



Unitarity Approaches to Two-Loop All-Plus Amplitudes

Sebastian Pögel

► To cite this version:

Sebastian Pögel. Unitarity Approaches to Two-Loop All-Plus Amplitudes. High Energy Physics - Theory [hep-th]. Université Paris-Saclay, 2021. English. NNT : 2021UPASP088 . tel-03506293

HAL Id: tel-03506293

<https://theses.hal.science/tel-03506293>

Submitted on 2 Jan 2022

HAL is a multi-disciplinary open access archive for the deposit and dissemination of scientific research documents, whether they are published or not. The documents may come from teaching and research institutions in France or abroad, or from public or private research centers.

L'archive ouverte pluridisciplinaire **HAL**, est destinée au dépôt et à la diffusion de documents scientifiques de niveau recherche, publiés ou non, émanant des établissements d'enseignement et de recherche français ou étrangers, des laboratoires publics ou privés.

Unitarity Approaches to Two-Loop All-Plus Amplitudes

Approches d'unitarité pour des amplitudes
«tout-plus» à deux boucles

Thèse de doctorat de l'université Paris-Saclay

École Doctorale n° 564 : Physique en Île-de-France (PIF)

Spécialité de doctorat: Physique

Unité de recherche: Université Paris-Saclay, CNRS, CEA, Institut de physique théorique,
91191, Gif-sur-Yvette, France

Referent: Faculté des sciences d'Orsay

Thèse présentée et soutenue à Paris-Saclay, le 29 Septembre 2021, par

Sebastian Eike PÖGEL

Composition du jury:

Claude DUHR Professeur, Université rhénane Frédéric-Guillaume de Bonn	Président et Rapporteur
David DUNBAR Professeur, Université de Swansea	Rapporteur et Examineur
Simon BADGER Maître de conférences, Université de Turin	Examineur
Lance DIXON Professeur, Université Stanford	Examineur
Fernando FEBRES CORDERO Maître de conférences, Université d'État de Floride	Examineur
Gregory SOYEZ Directeur de recherche CNRS, CEA-Saclay	Examineur
David KOSOWER Directeur de recherche, CEA-Saclay	Directeur de thèse
John Joseph CARRASCO Maître de conférences, Université Northwestern	Co-encadrant
Gregory KORCHEMSKY Directeur de recherche CNRS, CEA-Saclay	Invité

Titre: Approches d'unitarité pour des amplitudes «tout-plus» à deux boucles

Mots clés: Amplitudes de Diffusion, Calculs de Précision en QCD, Unitarité Généralisée

Résumé: Avec la progression de la précision des mesures expérimentales au Grand Collisionneur de hadrons (LHC) du CERN, de nouvelles prédictions théoriques de haut précision sont nécessaires pour évaluer la validité du modèle standard de la physique des particules (SM). Un ingrédient essentiel sont les prédictions pour des processus de chromodynamique quantique (QCD). Celles-ci représentent la majorité des processus connus dans les mesures expérimentales au LHC. Une compréhension précise de ces processus est donc essentielle pour les recherches de physique au-delà du modèle standard.

Les prédictions théoriques de haute précision nécessitent des corrections virtuelles en ordre sub-sub-dominant (NNLO), qui sont typiquement fondées sur des amplitudes de diffusion à deux boucles. Puisque le calcul des amplitudes nécessaires pour les expériences est une tâche complexe, il est utile d'examiner des exemples simplifiés, pour développer de nouvelles techniques et trouver de nouvelles structures.

Dans cette thèse, je traite le calcul d'une classe d'amplitudes simples, appelées amplitudes «tout-plus». Celles-ci sont hautement symétriques, puisqu'elles caractérisent les interactions des gluons, qui ont tous la même hélicité. Les propriétés de la configuration «tout-plus» entraînent une simplification de l'expression de ces amplitudes, elles sont donc particulièrement accessibles à examiner.

Un aspect remarquable des amplitudes tout-plus, observer jusqu'au niveau deux boucles, est une réduction de la complexité de leur calcul. Les amplitudes en arbre sont nulles, tandis que les amplitudes à une boucle peuvent être obtenues avec des techniques qui sont similaires à celles utilisées au niveau arbre. Au niveau de deux boucles, il a été établi que la plupart des ampli-

tudes sont accessibles par des techniques au niveau d'une boucle.

Les termes des amplitudes tout-plus à deux boucles, pour lesquelles une telle construction n'est pas connue actuellement, sont les termes rationnels. Ces termes représentent la part de l'amplitude qui ne contient pas de polylogarithmes ou de pôles lors de la régularisation dimensionnelle.

Fondée sur une conjecture du Badger, Mogull et Peraro, je présente dans cette thèse une approche pour le calcul des termes rationnels des amplitudes tout-plus à deux boucles, qui s'appuie entièrement sur des techniques d'unitarité généralisée à une boucle. Cette approche n'est pas limitée à l'ordre dominant en couleur, mais semble aussi s'étendre aux ordres sub-dominants. Je montre que cette méthode reproduit tous les résultats connus pour ces termes rationnels, y compris pour des amplitudes non-planaires allant jusqu'à sept gluons. Les résultats concordent aussi avec les termes rationnels de l'amplitude sub-dominante à sept gluons avec une seule trace de couleur, qui n'est actuellement connue que dans le cadre d'une conjecture.

De plus, je montre que les termes rationnels peuvent être obtenus à partir d'un calcul d'unitarité généralisée à une boucle niché. Dans ce cas, une des boucles est présente en tant que termes rationnels d'une amplitude à une boucle. Ceci reflète une approche similaire trouver pour les termes polylogarithmiques des amplitudes dominantes en couleur.

Enfin, je présente de nouvelles relations entre les amplitudes partielles de la configuration tout-plus à deux boucles, qui incluent des invariants de Mandelstam. Ces relations ont donc une similarité frappante avec les relations BCJ, qui associent des amplitudes en arbre et des intégrandes au niveau boucle à ces mêmes invariants.

Title: Unitarity Approaches to Two-Loop All-Plus Amplitudes

Keywords: Scattering Amplitudes, Precision QCD Calculations, Generalised Unitarity

Abstract: With the continued advances in experimental measurements at the Large Hadron Collider (LHC), new high precision theoretical predictions are required to further test the validity of the Standard Model of particle physics (SM). An essential ingredient for such searches are predictions for processes in Quantum Chromodynamics (QCD). These make up the majority of the understood background in LHC measurements. A precise understanding of these processes is therefore vital for the search of physics beyond the SM.

High precision theory predictions require next-to-next-to-leading order virtual corrections, typically based on two-loop scattering amplitudes. As the computation of such amplitudes for experiments is generally a complex task, it is useful to study simplified cases, in order to develop computational techniques and search for new structures.

In this thesis I discuss the computation of such a simpler class of amplitudes, called all-plus amplitudes. They are highly symmetric, as they describe the interaction of gluons which all have the same helicity. The properties of the all-plus configuration lead to particularly compact forms, making all-plus amplitudes convenient objects to study.

A striking feature of all-plus amplitudes found so far for up to two loops is a reduction in computational complexity. Their tree amplitudes vanish, while their one-loop amplitudes can be obtained from techniques, which resemble those used at tree-level. In the two-loop case, many parts of these amplitudes have been shown to be

computable using only one-loop techniques.

A part of two-loop all-plus amplitudes for which such a construction from one-loop techniques is presently not known in general are their rational parts. These are the parts of the amplitude that are free of polylogarithms and poles in dimensional regularization. Based on a previous conjecture, I present in this thesis an approach for the computation of the rational part of two-loop all-plus amplitudes based solely on one-loop generalized unitarity techniques. This approach is not limited to leading color, but appears to extend to the full-color amplitude. I show that this method reproduces all known results for such rational parts, including the non-planar ones, for up to seven gluons. It also matches the rational part of the seven gluon subleading single-trace amplitude, whose form is presently only known as part of an all- n conjecture.

Furthermore, I show that the rational parts can be determined not only from one-loop techniques, but also from a nested one-loop generalized unitarity computation. Here, one of the loops appears as the rational part of a one-loop amplitude. This mirrors a similar derivation found for the leading-color polylogarithmic parts of the amplitude.

Finally, I present new relations between the two-loop partial amplitudes of the all-plus, which involve powers of Mandelstam invariants. As such they have a striking similarity to BCJ relations, which relate tree-level amplitudes and loop-level integrands via powers of such invariants.

Acknowledgements

First and foremost, I would like to thank my advisor David Kosower for introducing me to the subject of scattering amplitudes, and for the continuous support over the last three years.

This project has received funding from the European Unions Horizon 2020 research and innovation programme under the Marie Skłodowska-Curie grant agreement No. 764850 “SAGEX”, and I would like to express my sincere gratitude to everyone who helped organize and run this amazing network. I would like to especially thank Gabriele Travaglini and Jenna Lane for their vital role in getting the project started, and keeping it running so smoothly.

I want to thank the RISC GmbH and their Medical Informatics Group for hosting me during my SAGEX industry secondment. Here I particularly thank Stefan Thumfart and Bertram Sabrowsky-Hirsch for their support and for creating such a welcoming environment.

I would like to thank everybody at the IPhT and CEA-Saclay for the great three years of my PhD. I would like to extend my sincere thanks to John Joseph Carrasco for his help and acting as my co-supervisor. Special thanks go to Gregory Soyez and Gregory Korchemsky for helping and guiding me in my PhD as part of my comite de suivi. I would also like to particularly thank Laurent Sengmanivanh for all the technical support he provided. Thanks to Veronique Terras, who helped me navigate the french doctoral system, and was amazingly patient in answering my numerous questions. I also would like to express my sincere gratitude to Ben Page, who in our discussion over the years helped me with his many comments and suggestions. Special thanks also go to Maxence Grandadame for being an amazing office mate. My time at the lab would have been a lot duller without you.

I would like to thank all of the SAGEX PhD students, Manuel Accettulli Huber, Luke Corcoran, Andrea Cristofoli, Stefano De Angelis, Nikolai Fadeev, Jordi Frias Navarro, Gabriele Dian, Riccardo Gonzo, Kays Haddad, Davide Polvara, Lorenzo Quintavalle, Marco Saragnese, Canxin Shi, and Ingrid Vazquez-Holm. I am so grateful that I had the chance of getting to know all of you, and spend so much time with you at the various SAGEX events. I would like to particularly thank Manuel for providing me with an early version of his **SpinorHelicity6D`** package, on which most of the work in this thesis is based. Special thanks also go to Canxin for (again) being my office mate during our time at RISC. Your company greatly helped make the secondment such an enjoyable experience. I am also very grateful to Ingrid for all the moral support in the face of the French bureaucracy.

Thanks to George, Melih, Nicolas and Tuan for being such great friends over the years. I hope we are able to travel together many more times.

Finally, I want to express my deep gratitude to my family for all their support and encouragement, before and during my studies.



Synthèse en français

Avec les progrès continus des mesures expérimentales au Grand Collisionneur de Hadrons (LHC), de nouvelles prédictions théoriques de haute précision sont nécessaires pour tester d'avantage la validité du modèle standard de la physique des particules (SM). Un ingrédient essentiel pour de telles recherches est la prédiction des processus en Chromodynamique Quantique (QCD). Ces processus constituent la majorité du bruit de fond compris dans les mesures du LHC. Une compréhension précise de ces processus est donc vitale pour la recherche de la physique au-delà du SM.

Pour obtenir des prédictions théoriques de haute précision, des corrections à lordre sub-sub-dominant sont nécessaires, ce qui requiert généralement des amplitudes de diffusion à deux boucles. Comme le calcul de ces amplitudes pour les expériences est généralement une tâche complexe, il est utile d'étudier des cas simplifiés, afin de développer des techniques de calcul et d'explorer la structure analytique de ces amplitudes.

Dans cette thèse, je discute du calcul d'une telle classe d'amplitudes plus simples, appelées amplitudes tout-plus. Ce sont les amplitudes de Yang-Mills les plus symétriques, car elles décrivent l'interaction de gluons qui ont tous la même hélicité. Les propriétés de la configuration tout-plus conduisent à des formes particulièrement compactes, faisant des amplitudes tout-plus des objets pratiques à étudier.

Une caractéristique frappante des amplitudes tout-plus est une complexité de calcul réduite, qui ne correspond pas à celle des configurations d'hélicité générales au même ordre de boucle. Notamment, leurs amplitudes d'arbre disparaissent,

$$A^{(0)}(1^+ \dots n^+) = 0 \quad (1)$$

alors qu'à une boucle, elles ont une complexité comparable aux amplitudes d'arbres génériques. Pour l'amplitude partielle en couleur principale, la forme générale pour un nombre arbitraire de gluons a été conjecturée dans la réf. [1]

$$A^{(1)}(1^+ \dots n^+) = -\frac{1}{3} \frac{\sum_{1 \leq i < j < k < l \leq n} \langle i | jkl | i \rangle}{\langle 12 \rangle \langle 23 \rangle \dots \langle (n-1)n \rangle \langle n1 \rangle} + \mathcal{O}(\epsilon), \quad (2)$$

puis prouvée dans la ref. [2] cette forme fait apparaître deux caractéristiques des amplitudes tout-plus à une boucle : d'une part, elles ne contiennent aucun terme proportionnel aux puissances de $\frac{1}{\epsilon}$ dans la régularisation dimensionnelle. Elles ne sont donc ni UV ni IR divergentes. D'autre part, elles ne contiennent pas non plus de contributions polylogarithmiques, et sont donc exemptes de coupures de branches dans la cinématique externe.

Au niveau à deux boucles, les amplitudes tout-plus présentent également une complexité considérablement réduite. Les premiers signes de simplification peuvent être observés en étudiant leur

structure singulière UV et IR. Une amplitude générique à deux boucles peut être décomposée de la façon suivante [3],

$$A^{(2)} = A^{(0)}I^{(2)} + A^{(1)}I^{(1)} + F^{(2)} + \mathcal{O}(\epsilon). \quad (3)$$

Ici, $I^{(2)}$ est une fonction avec des divergences d'ordre $\frac{1}{\epsilon^4}$, tandis que $I^{(1)}$ est d'ordre $\frac{1}{\epsilon^2}$. $F^{(2)}$ est finie en régularisation dimensionnelle, et peut contenir des termes rationnels et polylogarithmiques. Alors que les amplitudes à deux boucles ont généralement des termes divergents d'ordre $\frac{1}{\epsilon^4}$, la disparition de $A^{(0)}$ et la finitude de $A^{(1)}$ dans le cas de la configuration tout-plus ne permettent que des termes avec des divergences d'ordre $\frac{1}{\epsilon^2}$, comme on s'y attendrait habituellement dans une amplitude à une boucle. Dans la réf. [4], une forme générique pour la partie divergente $A^{(1)}I^{(1)}$ de l'amplitude tout-plus est donnée pour un nombre arbitraire de gluons et toutes les amplitudes partielles. Comme nous pouvons obtenir les parties divergentes de $A^{(2)}$ par ce comportement universel, seule la partie finie $F^{(2)}$ doit être déterminée.

Nous pouvons diviser $F^{(2)}$ en ses composantes polylogarithmique et rationnelle, $P^{(2)}$ et $R^{(2)}$, de sorte que

$$F^{(2)} = P^{(2)} + R^{(2)}. \quad (4)$$

La partie polylogarithmique $P^{(2)}$ possède des coupures de branches et est donc accessible par un calcul d'unitarité généralisé à quatre dimensions. Dans les références [4–10], il a été montré que les parties divergentes et polylogarithmiques finies peuvent être obtenues à partir d'un calcul d'unitarité généralisée à une boucle, dans lequel chaque coupe implique une amplitude tout-plus à une boucle,

$$\begin{aligned} & \left[A^{(1)}I^{(1)} + P^{(2)} \right] (1^+ \dots n^+) \\ &= \sum \text{diagram 1} + \sum \text{diagram 2} + \sum \text{diagram 3} + \sum \text{diagram 4} \end{aligned} \quad (5)$$

Ainsi, ces parties de l'amplitude suivent le modèle du cas à une boucle, et ont une complexité de calcul réduite.

Il ne nous reste donc que les parties rationnelles finies $R^{(2)}$. Par définition, celles-ci ne contiennent pas de coupures de branche dans la cinématique, et ne peuvent donc être obtenues qu'à partir de l'unitarité D -dimensionnelle.

Les amplitudes de diffusion dépendent généralement de la valeur de la dimension espace-temps D_s , qui correspond à la trace du tenseur métrique g_μ^μ . Cette dimension contrôle le nombre d'états d'hélicité pour un champ. Dans le cas de bosons de jauge sans masse, tels que les gluons, le nombre d'états d'hélicité est donné par $(D_s - 2)$, ce qui dans $D_s = 4$ correspond au cas habituel de gluons à hélicité positive et négative. Il est important de noter que les amplitudes de boucle ont une dépendance polynomiale par rapport à D_s , car chaque boucle peut au maximum générer une seule trace g_μ^μ .

Au niveau de la couleur dominante, les réfs. [11, 12] relient les contributions rationnelles polylogarithmiques finies des amplitudes tout-plus à deux boucles à leur représentation comme polynômes en puissance de $(D_s - 2)$. Plus précisément, jusqu'à l'ordre ϵ^0 , les contributions polylogarithmiques finies $P_n^{(2)}$ proviennent entièrement du coefficient de $(D_s - 2)$, tandis que les termes rationnels $R_n^{(2)}$

sont entièrement déterminés par le coefficient de $(D_s - 2)^2$,

$$F_{n:1}^{(2)}(1^+ \dots n^+) = \underbrace{(D_s - 2)\mathcal{P}^{(2)}(1^+ \dots n^+)}_{P_n^{(2)}} + \underbrace{(D_s - 2)^2\mathcal{R}^{(2)}(1^+ \dots n^+)}_{R_n^{(2)}} + \mathcal{O}(\epsilon). \quad (6)$$

Ainsi, pour obtenir la partie rationnelle $R^{(2)}$ des amplitudes complètes tout-plus à deux boucles, il suffit de calculer la partie rationnelle de son coefficient $(D_s - 2)^2$.

La méthode de reconstruction dimensionnelle permet de retrouver la dépendance explicite des amplitudes de boucle sur la dimension D_s . En tant que polynômes dans D_s , il suffit d'évaluer ces amplitudes à plusieurs valeurs différentes de D_s pour fixer tous les coefficients. Les amplitudes à deux boucles sont des polynômes quadratiques, de sorte que nous avons besoin de trois évaluations de ce type. Les choix commodes pour ces évaluations sont $D_s = 6, 7, 8$. Les amplitudes dans $D_s = 7, 8$ peuvent alors être reliées, par réduction de Kaluza-Klein, à des combinaisons linéaires d'amplitudes à six dimensions, dans lesquelles les boucles portent soit des gluons à six dimensions, soit des scalaires à six dimensions,

$$A_{D_s}^{(2)} = A_6^{(2)} + (D_s - 6)A_{6,1,0}^{(2)} + (D_s - 6)^2 A_{6,2,0}^{(2)} + (D_s - 6)(D_s - 7)A_{6,1,1}^{(2)}. \quad (7)$$

Ici, $A_6^{(2)}$ est l'amplitude purement gluonique, à six dimensions. L'amplitude $A_{6,1,0}^{(2)}$ possède une boucle scalaire, tandis que $A_{6,2,0}^{(2)}$ et $A_{6,1,1}^{(2)}$ portent des scalaires dans leurs deux boucles. La différence entre ces deux dernières est la manière dont les deux boucles scalaires sont connectées: dans $A_{6,2,0}^{(2)}$, les scalaires des deux boucles échangent un gluon, tandis que dans $A_{6,1,1}^{(2)}$, les lignes scalaires sont directement couplées via un terme de contact à quatre scalaires.

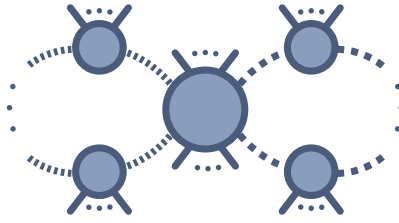
Nous connectons ensuite la proposition de ref. [12] pour les contributions finies avec le schéma de reconstruction dimensionnelle. En réarrangeant eq. (7) et en comparant avec eq. (6), nous obtenons les relations suivantes pour les contributions polylogarithmiques et rationnelles finies,

$$P^{(2)}(1^+ \dots n^+) = (D_s - 2)\mathcal{F} \left[A_{6,1,0}^{(2)} - 2 \times 4(A_{6,2,0}^{(2)} + A_{6,1,1}^{(2)}) - A_{6,1,1}^{(2)} \right] (1^+ \dots n^+), \quad (8)$$

$$R^{(2)}(1^+ \dots n^+) = (D_s - 2)^2 \mathcal{F} \left[A_{6,2,0}^{(2)} + A_{6,1,1}^{(2)} \right] (1^+ \dots n^+), \quad (9)$$

où \mathcal{F} représente l'opération d'extraction de la partie finie, en laissant tomber les termes d'ordre ϵ .

L'avantage de cette représentation en termes de $A_{6,2,0}^{(2)}$ et $A_{6,1,1}^{(2)}$ réside dans les topologies des intégrales qui peuvent contribuer à ces amplitudes. Plus précisément, les règles de Feynman pour les scalaires sont telles que les deux impulsions de boucle ne peuvent jamais apparaître dans le même propagateur. Toutes les intégrales de base qui peuvent apparaître dans un calcul d'unitarité généralisée de ces amplitudes se factorisent donc en un produit d'intégrales à une boucle, et toute coupure généralisée que nous devons calculer est de la forme suivante

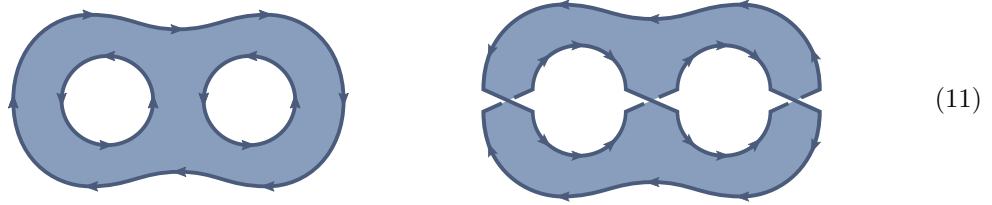


$$. \quad (10)$$

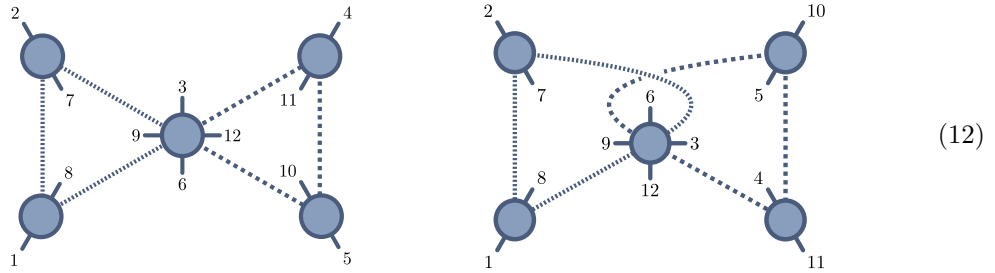
Les deux boucles se rejoignent dans une amplitude quadri-scalaire, qui ne relie les lignes scalaires

que par un échange de gluons ou un terme de contact. Comme les intégrales se factorisent, nous pouvons procéder au calcul des coefficients boucle par boucle, ne nécessitant à chaque fois que des techniques d'unitarité généralisée à une boucle. Alors que nous devrions généralement utiliser des amplitudes de scalaires sans masse à six dimensions dans le calcul, je soutiens que dans ces calculs il est suffisant d'utiliser des amplitudes de scalaires massifs à quatre dimensions. Les parties rationnelles à deux boucles de la couleur principale montrent donc la même réduction de complexité que celle déjà observée dans les parties divergentes et polylogarithmiques.

Alors que cette construction au carré à une boucle à la couleur principale a été présentée sous une forme similaire dans les refs. [11, 12], jusqu'à présent on ne savait pas si les parties rationnelles des amplitudes partielles sub-dominantes en couleur présentaient une structure similaire. Dans cette thèse, je présente une construction à une boucle au carré qui étend naturellement la construction à une boucle au carré à toutes les amplitudes partielles non planes. Je montre comment générer toutes les coupes au carré à une boucle appartenant aux différentes structures de traces dans la décomposition en couleur à deux boucles. Dans cette procédure, j'utilise l'origine des traces de couleur dans la théorie des cordes comme guide. Dans les amplitudes de cordes ouvertes, les surfaces de genre 2 suivantes peuvent apparaître,



Lorsqu'on habille les cordes avec des facteurs de Chan-Paton, chaque frontière de ces surfaces contribue finalement à une seule trace de couleur. Pour la topologie de gauche, on obtient donc trois traces, les traces vides se transformant en facteurs de N_c . La topologie de droite ne produit qu'une seule trace. En adhérant à ces topologies, nous obtenons les types suivants de coupes au carré à une boucle



Les coupes du type illustré à gauche appartiennent aux amplitudes partielles $A_{n:1}^{(2)}$, $A_{n:i}^{(2)}$ et $A_{n:i,r}^{(2)}$; celles appartenant au type illustré à droite conduisent à des amplitudes partielles sub-dominantes à trace unique $A_{n:1B}^{(2)}$. Par des évaluations explicites, je montre qu'en additionnant toutes les coupes uniques de ces types, nous récupérons les parties rationnelles de toutes les amplitudes partielles à quatre, cinq et six gluons, pour lesquelles des expressions analytiques sont disponibles dans la littérature [4–10, 13–17]. De plus, cette approche est en accord numérique avec l'expression de la couleur principale des sept gluons de la réf. [8], ainsi qu'avec le résultat conjecturé pour la partie rationnelle de l'amplitude sub-dominante de la trace unique des sept gluons $A_{7:1B}^{(2)}$ [18].

Alors que la construction à une boucle au carré montre que le calcul des parties rationnelles à

deux boucles des amplitudes tout-plus est d'un niveau à une boucle, les parties polylogarithmiques permettent une construction à une boucle encore plus explicite, comme on peut le voir dans l'eq. (5). Dans cette thèse, je montre qu'une construction similaire existe également pour les termes rationnels. Plus précisément, ils peuvent aussi être obtenus à partir d'un calcul d'unitarité généralisée à une boucle imbriquée, où l'une des boucles apparaît comme la partie rationnelle d'une autre amplitude à une boucle,

$$R^{(2)}(1^+ \dots n^+) = \text{diagram 1} + \text{diagram 2} + \text{diagram 3} .$$

Je justifie une telle construction en l'interprétant comme une réorganisation de l'approche de la coupe carrée à une boucle : Étant donné une coupe spécifique d'une des boucles, nous pouvons rassembler toutes les coupes appartenant à la deuxième boucle,

$$\text{diagram 1} + \text{diagram 2} + \text{diagram 3} + \dots \longrightarrow \text{diagram 4} .$$

Les sommets à une boucle qui apparaissent dans ces coupes sont les parties rationnelles d'un type particulier d'amplitude quadridimensionnelle à une boucle qui ont deux scalaires massifs externes et un nombre de gluons d'hélicité positive. Dans cette thèse, je présente une méthode pour calculer ces parties rationnelles à une boucle directement à partir de la récursion complexe. L'un des principaux défis du calcul récursif des amplitudes à une boucle est l'apparition de pôles uniques qui ne sont pas associés à la factorisation de l'amplitude. Une approche permettant d'obtenir ces termes de pôles supplémentaires est la procédure de récursion augmentée de la réf. [19], qui les détermine à partir de courants off-shell particuliers. Cette méthode a été appliquée avec succès dans un certain nombre de calculs à une boucle [20–22], et a été utilisée pour déterminer les contributions rationnelles des amplitudes tout-plus à deux boucles dans les refs. [4–10]. Dans cette thèse, je présente une approche hybride alternative, qui combine l'unitarité généralisée et la récursion complexe. En particulier, je montre que les termes de pôle manquants peuvent être obtenus à partir de seulement deux coupes d'unitarité. En conséquence, cette approche ne repose que sur des quantités on-shell. En utilisant cette approche hybride, je détermine des formes analytiques compactes pour les sommets à une boucle dans le cas de deux et trois gluons externes à hélicités positives. Je vérifie ensuite numériquement pour les parties rationnelles tout-plus à deux boucles $R_{4:1}^{(2)}$, $R_{4:3}^{(2)}$, $R_{4:11B}^{(2)}$ et $R_{5:1}^{(2)}$ qu'en additionnant toutes les coupures à une boucle appropriées impliquant ces sommets, nous obtenons effectivement un accord avec les résultats de la littérature. Enfin, dans le dernier chapitre, je présente brièvement de nouvelles relations entre les amplitudes partielles à deux boucles de configuration tout-plus, qui font apparaître des puissances d'invariants de Mandelstam. En tant que telles, elles présentent une similitude frappante avec les relations BCJ, qui relient les amplitudes au niveau de l'arbre et les intégrandes au niveau de la boucle via les puissances de ces mêmes invariants.

Contents

Introduction	1
1 Amplitudes Basics	5
1.1 Yang–Mills Theory	5
1.2 Spinor Helicity Formalism	8
1.2.1 Amplitudes and Spinors	11
1.3 Tree-Amplitudes	14
1.3.1 Tree-Level Color-Decomposition	15
1.3.2 BCFW Recursion	19
1.4 Loop Amplitudes	22
1.4.1 Feynman Integrals	23
1.4.2 Color-Decomposition for Loop Amplitudes	26
2 Generalized Unitarity	29
2.1 One-Loop Feynman Integrals	29
2.2 Four-Dimensional Generalized Unitarity	34
2.2.1 Unitarity Cuts and Loop-Momentum Parametrizations	36
2.3 D -Dimensional Generalized Unitarity	48
2.3.1 One-Loop Integral Basis in D Dimensions	49
2.3.2 SUSY Decomposition	50
2.3.3 Loop-Momentum Parametrization for D -Dimensional Cuts	51
2.4 Color-Dressed Unitarity	54
2.5 Generalized Unitarity Implementation in Mathematica	55
3 Two-Loop Rational Terms from One-Loop Unitarity	59
3.1 The All-Plus: A Brief Review	60
3.2 Dimensional Reconstruction	64
3.3 Separability and Two-Loop Rational Terms	71
3.4 One-Loop Squared Cuts	73
3.4.1 Two-Loop Color Dressed Unitarity	73
3.4.2 Generating Sets of Cuts	76
3.5 Six-Dimensional Amplitudes	80
3.5.1 Tree Amplitudes with One Scalar Pair	80
3.5.2 Tree-Amplitudes with Two Scalar Pairs	81
3.6 Momentum Twistor Parametrization	87
3.7 Results	89

3.7.1	The Four-Gluon Amplitude Analytically	89
3.7.2	The Five-Gluon Amplitude Analytically	96
3.7.3	The Six- and Seven-Gluon Amplitudes: Numeric Results	97
3.7.4	Agreement with Seven-Gluon $R_{7:1B}^{(2)}$ Conjecture	101
4	Integrating A Loop: The Effective One-Loop Picture	105
4.1	Four-Gluon Rational Terms from a One-Loop Vertex	106
4.2	One-Loop Massive Scalar Amplitudes	111
4.2.1	One-Loop BCFW	112
4.2.2	Contact Term Amplitudes	120
4.2.3	One-Loop Gluon-Exchange Amplitudes	124
4.2.4	Combining $R_{\text{contact}}^{(1)}$ and $R_{\text{gluon}}^{(1)}$ Amplitudes	126
4.3	One Loop Construction of $R^{(2)}(1^+2^+3^+4^+5^+)$	127
5	BCJ-Like Relations for Two-Loop All-Plus Amplitudes	129
5.1	Linear Relations	130
5.2	Relations Involving Mandelstam Invariants	131
	Conclusion	139
	Appendix A	141
A.1	The Vanishing of $A^{(0)}(1^\pm 2 + \dots n^+)$	141
A.2	Single-Minus One-Loop Amplitudes	142
A.3	Tree-Level Soft Functions	143
A.4	Computing One-Loop μ^2 Integrals	145
	Appendix B	153
B.1	Scalar Tree Amplitudes	153
B.2	Analytic Expressions for $R_{5:1}^{(2)}$	154

Introduction

The Large Hadron Collider (LHC) is currently our most promising window to exploring the fundamental structures of our universe. The Standard Model of particle physics (SM) has so far been able to accurately describe all observations in collider experiments. It is incomplete, making it presumably only the effective theory of a more comprehensive underlying theory. So far no significant deviations from the SM have been detected directly in the energy regime accessible to the LHC. Attempts of detecting physics beyond the Standard Model (BSM) will thus have to rely on high-precision measurements, looking for small discrepancies from SM predictions.

In order to subtract the backgrounds of known SM processes from the experimental data we require high-precision theory predictions in the form of higher-order corrections. The LHC is a proton–proton collider, making quantum chromodynamics (QCD) the main source of such backgrounds. For these, leading-order (LO) computations provide mostly qualitative results, with predictions of approximately the correct order of magnitude. At next-to-leading order (NLO), predictions become quantitatively more reliable, with uncertainties of the order of 15%. For precision measurements we require next-to-next-to-leading order (NNLO) corrections, which promise uncertainties of just a few percent. While NLO predictions are well understood and are used extensively for collider phenomenology today, NNLO predictions are still the subject of current research. NNLO predictions for experiments like the LHC rely on two-loop scattering amplitudes in QCD, whose computation presents a formidable challenge.

The study of scattering amplitudes has provided many insights into the structures present in the interactions of fundamental particles. Particularly the on-shell techniques developed over the last 20 years, have proven to be powerful tools to rein in the complexities of computing higher-order virtual corrections.

In the traditional approach, scattering amplitudes are computed from the sum of Feynman diagrams contributing to a process. A significant downside in applying this method to gauge theories is the inclusion of gauge redundancies. While every diagram is dependent on the choice of gauge, the sum of all diagrams is not. This can lead to complicated intermediate results, and many non-trivial cancellations need to occur to recover the final result, which tends to be much simpler. In the on-shell approach, Feynman diagrams are avoided all together. Instead, on-shell tree-amplitudes are taken as the fundamental objects from which more complicated amplitudes are constructed [23, 24]. As scattering amplitudes need to satisfy locality and unitarity, they have to factorize again into amplitudes when internal propagators go on-shell. By harnessing this feature, complicated amplitudes can be built up from simpler ones without introducing gauge redundancies, providing a shortcut to the compact gauge-invariant result.

An important technique in the on-shell approach for loop-amplitudes is generalized unitarity [24–26]. Amplitudes are multivalued functions in the kinematics, which develop singularities and branch cuts for internal propagators going on-shell. Instead of computing an amplitude directly, in generalized unitarity an amplitude is expressed in terms of a basis of Feynman integrals, called Master Integrals. To determine the basis coefficients, generalized cuts are used to project the amplitude onto the basis, according to their discontinuities. These generalized cuts—an extension of physical unitarity cuts introduced by Cutkosky [27]—determine the discontinuities associated to an arbitrary number of propagators going on-shell by computing the associated residues. Computing the residues “freezes” parts of the loop-momentum, and the basis integral coefficients can be entirely determined from on-shell tree-amplitudes. By computing cuts of a dimensionally regulated amplitude with D -dimensional loop-momentum, it is possible to construct the entire amplitude in this manner, including contributions that do not contain branch cuts in four dimensions. The generalized unitarity technology at one loop has been made accessible to collider phenomenology through various automated software packages, such as **BlackHat** [28, 29], **CutTools** [30, 31], **ROCKET** [32], **HELAC1L** [33], **OpenLoops** [34, 35] or **NJet** [36]. At the two-loop level, it has been used to obtain amplitudes relevant for virtual NNLO QCD corrections [16, 17, 37–40]. On-shell techniques have therefore become an essential tool for many collider predictions.

Due to the complexity of computing virtual corrections for experiments, it is often fruitful to first consider simplified cases, which allow the development of new techniques and the discovery of structures in amplitudes. The gained insights can then be used to further push the boundary of theoretical predictions for particle phenomenology.

The archetype of non-abelian gauge-theories are Yang–Mills theories, which describe the interaction of gauge-bosons in the adjoint representation of a non-abelian gauge-group, typically $SU(N_c)$ or $U(N_c)$. QCD is an example of a Yang–Mills theory with $N_c = 3$, coupled to fermions transforming in the fundamental representation. Careful study of amplitudes in pure Yang–Mills theory, *i.e.* without fermions, can therefore lead to an improved understanding of the strong interaction.

While pure Yang–Mills amplitudes already represent a simplification compared to those of QCD, for generic helicity configurations they are still challenging to compute. It is therefore useful to consider simple cases, which can act as laboratories for the development of new techniques. A common example is that of amplitudes in $\mathcal{N} = 4$ super-Yang–Mills theory (SYM), which is the supersymmetric extension of Yang–Mills with the maximal number of supersymmetries allowed in four dimensions for particles of spin 1. While these show a rich structure due their many symmetries, their supersymmetric nature sets them apart from QCD amplitudes, required for collider physics.

Without resorting to supersymmetry, the next easiest class of gauge-theory amplitudes to consider are Yang–Mills amplitudes, where all gluons have the same helicity. Typically the helicity is chosen to be positive, and these amplitudes are often referred to as all-plus amplitudes. They are the most symmetric class of Yang–Mills amplitudes, and as a consequence show a great amount of simplicity, making them a good laboratory as well. Furthermore, as they are proper Yang–Mills amplitudes, and insights for all-plus amplitudes are more likely to be applicable to phenomenologically relevant cases.

As a consequence of the properties of the all-plus configuration, their computational complexity tends to be of lower-loop level. They vanish at tree level, and are entirely rational at one loop. Generically two-loop amplitudes in dimensional regularization can be split into a divergent,

a polylogarithmic finite and a rational finite piece. For two-loop all-plus amplitudes, Dunbar, Perkins and Jehu showed [5–7] that one-loop techniques are sufficient to compute the divergent and polylogarithmic finite parts. This eventually led to the determination of an analytic form for these contributions at leading color, valid for an arbitrary number of gluons [7]. Thus, at least at leading color, a complete understanding of these amplitudes requires only a general form of the finite rational parts. Through extensive efforts over the last two decades, the full-color rational parts are today known analytically for up to six gluons: the four-gluon results were first derived by Bern, Dixon and Kosower [13], with the planar five-gluon amplitude following in ref. [16] through the work of Gehrmann, Henn and Presti. The full-color five-gluon results were first presented by Badger, Chicherin, Heinrich, Henn, Peraro, Wasser, Zhang and Zoia in ref. [17], and later rederived by Dunbar, Perkins, Godwin, Strong in ref. [4] using complex recursion. Using the same technique, Dalgleish, Dunbar, Perkins, Godwin and Strong were able to obtain the first result for the full-color six-gluon amplitude in ref. [10]. For seven gluons, only an expression for the leading color contribution is known [8], due to Dunbar, Godwin, Jehu and Perkins. Pairing the explicit results for five and six gluons with a simplified collinear behavior, Dunbar, Perkins and Strong were additionally able to formulate an all- n conjecture for the rational part of the subleading single-trace partial amplitude in ref. [18].

Extending a previous conjecture of Badger, Mogull and Peraro [11, 12], I developed and implemented a unitarity approach for the computation of rational terms applicable to all two-loop all-plus partial amplitudes. In refs. [11, 12] it was first demonstrated that only one-loop squared integrals contribute to the leading color two-loop all-plus rational terms. In these two-loop integrals, no propagator carries the loop momentum of both loops. They therefore factorize into a product of one-loop integrals, allowing the integral coefficient to be evaluated loop by loop. This reduces the effective complexity of computing the two-loop rational parts to one loop. I will show in this thesis that this approach is not only valid for leading color amplitudes, but also allows the computation of subleading rational parts via one-loop unitarity. As rational contributions cannot be computed from unitary cuts in four dimensions, we must work in higher dimensions, in this case six. However, as we will apply one-loop D -dimensional unitarity techniques, it will suffice to work with massive four-dimensional amplitudes, with the mass encoding the $(D - 4)$ -dimensional part of the loop momentum. Due to the substantial number of unitarity cuts involved in extending the computations to high multiplicity, I created automated tools that allow both pure numerical evaluation, as well as obtaining analytical results. Using my approach I am able to reproduce all existing results at leading and subleading color.

Following the one-loop squared construction, I will show that the rational terms of two-loop all-plus amplitudes can also be obtained from a nested one-loop computation, with one of the loops appearing as part of a one-loop amplitude. This mirrors the approach for determining the divergent and polylogarithmic finite parts of ref. [7].

Finally, I will briefly present new relations between the five-gluon all-plus partial amplitudes. While some of these are linear relations, others include powers of Mandelstam invariants. They are therefore similar in structure to BCJ relations, which usually only hold for integrands of loop amplitudes.

To summarize, the primary results presented in this thesis are

- A construction of two-loop all-plus partial amplitudes (including non-planar ones) using only

one-loop unitarity techniques

- An effective one-loop unitarity construction of such partial amplitudes using a one-loop vertex
- New relations between five-gluon two-loop all-plus partial amplitudes, which involve powers of Mandelstam invariants, with a BCJ-like structure.

Interesting secondary results include

- A momentum twistor parameterization for an arbitrary number of massless particles
- Analytic results for tree amplitudes involving two massive scalar lines
- Analytic results for rational terms of one-loop amplitudes involving a massive scalar line
- A generalized unitarity approach for the computation of subleading single poles in BCFW computations of one-loop amplitudes.

Chapter 1

Amplitudes Basics

In this chapter we will discuss the basic concepts in the study of scattering amplitudes that will be required for later discussions. We will first provide a brief review of Yang–Mills theory, summarizing information that can be found in most textbooks on quantum field theory. After a short introduction to the spinor-helicity formalism useful for expressing amplitudes compactly, we discuss tree-level amplitudes and some basic methods used to compute them using the on-shell approach. Afterwards, we briefly cover some preliminaries for loop amplitudes, leaving the discussion of their on-shell construction for the following chapter.

1.1 Yang–Mills Theory

The part of the Standard Model of particle physics that describes the interactions of quarks and gluons is called Quantum Chromodynamics, or QCD for short. It is an example of a Yang–Mills (YM) theory, which describes massless spin-1 particles with a gauge-symmetry described by a generally non-Abelian Lie group. Chen Ning Yang and Robert Mills were the first to study these types of theories [41], and since then they have played a crucial role in describing the interactions of fundamental particles. Quantum Electrodynamics is derived from an abelian $U(1)$ gauge-theory, and weak interactions are described by a non-abelian $SU(2)$ Yang–Mills theory. However, the physical vacuum does not respect the full symmetry $U(1) \times SU(2)$, leading to electroweak symmetry breaking. QCD is therefore the only realization of a Yang–Mills theory in the Standard Model with an unbroken gauge-group, namely $SU(3)$. The degree of the gauge group corresponds to the number of colors in QCD, and is therefore typically denoted by N_c .

While we might only be interested in theories with $N_c = 3$ for particle phenomenological purposes, Yang–Mills theories are the archetype of many Quantum Field Theories, and therefore merit more fundamental investigations. Thus, we usually leave N_c unspecified, and study Yang–Mills theories with a general gauge group $SU(N_c)$. This is further justified by the fact that it is possible to separate the kinematic dependence of scattering amplitudes from their color structure. I will discuss this point in a following section.

As the underlying Lie group is essential to any gauge theory, we first spend a few moments reviewing some basic properties of Lie groups. We will be considering gauge theories, whose

fields transform in the adjoint representation of the non-Abelian Lie groups $SU(N_c)$ and $U(N_c)$, generated by the Lie algebras $\mathfrak{su}(N_c)$ and $\mathfrak{u}(N_c)$. These algebras are spanned by generators T^a , where $a \in (1, \dots, N_c^2 - 1)$ for $\mathfrak{su}(N_c)$ and $a \in (1, \dots, N_c^2)$ for $\mathfrak{u}(N_c)$. Represented as matrices, the T^a are hermitian matrices in $\mathbb{C}^{N_c \times N_c}$, which in the case of $\mathfrak{su}(N_c)$ have to be traceless. We will use bases of generators that are normalized to

$$\text{Tr}(T^a T^b) = \delta^{ab}. \quad (1.1)$$

The generators are related to structure constants f^{abc} via

$$[T^a, T^b] = i\sqrt{2}f^{abc}T^c, \quad (1.2)$$

or conversely

$$\begin{aligned} i\sqrt{2}f^{abc} &= i\sqrt{2}f^{abd}\text{tr}(T^d T^c) = \text{tr}([T^a, T^b]T^c) \\ &= \text{tr}(T^a T^b T^c) - \text{tr}(T^b T^a T^c). \end{aligned} \quad (1.3)$$

In the case of $U(N_c)$ gauge groups we make use of the decomposition $U(N_c) = SU(N_c) \times U(1)$, which allows us to extend the generators of $SU(N_c)$ to those of $U(N_c)$ by adding

$$T_{U(1)} = \frac{1}{\sqrt{N_c}}\mathbb{I}_{N_c}, \quad (1.4)$$

The normalization is consistent with that of eq. (1.1).

An explicit example of a generator basis as described above are the Gell-Mann matrices, which normalized according to eq. (1.1) take the form

$$\begin{aligned} T^1 &= \frac{1}{\sqrt{2}} \begin{pmatrix} 0 & 1 & 0 \\ 1 & 0 & 0 \\ 0 & 0 & 0 \end{pmatrix} & T^2 &= \frac{1}{\sqrt{2}} \begin{pmatrix} 0 & -i & 0 \\ i & 0 & 0 \\ 0 & 0 & 0 \end{pmatrix} & T^3 &= \frac{1}{\sqrt{2}} \begin{pmatrix} 1 & 0 & 0 \\ 0 & -1 & 0 \\ 0 & 0 & 0 \end{pmatrix} \\ T^4 &= \frac{1}{\sqrt{2}} \begin{pmatrix} 0 & 0 & 1 \\ 0 & 0 & 0 \\ 1 & 0 & 0 \end{pmatrix} & T^5 &= \frac{1}{\sqrt{2}} \begin{pmatrix} 0 & 0 & -i \\ 0 & 0 & 0 \\ i & 0 & 0 \end{pmatrix} & T^6 &= \frac{1}{\sqrt{2}} \begin{pmatrix} 0 & 0 & 0 \\ 0 & 0 & 1 \\ 0 & 1 & 0 \end{pmatrix} \\ T^7 &= \frac{1}{\sqrt{2}} \begin{pmatrix} 0 & 0 & 0 \\ 0 & 0 & -i \\ 0 & i & 0 \end{pmatrix} & T^8 &= \frac{1}{\sqrt{6}} \begin{pmatrix} 1 & 0 & 0 \\ 0 & 1 & 0 \\ 0 & 0 & -2 \end{pmatrix}. \end{aligned}$$

These form a basis of $\mathfrak{su}(3)$.

An important property of $SU(N_c)$ and $U(N_c)$ generators are the Fierz identities,

$$\sum_a (T^a)_i^j (T^a)_k^l = \begin{cases} \delta_i^l \delta_k^j, & U(N_c), \\ \delta_i^l \delta_k^j - \frac{1}{N_c} \delta_i^j \delta_k^l, & SU(N_c). \end{cases} \quad (1.5)$$

In practice we typically omit the explicit sum over repeated color indices. As we will be mainly concerned with traces of generators

$$\text{Tr}(T^{a_1} \dots T^{a_n}) \quad (1.6)$$

we translate the Fierz identities into relations of such traces. For $U(N_c)$ they correspond to concatenation and splitting of traces,

$$\begin{aligned}\mathrm{Tr}(A T^a B) \mathrm{Tr}(C T^a D) &= \mathrm{Tr}(ADCB), \\ \mathrm{Tr}(AB T^a C D T^a) &= \mathrm{Tr}(AB) \mathrm{Tr}(CD),\end{aligned}\tag{1.7}$$

while for $SU(N_c)$ we have to add a term proportional to $\frac{1}{N_c}$,

$$\begin{aligned}\mathrm{Tr}(A T^a B) \mathrm{Tr}(C T^a D) &= \mathrm{Tr}(ADCB) - \frac{1}{N_c} \mathrm{Tr}(AB) \mathrm{Tr}(CD) \\ \mathrm{Tr}(AB T^a C D T^a) &= \mathrm{Tr}(AB) \mathrm{Tr}(CD) - \frac{1}{N_c} \mathrm{Tr}(ABCD).\end{aligned}\tag{1.8}$$

The Lagrangian of Yang–Mills theory is,

$$\mathcal{L}_{\mathrm{QCD}} = -\frac{1}{4} F_{\mu\nu}^a F^{a\mu\nu}\tag{1.9}$$

The gauge bosons transform in the $(N_c^2 - 1)$ -dimensional adjoint representation of $\mathfrak{su}(N_c)$, labelled by $a = 1, \dots, (N_c^2 - 1)$. As the strong force of the Standard Model is described by an $SU(3)$ gauge theory, these gauge bosons are typically referred to as gluons, even when considering general gauge groups $SU(N_c)$. The field-strength tensor appearing in the Lagrangian is given by,

$$F_{\mu\nu}^a = \partial_\mu A_\nu^a - \partial_\nu A_\mu^a + g f^{abc} A_\mu^b A_\nu^c.\tag{1.10}$$

The last term, proportional f^{abc} , is the defining aspect of non-abelian gauge theories, as it generates three- and four-gluon self-interactions.

While pure Yang–Mills is already a formidable topic of study, we can also choose to couple it to matter fields. For example, in the case of QCD we add quarks through the Lagrangian,

$$\mathcal{L}_f = \bar{q}_i (i \not{D}_{ij} - m_{ij}) q_j.\tag{1.11}$$

The q_i are fermionic fields, which transform in the fundamental \mathbf{N}_c representations of $SU(N_c)$ in the indices $i, j = 1, \dots, N_c$. To ensure gauge invariance we use the covariant derivative D_μ ,

$$D_\mu q_i = (\partial_\mu - ig A_\mu^a T^a) q_i,\tag{1.12}$$

to couple the fermions to the gluons. More details are readily found in any modern QFT textbook, see for example refs. [42–45].

Choosing Feynman gauge, the pure Yang–Mills Feynman rules are therefore [42],

$$\begin{aligned}
& \text{Diagram 1: A vertex with three external lines. Line 1 (left) has index 1^{μ_1} and label a. Line 2 (top right) has index 2^{μ_2} and label b. Line 3 (bottom right) has index 3^{μ_3} and label c.} \\
& = g f^{abc} \left[g^{\mu_1 \mu_2} (p_1 - p_2)^{\mu_3} + g^{\mu_2 \mu_3} (p_2 - p_3)^{\mu_1} + g^{\mu_3 \mu_1} (p_3 - p_1)^{\mu_2} \right] \\
& \text{Diagram 2: A four-point vertex with external lines labeled a, b, c, d and indices $1^{\mu_1}, 2^{\mu_2}, 3^{\mu_3}, 4^{\mu_4}$. Lines a and b cross each other.} \\
& = -ig^2 \left[f^{abe} f^{cde} (g^{\mu_1 \mu_3} g^{\mu_2 \mu_4} - g^{\mu_1 \mu_4} g^{\mu_2 \mu_3}) + f^{ace} f^{bde} (g^{\mu_1 \mu_2} g^{\mu_3 \mu_4} - g^{\mu_1 \mu_4} g^{\mu_2 \mu_3}) \right. \\
& \quad \left. + f^{ade} f^{bce} (g^{\mu_1 \mu_2} g^{\mu_3 \mu_4} - g^{\mu_1 \mu_3} g^{\mu_2 \mu_4}) \right] \\
& \text{Diagram 3: A two-point vertex with external lines labeled a, b and indices p^μ, p^ν.} \\
& = \frac{-ig^{\mu\nu} \delta^{ab}}{p^2 + i0}
\end{aligned} \tag{1.13}$$

As we are working in a non-abelian gauge theory we would in principle also need to include Faddeev–Popov ghosts [46]. However, these are only required in Feynman diagrammatic computations of loop amplitudes. As we will soon review, there are methods better suited to compute such amplitudes.

1.2 Spinor Helicity Formalism

Before we dive into the topic of scattering amplitudes, we will first review the spinor-helicity formalism. Spinors are a convenient language to express amplitudes, as they allow us to encode both the helicity information and kinematics of external particles. They are thus a natural choice of variables to express on-shell quantities. Reviews of the formalism can be found in refs. [47, 48]. Here, we loosely follow the discussion of ref. [47], though with a different metric.

In this thesis we will always use the “mostly-minus”, or Bjorken–Drell metric

$$\eta^{\mu\nu} = \text{diag}(+1, -1, \dots, -1). \tag{1.14}$$

Let us begin with a massless momentum p^μ , for which we would like to find an associated spinorial representation. As a reminder, Weyl spinors transform in the $(\frac{1}{2}, 0)$ and $(0, \frac{1}{2})$ representations of the Lorentz group. As a Lorentz vector, p transforms in the $(\frac{1}{2}, \frac{1}{2})$ representation, and we might therefore expect to find two spinors associated p , one for either representation.

To construct such spinors we use the Pauli matrices supplemented with the identity σ^i ,

$$\sigma^0 = \begin{pmatrix} 1 & 0 \\ 0 & 1 \end{pmatrix}, \quad \sigma^1 = \begin{pmatrix} 0 & 1 \\ 1 & 0 \end{pmatrix}, \quad \sigma^2 = \begin{pmatrix} 0 & -i \\ i & 0 \end{pmatrix}, \quad \sigma^3 = \begin{pmatrix} 1 & 0 \\ 0 & -1 \end{pmatrix}. \tag{1.15}$$

Further defining,

$$(\bar{\sigma}^0, \bar{\sigma}^i) = (\sigma^0, -\sigma^i), \tag{1.16}$$

we can define,

$$\begin{aligned}
p_{ab} &= p^\mu (\sigma_\mu)_{ab}, \\
p^{\dot{a}b} &= p^\mu (\bar{\sigma}_\mu)^{\dot{a}b}.
\end{aligned} \tag{1.17}$$

The spinors we are after have to satisfy the Weyl equation

$$p_{a\dot{b}} |p\rangle^{\dot{b}} = 0, \quad \langle p|^a p_{ab} = 0, \quad (1.18)$$

$$p^{\dot{a}b} |p\rangle_b = 0, \quad [p]_{\dot{a}} p^{\dot{a}b} = 0. \quad (1.19)$$

Here $\langle p|^a$, $[p]_{\dot{a}}$ are Weyl spinors associated to p that transform in the $(\frac{1}{2}, 0)$ and $(0, \frac{1}{2})$ representations of the Lorentz group. We sometimes refer to spinors in the different representations as “angle” and “bracket” spinors, respectively. By convention, we will always use undotted indices $a = 1, 2$ for the $(\frac{1}{2}, 0)$ representation, and dotted indices $\dot{a} = \dot{1}, \dot{2}$ for the $(0, \frac{1}{2})$ representation. As objects transforming in representations of $SU(2)$, we can raise and lower the spinor indices using the antisymmetric tensors ϵ^{ab} and $\epsilon^{\dot{a}\dot{b}}$,

$$|p\rangle_a = \epsilon_{ab} \langle p|^b, \quad [p]^{\dot{a}} = \epsilon^{\dot{a}\dot{b}} [p]_{\dot{b}}. \quad (1.20)$$

We use the sign convention,

$$\epsilon^{12} = -\epsilon_{12} = +1. \quad (1.21)$$

We can further build $SU(2)$ invariant spinor products,

$$\langle pk\rangle = \langle p|^a \langle k|^b \epsilon_{ab} = \langle p|^a |k\rangle_a \quad [pk] = [p]_{\dot{a}} [k]_{\dot{b}} \epsilon^{\dot{a}\dot{b}} = [p]_{\dot{a}} |k\rangle^{\dot{a}}, \quad (1.22)$$

which are naturally antisymmetric,

$$\langle pk\rangle = -\langle kp\rangle, \quad [pk] = -[kp]. \quad (1.23)$$

In amplitude calculations we deal with a set of numbered momenta $\{p_1, \dots, p_n\}$ associated to the external particles. To reduce clutter in computations, the spinors of these momenta are usually labelled by their indices,

$$\langle 12\rangle \equiv \langle p_1 p_2\rangle, \quad [12] \equiv [p_1 p_2]. \quad (1.24)$$

From the Weyl equation we see that both $p_{a\dot{b}}$ and $p^{\dot{a}b}$ have a complex one-dimensional nullspace. As they are matrices in $\mathbb{C}^{2 \times 2}$, we can therefore express them as the outer product of two complex, two-dimensional vectors. These vectors are the spinors associated to the momentum,

$$p_{a\dot{b}} = |p\rangle_a [p]_{\dot{b}} \quad (1.25)$$

$$p^{\dot{a}b} = [p]^{\dot{a}} \langle p|^b.$$

This representation trivializes the Weyl equations of eq. (1.18). We can also express momentum conservation in spinorial form as follows,

$$\sum_i p_i^\mu = 0 \Rightarrow \begin{cases} \sum_i p_i^{a\dot{a}} &= \sum_i |i\rangle^a [i]^{\dot{a}} = 0 \\ \sum_i p_{i,\dot{a}a} &= \sum_i [i]_{\dot{a}} \langle i|_a = 0 \end{cases} \quad (1.26)$$

The Weyl spinors can be associated to components of Dirac bispinors of specific helicities [47],

$$\begin{pmatrix} u_-(p) \\ v_+(p) \end{pmatrix} \rightarrow \begin{pmatrix} 0 \\ [p]^{\dot{a}} \end{pmatrix}, \quad \begin{pmatrix} u_+(p) \\ v_-(p) \end{pmatrix} \rightarrow \begin{pmatrix} |p\rangle_a \\ 0 \end{pmatrix} \quad (1.27)$$

$$\begin{pmatrix} \bar{u}_-(p) \\ \bar{v}_+(p) \end{pmatrix} \rightarrow \left(\langle p|^a, 0 \right), \quad \begin{pmatrix} \bar{u}_+(p) \\ \bar{v}_-(p) \end{pmatrix} \rightarrow \left(0, [p]_a \right). \quad (1.28)$$

u_{\pm}/\bar{u}_{\pm} are in- and outgoing fermions, and v_{\pm}/\bar{v}_{\pm} are in- and outgoing anti-fermions. As momenta are always defined to be outgoing, a fermion with helicity $\pm\frac{1}{2}$ is associated to \bar{u}_{\pm} , or, in the spinor language, to bracket and angle spinors respectively.

The Pauli matrices σ^{μ} and $\bar{\sigma}^{\mu}$ fulfill the identity

$$\text{tr}(\sigma^{\mu}\bar{\sigma}^{\nu}) = (\sigma_{\mu})_{a\dot{a}}(\bar{\sigma}^{\nu})^{\dot{a}a} = 2\eta^{\mu\nu}, \quad (1.29)$$

as well as

$$\begin{aligned} (\sigma^{\mu})_{a\dot{a}}(\sigma_{\mu})_{b\dot{b}} &= 2\epsilon_{\dot{a}\dot{b}}\epsilon_{ab} \\ (\bar{\sigma}^{\mu})^{\dot{a}a}(\bar{\sigma}_{\mu})^{\dot{b}b} &= 2\epsilon^{\dot{a}\dot{b}}\epsilon^{ab}. \end{aligned} \quad (1.30)$$

With the identities

$$\langle a|\bar{\sigma}^{\mu}|b\rangle(\bar{\sigma}_{\mu})^{\dot{a}a} = 2|b]^{\dot{a}}\langle a|^a, \quad [a|\sigma^{\mu}|b\rangle(\sigma_{\mu})_{a\dot{a}} = 2|b\rangle_a[a]_{\dot{a}}, \quad (1.31)$$

we can show that the four-momentum p^{μ} is recovered from its spinors via,

$$p^{\mu} = \frac{1}{2}|p|\sigma^{\mu}|p\rangle. \quad (1.32)$$

These identities also give us the Fierz identity,

$$\langle a|\gamma^{\mu}|b\rangle\langle c|\gamma_{\mu}|d\rangle = 2\langle ab\rangle[dc]. \quad (1.33)$$

Using eq. (1.32) and the Fierz identity we can derive a relation between products of four-momenta and the products of their spinors,

$$2p_i \cdot p_j = \frac{1}{2}\langle i|\sigma^{\mu}|i\rangle\langle j|\sigma_{\mu}|j\rangle = \langle ij\rangle[ji]. \quad (1.34)$$

As vectors in a two-dimensional complex vector space, any set of three spinors must be linearly dependent over \mathbb{C} . In other words, given $|i\rangle$, $|j\rangle$ and $|k\rangle$, there exist $a_j, a_k \in \mathbb{C}$, such that

$$|i\rangle = a_j|j\rangle + a_k|k\rangle. \quad (1.35)$$

The constants can be obtained from projecting $|i\rangle$ on $|j\rangle$ and $|k\rangle$,

$$|i\rangle = \frac{\langle ki\rangle}{\langle kj\rangle}|j\rangle + \frac{\langle ji\rangle}{\langle jk\rangle}|k\rangle, \quad (1.36)$$

or equivalently

$$\langle jk\rangle|i\rangle + \langle ki\rangle|j\rangle + \langle ij\rangle|k\rangle = 0, \quad (1.37)$$

This is the Schouten identity. A more general form of this identity for strings of spinors takes the form

$$[a|\dots b|c\rangle\langle d|e\dots|f] = [a|\dots b|d\rangle\langle c|e\dots|f] - \langle cd\rangle[a|\dots b|e\dots|f]. \quad (1.38)$$

When defining the spinors as in eq. (1.25) we have a remaining freedom to rescale both angle and bracket spinors simultaneously. The sets of spinors

$$\begin{pmatrix} \langle p| \\ [p] \end{pmatrix}, \quad \begin{pmatrix} a \langle p| \\ \frac{1}{a} [p] \end{pmatrix} \quad (1.39)$$

both belong to the same momentum p , which can be verified via eq. (1.32). Spinors are therefore not uniquely defined. The source of this ambiguity are transformations of the little group. This subgroup of the Lorentz-group is defined by all transformations that leave the momentum p invariant. By moving to a frame

$$p'^\mu = \Lambda^\mu_\nu p^\nu = \frac{E}{2}(1, 0, 0, 1), \quad (1.40)$$

we identify the little group transformations as those that in the new frame rotate components $(p')^1$ and $(p')^2$. The little group for a massless particle is therefore $U(1)$. The scale invariance in the definition of spinors $\langle p|$, $[p]$ is the manifestation of this invariance.

Note that for real momenta, $\langle p|$ and $[p]$ are linked by complex conjugation; the transformations are therefore limited to be purely phases, *i.e.* $a = e^{i\phi}$. If the momenta are complex, the spinors are independent of each other, and we have $a \in \mathbb{C}$.

Finally we note that the polarization vectors of gauge bosons can also be expressed in terms of spinors [49],

$$\varepsilon_+^\mu(p; q) = -\frac{1}{\sqrt{2}} \frac{[p|\gamma^\mu|q\rangle}{\langle pq\rangle}, \quad \varepsilon_-^\mu(p; q) = \frac{1}{\sqrt{2}} \frac{\langle p|\gamma^\mu|q\rangle}{[pq]}, \quad (1.41)$$

where we have to introduce an arbitrary massless reference momentum q . These definitions satisfy the usual conditions of polarization vectors for circular polarizations, namely¹

$$\varepsilon(p) \cdot p = 0, \quad \varepsilon_+ \cdot \varepsilon_- = -1. \quad (1.42)$$

1.2.1 Amplitudes and Spinors

In the discussion of the spinor-helicity formalism we saw that spinors are only defined up to a rescaling, as the associated momentum is invariant under opposite scaling of both angle and bracket spinors. Such scaling has direct ramifications for scattering amplitudes. While kinematic factors such as Mandelstam invariants s_{ij} are constant under such scaling, the polarization vectors or spinors of external gluons or fermions are not. Let us rescale the spinors of momentum p as previously shown,

$$\begin{pmatrix} \langle p| \\ [p] \end{pmatrix} \longrightarrow \begin{pmatrix} a \langle p| \\ \frac{1}{a} [p] \end{pmatrix}. \quad (1.43)$$

¹While the relative sign of ε_+ and ε_- is fixed by the condition that $\varepsilon_+ \cdot \varepsilon_- = -1$, the absolute sign is a Feynman rule convention. We could equivalently choose the opposite signs in eq. (1.41), as long as we also flip the sign of the three-gluon Feynman vertex.

Positive-helicity fermions are associated to bracket spinors, while negative helicity ones are associated to angle spinors. Fermionic amplitudes will therefore scale as

$$\begin{aligned} A(\dots p_f^{+\frac{1}{2}} \dots) &= [p]_{\dot{b}} \mathcal{M}^{\dot{b}}(\dots p_f \dots) \rightarrow \frac{1}{a} A(\dots p_f^{+\frac{1}{2}} \dots), \\ A(\dots p_f^{-\frac{1}{2}} \dots) &= \langle p \rangle^{\dot{b}} \mathcal{M}_{\dot{b}}(\dots p_f \dots) \rightarrow a A(\dots p_f^{-\frac{1}{2}} \dots). \end{aligned} \quad (1.44)$$

Similarly, by expressing gluon polarization vectors in terms of spinors, we find that gluon amplitudes scale as follows,

$$A(\dots p_g^{\pm} \dots) = \varepsilon_{\mu}^{\pm}(p) \mathcal{M}^{\mu}(\dots p_g \dots) \rightarrow \begin{cases} \frac{1}{a^2} A(\dots p_g^{+} \dots), \\ a^2 A(\dots p_g^{-} \dots). \end{cases} \quad (1.45)$$

This scaling behavior generalizes to particles with arbitrary helicity h [47],

$$A(\dots p^h \dots) \rightarrow a^{-2h} A(\dots p^h \dots). \quad (1.46)$$

This scaling property provides constraints on the final form of the amplitude. For one, it is a useful cross-check during the computation of amplitudes. Furthermore, in the case of tree-level amplitudes of three gluons,

$$A^{(0)}(1^{h_1} 2^{h_2} 3^{h_3}), \quad (1.47)$$

requiring the correct scaling behavior under little group transformations is sufficient to fix the form of the amplitude entirely. Normally, such amplitudes of three massless particles are forbidden by on-shell kinematics. However, this is only true for real kinematics. For complex momenta these amplitudes are well defined. As we will see shortly, they are a useful building block to recursively construct more complicated amplitudes.

Let us see how the form of these three-particle amplitudes in the case of gluons can be derived using only scaling arguments. We follow here the procedure of refs. [47, 50, 51]. Ref. [51] also provides a more general discussion of bootstrapping scattering amplitudes based on physical constraints. First we realize that for non-zero momenta, all spinors $\langle i|$ and $[i]$ need to be non-zero. Using momentum conservation we further see that all angle and bracket spinor products need to be proportional to one another, as for example

$$\begin{aligned} \langle 12 \rangle &= \langle 12 \rangle \frac{[2q]}{[2q]} = - \langle 13 \rangle \frac{[3q]}{[1q]}, \\ [12] &= [12] \frac{\langle 2q \rangle}{\langle 2q \rangle} = - [13] \frac{\langle 3q \rangle}{\langle 1q \rangle}. \end{aligned} \quad (1.48)$$

Similar relations hold for $\langle 13 \rangle$, $[13]$, $\langle 23 \rangle$ and $[23]$. Here we use the spinors $\langle q|$ and $[q]$ of some arbitrary massless reference momentum q , which we explicitly choose to be neither p_1 , p_2 or p_3 . Momentum conservation further requires that

$$\begin{aligned} (p_1 + p_2)^2 = p_3^2 = 0 &\Rightarrow \langle 12 \rangle [21] = 0 \\ (p_1 + p_3)^2 = p_2^2 = 0 &\Rightarrow \langle 13 \rangle [31] = 0 \\ (p_2 + p_3)^2 = p_1^2 = 0 &\Rightarrow \langle 23 \rangle [32] = 0 \end{aligned} \quad (1.49)$$

As the spinors are assumed to be non-zero and the spinor products are proportional to one another,

all three relations can only be fulfilled if either all angle or all bracket spinor products vanish. A non-trivial amplitude that only depends on three massless momenta therefore can only contain either angle *or* bracket spinor products. As angle and bracket spinors are each other's complex conjugate for real momenta, a gluonic three-point amplitude therefore can only be non-zero for complex momenta. In this case angle and bracket spinors are independent.

Using this knowledge, let us write down an Ansatz for the spinor structure of the three-gluon tree amplitude with two negative helicities and one positive helicity. We make the assumption that all bracket spinors vanish, such that the most general form for this amplitude is,

$$A^{(0)}(1^-2^-3^+) \propto \langle 12 \rangle^{x_1} \langle 13 \rangle^{x_2} \langle 23 \rangle^{x_3}, \quad (1.50)$$

where the proportionality factor does not depend on the kinematics. We can now use the little-group scaling of this amplitude to solve for the exponents x_1 , x_2 and x_3 . Under scaling of $\langle 1|$, we require that,

$$a^2 A^{(0)}(1^-2^-3^+) = a^{x_1+x_2} A^{(0)}(1^-2^-3^+) \quad (1.51)$$

such that,

$$x_1 + x_2 = -2. \quad (1.52)$$

Scaling $\langle 2|$ and $\langle 3|$ in the same manner leads us to the system of equations

$$\begin{aligned} x_1 + x_2 &= 2, \\ x_1 + x_3 &= 2, \\ x_2 + x_3 &= -2, \end{aligned} \quad (1.53)$$

which has the solution

$$x_1 = 3, \quad x_2 = -1, \quad x_3 = -1. \quad (1.54)$$

The expected form of this amplitude is therefore

$$A(1^-2^-3^+) \propto \frac{\langle 12 \rangle^3}{\langle 23 \rangle \langle 13 \rangle}, \quad (1.55)$$

which agrees with the form of the Parke–Taylor amplitude shown in eq. (1.60) below. By assuming all angle spinor products to vanish, we similarly determine,

$$A(1^+2^+3^-) \propto \frac{[12]^3}{[23][13]}, \quad (1.56)$$

A diagrammatic computation agrees with these kinematic structures, and allows us to determine the prefactors. We find from color ordered Feynman rules,

$$\begin{aligned} A^{(0)}(1^-2^-3^+) &= \frac{\langle 12 \rangle^3}{\langle 23 \rangle \langle 31 \rangle}, \\ A^{(0)}(1^+2^+3^-) &= -\frac{[12]^3}{[23][31]}, \end{aligned} \quad (1.57)$$

Note that these are so-called color-ordered amplitudes, which have been stripped of any color

structures and couplings. We will discuss such amplitudes in the next section. Aside from the three-gluon case, tree amplitudes vanish unless at least two helicities differ from the rest, such that

$$A^{(0)}(1^\pm 2^+ \dots n^+) = A^{(0)}(1^\mp 2^- \dots n^-) = 0. \quad (1.58)$$

In appendix A.1 we review an argument for this vanishing based on making suitable choices for gluon reference momenta.

The first non-vanishing helicity configuration $A(1^- 2^- 3^+ \dots n^+)$ is called the MHV, or maximally helicity violating, amplitude [52, 53]. An additional negative helicity yields the NMHV, or next-to-maximally helicity violating, amplitude. This principle generalizes to N^k MHV amplitudes. If all helicities are flipped, they are often called the anti-MHV/ N^k MHV, or $\overline{\text{MHV}}/\overline{N^k\text{MHV}}$ amplitudes.

Note, that the vanishing of the amplitudes in eq. (1.58) holds only at tree level in non-supersymmetric theories. In fact, Yang–Mills all-plus amplitudes at loop level have an interesting structure, and are the main focus of this thesis.

1.3 Tree-Amplitudes

Tree amplitudes are the natural starting point in the discussion of scattering amplitudes and the use of on-shell methods in their computation. Even in the absence of loops there exist rich structures to be explored. In addition, tree amplitudes ultimately form the basis from which we will construct loop amplitudes.

We define tree amplitudes as

$$\mathcal{A}^{(0)} = (-i) \times \text{sum of tree-level Feynman diagrams}. \quad (1.59)$$

The included normalization of $(-i)$ ensures that the amplitude expression will be free of factors of i . A common observation in the Feynman diagrammatic computation of gauge-theory amplitudes is the appearance of large intermediate expressions. At the same time, the final result is usually expressible in a considerably more compact form. A famous example is the Parke–Taylor amplitude, describing the interaction of two gluons of negative helicity with the rest having positive helicity. The general form of this amplitude was first presented in ref. [52], and later proven in ref. [54]. Expressed in terms of spinors products,

$$A^{(0)}(1^+ 2^+ \dots i^- \dots j^- \dots (n-1)^+ n^+) = \frac{\langle ij \rangle^4}{\langle 12 \rangle \langle 23 \rangle \dots \langle (n-1)n \rangle \langle n1 \rangle}. \quad (1.60)$$

This suggests that Feynman diagrams are not always the ideal approach to computing amplitudes, and that other methods should exist to obtain the compact result in a more direct manner. One significant source of complexity in amplitudes of gauge theory is gauge redundancy. While the final on-shell amplitude may be gauge invariant, the individual Feynman diagrams are not. We therefore require non-trivial cancellations to occur between the diagrams to obtain a manifestly gauge invariant quantity. At this point on-shell methods come to our rescue. They allow us to construct on-shell amplitudes from lower-point on-shell amplitudes. Each step is therefore manifestly gauge-invariant, and we are able to derive compact gauge invariant expressions with

relative ease. In the following we will review common techniques used in the computation of tree amplitudes, which will be important for the later chapters of this thesis.

1.3.1 Tree-Level Color-Decomposition

The first complication when dealing with amplitudes in gauge theory is the fact that particles transform in representations of the gauge group. Such amplitudes are therefore a mixture of kinematic and group theory structures, which generally need to be manipulated simultaneously. In QCD the latter are related to the particles' color charge. Therefore, even in general $SU(N_c)$ Yang–Mills theories these group structures are often referred to as color structures.

A useful technique to separate the two classes is the color decomposition of gauge theory amplitudes. Color decomposition relies on finding a basis of independent color structures, in which the amplitudes gauge-group dependence can be encoded. The coefficients of these basis elements are then dependent only on the external kinematics, and can be obtained directly from special “color-ordered” Feynman rules. There are various options for choosing such a basis [55, 56], however a common choice is the set of color traces

$$\left\{ \text{Tr}(T^{a_{\sigma(1)}} T^{a_{\sigma(2)}} \dots T^{a_{\sigma(n)}}) \mid \sigma \in S_n / C_n \right\} \quad (1.61)$$

where S_n is the symmetric group of n elements, and C_n the cyclic group. We only need to consider the quotient group of the two due to the cyclic symmetry of the traces. Given such a basis of color traces, we are able to express any tree-amplitude in the form,

$$\begin{aligned} \mathcal{A}_n^{(0)}(1^{h_1, a_1}, 2^{h_2, a_2}, \dots, n^{h_n, a_n}) \\ = g^{n-2} \sum_{\sigma \in S_n / C_n} \text{Tr}(T^{a_{\sigma(1)}} \dots T^{a_{\sigma(n)}}) A_n^{(0)}(\sigma(1^{h_1}), \dots, \sigma(n^{h_n})). \end{aligned} \quad (1.62)$$

Here, $\mathcal{A}_n^{(0)}$ is the amplitude obtained from the usual Feynman rules involving color structures, sometimes also referred to as the “full-color” amplitude. The $A_n^{(0)}$ are called partial-, or color-ordered amplitudes, and only depend on the momenta and helicities of the external momenta. The name “color-ordered” derives from the fact that we can compute the $A_n^{(0)}$ based on Feynman diagrams which are planar, such that the relative order of the particles is fixed. The planarity of the diagrams contributing to $A^{(0)}$ is a feature of tree-level amplitudes, and does not hold at loop level. However, the color-trace organisation will still be present.

A convenient feature of partial amplitudes is their invariance under gauge transformations. As $\mathcal{A}^{(0)}$ is an on-shell quantity, it has to be invariant under such transformations. Gauge transformations do not mix the color traces. Therefore, for $\mathcal{A}^{(0)}$ to be invariant under the residual on-shell gauge transformations, cancellations need to occur for each coefficient separately. The $A_n^{(0)}$ therefore need to be separately gauge-invariant objects.

As an example, consider the four-gluon amplitude

$$\mathcal{A}(1^{h_1, a} 2^{h_2, b} 3^{h_3, c} 4^{h_4, d}) = \text{diagram 1} + \text{diagram 2} + \text{diagram 3} + \text{diagram 4} \quad (1.63)$$

Focusing just on their color structure, these diagrams give the contributions²

$$\begin{aligned}
& \text{Diagram 1: } \begin{array}{c} 2 \quad b \quad c \quad 3 \\ \diagdown \quad \diagup \\ e \\ \diagup \quad \diagdown \\ 1 \quad a \quad d \quad 4 \end{array} = g^2 2 f^{abe} f^{cde} G_1, \\
& \text{Diagram 2: } \begin{array}{c} 2 \quad b \quad c \quad 3 \\ \diagdown \quad \diagup \\ e \\ \diagup \quad \diagdown \\ 1 \quad a \quad d \quad 4 \end{array} = g^2 2 f^{aed} f^{bce} G_2, \\
& \text{Diagram 3: } \begin{array}{c} 2 \quad b \quad c \quad 3 \\ \diagdown \quad \diagup \\ e \\ \diagup \quad \diagdown \\ 1 \quad a \quad d \quad 4 \end{array} = g^2 2 f^{aec} f^{bde} G_3, \\
& \text{Diagram 4: } \begin{array}{c} 2 \quad b \quad c \quad 3 \\ \diagdown \quad \diagup \\ \diagup \quad \diagdown \\ 1 \quad a \quad d \quad 4 \end{array} = g^2 2 (f^{abe} f^{cde} G_{4,1} + f^{ace} f^{bde} G_{4,2} + f^{ade} f^{bce} G_{4,3}),
\end{aligned} \tag{1.64}$$

where the G_i depend only on the kinematics. For simplicity, we assume the gauge group to be $U(N)$. We expect a basis of $|S_4/C_4| = \frac{4!}{4} = 6$ color traces,

$$\text{Tr}(T^a T^b T^c T^d), \quad \text{Tr}(T^a T^c T^d T^b), \quad \text{Tr}(T^a T^d T^b T^c), \tag{1.65}$$

$$\text{Tr}(T^a T^b T^d T^c), \quad \text{Tr}(T^a T^d T^c T^b), \quad \text{Tr}(T^a T^c T^b T^d), \tag{1.66}$$

such that,

$$\begin{aligned}
\mathcal{A}^{(0)}(1^{h_1,a} 2^{h_2,b} 3^{h_3,c} 4^{h_4,d}) = g^2 & \left[\text{Tr}(T^a T^b T^c T^d) A^{(0)}(1^{h_1} 2^{h_2} 3^{h_3} 4^{h_4}) \right. \\
& + \text{Tr}(T^a T^c T^d T^b) A^{(0)}(1^{h_1} 3^{h_3} 4^{h_4} 2^{h_2}) \\
& + \text{Tr}(T^a T^d T^b T^c) A^{(0)}(1^{h_1} 4^{h_4} 2^{h_2} 3^{h_3}) \\
& + \text{Tr}(T^a T^b T^d T^c) A^{(0)}(1^{h_1} 2^{h_2} 4^{h_4} 3^{h_3}) \\
& + \text{Tr}(T^a T^d T^c T^b) A^{(0)}(1^{h_1} 4^{h_4} 3^{h_3} 2^{h_2}) \\
& \left. + \text{Tr}(T^a T^c T^b T^d) A^{(0)}(1^{h_1} 3^{h_3} 2^{h_2} 4^{h_4}) \right].
\end{aligned} \tag{1.67}$$

We can use the relation of eq. (1.3) as well as the Fierz identities (1.7) to rewrite the color factor of the first diagram as

$$\begin{aligned}
2f^{abe} f^{cde} &= -[\text{Tr}(T^a T^b T^e) - \text{Tr}(T^b T^a T^e)] [\text{Tr}(T^c T^d T^e) - \text{Tr}(T^d T^c T^e)] \\
&= -\text{Tr}(T^a T^b T^c T^d) + \text{Tr}(T^a T^b T^d T^c) + \text{Tr}(T^a T^c T^d T^b) - \text{Tr}(T^a T^d T^c T^b)
\end{aligned} \tag{1.68}$$

Repeating these steps for the remaining three diagrams, and collecting on the six color traces leads

²We also pull out a factor of 2 due to the choice of normalization for the gauge group generators in eq. (1.1)

us to the partial amplitudes,

$$\begin{aligned}
A^{(0)}(1^{h_1} 2^{h_2} 3^{h_3} 4^{h_4}) &= -G_1 - G_2 - G_{4,1} + G_{4,3} \\
A^{(0)}(1^{h_1} 4^{h_4} 2^{h_2} 3^{h_3}) &= G_1 - G_3 + G_{4,1} + G_{4,2} \\
A^{(0)}(1^{h_1} 2^{h_2} 4^{h_4} 3^{h_3}) &= G_2 + G_3 - G_{4,2} - G_{4,3} \\
A^{(0)}(1^{h_1} 3^{h_3} 2^{h_2} 4^{h_4}) &= G_1 - G_3 + G_{4,1} + G_{4,2} \\
A^{(0)}(1^{h_1} 4^{h_4} 3^{h_3} 2^{h_2}) &= -G_1 - G_2 - G_{4,1} + G_{4,3} \\
A^{(0)}(1^{h_1} 3^{h_3} 4^{h_4} 2^{h_2}) &= G_2 + G_3 - G_{4,2} - G_{4,3}.
\end{aligned} \tag{1.69}$$

At first glance this representation appears more complicated. However, there exist Feynman rules that allow us to obtain these partial amplitudes directly, namely

$$\begin{aligned}
\begin{array}{c} \text{Diagram 1: } 1^{\mu_1} \text{ --- } \text{Y-junction} \begin{array}{l} \nearrow 2^{\mu_2} \\ \searrow 3^{\mu_3} \end{array} \end{array} &= \frac{i}{\sqrt{2}} [g^{\mu_1 \mu_2} (p_1 - p_2)^{\mu_3} + g^{\mu_2 \mu_3} (p_2 - p_3)^{\mu_1} + g^{\mu_3 \mu_1} (p_3 - p_1)^{\mu_2}], \\
\begin{array}{c} \text{Diagram 2: } 2^{\mu_2} \text{ --- } \text{X-junction} \begin{array}{l} \nwarrow 1^{\mu_1} \\ \nearrow 4^{\mu_4} \end{array} \end{array} &= i \left[g^{\mu_1 \mu_3} g^{\mu_2 \mu_4} - \frac{1}{2} (g^{\mu_1 \mu_2} g^{\mu_3 \mu_4} + g^{\mu_2 \mu_3} g^{\mu_4 \mu_1}) \right], \\
\text{Diagram 3: } p^\mu \text{ --- } p^\nu &= \frac{-i}{p^2 + i0}.
\end{aligned} \tag{1.70}$$

With these, each of the partial amplitudes is given by the sum of three color-ordered Feynman diagrams,

$$A^{(0)}(1^{h_1} 2^{h_2} 3^{h_3} 4^{h_4}) = \begin{array}{c} \text{Diagram 1: } 1 \text{ --- } \text{Y-junction} \begin{array}{l} \nearrow 2 \\ \searrow 3 \end{array} \end{array} + \begin{array}{c} \text{Diagram 2: } 1 \text{ --- } \text{Y-junction} \begin{array}{l} \nearrow 3 \\ \searrow 2 \end{array} \end{array} + \begin{array}{c} \text{Diagram 3: } 1 \text{ --- } \text{X-junction} \begin{array}{l} \nwarrow 2 \\ \nearrow 3 \end{array} \end{array}. \tag{1.71}$$

While the color traces are independent of one another, the same cannot be said about the partial amplitudes. An important class of relations between the partial amplitudes are the U(1)-, or photon-decoupling identities. To derive them we consider amplitudes of a Yang–Mills theory with gauge group $U(N_c)$. As mentioned in section 1.1 we can separate the generators of the group $U(N_c)$ into those of $SU(N_c)$, together with a generator of $U(1)$ which corresponds to the trace. Analogously we can also separate the gauge bosons of $U(N_c)$ Yang–Mills theory according to these two subgroups. We will refer to the gauge bosons of $SU(N_c)$ as gluons and to the one of $U(1)$ as photon. The U(1)-decoupling identities rely on the observation that any mixed gluon-photon amplitude has to vanish. One naïve argument can be made on the basis of the Yang–Mills field strength tensor

$$F_{\mu\nu}^a = \partial_\mu A_\nu^a - \partial_\nu A_\mu^a + g f^{abc} A^b A^c. \tag{1.72}$$

The third term is the one of interest, as it generates the gauge boson self-interactions. In the case of photon-gluon interactions, one of the indices of the structure constant f^{abc} is associated with the photon generator. As this generator has to be proportional to the identity $\mathbb{1}_{N_c}$, such a structure function is guaranteed to vanish, which can be seen via the relation (1.3). Thus, photons and

gluons cannot interact with one another, and any amplitudes that involves even a single photon has to vanish.

We can further see that the partial amplitudes have to be the same in both $U(N_c)$ and $SU(N_c)$ Yang–Mills theories. Due to the Feynman rules being the same, we could carry out the color decomposition entirely oblivious of the fact that photon structure constants vanish. We would therefore necessarily end up with the same kinematic structures, *i.e.* partial amplitudes.

At tree level, instead of computing $U(N_c)$ and $SU(N_c)$ amplitudes separately, we can start from the color decomposed $SU(N_c)$ amplitude involving only gluons. To transform a gluon into a photon we exchange the corresponding generator with the $U(1)$ generator. As this generator is proportional to the identity, it can always be removed from the traces, such that multiple partial amplitudes end up with the same color structure. The vanishing of the full amplitude therefore leads to linear relations between these partial amplitudes.

As an example, consider our previous four-gluon amplitude,

$$\mathcal{A}(1_g^{h_1,a} 2_g^{h_2,b} 3_g^{h_3,c} 4_g^{h_4,d}). \quad (1.73)$$

We now turn gluon 1 into a photon by replacing its generator T^a in the color decomposition with $\frac{1}{\sqrt{N_c}} \mathbb{1}_{N_c}$. Rearranging the terms in eq. (1.67) then leads to,

$$\begin{aligned} 0 = \mathcal{A}^{(0)}(1_\gamma^{h_1} 2_g^{h_2,b} 3_g^{h_3,c} 4_g^{h_4,d}) = \\ \frac{g^2}{\sqrt{N_c}} \left[\text{Tr}(T^b T^c T^d) \left(A^{(0)}(1^{h_1} 2^{h_2} 3^{h_3} 4^{h_4}) + A^{(0)}(1^{h_1} 3^{h_3} 4^{h_4} 2^{h_2}) + A^{(0)}(1^{h_1} 4^{h_4} 2^{h_2} 3^{h_3}) \right) \right. \\ \left. + \text{Tr}(T^b T^d T^c) \left(A^{(0)}(1^{h_1} 2^{h_2} 4^{h_4} 3^{h_3}) + A^{(0)}(1^{h_1} 4^{h_4} 3^{h_3} 2^{h_2}) + A^{(0)}(1^{h_1} 3^{h_3} 2^{h_2} 4^{h_4}) \right) \right]. \end{aligned} \quad (1.74)$$

As the color structures are independent, we obtain the two relations,

$$\begin{aligned} 0 &= A^{(0)}(1^{h_1} 2^{h_2} 3^{h_3} 4^{h_4}) + A^{(0)}(1^{h_1} 3^{h_3} 4^{h_4} 2^{h_2}) + A^{(0)}(1^{h_1} 4^{h_4} 2^{h_2} 3^{h_3}), \\ 0 &= A^{(0)}(1^{h_1} 2^{h_2} 4^{h_4} 3^{h_3}) + A^{(0)}(1^{h_1} 4^{h_4} 3^{h_3} 2^{h_2}) + A^{(0)}(1^{h_1} 3^{h_3} 2^{h_2} 4^{h_4}). \end{aligned} \quad (1.75)$$

This procedure generalizes, and the tree-level $U(1)$ -decoupling relations can be summarized as,

$$0 = A^{(0)}(1_\gamma 2_g 3_g \dots n_g) + A^{(0)}(2_g 1_\gamma 3_g \dots n_g) + \dots + A^{(0)}(2_g 3_g \dots 1_\gamma n_g) \quad (1.76)$$

and permutations thereof. At loop level, the $U(1)$ -decoupling lead to important relations between partial amplitudes, which we discuss in later sections.

Another class of relations between the tree-level partial amplitudes are the Kleiss–Kuijf relations [57]. These can be concisely summarized as [47],

$$A^{(0)}(1, \{\alpha\}, i, \{\beta\}) = (-1)^{|\beta|} \sum_{\sigma \in (\{\alpha\} \sqcup \{\beta\}^T)} A^{(0)}(1, \sigma, i), \quad (1.77)$$

where $\{\beta\}^T$ is the set $\{\beta\}$ in reversed order. The symbol \sqcup refers to the shuffle product, defined as all mergers of the sets that preserve the ordering within each set. Note that at tree level, the $U(1)$ decoupling identities are included in the Kleiss–Kuijf relations.

1.3.2 BCFW Recursion

A common technique in the on-shell approach to tree amplitudes is complex recursion [58, 59]. A tree-level amplitudes factorize into smaller amplitudes when internal propagators go on-shell, and we can exploit this property to recursively construct gauge-theory amplitudes in many cases.

The main feature of scattering amplitudes enabling this approach is their analyticity in the kinematics. At tree level this is evident, as they are rational functions in momenta and spinors. To understand the basic idea, let us consider a tree amplitude $A^{(0)}$ involving n massless particles with momenta p_k . By shifting the momenta by terms proportional to a—generally complex—parameter z , the amplitude becomes an analytic function in z , which we call $A^{(0)}(z)$. As we only shifted the momenta, we recover the original amplitude in the limit of vanishing z , *i.e.*

$$A^{(0)}(0) = A^{(0)}. \quad (1.78)$$

As $A^{(0)}(z)$ is an analytic function we can alternatively express this property via a contour integral. Choosing a contour γ that only encircles $z = 0$, while avoiding any other poles, we find that

$$\int_{\gamma} dz \frac{A^{(0)}(z)}{z} = (2\pi i) \operatorname{Res}_{z=0} \left[\frac{A^{(0)}(z)}{z} \right] = (2\pi i) A^{(0)}(0) = (2\pi i) A^{(0)}. \quad (1.79)$$

Let us expand the contour to infinity. We now have to acknowledge the fact that $A^{(0)}(z)$ contains poles as well: Through the shifted momenta, a subset of propagators will depend on z . For each such propagator we can find a value of z , so that the propagator becomes on-shell. The value of z , for which $A^{(0)}(z)$ develops a pole due to a propagator $1/(p_i + p_j + \dots p_k)^2$, will be denoted by $z_{ij\dots k}$. As we expand the contour we have to account for every such pole in z that we cross by subtracting the associated residue. We therefore end up with

$$\int_{\gamma} dz \frac{A^{(0)}(z)}{z} = -(2\pi i) \sum_{\substack{\text{poles} \\ z_{ij\dots k}}} \operatorname{Res}_{z=z_{ij\dots k}} \left[\frac{A^{(0)}(z)}{z} \right] + \int_{\gamma_{\infty}} dz \frac{A^{(0)}(z)}{z}. \quad (1.80)$$

In the last term, the contour γ_{∞} encircles the point at complex infinity, and it is this integral that could spoil our computation. While the residues at finite values of z are associated to on-shell propagators, a pole at infinity does not immediately allow for such an interpretation. There exist methods to obtain such contributions from multiple different shifts [60]. However for simplicity we assume here that under the specific shift we chose, the amplitude $A^{(0)}(z)$ falls off as $1/z$ in the large- z limit. In this case we can safely ignore the last integral. Combining eqs.(1.79) and (1.80), we are therefore able to relate the amplitude $A^{(0)}$ to the poles of $A^{(0)}(z)$ via

$$A^{(0)} = - \sum_{\substack{\text{poles} \\ z_{ij\dots k}}} \operatorname{Res}_{z=z_{ij\dots k}} \left[\frac{A^{(0)}(z)}{z} \right] \quad (1.81)$$

To relate the residues to the factorization of tree amplitudes, we will consider a specific choice of shift, presented in [58, 59]. Given a set of massless momenta p_k , $k = 1 \dots n$, we define a so-called

BCFW $[i, j]$ -shift of these momenta by introducing hatted set of momenta \hat{p}_k ,

$$\begin{aligned}\hat{p}_i^\mu &= p_i - \frac{z}{2} \langle i | \gamma^\mu | j \rangle \\ \hat{p}_j^\mu &= p_j + \frac{z}{2} \langle i | \gamma^\mu | j \rangle \\ \hat{p}_k &= p_k, \quad k \neq i, j\end{aligned}\tag{1.82}$$

where the spinors of p_i, p_j are given by

$$\begin{aligned}\hat{\lambda}_i &= \lambda_i, \quad \hat{\tilde{\lambda}}_i = \tilde{\lambda}_i - z \tilde{\lambda}_j \\ \hat{\tilde{\lambda}}_j &= \tilde{\lambda}_j, \quad \hat{\lambda}_j = \lambda_j + z \lambda_j.\end{aligned}\tag{1.83}$$

We introduce the parameter z , generally assumed to be complex, which causes the hatted momenta to be complex as well. The \hat{p}_k defined in such a way are again massless, conserve total momentum, and fulfill the properties

$$\hat{p}_i \cdot \hat{p}_j = p_i \cdot p_j, \quad \langle \hat{i} \hat{j} \rangle = \langle ij \rangle, \quad [\hat{i} \hat{j}] = [ij].\tag{1.84}$$

These properties will help in improving the large- z behavior of $A^{(0)}$. We now need to identify the propagators that develop poles in z under this shift. Since

$$\hat{p}_i + \hat{p}_j = p_i + p_j\tag{1.85}$$

the only z -dependent propagators are those involving *either* \hat{p}_i or \hat{p}_j . As the two cases are related by momentum conservation, let us focus on a propagator carrying \hat{p}_i , with the remaining momenta collected in Q . Extracting the pole in z , we obtain

$$\begin{aligned}\frac{1}{(\hat{p}_i + Q)^2} &= \frac{1}{(p_i + Q)^2 - z \langle i | Q | j \rangle} \\ &= -\frac{1}{\langle i | Q | j \rangle} \left[z - \frac{\langle i | Q | i \rangle}{\langle i | Q | j \rangle} \right]^{-1} \\ &= -\frac{z_{iQ}}{(p_i + Q)^2} \frac{1}{z - z_{iQ}}\end{aligned}\tag{1.86}$$

Taking the residue of $A^{(0)}(1 \dots \hat{i} \dots \hat{j} \dots n)$ at z_{iQ} thus sets this internal propagator on-shell, and replaces its denominator with $-\frac{z_{iQ}}{(p_i + Q)^2}$. In the case of the propagator belonging to a gluon, we additionally have to deal with a non-trivial numerator. Here the completeness relation of gluon polarization vectors comes to our aid. It ensures that if a gluon propagator goes on-shell, the propagator's numerator turns into the sum over polarization vectors. This is simplest to see in axial gauge, where the propagator takes the form³

$$\text{prop}_g^{\mu\nu}(p) = \frac{i}{p^2} \left(-g^{\mu\nu} + \frac{2p^{(\mu} q^{\nu)}}{2p \cdot q} \right),\tag{1.87}$$

³Here we are using the symmetrization over indices $p^{(\mu} q^{\nu)} = \frac{1}{2}(p^\mu q^\nu + p^\nu q^\mu)$.

By using the definition of the polarization vectors in eq. (1.41), we have

$$\begin{aligned}
\sum_{h=\pm} \varepsilon_h^\mu \varepsilon_h^\nu &= \varepsilon_+^\mu \varepsilon_-^\nu + \varepsilon_-^\mu \varepsilon_+^\nu \\
&= + \frac{1}{2} \frac{\langle p | \gamma^{(\mu} q \gamma^{\nu)} | p \rangle}{2p \cdot q} \\
&= \frac{1}{4p \cdot q} \left(2q^{(\nu} \langle p | \gamma^{\mu)} | p \rangle - \langle p | \gamma^{(\mu} \gamma^{\nu)} q | p \rangle \right) \\
&= \frac{1}{4p \cdot q} \left(4q^{(\mu} p^{\nu)} - 2g^{\mu\nu} 2p \cdot q \right) \\
&= -g^{\mu\nu} + \frac{2q^{(\mu} p^{\nu)}}{2p \cdot q}.
\end{aligned} \tag{1.88}$$

As we end up with on-shell quantities the choice of gauge is irrelevant, and we can use this identification generally. When computing the residue, gluon propagator therefore turns into

$$\text{prop}_g^{\mu\nu}(\hat{p}_i + Q) \xrightarrow{\text{Res}_{z=z_i Q}} -i \frac{z_i Q}{(p_i + Q)^2} \sum_{h=\pm} \varepsilon_h^\mu \varepsilon_h^\nu \tag{1.89}$$

At the level of the amplitude, the evaluation of the residue therefore leads to

$$\begin{aligned}
&- \text{Res}_{z=z_i Q} \left[\frac{A^{(0)}(1 \dots \hat{i} \dots \hat{j} \dots n)}{z} \right] \\
&= - \sum_{h=\pm} \left[A^{(0)}(\dots \hat{i} \dots (-\hat{p}_i - Q)^{\bar{h}}) \frac{1}{(p_i + Q)^2} A^{(0)}((\hat{p}_i + Q)^h \dots \hat{j} \dots) \right] \Big|_{z=z_i Q}
\end{aligned} \tag{1.90}$$

Note that the overall minus sign is due to the normalization of $(-i)$ which we include in every amplitude. In computations we will often omit the explicit value of z at which we need to evaluate the product of trees, though it is always implied. The factorization channel will always be evident through the propagator-like factor.

A famous illustration of the power of complex recursion is the proof of the Parke-Taylor amplitude [52],

$$A^{(0)}(1^+ \dots i^- \dots j^- \dots n^+) = \frac{\langle ij \rangle^4}{\langle 12 \rangle \dots \langle n1 \rangle} \tag{1.91}$$

This was first presented in ref. [59], and we will sketch the arguments here. The proof follows from induction. We already saw in eq. (1.57) that the form of eq. (1.91) applies for $n = 3$. We therefore only need to show the inductive step. We choose a BCFW $[i, i+1]$ -shift

$$\begin{aligned}
\hat{p}_i^\mu &= p_i^\mu - \frac{z}{2} \langle i | \gamma^\mu | i+1 \rangle \\
\hat{p}_{i+1}^\mu &= p_{i+1}^\mu + \frac{z}{2} \langle i | \gamma^\mu | i+1 \rangle
\end{aligned} \tag{1.92}$$

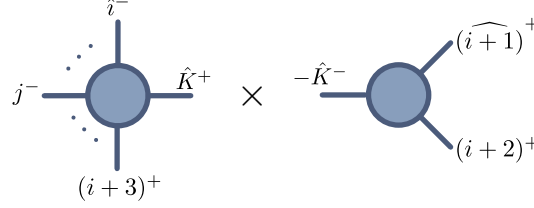
with spinors

$$\begin{aligned}
\hat{\lambda}_i &= \lambda_i, & \hat{\tilde{\lambda}}_i &= \tilde{\lambda}_i - z \tilde{\lambda}_{i+1} \\
\hat{\tilde{\lambda}}_{i+1} &= \tilde{\lambda}_{i+1}, & \hat{\lambda}_{i+1} &= \lambda_{i+1} + z \lambda_i.
\end{aligned} \tag{1.93}$$

Evaluating the general form in eq. (1.91) on the shifted kinematics, we see that the amplitude scales as $\frac{1}{z}$. We should therefore be able to reconstruct this amplitude from its poles at finite

values of z .

As single-minus tree amplitudes vanish except for the three-point case, the only factorization allowed is



$$(1.94)$$

or more precisely

$$\begin{aligned} A^{(0)}(1^+ \dots i^- \dots j^- \dots n^+) \\ = -\frac{1}{s_{(i+1)(i+2)}} A^{(0)}(1^+ \dots \hat{i}^- \hat{K}^+(i+3)^+ \dots j^- \dots n^+) A^{(0)}((- \hat{K})^- \widehat{(i+1)}^+ (i+2)^+) \end{aligned} \quad (1.95)$$

One of the tree amplitudes is the Parke–Taylor amplitude with one fewer positive helicity gluons, and we can therefore apply eq. (1.91) as the inductive assumption. The form of the second amplitude in the factorization is given in eq. (1.57). As one of the momenta is negative, we need to define spinors of a negative momentum. In this thesis we will always use the symmetric continuation

$$\langle -p| = i \langle p|, \quad [-p] = i [p]. \quad (1.96)$$

We can then evaluate eq. (1.95)

$$\begin{aligned} A^{(0)}(1^+ \dots i^- \dots j^- \dots n^+) \\ = -\frac{1}{s_{(i+1)(i+2)}} \frac{\langle ij \rangle^4}{\langle 12 \rangle \dots \langle (i-1)i \rangle \langle (i+3)(i+4) \rangle \dots \langle n1 \rangle} \frac{[(i+1)(i+2)]^3}{[\hat{K}(i+1)] [(i+2)\hat{K}] \langle i\hat{K} \rangle \langle \hat{K}(i+3) \rangle} \\ = \frac{\langle ij \rangle^4}{\langle 12 \rangle \dots \langle (i-1)i \rangle \langle (i+1)(i+2) \rangle \langle (i+3)(i+4) \rangle \dots \langle n1 \rangle} \frac{[(i+1)(i+2)]^2}{\langle (i+3)|\hat{K}|(i+1) \rangle [(i+2)|\hat{K}|i]} \\ = \frac{\langle ij \rangle^4}{\langle 12 \rangle \dots \langle (i-1)i \rangle \langle i(i+1) \rangle \langle (i+1)(i+2) \rangle \langle (i+2)(i+3) \rangle \langle (i+3)(i+4) \rangle \dots \langle n1 \rangle}, \end{aligned} \quad (1.97)$$

which is exactly the form expected from eq. (1.91), completing the proof. In this computation we never had to evaluate any spinors at the specific pole, as we were always able to eliminate any contributions of shifted momenta through spinor products involving $\langle i|$ and $[i+1]$. This is not possible in general, and the evaluation at the specific value of z usually leads to spurious denominators, which only cancel between multiple factorization channels.

1.4 Loop Amplitudes

As explained in the introduction, tree-level amplitudes are not sufficient to explain physical observations in experiments and it is necessary to include loop corrections. Here we will look at some general properties of loop amplitudes, as well as some basic methods used in their computation.

The characteristic feature of loop amplitudes are virtual particles that form closed loops in the Feynman diagrams. These loops carry an associated four-momentum, over which we need to

integrate. An L -loop amplitude can be written as [47],

$$\mathcal{A}_n^{(L)} = (-i)(4\pi)^{LD/2} \sum_{G_L} \int \left(\prod_{i=1}^L \frac{d^D \ell_i}{(2\pi)^D} \right) \frac{1}{S_{G_L}} \frac{c_{G_L} \mathcal{N}_{G_L}[\{p_j\}, \ell_i]}{\prod_{\alpha_{G_L} \in G_L} p_{\alpha_{G_L}}^2}. \quad (1.98)$$

The sum runs over all L -loop Feynman diagrams G_L , whose propagators are labelled by α_{G_L} . The numerators c_{G_L} and \mathcal{N}_{G_L} are respectively color and kinematic factors, and the $\frac{1}{S_{G_L}}$ provide possible symmetry factors, depending on the diagram topology. The $d^D \ell_i$ integrals run over the entire D -dimensional Minkowskian momentum space, where the dimension is left unspecified for the moment.

1.4.1 Feynman Integrals

The central feature of loop amplitudes are the integrations over the loop momentum. These integrals present one of the main challenges in pushing perturbation theory to higher orders, as their computation generally presents a formidable challenge. While one-loop integrals are well understood, two-loop integrals are still a topic of current research, and many advanced techniques have been developed over the past decades to aid in their computation.

As the computation of Feynman integrals has not been an integral part of my doctoral research, and due to the wide breadth of topics that would have to be covered, I will only present a brief overview.

Following the discussion in ref. [61], we will define the Feynman integral $\mathcal{I}_G^{(L),D}$ of an L -loop Feynman graph G with n external particles in D dimensions as

$$(2\pi)^D \delta^D \left(\sum_i p_i \right) \mathcal{I}_G^{(L),D} = \int \left(\prod_{i=1}^I \frac{d^D k_i}{(2\pi)^D} \frac{1}{(k_i^2 - m_i^2 + i\epsilon)} \right) \prod_{v=1}^V (2\pi)^D \delta^D \left(P_v - \sum_{i=1}^I \kappa_{iv} k_i \right) \quad (1.99)$$

The p_i , $i \in 1, \dots, n$ are the momenta of the external particles, while I and V denote the number of internal lines and vertices in the graph G . For each vertex v the momentum P_v is the sum of external momenta incident to that vertex. The incidence matrix κ_{iv} states whether the internal momentum k_i is flowing out of ($\kappa_{iv} = -1$), flowing into ($\kappa_{iv} = +1$) or not attached to the vertex v ($\kappa_{iv} = 0$). Note that in comparison to ref. [61] we are not including the factors of i in the propagators.

Using the identities [61],

$$\frac{1}{(q^2 - m^2 + i\epsilon)^\nu} = \frac{1}{\Gamma(\nu)} \int_0^\infty d\alpha \alpha^{\nu-1} \exp(-\alpha(q^2 - m^2 + i\epsilon)), \quad (1.100)$$

and,

$$(2\pi)^D \delta^{(D)} \left(P_v - \sum_{i=1}^I \kappa_{iv} k_i \right) = \int d^D y_v \exp \left[-iy_v \left(P_v - \sum_{i=1}^I \kappa_{iv} k_i \right) \right], \quad (1.101)$$

we can carry out the integrals over the internal momenta k_l , and obtain for $\mathcal{I}_G^{(L),D}$ the form [61],

$$\mathcal{I}_G^{(L),D} = \frac{(-1)^I}{i^L (4\pi)^{LD/2}} \Gamma(I - L \frac{D}{2}) \left(\prod_i \int_0^\infty d\alpha_i \right) \delta(1 - \sum_i \alpha_i) \frac{\mathcal{U}^{I-(L+1)D/2}}{\mathcal{F}^{I-LD/2}}. \quad (1.102)$$

ψ and φ are the first and second Symanzik polynomials, which are polynomials in the variables Schwinger parameters α_i . Their form can be related to the graph associated to the Feynman integral's propagators, as presented for example in ref. [62].

An important feature of Feynman integrals are their divergences. While we are mainly interested in the case $D = 4$, many integrals of interest diverge for this choice, and we need to regulate them. The most common method is dimensional regularization, in which we use $D = 4 - 2\epsilon$. By working in non-integer dimension, we are able to evaluate the integrals as a Laurent expansion in ϵ , where the divergences appear as powers of $\frac{1}{\epsilon}$. There are generally two classes of singularities that can appear in a Feynman integral: ultraviolet (UV) and infrared (IR).

As the name suggests, ultraviolet divergences originate from regions of large loop momentum in the integration. Consider for example the integral

$$\int d^D \ell \frac{1}{\ell^2 (\ell - K)^2} \quad (1.103)$$

For large ℓ the integral measure and integrand scale together as ℓ^{D-4} . This corresponds to a logarithmic divergence in $D = 4 - 2\epsilon$, which would appear as a $\frac{1}{\epsilon}$ pole in the regulated integral. The source of these divergences in the Schwinger parameter representation of eq. (1.102) is the prefactor $\Gamma(I - L \frac{D}{2})$ [62]. Substituting the appropriate values for our example integral, this prefactor takes the form

$$\Gamma\left(2 - \frac{4 - 2\epsilon}{2}\right) = \Gamma(\epsilon) = \frac{1}{\epsilon} - \gamma + \mathcal{O}(\epsilon) \quad (1.104)$$

where γ is the Euler-Mascheroni constant. Assuming a renormalizable theory like Yang-Mills, these divergences can always be absorbed into physical quantities through renormalization, as discussed in QFT textbooks, for example refs. [42–45].

The second type of singularity is called infrared, as such singularities occur in the regions of small, or at least finite loop momentum. There exist two types of IR singularities, namely soft and collinear, and in the integral representation of eq. (1.102) they originate from the integrals over the α_i . The Landau equations [63] rigorously specify the locations of these singularities. At one-loop they can also be understood from power counting arguments, which we will review here. These arguments were first first presented in ref. [64].

The soft divergences appear in the limit of vanishing loop momentum. Take for example the one-loop integral with four external massless momenta p_1, p_2, p_3, p_4 and four propagators

$$\int d^D \ell \frac{1}{\ell^2 (\ell - p_1)^2 (\ell - p_1 - p_2)^2 (\ell + p_4)^2} \quad (1.105)$$

For small ℓ , the measure scales as ℓ^D . The first propagator naturally behaves as ℓ^{-2} , while the third is finite as

$$\frac{1}{(\ell - p_1 - p_2)^2} = \frac{1}{\ell^2 - 2\ell \cdot (p_1 + p_2) + s_{12}} \stackrel{\ell \rightarrow 0}{\approx} \frac{1}{s_{12}} \quad (1.106)$$

The second and fourth propagators on the other hand scale as ℓ^{-1} , as for example

$$\frac{1}{(\ell - p_1)^2} = \frac{1}{\ell^2 - 2\ell \cdot p_1} \stackrel{\ell \rightarrow 0}{\approx} -\frac{1}{2\ell \cdot p_1} \quad (1.107)$$

The entire integral therefore scales as $(\frac{1}{\ell})^{4-D}$. It therefore has a logarithmic singularity, which appears as a $\frac{1}{\epsilon}$ pole in the dimensionally regulated integral.

Collinear singularities originate from finite regions of the loop momentum integration, where ℓ becomes proportional to a massless external momentum. Below we use arguments and notation of ref. [65]. Let us again consider the integral

$$\int d^D \ell \frac{1}{\ell^2 (\ell - p_1)^2 (\ell - p_1 - p_2)^2 (\ell + p_4)^2}. \quad (1.108)$$

To find the divergence for ℓ becoming collinear with p_1 we can use a Sudakov decomposition of the loop momentum with respect to p_1 [65, 66],

$$\ell = \alpha p_1 + \beta p_1^- + \ell_\perp. \quad (1.109)$$

Here α and β are new parameters, while p_1^- is defined to be $p_1^{-\mu} = (p_1^0, -p_1^i)$, so that $(p_1^-)^2 = 0$. The momentum ℓ_\perp has to be orthogonal to both p_1 and p_1^- , *i.e.* $(\ell_\perp \cdot p_1) = (\ell_\perp \cdot p_1^-) = 0$. Through α , β and ℓ_\perp , ℓ is fully parametrized. The collinear limit with respect to p_1 is obtained for vanishing β and ℓ_\perp , while keeping α at an arbitrary, but fixed value. We can parametrize this limit by making the replacements,

$$\beta \rightarrow \delta \beta, \quad \ell_\perp \rightarrow \delta^{\frac{1}{2}} \ell_\perp, \quad (1.110)$$

We then approach the collinear region for $\delta \rightarrow 0$.

Let us first see the effect on the integration measure, which in the Sudakov decomposition takes the form [66],

$$d^D \ell = (p_1 \cdot p_1^-) d\alpha d\beta d^{D-2} \ell_\perp. \quad (1.111)$$

Leaving α fixed, the scaling of eq. (1.110) leads to a scaling of the measure

$$d^D \ell \stackrel{\delta \rightarrow 0}{\sim} \delta^{\frac{D}{2}}. \quad (1.112)$$

In the integral of eq. (1.108), the last two propagators are finite in the small δ limit. For example,

$$\frac{1}{(\ell + p_4)^2} = \frac{1}{\ell^2 + 2\ell \cdot p_4} \stackrel{\delta \rightarrow 0}{\approx} \frac{1}{\alpha s_{14}}. \quad (1.113)$$

Each of the first two propagators however scale homogeneously as $\frac{1}{\delta}$,

$$\begin{aligned} \frac{1}{\ell^2} &= \frac{1}{\ell_\perp^2 + 2\alpha\beta(p_1 \cdot p_1^-)} \stackrel{\delta \rightarrow 0}{\approx} \frac{1}{\delta}, \\ \frac{1}{(\ell - p_1)^2} &= \frac{1}{\ell_\perp^2 + 2(\alpha - 1)\beta(p_1 \cdot p_1^-)} \stackrel{\delta \rightarrow 0}{\approx} \frac{1}{\delta}. \end{aligned} \quad (1.114)$$

The quadratic appearance of ℓ_\perp and only The entire integral therefore scales as $(\frac{1}{\delta})^{2-\frac{D}{2}}$. This is yet another logarithmic divergence, which also leads to a factor of $\frac{1}{\epsilon}$. Note that in the limit

of vanishing α the collinear and soft divergences can overlap. A one-loop integral can therefore have divergences up to $\frac{1}{\epsilon^2}$. Contrary to UV divergences these IR divergences cannot be removed at the level of the loop amplitude. Rather, they cancel once we compute an observable. Since colliders have a finite resolution, we have to include processes with soft real emissions that are indistinguishable from the original process. At fixed order in the coupling, a one-loop virtual process needs to be combined with a single real emission, that is either soft or collinear with respect to the other particles. The phase-space integral of the real emission develops singularities, which cancel the infrared divergences of the loop amplitude point-by-point. For multi-loop corrections, multiple such real emissions are required for the cancellation to occur. The exact cancellation of these infrared divergences at any order in the coupling is guaranteed by the KLN theorem [64, 67].

Feynman integrals are not independent functions, and it is often possible to reduce the integrals appearing in an amplitude to a minimal set, often called master integrals. Such a basis of integrals is not uniquely defined, and there are many different choices for the set of master integrals of a given amplitude. While at one loop it is simple to find such a basis of integrals—as we will see in the next chapter—finding such a basis for multi-loop amplitudes can be a difficult task. Several approaches for such integral reductions have been developed over the years [68–71], and specialized software packages are available, such as **Reduze** [72, 73], **AIR** [74], **Kira** [75–77] or **FIRE** [78–81].

1.4.2 Color-Decomposition for Loop Amplitudes

Just as in the tree-level case, we can separate the color and kinematic parts of loop amplitudes through color decomposition. In contrast to tree amplitudes, the basis of color structures does not only contain single traces of color generators. For an L -loop amplitude we can have at most $L + 1$ such traces, which can include powers of N_c . Furthermore, the color decomposition of $SU(N_c)$ and $U(N_c)$ loop amplitudes differ. In the former any trace of a single color generator vanishes, while for the latter these are allowed in the case of the additional $U(1)$ generator.

At this point I just state the general form of $SU(N_c)$ decompositions of one- and two-loop amplitudes. We will further discuss their origin in the next chapter.

1.4.2.1 One Loop

The color decomposition of a generic one-loop amplitude with $SU(N_c)$ gauge group takes the form

$$\begin{aligned} \mathcal{A}_n^{(1)} = g^n & \left[N_c \sum_{\sigma \in S_n / C_n} \text{Tr}[T^{\sigma(1)} \dots T^{\sigma(n)}] A_{n,1}^{(1)}(\sigma(1) \dots \sigma(n)) \right. \\ & + \sum_{r=3}^{\lfloor \frac{n}{2} \rfloor + 1} \sum_{\sigma \in S_n / P_{n,r}} \text{Tr}[\sigma(1) \dots \sigma(r-1)] \text{Tr}[\sigma(r) \dots \sigma(n)] \\ & \left. \times A_{n:r}^{(1)}(\sigma(1) \dots \sigma(r-1); \sigma(r) \dots \sigma(n)) \right]. \end{aligned} \quad (1.115)$$

Here, S_n and C_n are the symmetric and cyclic group of n elements. The $P_{n:r}$, defined as

$$P_{n:r} = \begin{cases} C_{r-1} \times C_{r-1} \times S_2, & n = 2(r-1), \\ C_{r-1} \times C_{n-r-1}, & \text{otherwise} \end{cases} \quad (1.116)$$

account for the cyclic symmetry of the traces (C_i), as well as the permutations of the traces (S_i), should they have equal length. The factor N_c in the decomposition can be interpreted as traces containing the identity \mathbb{I}_{N_c} .

We now have two classes of partial amplitude, those of a single color trace $A_{n:1}^{(1)}$, and those of the double traces $A_{n:i}^{(1)}$. Due to the power of N_c , the former are called leading in color, while the latter are referred to as subleading in color. The subleading partial amplitudes are entirely determined by the leading ones via the relation [82, 83],

$$A_{n:j}^{(1)}(1, 2, \dots, j-1; j, j+1, \dots, n) = \sum_{\sigma \in \text{COP}\{\alpha\}\{\beta\}} A_{n:1}^{(1)}(\sigma(1), \dots, n). \quad (1.117)$$

This was derived using the one-loop U(1)-decoupling identities, and is a feature of one-loop amplitudes.

1.4.2.2 Two Loops

Two-loop Yang–Mills amplitudes with gauge group $\text{SU}(N_c)$ can be generically decomposed in terms of color traces as follows [4, 10],

$$\begin{aligned} \mathcal{A}_n^{(2)} = & g^{n+2} \left[N_c^2 \sum_{\sigma \in S_n/C_n} \text{Tr}[T^{\sigma(1)} \dots T^{\sigma(n)}] A_{n:1}^{(2)}(\sigma(1) \dots \sigma(n)) \right. \\ & + N_c \sum_{r=3}^{\lfloor \frac{n}{2} \rfloor + 1} \sum_{\sigma \in S_n/P_{n:r}} \text{Tr}[\sigma(1) \dots \sigma(r-1)] \text{Tr}[\sigma(r) \dots \sigma(n)] \\ & \quad \times A_{n:r}^{(2)}(\sigma(1) \dots \sigma(r-1); \sigma(r) \dots \sigma(n)) \\ & + \sum_{r=2}^{\lfloor \frac{n}{2} \rfloor} \sum_{k=r}^{\lfloor \frac{n-r}{2} \rfloor} \sum_{\sigma \in S_n/P_{n:r,k}} \text{Tr}[\sigma(1) \dots \sigma(r)] \text{Tr}[\sigma(r+1) \dots \sigma(r+k)] \text{Tr}[\sigma(r+k+1) \dots \sigma(n)] \\ & \quad \times A_{n:r,k}^{(2)}(\sigma(1) \dots \sigma(r); \sigma(r+1) \dots \sigma(r+k); \sigma(r+k+1) \dots \sigma(n)) \\ & \left. + \sum_{\sigma \in S_n/C_n} \text{Tr}[\sigma(1), \dots, \sigma(n)] A_{n:1B}^{(2)}(\sigma(1), \dots, \sigma(n)) \right], \end{aligned} \quad (1.118)$$

where $P_{n:r}$ is defined as in eq. (1.116), and

$$P_{n:r,k} = \begin{cases} C_r \times C_r \times C_r \times S_3, & r = k, n = 3r, \\ C_r \times C_k \times C_k \times S_2, & n = r + 2k, \\ C_r \times C_r \times C_{n-2r} \times S_2, & r = k, \\ C_r \times C_k \times C_{n-r-k}, & \text{otherwise} \end{cases}. \quad (1.119)$$

In eq. (1.119), $P_{n:r,k}$ has the same function as $P_{n:r}$ in the one-loop case, namely to remove trace color-trace structures based on their symmetries. The factors of N_c in the decomposition can again be interpreted as traces containing the identity \mathbb{I}_{N_c} . In this definition, the traces are ordered with respect to their length,

For two loops, there exist four classes of partial amplitudes: the leading color single trace $A_{n:1}^{(2)}$, the subleading color double and triple trace amplitudes $A_{n:r}^{(2)}$ and $A_{n:r,k}^{(2)}$, as well as the subleading color single trace amplitudes $A_{n:1B}^{(2)}$. While relations connecting the leading and subleading amplitudes exist also for two loops, they generally do not fix all subleading amplitudes, and they have to be computed separately.

Chapter 2

Generalized Unitarity

In this chapter, we discuss the main technique we will be using throughout the thesis for the computation of loop amplitudes: generalized unitarity. For a given amplitude, the relations between Feynman integrals allow us to find a minimal basis of independent integrals. Once expressed in such a basis, we are then able to find the integral coefficients of the amplitude from generalized unitarity cuts. These in a sense project the amplitude onto the basis of integrals via their branch-cut structure.

While we will discuss the computation of two-loop all-plus amplitudes in the following chapters, a central point will be the explicit avoidance of two-loop unitarity techniques. Instead we find that for our purposes we can rely solely on the well-developed one-loop technology, which is significantly simpler. In this chapter I therefore choose to entirely omit multi-loop unitarity techniques, and provide a more thorough discussion of the one-loop technology we will require later.

2.1 One-Loop Feynman Integrals

To discuss the required Feynman integrals for one-loop amplitudes, let us specialize the definition of section 1.4.1 to $L = 1$. At one loop we need only consider the Feynman integrals of graphs forming an n -sided polygon, as shown in Figure 2.1. We will require this class of integrals for the

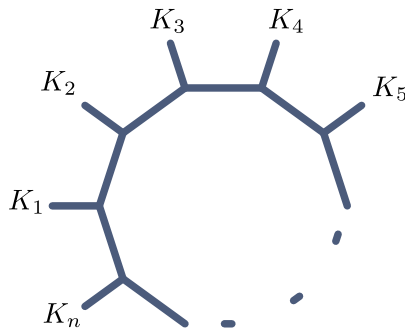


Figure 2.1: All Feynman integrals appearing in one-loop amplitudes can be associated with graphs $G_{n\text{-poly}}$ taking the shape of an n -sided polygon. The momenta K_i are generally massive.

remainder of the thesis. We use the normalization of ref. [84]

$$I_n^D[\mathcal{N}[\ell]] = I_{G_{n\text{-poly}}}^{(1),D}[\mathcal{N}[\ell]] = (-i)(-1)^n(4\pi)^{D/2}\mathcal{I}_n^D[\mathcal{N}[\ell]], \quad (2.1)$$

where

$$\mathcal{I}_n^D[\mathcal{N}[\ell]] \equiv \mathcal{I}_{G_{n\text{-poly}}}^{(1),D}[\mathcal{N}[\ell]] = \int \frac{d^D\ell}{(2\pi)^D} \frac{\mathcal{N}[\ell]}{\ell^2(\ell - K_1)^2 \dots (\ell - K_{12\dots(n-1)})^2}. \quad (2.2)$$

The K_i are the—generally massive—momenta attached to the loop, for which we also use the notation,

$$K_{i_1 i_2 \dots i_k} = K_{i_1} + K_{i_2} + \dots + K_{i_k}. \quad (2.3)$$

While graphs at higher loops can in general be non-planar, at one loop we can bring any graph into the planar form of Figure 2.1.

Including loop-momentum dependent numerators, a one-loop n -particle amplitude computed via Feynman diagrams generally contains integrals of the form $I_n^D[\mathcal{N}[\ell]]$. However, as mentioned in section 1.4.1, Feynman integrals are not independent, and this property is nowhere easier to observe than in one-loop amplitudes. For external kinematics in four dimensions we can show that it is sufficient to consider scalar integrals with up to four propagators. First, we can see that any tensor integrals that may appear can be reduced to scalar ones via Passarino-Veltmann reduction [85] or similar reduction schemes [86]. The fact that we only require integrals with up to four propagators is due to the four-dimensionality of the kinematics. Given four linearly independent four-momenta $\{K_1, K_2, K_3, K_4\}$ we can express any additional momentum Q as a linear combination of the K_i . We can use this property to rewrite any integral with $n > 4$ propagators as a linear combination of integrals with $(n - 1)$ propagators. More complete reviews of this procedure can be found for example in refs. [48, 70]; here we will only provide a short summary of these.

A convenient way to express linear dependence between momenta is the Gram determinant, defined by,

$$G \begin{pmatrix} p_1 & p_2 & \dots & p_m \\ k_1 & k_2 & \dots & k_m \end{pmatrix} = \begin{vmatrix} (p_1 \cdot k_1) & \dots & (p_1 \cdot k_m) \\ \vdots & \ddots & \vdots \\ (p_m \cdot k_1) & \dots & (p_m \cdot k_m) \end{vmatrix} \quad (2.4)$$

It vanishes if either one of the sets $\{p_i\}$ or $\{k_i\}$ is linearly dependent. Say for example that p_m can be expressed as a linear combination of the remaining $(m - 1)$ momenta. We can then row reduce the matrix to eliminate the lowest row, proving that the determinant vanishes. For the q_i we could perform the same operations on the columns. Due to the four-dimensionality of our kinematics we particularly have for any $p_i, k_i, i \in \{1, \dots, n\}, n > 5$,

$$G \begin{pmatrix} p_1 & p_2 & \dots & p_n \\ k_1 & k_2 & \dots & k_n \end{pmatrix} = 0. \quad (2.5)$$

We can use this fact to reduce an n -point integral to a linear combination of $(n - 1)$ -point integrals through [70]

$$I_n^D \left[G \begin{pmatrix} K_1 & K_{12} & K_{123} & K_{1234} & \ell \\ K_1 & K_{12} & K_{123} & K_{1234} & K_{12345} \end{pmatrix} \right] = 0. \quad (2.6)$$

Each term in the determinant will contain a product $(\ell \cdot K_{\dots})$. We can complete these to inverse

propagators,

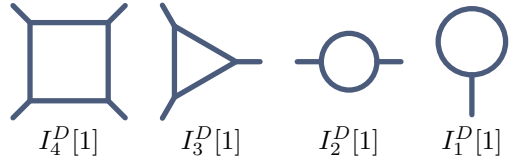
$$(\ell \cdot K_{\dots}) = \frac{1}{2} ((\ell + K_{\dots})^2 - \ell^2 - K_{\dots}^2). \quad (2.7)$$

The first two terms each cancel one of the integral propagators, while the third will be proportional to the original integral. By collecting the ℓ independent terms in the determinant then allows us to rewrite the n -propagator integral in terms of a sum over $(n-1)$ -point integrals with kinematic coefficients.

In the case of $n=5$ we have to take care of a subtlety originating from dimensional regularization. Assuming ℓ to be D -dimensional with $D = (4-2\epsilon)$, the gram determinant vanishes only up to contributions stemming from the (-2ϵ) -components of the loop momentum. These will ultimately lead to terms of order ϵ , so that we can loosely write,

$$G \begin{pmatrix} K_1 & K_{12} & K_{123} & K_{1234} & \ell \\ K_1 & K_{12} & K_{123} & K_{1234} & K_{12345} \end{pmatrix} = \mathcal{O}(\epsilon) \quad (2.8)$$

In section 2.3 we will discuss how to deal with these additional contributions. However, for the moment we will assume the loop momentum to be four dimensional, such that the Gram determinant in eq. (2.8) vanishes. Recursive application of this reduction thus allows us to express any integral $I_n^D[N[\ell]]$ as a linear combination of integrals belonging to the four classes,

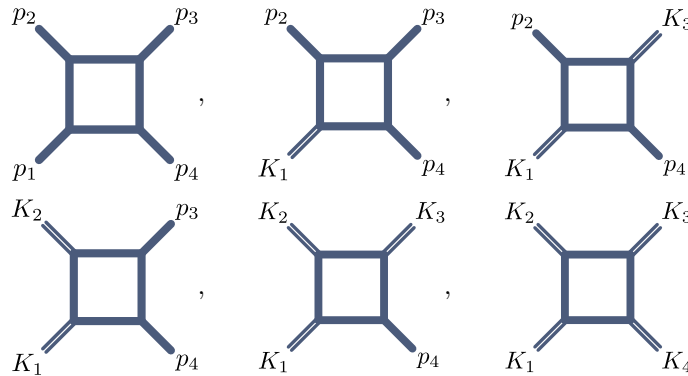


$$I_4^D[1] \quad I_3^D[1] \quad I_2^D[1] \quad I_1^D[1] \quad (2.9)$$

Due to their geometry they are usually called the box, triangle, bubble and tadpole integrals, and they form a (four-dimensional) basis of Feynman integrals at one-loop. We will mainly concern ourselves with amplitudes of Yang–Mills theory. We therefore usually ignore the tadpole integrals, as they would be scaleless integrals, which vanish in dimensional regularization.

In determining these integrals as a Laurent series in ϵ we have to distinguish between cases where different sets of external momenta are massive, as the massless limit and the expansion in ϵ do not necessarily commute [84]. The internal propagators could generally be massive as well, though for simplicity we ignore those cases here.

Starting with the box integrals, we have six different distinct cases,



$$\begin{array}{ccc} \begin{array}{c} p_2 \quad p_3 \\ \diagdown \quad \diagup \\ \text{Box} \\ \diagup \quad \diagdown \\ p_1 \quad p_4 \end{array} & , & \begin{array}{c} p_2 \quad p_3 \\ \diagdown \quad \diagup \\ \text{Box} \\ \diagup \quad \diagdown \\ K_1 \quad p_4 \end{array} & , & \begin{array}{c} p_2 \quad p_3 \\ \diagdown \quad \diagup \\ \text{Box} \\ \diagup \quad \diagdown \\ K_1 \quad p_4 \end{array} & , \\ \begin{array}{c} K_2 \quad p_3 \\ \diagdown \quad \diagup \\ \text{Box} \\ \diagup \quad \diagdown \\ K_1 \quad p_4 \end{array} & , & \begin{array}{c} K_2 \quad K_3 \\ \diagdown \quad \diagup \\ \text{Box} \\ \diagup \quad \diagdown \\ K_1 \quad p_4 \end{array} & , & \begin{array}{c} K_2 \quad K_3 \\ \diagdown \quad \diagup \\ \text{Box} \\ \diagup \quad \diagdown \\ K_1 \quad K_4 \end{array} & . \end{array} \quad (2.10)$$

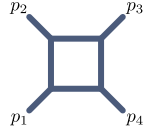
Here we label massless momenta by p_i and single lines, while massive momenta have labels K_i and

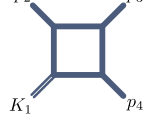
are represented by double lines. In the case of two massive momenta we have two distinct cases, as the massive momenta can be either opposite or adjacent to one another. These are sometimes called the easy and hard two-mass box integrals, reflecting the complexity of their derivation.

Defining the common prefactor of gamma functions,

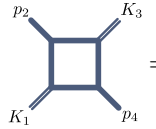
$$r_\Gamma = \frac{\Gamma(1+\epsilon)\Gamma^2(1-\epsilon)}{\Gamma(1-2\epsilon)}, \quad (2.11)$$

these integrals can be expressed in terms of logarithms and dilogarithms up to order ϵ as follows [84, 87–89],

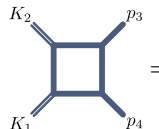


$$= I_{4,0m}^D[1] = 2r_\Gamma \left[\frac{1}{\epsilon^2} ((-s_{12})^{-\epsilon} + (-s_{23})^{-\epsilon}) - \frac{1}{2} \log^2 \left(\frac{-s_{12}}{-s_{23}} \right) - \frac{\pi^2}{2} \right] + \mathcal{O}(\epsilon), \quad (2.12)$$


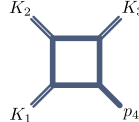
$$= I_{4,1m}^D[1] = \frac{2r_\Gamma}{s_{23}s_{34}} \left[\frac{1}{\epsilon^2} ((-s_{23})^{-\epsilon} + (-s_{34})^{-\epsilon} - (-K_1^2)^{-\epsilon}) \right. \\ \left. - \text{Li}_2 \left(1 - \frac{K_1^2}{s_{23}} \right) - \text{Li}_2 \left(1 - \frac{K_1^2}{s_{34}} \right) - \frac{1}{2} \log^2 \left(\frac{-s_{12}}{-s_{23}} \right) - \frac{\pi^2}{6} \right] + \mathcal{O}(\epsilon), \quad (2.13)$$



$$= I_{4,2m\epsilon}^D[1] = \frac{2r_\Gamma}{s_{12}s_{23} - K_1^2 K_3^2} \left[\frac{1}{\epsilon^2} ((-s_{23})^{-\epsilon} + (-s_{34})^{-\epsilon} - (-K_1^2)^{-\epsilon} - (-K_3^2)^{-\epsilon}) \right. \\ \left. - \text{Li}_2 \left(1 - \frac{K_1^2}{s_{12}} \right) - \text{Li}_2 \left(1 - \frac{K_1^2}{s_{23}} \right) - \text{Li}_2 \left(1 - \frac{K_3^2}{s_{12}} \right) \right. \\ \left. - \text{Li}_2 \left(1 - \frac{K_3^2}{s_{23}} \right) - \text{Li}_2 \left(1 - \frac{K_1^2 K_3^2}{s_{12}s_{23}} \right) - \frac{1}{2} \log^2 \left(\frac{-s_{12}}{-s_{23}} \right) \right] + \mathcal{O}(\epsilon), \quad (2.14)$$



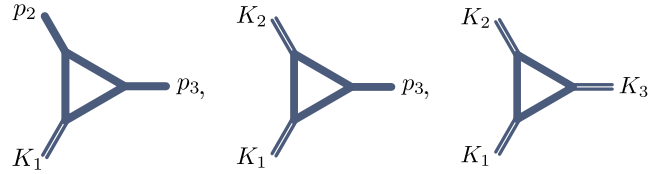
$$= I_{4,2mh}^D[1] = \frac{2r_\Gamma}{s_{12}s_{23}} \left[\frac{1}{\epsilon^2} ((-s_{23})^{-\epsilon} + (-s_{12})^{-\epsilon} - (-K_1^2)^{-\epsilon} - (-K_2^2)^{-\epsilon}) \right. \\ \left. + \frac{1}{\epsilon^2} \frac{(-K_1^2)^{-\epsilon}(-K_2^2)^{-\epsilon}}{(-s_{12})^{-\epsilon}} - \text{Li}_2 \left(1 - \frac{K_1^2}{s_{23}} \right) \right. \\ \left. - \text{Li}_2 \left(1 - \frac{K_2^2}{s_{23}} \right) - \frac{1}{2} \log^2 \left(\frac{-s_{12}}{-s_{23}} \right) \right] + \mathcal{O}(\epsilon), \quad (2.15)$$



$$= I_{4,3m}^D[1] = \frac{2r_\Gamma}{s_{12}s_{23} - K_1^2 K_3^2} \times \left[\frac{1}{\epsilon^2} ((-s_{23})^{-\epsilon} + (-s_{34})^{-\epsilon} - (-K_1^2)^{-\epsilon} - (-K_2^2)^{-\epsilon} - (-K_3^2)^{-\epsilon}) \right. \\ \left. + \frac{1}{\epsilon^2} \frac{(-K_1^2)^{-\epsilon}(-K_2^2)^{-\epsilon}}{(-s_{12})^{-\epsilon}} + \frac{1}{\epsilon^2} \frac{(-K_2^2)^{-\epsilon}(-K_3^2)^{-\epsilon}}{(-s_{23})^{-\epsilon}} - \text{Li}_2 \left(1 - \frac{K_1^2}{s_{12}} \right) \right. \\ \left. - \text{Li}_2 \left(1 - \frac{K_3^2}{s_{23}} \right) + \text{Li}_2 \left(1 - \frac{K_1^2 K_3^2}{s_{12}s_{23}} \right) - \frac{1}{2} \log^2 \left(\frac{-s_{12}}{-s_{23}} \right) \right] + \mathcal{O}(\epsilon), \quad (2.16)$$

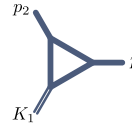
I omitted here the definition of the finite four mass box integral $I_{4,4m}^D[1]$, due to its lengthy definition. An explicit form can be found in ref. [84]. Ref. [89] also provides expressions for these integrals with internal masses in the propagators.

For triangle integrals we have three distinct cases, namely those integrals with one, two or three massive momenta,

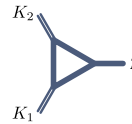


$$\quad (2.17)$$

The first two integrals are [84, 90],



$$= I_{3,1m}^D[1] = \frac{r_\Gamma}{\epsilon^2} \frac{(-K_1^2)^{-\epsilon}}{(-K_1^2)}, \quad (2.18)$$



$$= I_{3,2m}^D[1] = \frac{r_\Gamma}{\epsilon^2} \frac{(-K_1^2)^{-\epsilon} - (-K_2^2)^{-\epsilon}}{(-K_1^2) - (-K_2^2)}, \quad (2.19)$$


omitting again the finite three-mass integral $I_{3,3m}^D$. Its form can also be found in ref. [84].

Lastly we require the bubble integral



$$\quad (2.20)$$

As we are assuming the propagators to be massless, the external momentum K needs to be massive for this integral to be non-zero in dimensional regularization. Up to order ϵ terms the integral is then given by [89]



$$= I_2^D[1] = (-K^2)^{-\epsilon} \left(\frac{1}{\epsilon} + 2 \right) + \mathcal{O}(\epsilon). \quad (2.21)$$

2.2 Four-Dimensional Generalized Unitarity

In the previous section, we saw that any Feynman integral appearing in a one-loop amplitude $A^{(1)}$ has to be expressible as a linear combination of box, triangle or bubble integrals, with coefficients rational in the kinematics. Thus, we can express such an amplitude in terms of a basis of integrals,

$$A^{(1),D} = \sum C_{\text{Box}}^{(1)} I_4^D[1] + \sum C_{\text{Tri}}^{(1)} I_3^D[1] + \sum C_{\text{Bub}}^{(1)} I_2^D[1] + R^{(1)} + \mathcal{O}(\epsilon), \quad (2.22)$$

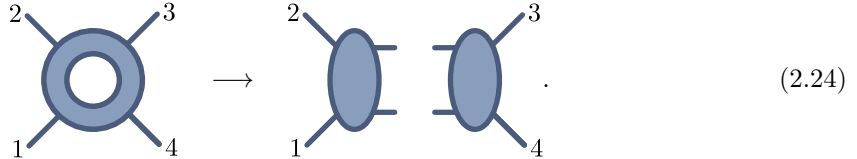
where the summations are assumed over all possible box, triangle and bubble configurations. As an example, consider the four gluon amplitude $A_{4;1}^{(1)}(1^+2^+3^-4^-)$. We should be able to express this amplitude as

$$\begin{aligned} A_{4;1}^{(1)}(1^+2^+3^-4^-) = & C_{\text{Box},1}^{(1)} I_4^D \left[\begin{array}{c} 2 \\ 1 \end{array} \begin{array}{c} 3 \\ 4 \end{array} \right] + C_{\text{Tri},1}^{(1)} I_3^D \left[\begin{array}{c} 2 \\ 1 \end{array} \begin{array}{c} 3 \\ 4 \end{array} \right] + C_{\text{Tri},2}^{(1)} I_3^D \left[\begin{array}{c} 1 \\ 4 \end{array} \begin{array}{c} 2 \\ 3 \end{array} \right] \\ & + C_{\text{Tri},3}^{(1)} I_3^D \left[\begin{array}{c} 4 \\ 3 \end{array} \begin{array}{c} 1 \\ 2 \end{array} \right] + C_{\text{Tri},4}^{(1)} I_3^D \left[\begin{array}{c} 3 \\ 2 \end{array} \begin{array}{c} 4 \\ 1 \end{array} \right] + C_{\text{Bub},1}^{(1)} I_2^D \left[\begin{array}{c} 2 \\ 1 \end{array} \begin{array}{c} 3 \\ 4 \end{array} \right] \\ & + C_{\text{Bub},2}^{(1)} I_2^D \left[\begin{array}{c} 1 \\ 4 \end{array} \begin{array}{c} 2 \\ 3 \end{array} \right] + R^{(1)} + \mathcal{O}(\epsilon). \end{aligned} \quad (2.23)$$

From a Feynman diagrammatic computation it would be exceedingly difficult to obtain the integral coefficients in all but the simplest cases. However, we are able project to amplitudes onto such a basis of Feynman integrals, and obtain the coefficients directly in terms of tree amplitudes. This approach of obtaining loop-amplitudes by sewing together tree-level ones was first established in refs. [23, 24], and later lead to the method of generalized unitarity [25, 91].

As discussed in section 1.4.1, Feynman integrals as analytic functions of the kinematics contain singularities. These singularities are associated to loop propagators going on-shell, and their precise location is given by the Landau equations. Each distinct Feynman integral has a unique set of singularities. By extracting the part of the amplitude which has the set of singularities specific to a given Feynman integral, we can deduce the basis coefficient belonging to that integral.

We have to distinguish between different classes of singularities: physical and anomalous ones. The physical singularities are related to thresholds caused by the possible intermediate on-shell particle production. As an example, consider a four-point one-loop amplitude $A^{(1)}(1234)$, with a massive particle running in the loop. If $s = (p_1 + p_2)^2 \geq 4m^2$, the loop can create an on-shell particle pair,



In this case, two of the internal propagators go on-shell. The particle creation is associated to a singularity of the amplitude, with branch point $s = 4m^2$, and a branch cut for $s > 4m^2$. Singularities associated to physical processes of particle creation are referred to as physical singularities. The discontinuity across their branch cuts can be computed via the Cutkosky cutting rule [27]: to obtain the discontinuity for a physical threshold with a set of propagators going on-shell, we

replace each involved propagator using the rule,

$$\frac{i}{(\ell - K)^2 - m^2} \rightarrow 2\pi\delta^+((\ell - K)^2 - m^2) \quad (2.25)$$

The delta function $\delta^+(P^2)$ ensures that momentum of the cut propagator has positive energy, *i.e.*

$$\delta^+(P^2) = \delta(P^2)\Theta(P^0). \quad (2.26)$$

A rigorous proof of the Cutkosky rules can be found in ref. [92].

The Cutkosky cutting rule are closely connected to the optical theorem, a classic result in quantum field theory. I summarize here the discussion of ref. [42]. Defining the S-matrix as

$$\mathbb{S} = \mathbb{1} + i\mathbb{T}, \quad (2.27)$$

with \mathbb{T} containing all non-trivial interactions, unitarity requires that,

$$1 = \langle\phi|\phi\rangle = \langle\phi'|\mathbb{S}^\dagger\mathbb{S}|\phi'\rangle. \quad (2.28)$$

The S-matrix therefore has to satisfy,

$$\mathbb{1} = \mathbb{S}^\dagger\mathbb{S} = \mathbb{1} - i\mathbb{T}^\dagger + i\mathbb{T} + \mathbb{T}^\dagger\mathbb{T}, \quad (2.29)$$

or in other words,

$$i\mathbb{T}^\dagger - i\mathbb{T} = \mathbb{T}^\dagger\mathbb{T}. \quad (2.30)$$

To see the consequence for amplitudes, we compute the expectation value with respect to external states ϕ_{out} and ϕ_{in}

$$i\langle\phi_{\text{out}}|\mathbb{T}^\dagger|\phi_{\text{in}}\rangle - i\langle\phi_{\text{out}}|\mathbb{T}|\phi_{\text{in}}\rangle = \langle\phi_{\text{out}}|\mathbb{T}^\dagger\mathbb{T}|\phi_{\text{in}}\rangle = \sum_{\phi_i} \langle\phi_{\text{out}}|\mathbb{T}^\dagger|\phi_i\rangle \langle\phi_i|\mathbb{T}|\phi_{\text{in}}\rangle, \quad (2.31)$$

where on the right-hand side we inserted an identity $\mathbb{1}$ in the form of a full set of single and multi-particle states. The summation runs over the number of particles, as well as particle types, while the integration represents a phase-space integral attributed to every particle. To make the connection with the Cutkosky rule clearer, we can rewrite each of these integrals as,

$$\int \frac{d^3p}{(2\pi)^3} \frac{1}{2E_p} = \int \frac{d^4p}{(2\pi)^4} (2\pi)\delta^+(p^2 - m^2). \quad (2.32)$$

The equality of eq. (2.31) has to hold at every order in perturbation theory. Looking at the order corresponding to one-loop amplitudes on the left-hand side, the right-hand side can only involve two-particle states ϕ_i , such that

$$iA^{(1)*}(\phi_{\text{in}} \rightarrow \phi_{\text{out}}) - iA^{(1)}(\phi_{\text{in}} \rightarrow \phi_{\text{out}}) = \sum_{\phi_i=\{\varphi_1, \varphi_2\}} A^{(0)}(\phi_{\text{in}} \rightarrow \{\varphi_1, \varphi_2\}) A^{(0)*}(\phi_{\text{out}} \rightarrow \{\varphi_1, \varphi_2\}) \quad (2.33)$$

Due to the analyticity of scattering amplitudes, the left-hand side can be interpreted as the discontinuity of $A^{(1)}$ in $s = \sum_{i \in \phi_{\text{in}}} p_i$. The right-hand side is precisely the one-loop amplitude with

two internal propagators cut via the Cutkosky rules

At next order in perturbation theory, the left-hand side of eq. (2.31) corresponds to the discontinuity of the two-loop amplitude, while the right-hand side can be interpreted as the two-loop amplitude with either two- or three propagators cut

$$\begin{aligned} \text{Disc } A^{(2)}(\phi_{\text{in}} \rightarrow \phi_{\text{out}}) = & \sum_{\phi_i=\{\varphi_1, \varphi_2\}}^f A^{(0)}(\phi_{\text{in}} \rightarrow \{\varphi_1, \varphi_2\}) A^{(1)*}(\phi_{\text{out}} \rightarrow \{\varphi_1, \varphi_2\}) \\ & + \sum_{\phi_i=\{\varphi_1, \varphi_2\}}^f A^{(1)}(\phi_{\text{in}} \rightarrow \{\varphi_1, \varphi_2\}) A^{(0)*}(\phi_{\text{out}} \rightarrow \{\varphi_1, \varphi_2\}) \\ & + \sum_{\phi_i=\{\varphi_1, \varphi_2, \varphi_3\}}^f A^{(0)}(\phi_{\text{in}} \rightarrow \{\varphi_1, \varphi_2, \varphi_3\}) A^{(0)*}(\phi_{\text{out}} \rightarrow \{\varphi_1, \varphi_2, \varphi_3\}). \end{aligned} \quad (2.34)$$

Thus, requiring unitarity of the S-matrix leads to exactly the relation between the discontinuity and cuts of an amplitude proven by Cutkosky [27]. Such cuts are therefore also called unitarity cuts.

As mentioned before, amplitudes, and as an extension Feynman integrals, possess additional singularities besides the physical ones, which are related to additional propagators going on-shell. These singularities are sometimes called anomalous, as they do not correspond to a physical process, with some being associated to complex momentum configurations. The precise determination of the discontinuities across their associated branch cuts is not covered by the Cutkosky cutting rule, as for example the delta function vanishes for complex arguments. A more rigorous approach of computing the discontinuities is based on computing the residue of poles associated to on-shell propagators [92–94]. This allows the computation of multiple discontinuities consecutively for all thresholds, physical or non-physical, with the result of cutting an amplitude into more than two parts. These are called generalized cuts, and form the basis of generalized unitarity method.

2.2.1 Unitarity Cuts and Loop-Momentum Parametrizations

We will now discuss the computation of the integral coefficients of eq. (2.22) using generalized unitarity cuts. We review the procedure and loop momentum parametrization presented in ref. [95], as these are well suited for analytic computations.

2.2.1.1 Box Coefficients

The easiest type of integral to consider in the basis of eq. (2.22) is the box integral. We will focus in the following on the construction of integral coefficients for a one-loop amplitude $A^{(1)}$ in Yang–Mills theory. Given such an amplitude and a box integral I_4^D in the basis of eq. (2.22), we would like to determine the associated coefficient $C_{\text{Box}}^{(1)}$. Let us assume the most general box integral, namely the integral with four massive external momenta K_1, K_2, K_3, K_4 . We choose the loop integration variable ℓ to be the momentum of the propagator between K_4 and K_1 as shown in Figure 2.2, such that,

$$I_4^D = \int \frac{d^D \ell}{(2\pi)^D} \frac{1}{\ell^2 (\ell - K_1)^2 (\ell - K_{12})^2 (\ell + K_4)^2}. \quad (2.35)$$

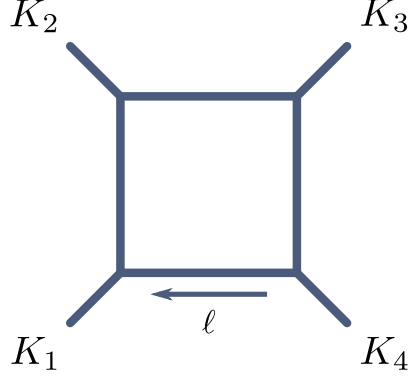


Figure 2.2: A generic box cut. The momenta K_1, K_2, K_3, K_4 are assumed to be massive. The loop momentum ℓ is defined to be flowing from the K_4 and into the K_1 corner.

We obtain $C_{\text{Box}}^{(1)}$ by projecting the amplitude onto I_4^D . Computing the discontinuities unique to I_4^D , *i.e.* the one associated to four on-shell conditions for the loop-momentum

$$\ell^2 = 0, \quad (\ell - K_1)^2 = 0, \quad (\ell - K_{12})^2 = 0, \quad (\ell + K_4)^2 = 0, \quad (2.36)$$

where $K_{12} = K_1 + K_2$. We can obtain this discontinuity through four generalized cuts. We will call this operation the box cut Cut_{Box} . As mentioned before, these discontinuities are not necessarily associated to physical or even real momentum configurations. Keeping the external kinematics fixed, we can assume the integration variable ℓ to be complex, and compute the residues through contour integrals around the associated poles.

First let us act with Cut_{Box} on the amplitude, which splits the integrand into four on-shell tree amplitudes. Assuming we are cutting gluon propagators, we can use the gluon polarization completeness relation to turn the cut propagators into sums over the polarization states, as discussed in section 1.3.2. In this case we end up with

$$\begin{aligned} \text{Cut}_{\text{Box}}[A^{(1)}] &= (-i)(4\pi)^{D/2} i^4 \sum_{h_i = \pm} \sum_{\ell = \ell^\pm} J A_1^{(0)} \left((-\ell)^{\bar{h}_1}, \{K_1\}, (\ell - K_1)^{h_2} \right) \\ &\quad \times A_2^{(0)} \left((-\ell + K_1)^{\bar{h}_2}, \{K_2\}, (\ell - K_{12})^{h_3} \right) \\ &\quad \times A_3^{(0)} \left((-\ell + K_{12})^{\bar{h}_3}, \{K_3\}, (\ell + K_4)^{h_4} \right) \\ &\quad \times A_4^{(0)} \left((-\ell - K_4)^{\bar{h}_4}, \{K_4\}, (\ell)^{h_1} \right) \\ &= (-i)(4\pi)^{D/2} J \sum_{\ell = \ell^\pm} A_1^{(0)}(\ell) A_2^{(0)}(\ell) A_3^{(0)}(\ell) A_4^{(0)}(\ell) + \mathcal{O}(\epsilon) \end{aligned} \quad (2.37)$$

The $A_i^{(0)}$ are tree-level color-ordered amplitudes, with $\{K_i\}$ being the set of external momenta which sum to the momentum K_i . For conciseness, we will refer to these amplitudes only by their indices. The factor of $(-i)$ is the overall normalization we chose for all amplitudes, *c.f.* eq. (1.59), while the factor of $(4\pi)^{D/2}$ is the normalization of one-loop partial amplitudes following eq. (1.98). The factor of i^4 originates from applying the amplitude normalization $(-i)$ to each of the $A_i^{(0)}$. Computing residues for the generalized cuts produces a factors $(-i)$ for every cut propagator, which are compensated by the factors of i in the propagator numerators.

The four cuts completely fix the four-dimensional part of ℓ . In four-dimensional unitarity we

content ourselves with this situation, and choose to ignore any contributions stemming from the (-2ϵ) -components of ℓ . We will describe their treatment in section 2.3. There exist generally two solutions, denoted ℓ^+ and ℓ^- , which we need to sum over. In J we collect all terms that cancel in the end, *i.e.* the integral $\int d^{-2\epsilon}\ell$, Jacobians and factors of 2π that originate from the residues and loop integrand.

Now that we know the action of Cut_{Box} on the left-hand side of eq. (2.22), let us see its effect on the right-hand side. The given box integral is the only one with the specific discontinuities, with all other integrals vanishing under the action of Cut_{Box} . Applying Cut_{Box} to $I_4^D[1]$ leads to,

$$\begin{aligned} \text{Cut}_{\text{Box}} \left[C_{\text{Box}}^{(1)} I_4^D[1] \right] &= C_{\text{Box}}^{(1)} (-i)(4\pi)^{D/2} (-i)^4 J \sum_{\ell=\ell^\pm} 1 \\ &= 2 C_{\text{Box}}^{(1)} (-i)(4\pi)^{D/2} J . \end{aligned} \quad (2.38)$$

Comparing eqs.(2.37) and (2.38), we obtain for the box coefficient [25],

$$C_{\text{Box}}^{(1)} = \frac{1}{2} \sum_{\ell=\ell^\pm} A_1^{(0)}(\ell) A_2^{(0)}(\ell) A_3^{(0)}(\ell) A_4^{(0)}(\ell) + \mathcal{O}(\epsilon) \quad (2.39)$$

The expression for the box coefficient in eq. (2.39) is independent of the particular realization of ℓ^\pm ; we use the parametrization presented in ref. [96]. Note that in the case of triangle and bubble cuts this will no longer hold, and the form of the coefficient will generally be parametrization dependent.

We construct the loop momentum fulfilling the four on-shell conditions in terms of the external kinematics. By projecting the massive momenta K_1, K_4 onto each other, we can obtain massless momenta K_1^b, K_4^b ,

$$K_1^b = \frac{\gamma^2 K_1 - \gamma K_1^2 K_4}{\gamma^2 - K_1^2 K_4^2}, \quad K_4^b = \frac{\gamma^2 K_4 - \gamma K_4^2 K_1}{\gamma^2 - K_1^2 K_4^2}. \quad (2.40)$$

In these expressions, γ is defined by,

$$(K_1^b)^2 = \frac{\gamma^4 K_1^2 + \gamma^2 (K_1^2)^2 K_4^2 - 2\gamma^3 K_1^2 (K_1 \cdot K_4)}{(\gamma^2 - K_1^2 K_4^2)^2} = 0 \quad (2.41)$$

$$\Leftrightarrow \gamma^2 K_1^2 + K_1^2 K_4^2 - 2\gamma (K_1 \cdot K_4) = 0 \quad (2.42)$$

$$\Rightarrow \gamma = (K_1 \cdot K_4) \pm \sqrt{(K_1 \cdot K_4)^2 - K_1^2 K_4^2}, \quad (2.43)$$

In case either K_1^2 or K_4^2 vanishes, the sign of the root is chosen such that γ is non-zero. We also find that,

$$\gamma = (K_1^b + K_4^b)^2 = 2(K_1^b \cdot K_4^b), \quad (2.44)$$

and that,

$$K_1 = K_1^b + \frac{K_1^2}{\gamma} K_4^b, \quad K_4 = K_4^b + \frac{K_4^2}{\gamma} K_1^b. \quad (2.45)$$

We use the momenta K_1^b and K_4^b to build an Ansatz for the loop-momentum. Following ref. [96], we assume that

$$\ell^\mu = c K_1^{b\mu} + d K_4^{b\mu} + \frac{1}{2} \left(t \langle K_1^b | \gamma^\mu | K_4^b \rangle + b \langle K_4^b | \gamma^\mu | K_1^b \rangle \right) + \mathcal{O}(\epsilon), \quad (2.46)$$

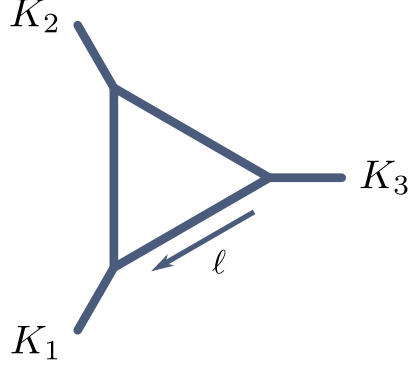


Figure 2.3: A generic triangle cut. The momenta K_1, K_2, K_3 are generally massive. The loop momentum ℓ is defined to flow out of the K_3 and into the K_1 corner.

where by $\mathcal{O}(\epsilon)$ we mean the (-2ϵ) -dimensional components of ℓ in dimensional regularization. In four-dimensional unitarity we ignore these contributions, and so we will drop them in this discussion, though their presence is always implicitly assumed.

The on-shell condition $\ell^2 = 0$ translates into

$$b = \frac{cd}{t}.$$

Next, $(\ell - K_1)^2 = 0$ and $(\ell + K_4)^2 = 0$ fix the parameters c and d to,

$$c = -\frac{K_4^2(\gamma + K_1^2)}{\gamma^2 - K_1^2 K_4^2}, \quad d = \frac{K_1^2(\gamma + K_4^2)}{\gamma^2 - K_1^2 K_4^2}. \quad (2.47)$$

The last on-shell condition $(\ell - K_{12})^2 = 0$ provides a quadratic relation for t , whose solutions are,

$$t^{\pm} = \frac{\Delta \pm \sqrt{\Delta^2 - 4cd \text{tr}_-(K_1^{\flat} K_2 K_4^{\flat} K_2)}}{2 \langle K_1^{\flat} | K_2 | K_4^{\flat} \rangle}, \quad \Delta = -(2K_2 \cdot (K_1 + cK_1^{\flat} + dK_4^{\flat}) + K_2^2). \quad (2.48)$$

2.2.1.2 Triangle Coefficients

We now turn to the computation of coefficients of triangle integrals $I_3^D[1]$. We again choose a generic representative with all external momenta K_1, K_2, K_3 being massive, with ℓ flowing between K_3 and K_1 . This configuration is shown in Figure 2.3.

We again make use of the discontinuities of the amplitude to project it onto the basis. As we are interested in the coefficient of a triangle integral, we only compute the discontinuities of three thresholds, cutting the loop amplitude into three tree amplitudes. Computing the discontinuities associated to the on-shell conditions

$$\ell^2 = 0, \quad (\ell - K_1)^2 = 0, \quad (\ell + K_3)^2 = 0, \quad (2.49)$$

defines the triangle cut operation Cut_{Tri} . However, the situation is complicated by the fact that more than one basis integral develop such discontinuities. While all bubble and all but one triangle integral vanish under application of Cut_{Tri} , a set of box integrals contain the same propagators, and will therefore not vanish when computing residues. We will therefore have to perform additional

steps to disentangle the triangle from the box contributions.

As mentioned in the previous section, the form of the triangle coefficients will depend on the particular loop momentum parametrization we use. A convenient choice is to reuse the parametrization of the box case, with the exception of leaving the parameter t unfixed. We again define the massless momenta associated to K_1 and K_3 ,

$$K_1^b = \frac{\gamma^2 K_1 - \gamma K_1^2 K_3}{\gamma^2 - K_1^2 K_3^2}, \quad K_3^b = \frac{\gamma^2 K_3 - \gamma K_3^2 K_1}{\gamma^2 - K_1^2 K_3^2}, \quad (2.50)$$

where

$$\gamma = (K_1 \cdot K_3) \pm \sqrt{(K_1 \cdot K_3)^2 - K_1^2 K_3^2}.$$

Again, for vanishing K_1^2 or K_3^2 we choose the sign in γ such that γ is non-zero. We already found a solution for the three on-shell conditions in eq. (2.49) in the box case, namely,

$$\ell^\mu = c K_1^{b\mu} + d K_3^{b\mu} + \frac{1}{2} \left(t \langle K_1^b | \gamma^\mu | K_3^b \rangle + \frac{cd}{t} \langle K_3^b | \gamma^\mu | K_1^b \rangle \right), \quad (2.51)$$

with

$$c = -\frac{K_3^2(\gamma + K_1^2)}{\gamma^2 - K_1^2 K_3^2}, \quad d = \frac{K_1^2(\gamma + K_3^2)}{\gamma^2 - K_1^2 K_3^2}. \quad (2.52)$$

Contrary to the box case, t is not fixed by the cuts, and needs to be integrated over.

Interestingly, just as in the box case we have two possible solutions for realizing the on-shell conditions in this form. In case that neither K_1^2 nor K_3^2 vanishes these are provided by the two different solutions for γ . Should one or both of the K_i^2 vanish, we have to choose the sign in γ such that it is non-zero. In this case the second solution can be obtained from the one in eq. (2.51) via complex conjugation,

$$\ell^{*\mu} = c K_1^{b\mu} + d K_3^{b\mu} + \frac{1}{2} \left(t [K_1^b | \gamma^\mu | K_3^b] + \frac{cd\gamma - \mu^2}{t\gamma} [K_3^b | \gamma^\mu | K_1^b] \right). \quad (2.53)$$

However, the fact that we have two solutions for the triangle loop momentum does not mean that imposing an additional on-shell condition for the box parametrization would lead to four solutions, which would be in conflict with section 2.2.1.1. Instead, the resulting solutions for ℓ would be degenerate, so we would still only have two distinct solutions.

To obtain the expression for the triangle coefficient $C_{\text{Tri}}^{(1)}$, let us again first act with Cut_{Tri} on the amplitude,

$$\begin{aligned} \text{Cut}_{\text{Tri}}[A^{(1,D)}] &= (-i)(4\pi)^{D/2} i^3 \sum_{h_i=\pm} \int dt J_t \left[A_1^{(0)} \left((-\ell)^{\bar{h}_1}, \{K_1\}, (\ell - K_1)^{h_2} \right) \right. \\ &\quad \times A_2^{(0)} \left((-\ell + K_1)^{\bar{h}_2}, \{K_2\}, (\ell + K_3)^{h_3} \right) \\ &\quad \left. \times A_3^{(0)} \left((-\ell - K_3)^{\bar{h}_3}, \{K_3\}, \ell^{h_1} \right) \right] \\ &= -(4\pi)^{D/2} \int dt J_t \sum_{\ell=\ell(t), \ell^*(t)} A_1^{(0)}(\ell) A_2^{(0)}(\ell) A_3^{(0)}(\ell) \end{aligned} \quad (2.54)$$

We again have to sum over the two solutions for the cut loop momentum $\ell(t)$ and $\ell^*(t)$. The

t -dependent factor J_t collects all remaining factors, whose exact form will end up being irrelevant to determining the triangle coefficients.

At this point the box and triangle contributions are still mixed together, and we need to separate the two. Fortunately this task is simple in this case. As we used the parameter t to enforce the fourth on-shell condition in the box case, box contributions will be associated with t poles of the product $A_1^{(0)}(\ell)A_2^{(0)}(\ell)A_3^{(0)}(\ell)$. All such poles have to be at finite values t_i . Thus to obtain the proper triangle contributions we need only remove all parts of the product of amplitudes that has a pole at finite values of t . This is a simple task when considering the large- t expansion of $A_1^{(0)}(\ell)A_2^{(0)}(\ell)A_3^{(0)}(\ell)$, as in this limit any finite pole will behave as

$$\frac{1}{t - t_i} = \frac{1}{t} + \mathcal{O}\left[\left(\frac{1}{t}\right)^2\right] \quad (2.55)$$

To make this separation of the pole terms from the triangle coefficient more explicit, we use the notation of refs. [60, 95, 96]. Given a function $f(x)$, we define $\text{Inf}_x[f(x)]$ as,

$$f(x) = \text{Inf}_x[f(x)] + \mathcal{O}\left[\left(\frac{1}{x}\right)^1\right], \quad (2.56)$$

such that in general

$$\text{Inf}_x[f(x)] = \sum_{i=0}^m c_i x^i. \quad (2.57)$$

The maximal power m is either an integer or ∞ , depending on the large- x behavior of $f(x)$. Using Inf , we can therefore express $f(x)$ via,

$$f(x) = \text{Inf}_x[f(x)] + \sum_{\text{poles } x_i} \frac{\text{Res}_{x=x_i}[f(x)]}{x - x_i}, \quad (2.58)$$

assuming $f(x)$ has only single poles in x . For later discussions we also define the notation,

$$\text{Inf}_{x_1 x_2 \dots x_n}[g(x)] \equiv \text{Inf}_{x_1} \circ \text{Inf}_{x_2} \circ \dots \circ \text{Inf}_{x_n}[g(x)]. \quad (2.59)$$

Applying eq. (2.58) to the product of trees in eq. (2.54) we obtain

$$A_1^{(0)}(\ell)A_2^{(0)}(\ell)A_3^{(0)}(\ell) = \text{Inf}_t \left[A_1^{(0)}(\ell)A_2^{(0)}(\ell)A_3^{(0)}(\ell) \right] + \sum_{\text{poles } t_i} \frac{\text{Res}_{t=t_i} \left[A_1^{(0)}(\ell)A_2^{(0)}(\ell)A_3^{(0)}(\ell) \right]}{t - t_i}. \quad (2.60)$$

When applying Cut_{Tri} to both sides of eq. (2.22), the $1/(t - t_i)$ terms would match up with box terms of the type $\text{C}_{\text{Box}}^{(1)} \text{Cut}_{\text{Tri}}[I_4^D[1]]$. As we have already determined the box coefficients we can just ignore these pole terms and focus on the Inf_t contribution belong to the triangle in question,

$$\text{Cut}_{\text{Tri}}[A^{(1),D}] = -(4\pi)^{D/2} \sum_{h_i=\pm} \int dt J_t \sum_{\ell=\ell(t), \ell^*(t)} \text{Inf}_t \left[A_1^{(0)}(\ell)A_2^{(0)}(\ell)A_3^{(0)}(\ell) \right] + (\text{Boxes}). \quad (2.61)$$

The Inf_t terms introduce integrals of the form,

$$\int dt J_t t^n. \quad (2.62)$$

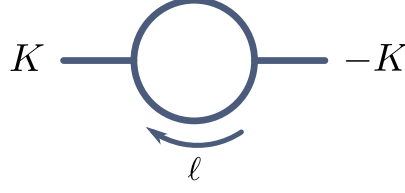


Figure 2.4: A generic bubble cut. Assuming the massive momentum K to be outgoing, we define the loop momentum ℓ to be flowing from the $-K$ and into the K corner.

They vanish for $n \neq 0$ [95, 97],

$$\int dt J_t t^n = 0, \quad \forall n \neq 0, \quad (2.63)$$

which is a special feature of the parametrization used. Eq.(2.61) therefore turns into,

$$\text{Cut}_{\text{Tri}}[A^{(1),D}] = -(4\pi)^{D/2} \sum_{h_i=\pm} \sum_{\ell=\ell(t),\ell^*(t)} \text{Inf}_t \left[A_1^{(0)}(\ell) A_2^{(0)}(\ell) A_3^{(0)}(\ell) \right]_{t^0} \int dt J_t + (\text{Boxes}). \quad (2.64)$$

where in $\text{Inf}_t [\dots]_{t^0}$ we only keep the term proportional to t^0 . Acting with Cut_{Tri} on our target triangle integral results in,

$$\begin{aligned} \text{Cut}_{\text{Tri}}[C_{\text{Tri}}^{(1)} I_3^D[1]] &= i(4\pi)^{D/2} C_{\text{Tri}}^{(1)} \int dt J_t (-i)^3 \sum_{\ell=\ell(t),\ell^*(t)} 1 \\ &= -2(4\pi)^{D/2} C_{\text{Tri}}^{(1)} \int dt J_t. \end{aligned} \quad (2.65)$$

Comparing eqs.(2.64) and (2.65) we can determine the coefficient $C_{\text{Tri}}^{(1)}$ to be,¹

$$C_{\text{Tri}}^{(1)} = \frac{1}{2} \sum_{h_i=\pm} \sum_{\ell=\ell(t),\ell^*(t)} \text{Inf}_t \left[A_1^{(0)}(\ell) A_2^{(0)}(\ell) A_3^{(0)}(\ell) \right]_{t^0}. \quad (2.66)$$

2.2.1.3 Bubble Coefficients

Finally, we need to determine the coefficients of bubble integrals in the basis of eq. (2.22). In bubble integrals we have only one external massive momentum K , and we define the loop momentum ℓ as shown in Figure 2.4.

We now apply two generalized cuts to either side of eq. (2.22). Computing the residues associated to the on-shell conditions,

$$\ell^2 = 0, \quad (\ell - K)^2 = 0 \quad (2.67)$$

defines the bubble cut Cut_{Bub} . In the basis this removes all unwanted bubble contributions, leaving us with the desired bubble integral. However, just as in the triangle case, there exist triangle and box integrals in the basis, which share these propagators, and therefore are non-vanishing under such bubble cuts. We will again have to perform additional steps to extract the pure bubble coefficient.

As in the triangle case, the derivation of the bubble coefficient will depend on the specific loop

¹The sign agrees with ref. [95] after accounting for the $(-i)$ normalization of amplitudes used in this thesis. The expression of ref. [96] requires a sign flip to match this result.

momentum parametrization we use to make the on-shell conditions manifest. We would like to choose a parametrization similar to the box and triangle case. However, in this case we cannot define such a parametrization entirely in terms of the external kinematics, as we have only a single momentum K . We therefore need to introduce an arbitrary reference momentum χ . Choosing χ to be lightlike, we define the flattened version of K to be,

$$K^b = K - \frac{K^2}{\gamma} \chi, \quad (2.68)$$

where

$$\gamma = 2(K \cdot \chi) = 2(K^b \cdot \chi). \quad (2.69)$$

In analogy to the box and triangle cases, we make the Ansatz for the loop-momentum ℓ [95],

$$\ell^\mu = y K^{b\mu} + d \chi^\mu + \frac{1}{2} \left(t \langle K^b | \gamma^\mu | \chi \rangle + b \langle \chi | \gamma^\mu | K^b \rangle \right). \quad (2.70)$$

The on-shell conditions $\ell^2 = 0$ and $(\ell - K)^2 = 0$ then fix the parameters b and d to be,

$$d = \frac{K^2(1-y)}{\gamma}, \quad b = \frac{yd}{t} = \frac{y(1-y)K^2}{t\gamma}, \quad (2.71)$$

such that

$$\ell^\mu(t, y) = y K^{b\mu} + \frac{K^2(1-y)}{\gamma} \chi^\mu + \frac{1}{2} \left(t \langle K^b | \gamma^\mu | \chi \rangle + \frac{y(1-y)K^2}{t\gamma} \langle \chi | \gamma^\mu | K^b \rangle \right). \quad (2.72)$$

In contrast to the box and triangle case there exists only one solution, dependent on two parameters t and y .

We again first act with Cut_{Bub} on the amplitude,

$$\begin{aligned} \text{Cut}_{\text{Bub}}[A^{(1),D}] &= (-i)(4\pi)^{D/2} i^2 \sum_{h_i=\pm} \int dt dy J_{t,y} \left[A_1^{(0)} \left((-\ell)^{\bar{h}_1}, \{K\}, (\ell - K)^{h_2} \right) \right. \\ &\quad \left. \times A_2^{(0)} \left((-\ell + K)^{\bar{h}_2}, \{-K\}, \ell^{h_1} \right) \right] \\ &= i(4\pi)^{D/2} \int dt dy J_{t,y} A_1^{(0)}(\ell(t, y)) A_2^{(0)}(\ell(t, y)), \end{aligned} \quad (2.73)$$

leaving us with two integrals over the parameters t and y . As we will see, the process of disentangling the bubble coefficient from the box and triangle contributions is more subtle here, so we will proceed slowly. We first apply the decomposition of eq. (2.58) to the product of tree amplitudes with respect to the variable y ,

$$\begin{aligned} \text{Cut}_{\text{Bub}}[A^{(1),D}] &= i(4\pi)^{D/2} \int dt dy J_{t,y} \left[\text{Inf}_y \left[A_1^{(0)}(\ell(t, y)) A_2^{(0)}(\ell(t, y)) \right] \right. \\ &\quad \left. + \sum_{\text{poles } y_i} \frac{\text{Res}_{y=y_i} \left[A_1^{(0)}(\ell(t, y)) A_2^{(0)}(\ell(t, y)) \right]}{y - y_i} \right]. \end{aligned} \quad (2.74)$$

The poles in y stem from additional propagators in either of the amplitudes $A_1^{(0)}$ or $A_2^{(0)}$. The term

$\text{Res}_{y=y_i} [A_1^{(0)}(\ell(t, y))A_2^{(0)}(\ell(t, y))]$ therefore descends from box and triangle integrals. On the other hand, $\text{Inf}_y [A_1^{(0)}(\ell(t, y))A_2^{(0)}(\ell(t, y))]$ by definition has no poles in y . An important consequence is that it does not possess any poles in t either. The source of the y poles is one additional propagator going on-shell. Each of these poles could equally be expressed as a t pole. However, as by definition the Inf_y term is entirely made up of contributions where no additional propagator can go on-shell, we certainly cannot have any poles in t . Another way of seeing this is to consider the effect of the Inf_y operation on an additional, uncut propagator with some momentum Q , *i.e.*

$$\frac{1}{(\ell(t, y) + Q)^2} = \left[y 2(Q \cdot K^\flat) + \frac{K^2(1-y)}{\gamma} 2(Q \cdot \chi) + t \langle K^\flat | K_3 | \chi \rangle + \frac{y(1-y)K^2}{t\gamma} \langle \chi | Q | K^\flat \rangle + Q^2 \right]^{-1}. \quad (2.75)$$

To obtain the Inf_y terms we have to series-expand this propagator for large values of y . As long as there remains any y dependence in the propagator, the resulting expansion does not contain any poles in t . The only case in which all y dependent terms in eq. (2.75) disappear is for Q to simultaneously satisfy the three conditions,

$$K_3 \cdot K^\flat = 0, \quad K_3 \cdot \chi = 0, \quad \langle \chi | K_3 | K^\flat \rangle = 0. \quad (2.76)$$

The only values of Q for which all conditions are satisfied is,

$$Q^\mu = C \times \langle \chi | \gamma^\mu | K^\flat \rangle, \quad (2.77)$$

for some constant C . As χ cannot be K^\flat , this Q would have to be complex, and the propagator would turn into,

$$\frac{1}{(\ell(t, y) + Q)^2} = -\frac{1}{C\gamma t}. \quad (2.78)$$

Besides always being able to choose a value of χ for which this alignment does not occur, ref. [95] showed that the associated t integral vanishes.

Returning to the cut amplitude, we now apply the decomposition of eq. (2.58) with respect to t , so that eq. (2.74) turns into,

$$\begin{aligned} \text{Cut}_{\text{Bub}}[A^{(1,D)}] = & i(4\pi)^{D/2} \int dt dy J_{t,y} \left[\text{Inf}_{t,y} [A_1^{(0)}(\ell(t, y))A_2^{(0)}(\ell(t, y))] \right. \\ & + \text{Inf}_t \left[\sum_{\text{poles } y_i} \frac{\text{Res}_{y=y_i} [A_1^{(0)}(\ell(t, y))A_2^{(0)}(\ell(t, y))]}{y - y_i} \right] \\ & \left. + \sum_{\text{poles } y_i} \sum_{\text{poles } t_i(y_i)} \frac{\text{Res}_{t=t_i} \left[\frac{\text{Res}_{y=y_i} [A_1^{(0)}(\ell(t, y))A_2^{(0)}(\ell(t, y))]}{y - y_i} \right]}{t - t_i(y_i)} \right], \end{aligned} \quad (2.79)$$

using the notation introduced in eq. (2.59). Note that the Inf and Res operations for t and y

generally do not commute. Particularly, the sum over poles in t includes only those left over after the y_i residue, which is the reason for the notation $t_i(y_i)$. The double residue terms belong to scalar box integrals, while the double Inf term will contribute to the bubble coefficient. The parameter integrals involved have been determined in ref. [95]. For positive powers in t they vanish

$$\int dt dy J_{t,y} t^{i \neq 0} y^j = 0. \quad (2.80)$$

Power counting limits the maximal power in y in gauge-theory amplitudes to two. The associated integrals

$$Y_i = \int dt dy J_{t,y} y^i \quad (2.81)$$

evaluate to [95]

$$Y_0 = 1, \quad Y_1 = -\frac{1}{2}, \quad Y_2 = \frac{1}{3}, \quad (2.82)$$

where I use the notation of ref. [96]. In practice this integration can be carried out via a simple replacement, as

$$\int dt dy J_{t,y} \text{Inf}_{t,y} \left[A_1^{(0)}(\ell(t,y)) A_2^{(0)}(\ell(t,y)) \right] \equiv \text{Inf}_{t,y} \left[A_1^{(0)} A_2^{(0)} \right] \Big|_{t^0, y^i \rightarrow Y_i}. \quad (2.83)$$

The mixed $\text{Inf}_t[\text{Res}_y]$ term in eq. (2.79) requires more careful consideration. The pole in y clearly identifies them as contributions originating from integrals with three propagators, *i.e.* triangle integrals. However, this does not mean that they belong entirely to triangle coefficients. We have to keep in mind that when the loop momentum appears in the numerator, we are dealing with tensor integrals, which after Passarino–Veltman reduction can contain terms with only two propagators. Such terms would also contribute to bubble coefficients. After the Inf_t operation, the second term of eq. (2.79) contains only positive powers of t in the numerator, and these powers of t can only appear through the presence of the loop momentum in the numerator. The t^0 terms do belong to the scalar triangle integrals, and therefore to triangle coefficients. For the remaining powers t^i we have to use Passarino–Veltman reduction to obtain the contribution to the bubble coefficient.

To obtain the tensor integral terms, we take a step back and relate the y_i pole terms of eq. (2.74) to triangle cuts. The poles in y originate from on-shell propagators, and as we saw in discussion of triangle cuts, three on-shell conditions lead to two distinct solutions. The poles in y_i will therefore always come in pairs, with each pair belonging to a specific third on-shell propagator. Let us therefore consider a specific propagator $(\ell + K')^2$. Its on-shell condition translates into,

$$\begin{aligned} & (\ell(t,y) + K')^2 = 0 \\ \Rightarrow & \left[y 2(K' \cdot K^b) + \frac{K^2(1-y)}{\gamma} 2(K' \cdot \chi) + t \langle K^b | K' | \chi \rangle + \frac{y(1-y)K^2}{t\gamma} \langle \chi | K' | K^b \rangle + (K')^2 \right] = 0, \end{aligned} \quad (2.84)$$

which we can solve for y [96],

$$y^\pm = \frac{c_1 \pm \sqrt{c_1^2 + 4c_0c_2}}{2c_2}, \quad (2.85)$$

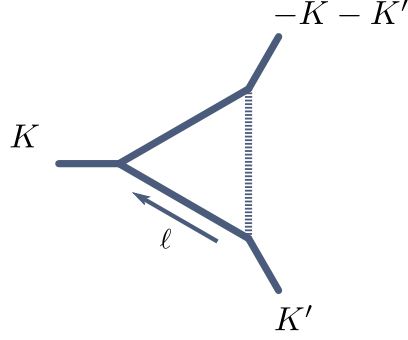


Figure 2.5: An example of a triangle cut contributing to the bubble coefficient. The momentum K and the solid lines are those belonging to the original bubble. The momentum K' and dashed lines are those of the additional on-shell condition.

with

$$\begin{aligned} c_0 &= t [\gamma(K')^2 + 2(K' \cdot \chi)K^2] + t^2 \gamma \langle K^\flat | K' | \chi \rangle, \\ c_1 &= K^2 \langle \chi | K' | K^\flat \rangle + t [\gamma 2(K' \cdot K^\flat) - K^2 2(K' \cdot \chi)], \\ c_2 &= K^2 \langle \chi | K' | K^\flat \rangle. \end{aligned} \quad (2.86)$$

We can make the poles of the propagator in y manifest by rewriting it in the form,

$$\frac{1}{(\ell + K')^2} = \frac{-t\gamma}{K^2 \langle \chi | K' | K^\flat \rangle} \frac{1}{(y - y^+)(y - y^-)}. \quad (2.87)$$

Let us further assume that this propagator is part of $A_2^{(0)}$ in eq. (2.79), and define,

$$\tilde{A}_2^{(0)} = (\ell + K')^2 A_2^{(0)}, \quad (2.88)$$

with this propagator removed, such that,

$$\begin{aligned} &\tilde{A}_2^{(0)} ((-\ell + K)^{h_2}, \{-K\}, \ell^{h_1}) \\ &\xrightarrow{(\ell + K')^2 \rightarrow 0} - \sum_{h'=\pm} A_{2,1}^{(0)} ((-\ell + K)^{h_2}, \{-K - K'\}, (\ell + K')^{h'}) A_{2,2}^{(0)} ((-\ell - K')^{h'}, \{K'\}, \ell^{h_1}). \end{aligned} \quad (2.89)$$

The factor of (-1) and sum over polarization states stem from the gluon propagator's numerator, as we have only removed its denominator². This configuration is shown in Figure 2.5. To compute the residues at y^\pm we need to decompose the propagator. Looking only at the poles y^\pm in the sum

²We also absorbed a factor of $-i$ into definition of the second amplitude

over poles y_i , the second term of eq. (2.74) can be written as

$$\begin{aligned}
& i(4\pi)^{D/2} \int dt dy J_{t,y} \sum_{y_i=y^\pm} \frac{1}{y-y_i} \text{Res}_{y=y_i} \left[A_1^{(0)}(\ell(t,y)) A_2^{(0)}(\ell(t,y)) \right] \\
&= i(4\pi)^{D/2} \int dt dy J_{t,y} \sum_{y_i=y^\pm} \frac{1}{y-y_i} \text{Res}_{y=y_i} \left[A_1^{(0)}(\ell(t,y)) \frac{\tilde{A}_2^{(0)}(\ell(t,y))}{(\ell+K_2)^2} \right] \\
&= i(4\pi)^{D/2} (2\pi i) \int dt \sum_{y_i=y^\pm} J_{t,y_i} \text{Res}_{y=y_i} \left[A_1^{(0)}(\ell(t,y)) \frac{\tilde{A}_2^{(0)}(\ell(t,y))}{(\ell+K_2)^2} \right] \\
&= -i(4\pi)^{D/2} (2\pi i) \int dt dy \tilde{J}'_t (\delta(y-y^+) + \delta(y-y^-)) A_1^{(0)}[\ell(t,y)] A_{2,1}^{(0)}[\ell(t,y)] A_{2,2}^{(0)}[\ell(t,y)]
\end{aligned} \tag{2.90}$$

This can be related to a triangle cut of the amplitude, where in the loop-momentum parametrization of eq. (2.72) we fix y to y^\pm to fulfill the third on-shell condition. We will call this operation $\text{Cut}_{\text{tri}/\text{bub}}$. Expressing the residue fixing y as two delta functions, careful evaluation of the Jacobians leads to [95],

$$\begin{aligned}
& \text{Cut}_{\text{tri}/\text{bub}} \left[A^{(1),D} \right] \\
&= -i(4\pi)^{D/2} i^3 \int dt dy J'_t (\delta(y-y^+) + \delta(y-y^-)) A_1^{(0)}[\ell(t,y)] A_{2,1}^{(0)}[\ell(t,y)] A_{2,2}^{(0)}[\ell(t,y)] \\
&= -i(4\pi)^{D/2} 2(2\pi i) \int dt dy \tilde{J}'_t (\delta(y-y^+) + \delta(y-y^-)) A_1^{(0)}[\ell(t,y)] A_{2,1}^{(0)}[\ell(t,y)] A_{2,2}^{(0)}[\ell(t,y)]
\end{aligned} \tag{2.91}$$

Comparing with the last line of eq. (2.90), we can identify the pole part of the bubble cut with triangle cuts of the amplitude using the bubble parametrization, up to a factor of 2.

Having connected the terms with poles in y to triangle cuts, we still need to expand this cut for large values of t , as indicated by the Inf_t operation in eq. (2.79). We then need to determine the parameter integrals of the triangle cut,

$$T_i = \int dt J'_t t^i. \tag{2.92}$$

We only need to consider integrals over non-zero powers of t , as only these are related to tensor integrals, and can therefore contain a bubble contribution. Performing the Passarino-Veltman reduction results in [95],

$$\begin{aligned}
T_1 &= -\frac{K^2 \langle \chi | K' | K^\flat \rangle}{2\gamma [(K \cdot K')^2 - K^2 K'^2]}, \\
T_2 &= \frac{3(K^2)^2 \langle \chi | K' | K^\flat \rangle^2}{8\gamma^2 [(K \cdot K')^2 - (K^2) K'^2]^2} [(K \cdot K') + K'^2] \\
T_3 &= -\frac{(K^2)^3 \langle \chi | K' | K^\flat \rangle^3}{48\gamma^3 [(K \cdot K')^2 - K^2 K'^2]^3}, \\
&\quad \times (11(K \cdot K')^2 + 30(K \cdot K') K'^2 + K'^2 (4K^2 + 15K'^2)).
\end{aligned} \tag{2.93}$$

Again, in practice this integration can be carried out by replacing each power of t^i in the Inf_t expansion by T_i ,

$$\text{Inf}_t \left[A_1^{(0)} A_2^{(0)} A_3^{(0)} \right] \Big|_{t^i > 0 \rightarrow T_i}. \tag{2.94}$$

We now have all ingredients to find a compact form for the bubble coefficient. Applying the bubble cut to the bubble basis integral leads to

$$\begin{aligned} \text{Cut}_{\text{Bub}}[C_{\text{Bub}}^{(1)} I_2^D[1]] &= i(4\pi)^{D/2} C_{\text{Bub}}^{(1)} \int dt dy J_{t,y} \\ &= i(4\pi)^{D/2} C_{\text{Bub}}^{(1)}, \end{aligned} \quad (2.95)$$

where in the second equality we use the definition of Y_0 of eq. (2.82). Comparing with eq. (2.79) and using the relation between the y pole terms and triangle cuts, we finally find for the bubble coefficient,

$$C_{\text{Bub}}^{(1)} = \text{Inf}_{t,y} [A_1^{(0)} A_2^{(0)}] \Big|_{t^0, y^i \rightarrow Y_i} + \frac{1}{2} \sum_{\substack{\text{triangle} \\ \text{cuts}}} \sum_{y^\pm} \text{Inf}_t [A_1^{(0)} A_2^{(0)} A_3^{(0)}] \Big|_{t^i > 0 \rightarrow T_i}. \quad (2.96)$$

2.3 D -Dimensional Generalized Unitarity

In the discussion of the four-dimensional generalized unitarity method of the previous section we ignored any contributions from the (-2ϵ) components of the D -dimensional loop momentum. Instead, as the name suggests, we formulated the on-shell conditions under the assumption that ℓ has four components, just as do the external momenta, hence the name. Such unitarity cuts probe branch cuts in the four-dimensional kinematics, allowing us to determine any parts of an amplitude that contain such discontinuities. However, loop amplitudes in Yang–Mills generally also contain terms that are rational in the kinematics, and therefore are not obtainable from four-dimensional unitarity. These can be interpreted as the result of cancellations between $\frac{1}{\epsilon}$ UV-poles of integrals with order ϵ parts of integral coefficients. Therefore, to capture these rational parts we need to compute the integral coefficients by cutting propagators carrying D -dimensional loop momenta. This technique is accordingly referred to as D -dimensional generalized unitarity [26, 98–103]. In the following we will review the procedure presented in ref. [96].

We will always take the external momenta to be purely four-dimensional. It is then convenient to split all loop-momenta ℓ_i into their 4- and $(D-4)$ -dimensional parts $\bar{\ell}_i, \tilde{\ell}_i$, such that,

$$\ell_i = \bar{\ell}_i + \tilde{\ell}_i. \quad (2.97)$$

Due to the external kinematics being four-dimensional, the $\tilde{\ell}_i$ are guaranteed to be conserved within each loop, and we can separate the integrations over $\bar{\ell}_i$ and $\tilde{\ell}_i$,

$$\int \frac{d^D \ell}{(2\pi)^D} \rightarrow \int \frac{d^{D/2-2} \mu^2}{(2\pi)^{D-4}} \int \frac{d^4 \bar{\ell}}{(2\pi)^4}. \quad (2.98)$$

Due to the external kinematics being four-dimensional, and requiring Lorentz invariance, guarantees that the only structures the $\tilde{\ell}$ can appear in are,

$$\tilde{\ell}_i \cdot \tilde{\ell}_i = \mu_i^2, \quad \tilde{\ell}_i \cdot \tilde{\ell}_j = \mu_{ij}. \quad (2.99)$$

Specializing to the one-loop case, we therefore extend the definition of one-loop Feynman integrals

in eq. (2.1) to include numerators $\mathcal{N}[\bar{\ell}, \mu^2]$ depending on μ^2 , such that,

$$I_n^D[\mathcal{N}[\bar{\ell}, \mu^2]] = (-i)(-1)^n (4\pi)^{D/2} \mathcal{I}_n^D[\mathcal{N}[\bar{\ell}, \mu^2]], \quad (2.100)$$

where,

$$\begin{aligned} \mathcal{I}_n^D[\mathcal{N}[\bar{\ell}, \mu^2]] &= \int \frac{d^D \ell}{(2\pi)^D} \frac{\mathcal{N}[\bar{\ell}, \mu^2]}{\ell^2 (\ell - K_1)^2 \dots (\ell - K_1 - \dots - K_{n-1})^2} \\ &= \int \frac{d^{D/2-2} \mu^2}{(2\pi)^{D-4}} \int \frac{d^4 \bar{\ell}}{(2\pi)^4} \frac{\mathcal{N}[\bar{\ell}, \mu^2]}{(\bar{\ell}^2 - \mu^2) ((\bar{\ell} - K_1)^2 - \mu^2) \dots ((\bar{\ell} - K_{1\dots n-1})^2 - \mu^2)}. \end{aligned} \quad (2.101)$$

2.3.1 One-Loop Integral Basis in D Dimensions

When cutting D -dimensional propagators, the on-shell condition for ℓ can be rewritten in terms of $\bar{\ell}$ and $\tilde{\ell}$ via

$$\ell^2 = 0 \Rightarrow \bar{\ell}^2 = -\tilde{\ell}^2 = \mu^2. \quad (2.102)$$

We can therefore treat cuts involving the D -dimensional loop momentum ℓ as four-dimensional cuts of the massive loop momentum $\bar{\ell}$, where the cut propagators include a mass term μ^2 [104, 105]. The resulting integral coefficients will be dependent on both the external kinematics, as well as μ^2 . As μ^2 vanishes for $D \rightarrow 4$ we can interpret this μ^2 dependence to represent contributions of higher order in ϵ .

The coefficients can only depend on powers of μ^2 , as any poles in μ^2 have to originate from additional propagators. The maximal power of μ^2 is limited by power counting, meaning that for boxes at most μ^4 can appear, while for triangles and bubbles, only powers up to μ^2 are allowed. The box μ^2 integral is of order ϵ , and therefore does not contribute.

To determine a basis of one-loop integrals in $D = 4 - 2\epsilon$ dimensions, we can again use the integral reduction arguments described in section 2.1. As the loop-momentum is now D -dimensional we can no longer ignore the -2ϵ components in the Gram determinant of eq. (2.8) when reducing pentagon integrals. We thus need to include such integrals in a full D -dimensional basis. However, if we are only interested in the amplitude up to terms of order ϵ , it is sufficient to work with an integral basis of the form [96],

$$\begin{aligned} A^{(1), 4-2\epsilon} &= \sum C_{\text{Box}, [0]}^{(1)} I_4^D[1] + \sum C_{\text{Tri}, [0]}^{(1)} I_3[1] + \sum C_{\text{Bub}, [0]}^{(1)} I_2[1] \\ &+ \sum C_{\text{Box}, [4]}^{(1)} I_4^D[\mu^4] + \sum C_{\text{Tri}, [2]}^{(1)} I_3[\mu^2] + \sum C_{\text{Bub}, [2]}^{(1)} I_2^D[\mu^2] + \mathcal{O}(\epsilon) \end{aligned} \quad (2.103)$$

The integrals without powers of μ^2 in their numerators are the parts of the amplitude obtainable from four-dimensional unitarity. The integrals with μ^2 numerator insertions evaluate to [96],

$$\begin{aligned} I_4^D[\mu^4] &= -\frac{1}{6} + \mathcal{O}(\epsilon), \quad I_3^D[\mu^2] = -\frac{1}{2} + \mathcal{O}(\epsilon), \\ I_2^D[\mu^2] &= -\frac{s}{6} + \mathcal{O}(\epsilon), \end{aligned} \quad (2.104)$$

where s is the square of the momentum flowing through the bubble. A derivation of these integrals, as well integrals with higher powers of μ^2 in the numerator can be found in appendix A.4. The

Amplitude	Vectors	Fermions	Scalars (complex)
$A_s^{(1)}$	-	-	1
$A_{\mathcal{N}=1}^{(1)}$ (chiral)	-	1	1
$A_{\mathcal{N}=4}^{(1)}$	1	4	3

Table 2.1: Particle spectrum appearing in the loop of scalar and supersymmetric one-loop amplitudes.

μ^2 integrals do not appear in the four-dimensional construction and make up the rational parts of the amplitude [96],

$$R^{(1)} = \sum C_{\text{Box},[4]}^{(1)} I_4^D[\mu^4] + \sum C_{\text{Tri},[2]}^{(1)} I_3[\mu^2] + \sum C_{\text{Bub},[2]}^{(1)} I_2^D[\mu^2] + \mathcal{O}(\epsilon). \quad (2.105)$$

2.3.2 SUSY Decomposition

In computing loop amplitudes from D -dimensional unitarity cuts, the states crossing cut propagators need to be D -dimensional. As we keep the external particles four-dimensional, we in principle need to use tree amplitudes with a mixture of D - and four-dimensional states. For gluons and fermions this is inconvenient as we would have to work with a non-integer number of states crossing the cut propagators. We would much prefer to work with amplitudes where the number of states does not depend on the dimension, which is only the case for scalars.

A common trick in D -dimensional generalized unitarity computations at one loop is to use the supersymmetry decomposition. A gluonic one-loop amplitude can be expressed in terms of supersymmetric amplitudes $A_{\mathcal{N}=4}^{(1)}$, $A_{\mathcal{N}=1}^{(1)}$, as well as amplitudes with a complex scalar in the loop $A_s^{(1)}$. The complex scalar appearing in $A_s^{(1)}$ can be thought of as a sum of two real scalars in the loop. In all of these, the external states are taken to be the same, such that they only differ by the particle spectrum in the loop, which is shown in Table 2.1.

An amplitude $A_g^{(1)}$ with only a gluon loop can be rewritten as,

$$A_g^{(1)} = A_{\mathcal{N}=4}^{(1)} - 4A_{\mathcal{N}=1}^{(1)} + A_s^{(1)}. \quad (2.106)$$

We can convince ourselves of this by counting the number of gluonic, fermionic and scalar states. The $\mathcal{N} = 4$ amplitude provides the two gluonic helicity states that we are after. At the same time it includes fermionic degrees of freedom, which we cancel by subtracting the $\mathcal{N} = 1$ amplitude four times. Both $A_{\mathcal{N}=4}^{(1)}$ and $A_{\mathcal{N}=1}^{(1)}$ come with additional scalars. Cancelling the fermions subtracted one too many complex scalars in the loop, such that we need to add back the scalar amplitude $A_s^{(1)}$. For an amplitude $A_f^{(1)}$ with only a fermion in the loop we find a similar decomposition,

$$A_f^{(1)} = A_{\mathcal{N}=1}^{(1)} - A_s^{(1)}. \quad (2.107)$$

Having determined most of the amplitude from four-dimensional unitarity, we only need to use D -dimensional unitarity to determine the rational part. The benefit of the supersymmetry decomposition is that supersymmetric amplitudes are entirely cut-constructible, and particularly do not contain any rational parts. Therefore, in the relations of eqs.(2.106) and (2.107) the only

source of rational terms are the scalar amplitudes $A_s^{(1)}$, such that,

$$R_g^{(1)} = R_s^{(1)}, \quad R_g^{(1)} = -R_s^{(1)}. \quad (2.108)$$

Computing $R_s^{(1)}$ via D -dimensional cuts is unproblematic: The cuts of D -dimensional massless scalar propagators are equivalent to four-dimensional cuts of massive scalars with mass μ^2 . We can therefore apply the D -dimensional unitarity approach, using tree-amplitudes of four-dimensional massive scalars in the cuts.

2.3.3 Loop-Momentum Parametrization for D -Dimensional Cuts

To be able to carry out the projection onto the new integral basis involving μ^2 terms, we need to adapt the loop momentum parameterization of section 2.2. Following the approach of interpreting the D -dimensional cut momenta as massive four-dimensional momenta with mass μ^2 , we parametrize $\bar{\ell}$, such that it fulfills the cut conditions $\bar{\ell}_i^2 = \mu^2$. Besides the parameters already introduced in the four-dimensional cuts, the loop momentum will additionally depend on μ^2 . This method presented here is that of ref. [96].

2.3.3.1 Boxes

Let us again start with the box cut. We use the same conventions as in the four-dimensional discussion, and make an Ansatz for the four-dimensional part of the loop momentum $\bar{\ell}$ in terms of the flattened momenta K_1^\flat and K_4^\flat ,

$$\bar{\ell}^\mu = cK_1^{\flat\mu} + dK_4^{\flat\mu} + \frac{1}{2} \left(t \langle K_1^\flat | \gamma^\mu | K_4^\flat \rangle + b \langle K_4^\flat | \gamma^\mu | K_1^\flat \rangle \right). \quad (2.109)$$

The on-shell conditions $\bar{\ell}^2 = \mu^2$ translates into

$$b = \frac{cd\gamma - \mu^2}{t\gamma}.$$

The on-shell conditions $(\bar{\ell} - K_1)^2 = 0$ and $(\bar{\ell} + K_4)^2 = 0$ fix the parameters c and d to the same values as in the four-dimensional case

$$c = -\frac{K_4^2(\gamma + K_1^2)}{\gamma^2 - K_1^2 K_4^2}, \quad d = \frac{K_1^2(\gamma + K_4^2)}{\gamma^2 - K_1^2 K_4^2}, \quad (2.110)$$

$$\gamma = (K_1 \cdot K_4) \pm \sqrt{(K_1 \cdot K_4)^2 - K_1^2 K_4^2}.$$

The last on-shell condition $(\bar{\ell} - K_1 - K_2)^2 = 0$ provides a quadratic relation for t , with μ^2 dependent solutions

$$t^\pm = \frac{\Delta \pm \sqrt{\Delta^2 - 4 \frac{cd\gamma - \mu^2}{\gamma} \text{tr}_-(K_1^\flat K_2 K_4^\flat K_2)}}{2 \langle K_1^\flat | K_2 | K_4^\flat \rangle}, \quad \Delta = -(2K_2 \cdot (K_1 + cK_1^\flat + dK_4^\flat) + K_2^2) \quad (2.111)$$

For rational terms we only require the leading coefficient in the large μ^2 expansion. In computations it is therefore sufficient to use the leading behavior of the parameterized loop momentum.

Expanding the solutions t^\pm of eq. (2.111) for large values of μ^2 , we obtain

$$t^\pm = \pm \sqrt{\frac{\mu^2}{\gamma}} \frac{\sqrt{\text{tr}_-(K_1^\flat K_2 K_4^\flat K_2)}}{\langle K_1^\flat | K_2 | K_4^\flat \rangle} + \mathcal{O} \left[\left(\frac{1}{\sqrt{\mu^2}} \right)^0 \right] \quad (2.112)$$

To obtain the box coefficients from the cut amplitude, we now require an additional step compared to the four-dimensional case. Applying the D -dimensional box cut

$$\begin{aligned} & \text{Cut}_{\text{Box}} \left[\frac{1}{\bar{\ell}^2 (\ell - K_1)^2 (\ell - K_{12})^2 (\ell + K_4)^2} \right] \\ & \rightarrow (-2\pi i)^4 \delta(\ell^2) \delta((\ell - K_1)^2) \delta((\ell - K_{12})^2) \delta((\ell + K_4)^2) \end{aligned} \quad (2.113)$$

to the amplitude results in a product of four tree-amplitudes, which still depends on μ^2 . We proceed in the same manner as in the case of the four-dimensional triangle and bubble coefficients, splitting the μ^2 dependence into a Inf_{μ^2} and a pole part as

$$\begin{aligned} & A_1^{(0)}(\ell(\mu^2)) A_2^{(0)}(\ell(\mu^2)) A_3^{(0)}(\ell(\mu^2)) A_4^{(0)}(\ell(\mu^2)) \\ & = \text{Inf}_{\mu^2} \left[A_1^{(0)}(\ell(\mu^2)) A_2^{(0)}(\ell(\mu^2)) A_3^{(0)}(\ell(\mu^2)) A_4^{(0)}(\ell(\mu^2)) \right] \\ & + \sum_{\text{poles } \mu_i^2} \frac{\text{Res}_{\mu^2=\mu_i^2} \left[A_1^{(0)}(\ell(\mu^2)) A_2^{(0)}(\ell(\mu^2)) A_3^{(0)}(\ell(\mu^2)) A_4^{(0)}(\ell(\mu^2)) \right]}{\mu^2 - \mu_i^2} \end{aligned} \quad (2.114)$$

The poles in μ^2 stem from an additional propagator, meaning pentagon integrals. As we are presently only interested in the rational contributions, we can discard the pole part as well as the μ^2 and μ^0 terms of Inf_{μ^2} expansion, and we identify μ^4 box coefficient as

$$C_{\text{Box},[4]}^{(1)} = \frac{1}{2} \sum_{t=t^\pm} \text{Inf}_{\mu^2} \left[A_1^{(0)} A_2^{(0)} A_3^{(0)} A_4^{(0)} \right] \Big|_{\mu^4} \quad (2.115)$$

2.3.3.2 Triangles

The procedure for triangle coefficients is largely the same as in the four-dimensional case. Using the same setup as in section 2.2, we parametrize $\bar{\ell}$ in terms of K_1^\flat and K_3^\flat . The D -dimensional on-shell conditions

$$\bar{\ell}^2 = \mu^2, \quad (\bar{\ell} - K_1)^2 = \mu^2, \quad (\bar{\ell} + K_3)^2 = \mu^2 \quad (2.116)$$

lead to the solution [96]

$$\bar{\ell}^\mu = c K_1^{\flat\mu} + d K_3^{\flat\mu} + \frac{1}{2} \left(t \langle K_1^\flat | \gamma^\mu | K_3^\flat \rangle + \frac{cd\gamma - \mu^2}{t\gamma} \langle K_3^\flat | \gamma^\mu | K_1^\flat \rangle \right) \quad (2.117)$$

where just as in the box case,

$$\begin{aligned} c &= -\frac{K_3^2(\gamma + K_1^2)}{\gamma^2 - K_1^2 K_3^2}, \quad d = \frac{K_1^2(\gamma + K_3^2)}{\gamma^2 - K_1^2 K_3^2}, \\ \gamma &= (K_1 \cdot K_3) \pm \sqrt{(K_1 \cdot K_3)^2 - K_1^2 K_3^2}. \end{aligned} \quad (2.118)$$

In the case of γ having only one non-zero value, the second triangle loop-momentum solution can be obtained from complex conjugation

$$\bar{\ell}^{*\mu} = cK_1^{b\mu} + dK_3^{b\mu} + \frac{1}{2} \left(t \langle K_3^b | \gamma^\mu | K_1^b \rangle + \frac{cd\gamma - \mu^2}{t\gamma} \langle K_1^b | \gamma^\mu | K_3^b \rangle \right) \quad (2.119)$$

We treat the additional dependence on μ^2 as in the box case. We first extract the massive “four-dimensional” triangle coefficient using the method of section 2.2. The integrals over non-zero powers of t also vanish for massive four-dimensional propagators, such that we again only require the t^0 terms. We then decompose this coefficient into μ^2 pole terms and the Inf_{μ^2} contribution. The pole terms again belong to coefficients of integrals with additional propagators. For the rational contribution we require the μ^2 triangle integral coefficient, which we obtain via

$$C_{\text{Tri},[2]}^{(1)} = \frac{1}{2} \sum_{\bar{\ell}, \bar{\ell}^*} \text{Inf}_{\mu^2, t} \left[A_1^{(0)} A_2^{(0)} A_3^{(0)} \right] \Big|_{\mu^2, t^0} \quad (2.120)$$

2.3.3.3 Bubble

Finally, we need to find the bubble coefficient proportional to μ^2 . Again, using the setup of the four-dimensional discussion, we find a parametrization of $\bar{\ell}$ in terms of the momentum K flowing through the bubble, as well as an arbitrary reference momentum χ . The on-shell conditions

$$\bar{\ell}^2 = \mu^2, \quad (\bar{\ell} - K)^2 = \mu^2 \quad (2.121)$$

are fulfilled for [96]

$$\bar{\ell}^\mu = yK_1^{b\mu} + \frac{s_1(1-y)}{\gamma} \chi^\mu + \frac{1}{2} \left(t \langle K_1^b | \gamma^\mu | \chi \rangle + \frac{y(1-y)s_1 - \mu^2}{t\gamma} \langle \chi | \gamma^\mu | K_1^b \rangle \right). \quad (2.122)$$

When applying the D -dimensional bubble cut to the amplitude, we again separate terms proportional to positive powers of μ^2 , *i.e.* Inf_{μ^2} , and terms that include poles in μ^2 . For the μ^2 bubble coefficient, the latter can again be discarded, and of the former we require only the μ^2 term, such that

$$C_{\text{Bub},[2]}^{(1)} = \text{Inf}_{\mu^2, t, y} \left[A_1^{(0)} A_2^{(0)} \right] \Big|_{\mu^2, t^0, y^i \rightarrow Y_i} + \frac{1}{2} \sum_{\text{triangle cuts}} \sum_{y^\pm} \left[\text{Inf}_{\mu^2, t} \left[A_1^{(0)} A_2^{(0)} A_3^{(0)} \right] \right] \Big|_{\mu^2, t^i \rightarrow T_i} \quad (2.123)$$

The solutions y^\pm used for the tensor triangle contribution to the bubble coefficient are now also dependent on μ^2 . The additional on-shell condition $(\bar{\ell} + K')^2 = \mu^2$ leads to [96]

$$y^\pm = \frac{c_1 \pm \sqrt{c_1^2 + 4c_0c_2}}{2c_2} \quad (2.124)$$

with

$$\begin{aligned} c_0 &= t [\gamma(K')^2 + 2(K' \cdot \chi)K^2] + t^2\gamma \langle K^b | K' | \chi \rangle - \mu^2 \langle \chi | K' | K^b \rangle \\ c_1 &= K^2 \langle \chi | K' | K^b \rangle + t [\gamma 2(K' \cdot K^b) - K^2 2(K' \cdot \chi)] \\ c_2 &= K^2 \langle \chi | K' | K^b \rangle \end{aligned} \quad (2.125)$$

We additionally need to use a new set of parameter integrals Y_i and T_i which are dependent on μ^2 . The dependence is precisely that of four-dimensional cuts of massive propagators with mass μ^2 . The parameter integrals for such cuts were determined in ref. [97], and specialize in our case to [96]

$$Y_0 = 1, \quad Y_1 = -\frac{1}{2}, \quad Y_2 = \frac{1}{3} \left(1 - \frac{\mu^2}{s} \right), \quad (2.126)$$

and

$$\begin{aligned} T_1 &= -\frac{K^2 \langle \chi | K' | K^\flat \rangle}{2\gamma [(K \cdot K')^2 - K^2 K'^2]}, \\ T_2 &= \frac{3(K^2)^2 \langle \chi | K' | K^\flat \rangle^2}{8\gamma^2 [(K \cdot K')^2 - (K^2)K'^2]^2} [(K \cdot K') + K'^2], \\ T_3 &= -\frac{(K^2)^3 \langle \chi | K' | K^\flat \rangle^3}{48\gamma^3 [(K \cdot K')^2 - K^2 K'^2]^3} \\ &\quad \times \left((K \cdot K')^2 \left(11 + 16 \frac{\mu^2}{K^2} \right) + 30(K \cdot K')K'^2 + K'^2 (4K^2 + 15K'^2 - 16\mu^2) \right). \end{aligned} \quad (2.127)$$

2.4 Color-Dressed Unitarity

In the discussion of generalized unitarity we have so far only focused on the kinematic part of amplitude, while largely ignoring color structures. In fact, in the discussion of one-loop cuts we have been using color-ordered tree amplitudes without properly motivating why these are a sensible choice, or even what color ordering the particle ought to have. In this section we will motivate this construction and see how to obtain unitarity cuts belonging to a specific color structure.

To understand the origin of the color structures in loop amplitudes, their origin from string theory amplitudes provides an instructive picture. An L -loop gauge theory amplitudes can be obtained from taking the infinite tension limit of amplitudes in open string-theory, where the world-sheet is an orientable surface of genus L with at least one boundary. At one-loop the only surface contributing is the annulus, which has two boundaries.

String amplitudes are constructed by placing vertex operators on the boundaries of the world-sheet. They further allow the addition of extra degrees of freedom to the ends of the open string. Endowing each string with a generator T_{ab} and associating the two indices with the ends of the string therefore allows us to realize a gauge group. These extra degrees of freedom are known as Chan-Paton factors. Along the world-sheet boundary the indices are conserved, and summing over all possible index values we recover the familiar traces of generators,

$$T_{a_1 a_2}^1 T_{a_2 a_3}^2 \dots T_{a_n a_1}^n = \text{Tr} (T^1 T^2 \dots T^n). \quad (2.128)$$

Using this construction, each boundary of the world-sheet provides us with exactly one trace. With empty traces simplifying to N_c , amplitudes with the topology of an annulus can therefore have color structures Tr^2 , and $N_c \text{Tr}$. These are exactly the color structures we expect from the color decomposition of one-loop gauge theory amplitudes.

Following this picture we can now motivate a construction of unitarity cuts belonging to the single and double trace gauge-theory amplitudes $A_{n,1}^{(1)}$ and $A_{n,r}^{(1)}$ of section 1.4.2.1. First we see

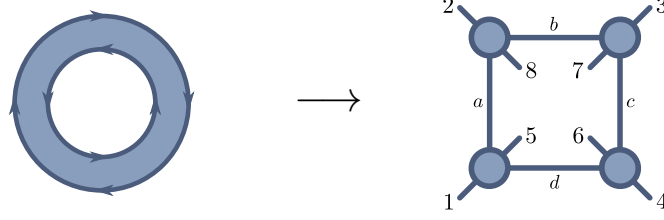


Figure 2.6: One-loop amplitudes in open string theory are obtained from a world-sheet with the topology of an annulus (left). Each boundary provides a trace over color generators. The associated unitarity cuts for gauge-theory amplitudes can be constructed by using color-ordered tree amplitudes, following this scheme (right). The shown cut belongs to an amplitude $A_{8;5}^{(1)}$, with color structure $\text{Tr}(T^1 T^2 T^3 T^4) \text{Tr}(T^5 T^6 T^7 T^8)$

that the single trace amplitudes proportional to N_c are just a special case of the double trace one, where one of the traces does not contain any generators. To build cuts belonging to a specific double trace color structure, we build cuts as explained in sections 2.2 and 2.3 using color-ordered tree amplitudes, choosing the color ordering such that particles of one trace are all on one side of the loop, while those of the second trace are all on the opposing side. As an example, consider the example shown in Figure 2.6. The cut on the right belongs to a double trace amplitude $A_{8;5}^{(1)}$ with color structure $\text{Tr}(T^1 T^2 T^3 T^4) \text{Tr}(T^5 T^6 T^7 T^8)$. We can verify this construction through explicit color algebra. We dress each of the tree amplitudes with their associated color traces, which are contracted via the gluon propagators. The color factor associated to the cut is thus,

$$\text{Tr}(T^1 T^a T^5 T^d) \text{Tr}(T^2 T^b T^8 T^a) \text{Tr}(T^3 T^c T^7 T^b) \text{Tr}(T^4 T^d T^6 T^c). \quad (2.129)$$

For simplicity we assume the gauge group to be $U(N_c)$. We can then use the rules of eq. (1.7) to simplify the contractions,

$$\begin{aligned} & \text{Tr}(T^1 T^a T^5 T^d) \text{Tr}(T^2 T^b T^8 T^a) \text{Tr}(T^3 T^c T^7 T^b) \text{Tr}(T^4 T^d T^6 T^c) \\ &= \text{Tr}(T^1 T^2 T^b T^8 T^5 T^d) \text{Tr}(T^3 T^4 T^d T^6 T^7 T^b) \\ &= \text{Tr}(T^1 T^2 T^3 T^4 T^d T^6 T^7 T^8 T^5 T^d) \\ &= \text{Tr}(T^1 T^2 T^3 T^4) \text{Tr}(T^5 T^6 T^7 T^8), \end{aligned} \quad (2.130)$$

resulting in the expected product of traces.

This method is sometimes referred to as color-dressed unitarity. As an alternative to using color-ordered tree amplitudes, it is also possible to construct cuts using full-color amplitudes. This approach is more efficient in numerical applications, and was for example explored in ref. [106]. Color-dressed unitarity has also been used for the computation of subleading two-loop all-plus partial amplitudes in refs. [4, 10], which are the main topic of this thesis. We will discuss the necessary two-loop extension in the next chapter.

2.5 Generalized Unitarity Implementation in Mathematica

I created a series of *Mathematica* packages that automate the evaluation of one-loop D -dimensional generalized unitarity cuts on kinematic points. These packages are written as addons to the *SpinorHelicity6D* package of ref. [107], which provides the implementation of the four- and six-

dimensional spinor-helicity formalism.

The main challenge in the computation of integral coefficients is the implementation of the `Inf` operation. As a reminder, given some function $f(x)$ that scales like x^p for $x \rightarrow \infty$, we define $\text{Inf}_x[f(x)]$ from its series expansion for large values of x , as,

$$f(x) = \sum_{i=0}^p c_i x^i + \mathcal{O}\left(\frac{1}{x}\right) = \text{Inf}_x[f(x)] + \mathcal{O}\left(\frac{1}{x}\right) \quad (2.131)$$

We use *Mathematica* to perform these series expansions symbolically. While this approach does not provide optimal numerical efficiency, we retain the full flexibility for choosing the kinematics. For one we can use rational kinematics to make exact comparisons with literature results. It also allows us to make use of the symbolic capabilities of *Mathematica* to perform computations on partially or fully parametrized kinematics. Sample applications are the exact verification of collinear behavior, obtaining analytic results from completely parametrized kinematics, or verifying the large- z behavior of loop amplitudes under a BCFW shift.

The products of trees in D -dimensional unitarity cuts are always rational functions in the loop-momentum parameters μ^2 , t and y , with coefficients generically being algebraic in the external kinematics. A significant downside of performing the series expansions symbolically are the possibly deeply nested intermediate expressions that can appear in the evaluation of such cuts even for numerical kinematic points. We therefore avoid the *Mathematica* built-ins `Series` and `SeriesCoefficient`, and instead use our own implementation of these functions `RationalSeries` and `RationalSeriesCoefficient`, which are optimized for expansions of rational functions. Our routines perform the series expansions recursively, caching intermediate results for improved performance.

In addition, we store any coefficients depending only on the external kinematics in symbolic objects called `NumSymb`. These can be defined recursively, and depend on `NumSymb` objects of previous steps in the computation. The dependence of every `NumSymb` object on other `NumSymb` objects can therefore be arranged in the form of directed acyclic graphs. Importantly, we assign the same `NumSymb` for repeated appearances of a specific subexpression, such that every `NumSymb` represents a unique kinematic structure. To avoid unnecessary computations we additionally perform a zero test on each newly defined `NumSymb` object, which can exactly and efficiently be performed using the *Mathematica* function `PossibleZeroQ` with the option `Method->ExactAlgebraics`³. For this zero test all kinematic parameters are set to random integer values with sufficient size to avoid accidental cancellations.

For cut coefficients, only the final result is known to be rational in the kinematics: on purely numeric rational kinematic points it will be a rational number, while for rational kinematics involving analytic parameters, it is a rational function in these parameters. Intermediate expressions can generically involve square roots, which are only guaranteed to vanish in the final result. Performing simplifications in intermediate steps is therefore costly. Furthermore, the final result will not necessarily depend on all of the `NumSymb` objects, as they may cancel or only contribute to powers in the loop-momentum parameters that are not required for the coefficient. We therefore choose to first perform the series expansion without any intermediate simplifications, storing the kinematic dependence in the `NumSymb` objects mentioned before. In the end, the result of the expansion will

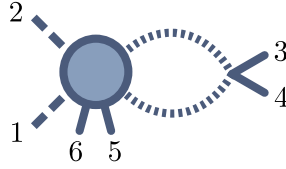
³When using this option the output of `PossibleZeroQ` is guaranteed to be correct [108].

	Rational Kinematics	BCFW shifted Rational Kinematics
Series	209s	automatic abort after 446s
RationalSeries	5.3s	25.3s/+15.5s for simplification

Table 2.2: Comparisons of timings between *Mathematica*'s **Series** and **RationalSeries** for evaluation of one-loop bubble coefficient shown in. The timings in the second column are for an evaluation on purely numeric rational kinematics. For the timings in the third column, the numerical rational kinematics shifted by a BCFW shift involving an analytic parameter z . For the evaluation using **Series** we provide *Mathematica* with the assumption that z is numeric.

be a single **NumSymb** object. We then simplify the result by traversing the dependency graph of this final **NumSymb** object, and perform simplifications from the bottom up, or depth-first. This ensures that we perform only simplifications required for the final result, and that every subexpression is processed only once.

To compare the performance of my **RationalSeries** method to *Mathematica*'s **Series**, we compute the cut,



belonging to a one-loop amplitude with two external massive scalars and four positive helicity gluons. The next chapter will make the interest in the rational part of such amplitudes more clear. For the benchmark the cut is evaluated on a rational kinematic point. To test the analytic capabilities, we also evaluate the cut on a BCFW shift, where momenta p_2 and p_3 are shifted using an analytic parameter z , with otherwise rational kinematics. The timings for the evaluation of the cut coefficient are provided in Table 2.2. We see that the **RationalSeries** routine provides much improved numerical performance compared to the *Mathematica* built-in function, and is capable of deriving analytic and semi-analytic results that are not obtainable using *Mathematica* own functionality.

Chapter 3

Two-Loop Rational Terms from One-Loop Unitarity

One of the simplest gluon amplitudes to consider is the scattering amplitude in which all gluons have the same helicity, typically called the “all-plus” configuration. The fact that we choose positive helicities for the name is purely convention, as there is little difference between an amplitude in which the gluons have all positive or all negative helicity, as the two cases are related by exchanging angle and bracket spinors.

Having reviewed the basics of computing amplitudes at tree and one-loop level, we now turn to main topic of the thesis. In the following we will discuss all-plus amplitudes of Yang–Mills theory. These amplitudes have only gluons as external or internal states, and the label “all-plus” refers to the helicity of the external particles. All gluons carry the same helicity, and a common convention is that all gluons have helicity¹+1. This is the most symmetric helicity configuration we could choose, and this symmetry is reflected in the form that these amplitudes take. We already saw that at tree level that these amplitudes have to vanish. At loop level we find further simplifications. All-plus amplitudes are usually regarded as the simplest gauge-theory amplitude to consider without resorting to supersymmetry.

At one loop, all-plus amplitudes are known for an arbitrary number of gluons, while at two loops a general form exists for their divergent and polylogarithmic finite parts. For the two-loop rational parts, an all- n conjecture is known only for the partial amplitudes $A_{n:1B}^{(2)}$ [18]. Up to six gluons, the rational parts of all partial amplitudes are known, while for seven gluons an analytic expression exists only at leading color. Based on findings of refs. [11, 12], we will here describe a method that allows the computation of rational parts of using only one-loop unitarity techniques.

We structure this chapter as follows: first, we will provide a review of the currently known results for all-plus amplitudes. We then extend the connection found between the leading color rational parts and the $(D_s - 2)^2$ coefficient of all-plus amplitudes found in refs. [11, 12] to the rational parts of all subleading partial amplitudes. We use the method of dimensional reconstruction to determine the unitarity cuts that make up the $(D_s - 2)^2$ coefficient. As was found for the leading color case in refs. [11, 12], these cuts have a one-loop squared topology, letting us evaluate them via one-loop

¹As the “all-plus” and “all-minus” cases are related by symmetry, a more accurate term would be “equal-helicity” amplitude

techniques. As a new result, we describe a method of computing the two-loop rational terms of arbitrary two-loop all-plus partial amplitudes. Using this technique we are able to reproduce all previous analytic results for such rational parts found in the literature. We are also able to independently verify the form of $R_{7:1B}^{(2)}$ that follows from the conjecture of ref. [18], as it has not been computed explicitly before.

3.1 The All-Plus: A Brief Review

Due to the simplicity of all-plus amplitudes they have been exceedingly well studied in the past. In this section we review the currently known results through two loops.

It is well known that all-plus amplitudes, along with single-minus amplitudes, vanish at tree level. In appendix A.1 we provide general arguments for this fact. The vanishing at tree level has direct ramifications for the loop level structure of all-plus amplitudes. At one-loop, we can decompose the all-plus amplitude as [3, 5]

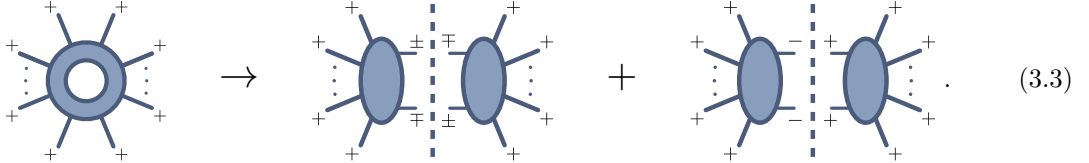
$$A^{(1)} = A^{(0)} I^{(1)} + F^{(1)} + \mathcal{O}(\epsilon). \quad (3.1)$$

Here, $F^{(1)}$ is finite in dimensional regularization, while $I^{(1)}$ is a singular function containing poles of the form $\frac{1}{\epsilon^2}$ and $\frac{1}{\epsilon}$. These poles contain the UV and IR divergences of the amplitude, and after renormalization, the $I^{(1)}$ term provides the universal behavior of one-loop amplitudes described in refs. [109–111]. From this decomposition we can immediately see that the vanishing of $A^{(0)}$ in the all-plus case directly leads to the absence of $1/\epsilon$ poles for their one-loop amplitudes.

We can further decompose the finite part $F^{(1)}$ into its polylogarithmic and rational parts $P^{(1)}$ and $R^{(1)}$, such that,

$$F^{(1)} = P^{(1)} + R^{(1)}. \quad (3.2)$$

$P^{(1)}$ contains four-dimensional branch cuts, and can be probed via four-dimensional unitarity cuts. $R^{(1)}$ is free of branch cuts, and can be determined from D -dimensional unitarity. However, if we were attempt to compute $P^{(1)}$, we would find that all cuts vanish. Placing any two propagators on-shell via a double cut leads to products of tree-amplitudes which contain either an amplitude of the all-plus or single-minus type,



$$\text{Diagram of a one-loop all-plus amplitude} \rightarrow \text{Sum of two tree-level diagrams with double cuts} \quad (3.3)$$

This argument holds for all partial amplitudes in the color decomposition, such that one-loop full-color all-plus amplitudes has to be free of branch cuts in four-dimensional kinematics. For every partial amplitude we therefore have,

$$A_{n:r}^{(1)}(1^+ \dots n^+) = R_{n:r}^{(1)}(1^+ \dots n^+) + \mathcal{O}(\epsilon). \quad (3.4)$$

For the leading-color partial amplitude, the general form for any number of gluons was conjectured

in ref. [1] to be,

$$A^{(1)}(1^+ \dots n^+) = -\frac{1}{3} \frac{\sum_{1 \leq i < j < k < l \leq n} \langle i|jkl|i \rangle}{\langle 12 \rangle \langle 23 \rangle \dots \langle (n-1)n \rangle \langle n1 \rangle} + \mathcal{O}(\epsilon), \quad (3.5)$$

by demanding correct collinear factorization. This form was later proven in ref. [2]. Ref. [112] additionally presented a construction of $A^{(1)}$ from complex recursion. The construction requires a three-particle Risager shift [113] to avoid a pole at infinity.

Subleading-color partial amplitudes at one-loop can always be obtained from the leading-color ones through color relations [82]. A compact form is known for these as well [4],

$$A_{n:r}^{(1)}(1^+ \dots (r-1)^+; r^+ \dots n^+) = -2 \frac{s_{1 \dots (r-1)}^2}{\langle 12 \rangle \langle 23 \rangle \dots \langle (r-1)1 \rangle \langle r(r+1) \rangle \dots \langle nr \rangle}, \quad (3.6)$$

where $r \geq 3$. Ref. [4] also provides an expression for the $U(N_c)$ partial amplitude $A_{n:2}^{(1)}$,

$$A_{n:2}^{(1)}(1^+; 2^+ \dots n^+) = -\frac{\sum_{2 \leq i < j \leq n} [1|ij|1]}{\langle 23 \rangle \langle 34 \rangle \dots \langle (n-1)n \rangle \langle n2 \rangle} \quad (3.7)$$

This amplitude is equivalent to the one-photon amplitude $A^{(1)}(1^- 2^+ \dots n^+)$, for which a compact all- n form was given earlier in ref. [1].

The absence of branch cuts and divergences in dimensional regularization are usually features of tree-level amplitudes. It is therefore curious to find a one-loop amplitude possessing these properties as well. We will see that this behavior continues in the two-loop amplitude, for which we find behavior more closely aligned with a generic one-loop amplitude.

One-loop all-plus amplitudes are further connected to MHV amplitudes of $\mathcal{N} = 4$ super-Yang–Mills theory via,

$$A^{(1)}(1^+ \dots n^+) = -2\epsilon(1-\epsilon)(4\pi)^2 \left[\frac{A_{\mathcal{N}=4}^{(1)}(1^+ \dots i^- \dots j^- \dots n^+)}{\langle ij \rangle^4} \right] \Big|_{\epsilon \rightarrow \epsilon-2} \quad (3.8)$$

The replacement $\epsilon \rightarrow \epsilon - 2$ amounts to shifting the dimension D from $4 - 2\epsilon$ to $8 - 2\epsilon$. At the level of the $\mathcal{N} = 4$ MHV integrand, the relation can be understood as replacing the supersymmetry preserving delta function via,

$$\delta^{(8)}(Q) \longrightarrow (D_s - 2)\mu^4, \quad (3.9)$$

where μ^2 is defined as in section 2.3 [12, 104]. This relation was first conjectured in ref. [104], and recently proven to hold to all orders in ϵ in ref. [114].

The first computation of a two-loop all-plus amplitude was presented in refs. [13–15], which provided analytic expressions for the full-color four-gluon amplitude. For five gluons, the planar and non-planar integrands were derived in refs. [115] and [116] respectively, together with results from numerical integration. Integrated expressions for these planar amplitude were presented in ref. [16]. Evaluation of the non-planar integrals in refs. [17] led to the first evaluation of the full-color two-loop all-plus amplitude.

Just as in the one-loop case, two-loop amplitudes can be decomposed with respect to their UV and IR singular structure [3], which leads us to a relation similar to that of eq. (3.1),

$$A^{(2)} = A^{(0)} I^{(2)} + A^{(1)} I^{(1)} + F^{(2)} + \mathcal{O}(\epsilon). \quad (3.10)$$

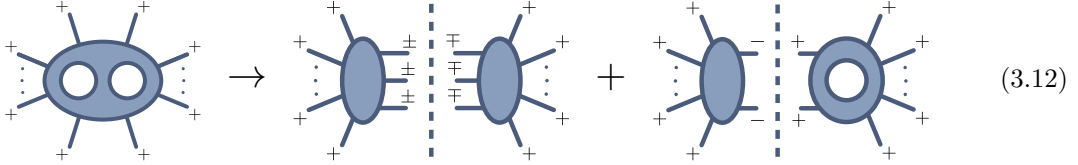
Here, $I^{(2)}$ is a function with divergences up to $\frac{1}{\epsilon^4}$, while $I^{(1)}$ is the same as in eq. (3.1). $F^{(2)}$ is finite in dimensional regularization, and can contain both rational and polylogarithmic terms. In the case of all-plus amplitudes we again find significant simplifications: while two-loop amplitudes generally have divergent terms of order $\frac{1}{\epsilon^4}$, the vanishing of $A^{(0)}$ and finiteness of $A^{(1)}$ only allow for terms up to $\frac{1}{\epsilon^2}$, as would usually be expected in a one-loop amplitude. In ref. [4], a generic form of the divergent part $A^{(1)}I^{(1)}$ of the all-plus is given for an arbitrary number of gluons and all partial amplitudes. As we can obtain the divergent parts of $A^{(2)}$ through this universal behavior, only the finite part $F^{(2)}$ needs to be determined.

Just as in the one-loop case we split $F^{(2)}$ into its polylogarithmic and rational components $P^{(2)}$, $R^{(2)}$, with

$$F^{(2)} = P^{(2)} + R^{(2)}. \quad (3.11)$$

While $P^{(2)}$ possesses branch cuts and is therefore accessible via four-dimensional generalized unitarity, $R^{(2)}$ does not contain such discontinuities and requires separate treatment.

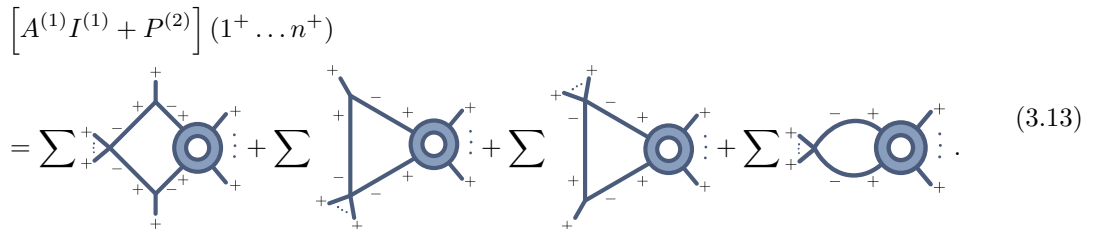
Let us first discuss $P^{(2)}$. To probe $P^{(2)}$, as well as the divergent parts $A^{(0)}I^{(2)}$ and $A^{(1)}I^{(1)}$, we compute the amplitude's discontinuities in four-dimensional kinematics. For the two-loop all-plus amplitude, the discontinuity of a physical singularity is associated to unitarity cuts of either two or three internal propagators



$$(3.12)$$

In the three particle cut on the left we obtain a product of two tree amplitudes. Due to the all-plus helicity configuration, these cuts have to vanish, as one of the tree amplitudes is guaranteed to be either of the single-minus or all-plus type. On the right we only cut one of the loops using the two-particle cut. We therefore end up with a cut, which due to the all-plus configuration has to be a product of a tree-level MHV and one-loop all-plus amplitude. We cannot place any additional cuts, as these would be related to branch cuts of the one-loop all-plus amplitude. We can therefore see that any discontinuity of the two-loop all-plus amplitude has to involve a product of amplitudes, one of which is again a one-loop all-plus amplitude.

This simplifications allow us to phrase the computation of the cut constructible parts of $A^{(2)}(1^+ \dots n^+)$ as a one-loop four-dimensional unitarity computation, with one of the amplitudes again being a one-loop all-plus one,

$$\begin{aligned} & \left[A^{(1)}I^{(1)} + P^{(2)} \right] (1^+ \dots n^+) \\ &= \sum \text{[diagram 1]} + \sum \text{[diagram 2]} + \sum \text{[diagram 3]} + \sum \text{[diagram 4]} \end{aligned} \quad (3.13)$$


The shown diagrams represent the combination of both cut coefficient and basis integral, with the propagators taken to be cut. The internal helicities of cuts are constrained by the all-plus configuration. Considering the expressions for the Feynman integrals provided in section 2.1,

we can identify origin of $P^{(2)}$ in the one-mass and two-mass easy box integrals. In ref. [6] this identification was used to derive $P^{(2)}$ for the leading-color five-gluon case. In ref. [7] a general form of $P^{(2)}$ for all leading color partial amplitudes was found in terms of the normalized finite parts of the two-mass easy box integral shown in eq. (2.14).

This leaves the two-loop rational part $R^{(2)}$. As discussed in chapter 2, these are not accessible from four-dimensional unitarity, as they do not develop branch cuts in the kinematics. As in the one-loop case they can be obtained from the two-loop extension of the D -dimensional generalized unitarity technique presented in chapter 2. This route was chosen in refs. [16] and [17], and the analytic results given therein include the rational parts $R_{5:1}^{(2)}$, $R_{5:3}^{(2)}$ and $R_{5:1B}^{(2)}$.

A second approach was followed in refs. [4–10]. Just as in the one-loop case, the two-loop rational parts of all-plus partial amplitudes can be obtained from complex recursion. As in the one-loop case, a Risager shift is required to obtain a construction only from poles at finite values of the shift parameter z . Using this method the five-, six- and seven-gluon leading-color, as well as all five- and six-gluon subleading rational parts were computed from the recursion approach. This appears like great news at first glance. Recursive computations are of significantly lesser complexity than those of generalized unitarity. They also make high multiplicity results easily accessible, even if the recursion may not be immediately solvable for a closed form.

However, in the case of $R^{(2)}$ there exists a significant barrier. While the construction of one-loop all-plus amplitudes from complex recursion proceeds much like a tree-level one, the previous discussion taught us that we ought to expect features of one-loop computations for two-loop all-plus amplitudes. In determining one-loop amplitudes from complex shifts we generally encounter two features not seen at tree level: double poles, and single poles not attributable to factorizations. And for the all-plus rational parts we encounter precisely these two features. While the double complex poles can be obtained from the universal collinear behavior of amplitudes [112], no general simple form is known for the additional single poles. Obtaining the latter presents therefore a significant challenge. We defer a more detailed discussion of one-loop recursion to the next chapter.

The main challenge of computing $R^{(2)}$ in refs. [4–10] was therefore determining the single pole terms of the recursion. The approach chosen for this task is the augmented recursion technique [19], which allows to obtain them from off-shell currents. Due to the complexity of these currents this approach is difficult to generalize to a large number of gluons, and we may want to look for alternative routes for obtaining $R^{(2)}$.

Ideally we would like to find a construction similar to that of $P^{(2)}$ in eq. (3.13). By finding an effective one-loop computation we made the one-loop structure of the polylogarithmic terms manifest. As we are now dealing with rational parts of a loop amplitude we would expect to find a D -dimensional unitarity construction of the form

$$R^{(2)}(1^+ \dots n^+) = \text{[Diagram 1]} + \text{[Diagram 2]} + \text{[Diagram 3]}$$

Assuming such a construction exists, the exact nature of the one-loop amplitude involved in the cuts is the main question: while for the polylogarithmic terms the one-loop amplitude in the cuts

was again an all-plus amplitude, for the rational parts we would expect amplitudes involving a massive scalar pair.

A first hint towards such an approach is provided in refs. [11, 12], which finds local integrands for the five- and six-gluon integrands of the two-loop all-plus at leading color. The basis of this construction is the connection of the all-plus and $\mathcal{N} = 4$ MHV amplitudes at the integrand level, similar to the one-loop integrand relation of eq. (3.9). For two-loop integral topologies of $\mathcal{N} = 4$ amplitudes, the associated all-plus integrands are connected to the local $\mathcal{N} = 4$ integrands of refs. [117, 118] via the replacement [11, 12],

$$\delta^{(8)}(Q) \rightarrow F_1 = (D_s - 2) (\mu_1^2 \mu_2^2 + (\mu_1^2 + \mu_2^2)^2 + 2\mu_{12}(\mu_1^2 + \mu_2^2)) + 16(\mu_{12}^2 - \mu_1^2 \mu_2^2). \quad (3.14)$$

Based on their observations, ref. [12] conjectured that at leading color, the finite polylogarithmic contributions $P_{n:1}^{(2)}$ are entirely determined by integrands connected to $\mathcal{N} = 4$ amplitudes. Furthermore, the leading-color rational parts $R_{n:1}^{(2)}$ are conjectured to originate from integrands not shared with $\mathcal{N} = 4$. These are all of the “one-loop squared” topology, which for example include,


(3.15)

Using these integrands, the relation for $R_{n:1}^{(2)}$ was verified in ref. [12] by direct computation for five and six gluons, comparing against the results of refs. [5, 16]. It is this one-loop squared construction of the leading-color $R^{(2)}$ on which the majority of this thesis rests.

In the following we will use the representation of the two-loop leading color finite part given in ref. [12],

$$F^{(2)} = (D_s - 2)\mathcal{P}^{(2)} + (D_s - 2)^2\mathcal{R}^{(2)} + \mathcal{O}(\epsilon).$$

Here, $\mathcal{P}^{(2)}$ is entirely polylogarithmic, while $\mathcal{R}^{(2)}$ is entirely rational. The construction of ref. [12] makes the dependence of the amplitude on the spin dimension D_s explicit. We can observe in the relation above that the rational parts are proportional to $(D_s - 2)^2$. Thus, assuming the conjecture holds, to obtain the rational part of the all-plus we need only to determine the rational part of its $(D_s - 2)^2$ dependent part.

In the following we review the dimensional reconstruction method, which will allow us to make the D_s dependence of an amplitude explicit.

3.2 Dimensional Reconstruction

Scattering amplitudes generically depend on the space-time dimension D_s . For gauge theories this dimension controls the number of states running in loops: for example, in Yang–Mills theory there are $(D_s - 2)$ polarization states, which in $D_s = 4$ corresponds to positive and negative helicity gluons. Different regularization schemes require specific choices of D_s , such as the four-dimensional helicity scheme (FDH) [119], where D_s is set to four, or the ’t Hooft Veltman scheme (HV) with $D_s = 4 - 2\epsilon$ [120]. As in the HV scheme, the value of D_s need in general not be an integer, which

further complicates computations. Details regarding the use of these regularization schemes can be found in the reference given, as well as ref. [121].

We already saw in section 2.3.2 that at least for the computation of rational parts of one-loop amplitudes, we can avoid using states of non-integer dimensions via the supersymmetry decomposition of such amplitudes. An approach to circumvent this problem more generally is dimensional reconstruction, first introduced for one-loop amplitudes in ref. [122]. Instead of working with a fixed value of D_s we rather take an amplitude to be a function of D_s . Evaluating the amplitude at a sufficient number of values for D_s allows us to completely fix the functional dependence. Once the generic form of the D_s dependence is found, obtaining the amplitude in a specific regularization scheme is a matter of substituting the desired value of D_s .

Using this approach we avoid non-integer values of D_s entirely. We are free to perform all evaluations in integer dimensions, while amplitudes in non-integer dimensions are obtained through interpolation. This makes dimensional reconstruction a useful technique for both analytic computations as well as automated codes. Note that for these evaluations we only set D_s to integer values. The loop integrals remain D -dimensional, as we still need to regulate UV and IR divergences.

As ref. [12] connects the rational contributions of two-loop all-plus amplitude to its dependence on the space-time dimension D_s , we will give here a brief review of the topic. The rest of the section is based on the discussion at one-loop in ref. [122], as well as the L -loop generalization presented in ref. [107].

The D_s dependence of loop amplitudes arises from contractions of the metric tensor $g^{\mu\nu}$ along loops, as any such contraction that closes in on itself yields the trace $g^\mu{}_\mu = D_s$. Gauge bosons in Yang–Mills carry a single vector index, such that an L -loop scattering amplitude in gauge theory can generically be written as a polynomial of degree L in D_s ,

$$A_{D_s}^{(L)} = \sum_{i=0}^L C_i D_s^i. \quad (3.16)$$

Computing an amplitude then amounts to determining the coefficients C_i through sampling $A_{D_s}^{(L)}$ at L different values of D_s . The exact values for D_s that can be used for sampling are subject to constraints that will be discussed below.

We will first discuss one-loop amplitudes, as they are the simplest case to consider. As we can have at most a single contraction $g^\mu{}_\mu = D_s$ they are linear in D_s , and generically take the form,

$$A_{D_s}^{(1)} = C_0 + C_1 D_s. \quad (3.17)$$

Thus, evaluating $A_{D_s}^{(1)}$ in some dimensions D_0 , D_1 , and solving for the coefficients C_0 , C_1 , we end up with,

$$A_{D_s}^{(1)} = \frac{D_s - D_0}{D_1 - D_0} A_{D_1}^{(1)} + \frac{D_s - D_1}{D_0 - D_1} A_{D_0}^{(1)}. \quad (3.18)$$

With the choice $D_1 = D_0 + 1$, the expression above simplifies to,

$$A_{D_s}^{(1)} = (D_s - D_0) A_{D_1}^{(1)} - (D_s - D_1) A_{D_0}^{(1)}. \quad (3.19)$$

Keeping the external kinematics four-dimensional, we need to choose $D_0 > 4$ to capture the

entire amplitude including rational contributions. However, we only need to choose D_0 large enough such that we can fully embed the loop momentum. For simplicity, we assume for the moment the loop momentum dimension to be D_i , later analytically continuing to $D = 4 - 2\epsilon$. As described in section 2.3, the $(D_0 - 4)$ -dimensional components of the loop-momentum in $A_{D_0}^{(1)}$ can only appear in the form of $\tilde{\ell}^2 = \bar{\ell}^2 = \mu^2$. At one-loop the simplest choice is therefore $D_0 = 5$.

We chose for simplicity $D_1 = D_0 + 1$, where the loop-momentum in $A_{D_1=6}^{(1)}$ has two $(D_1 - 4)$ components, namely $\ell^{(4)}$ and $\ell^{(5)}$. To simplify the following steps, we use Lorentz invariance to always set ℓ^5 to zero. In the one-loop case we therefore have the loop-momenta

$$\begin{aligned} D_0 = 5 : \quad \ell_i &= (\bar{\ell}_i, \ell_i^{(4)}) \\ D_1 = 6 : \quad \ell_i &= (\bar{\ell}_i, \ell_i^{(4)}, 0). \end{aligned} \tag{3.20}$$

$A_{D_0=5}^{(1)}$ can be determined via generalized unitarity with five-dimensional states and a five-dimensional loop-momentum. Just as in four dimensions, when cutting a propagator its numerators can be written as a sum over the $(D_0 - 2) = 3$ polarization states using the completeness relation of polarization vectors

$$\text{Cut}[\text{prop}^{\mu\nu}(\ell)] \rightarrow -(2\pi)\delta^+(\ell^2) \sum_{j=1}^{D_0-2} \varepsilon_j^\mu(\ell) \varepsilon_j^\nu(\ell), \tag{3.21}$$

where the polarization vectors ε_i satisfy the conditions

$$\varepsilon_i^\mu \varepsilon_{j\mu} = -\delta_{ij}, \quad \ell_\mu \varepsilon^\mu(\ell) = 0. \tag{3.22}$$

Turning to $A_{D_1=6}^{(1)}$, we can take advantage of the fact that $\ell^5 = 0$, and perform a Kaluza-Klein reduction [123, 124] of the six-dimensional gluon running in the loop. Since the loop momentum is still only five-dimensional, there are no additional cuts compared to the computation in $D_0 = 5$. However every cut in D_1 includes one additional polarization state in the sum of eq. (3.21). In $D_1 = 6$ we have four polarization states. Since ℓ in D_1 is only non-zero in the five-dimensional subspace, we identify three of the four polarizations to be those of dimension D_0 , *i.e.* polarization vectors of a massless five-dimensional gauge-boson. For the fourth polarization vector we make the choice $\varepsilon_4^\mu = \delta_5^\mu$, which is consistent with the conditions of eq. (3.22). As the external momenta are four-dimensional, and the loop momentum is five-dimensional, ε_4 is the only vector with a non-zero sixth-dimensional component, so that any contractions other than $\varepsilon_4 \cdot \varepsilon_4$ to vanish. ε_4 can therefore only appear contracted onto itself along the loop, coupling to the remaining polarization states as if belonging to an adjoint scalar field. In the following we will therefore treat this state separately, and due to its scalar-like behavior refer to it as φ .

We can directly derive Feynman rules for φ from the three- and four-point gluon vertices by

setting Lorentz indices associated to φ to 5,

$$\begin{aligned}
 V^3(1^\varphi 2^g 3^\varphi)^\mu &= \text{diagram} = \frac{i}{\sqrt{2}}(p_1 - p_3)^\mu, & V^4(1^g 2^g 3^\varphi 4^\varphi)^{\mu\nu} &= \text{diagram} = \frac{i}{2}g^{\mu\nu}, \\
 V^4(1^g 2^\varphi 3^g 4^\varphi)^{\mu\nu} &= \text{diagram} = -ig^{\mu\nu}, \\
 \text{prop}_\varphi &= \text{diagram} = \frac{i}{p^2}, & \text{prop}_g^{\mu\nu} &= \text{diagram} = \frac{-ig^{\mu\nu}}{p^2},
 \end{aligned} \tag{3.23}$$

with all other configurations vanishing. The contact terms are represented by a borderless disk, with the internal lines representing the flow of the scalar flavor. This is in line with the conventions of refs. [107, 115]. The Feynman rules exactly match those of an adjoint scalar field φ^a with Lagrangian [107]

$$\mathcal{L}_\varphi = \int dx D_\mu \varphi^a D^\mu \varphi^a, \tag{3.24}$$

where φ only couples to gluons through the covariant derivative.

Separating ε_4 from the five-dimensional polarization vectors allows us to decompose $A_{D_1}^{(1)}$ into the sum,

$$A_{D_1=D_0+1}^{(1)} = A_{D_0}^{(1)} + A_s^{(1)}, \tag{3.25}$$

where $A_s^{(1)}$ is an amplitude in D_0 dimensions with only φ circulating in the loop. Substituting this decomposition back into eq. (3.19) we obtain,

$$\begin{aligned}
 A_{D_s}^{(1)} &= (D_s - D_0) \left(A_{D_0}^{(1)} + A_s^{(1)} \right) - (D_s - D_1) A_{D_0}^{(1)} \\
 &= A_{D_0}^{(1)} + (D_s - D_0) A_s^{(1)}.
 \end{aligned} \tag{3.26}$$

Therefore, the full amplitude can be reconstructed from only a single value of D_s , while having to evaluate it with both vectors and scalars in the loop.

This construction of amplitudes generalizes to arbitrary loop order, as discussed in ref. [107]. We limit ourselves to the two-loop case required for the present work. Since there can be up to two contractions of the metric tensor, an amplitude is a quadratic polynomial in D_s ,

$$A^{(2)} = C_0 + C_1 D_s + C_2 D_s^2, \tag{3.27}$$

and we need to evaluate it for three values of D_s to fix all the coefficients. Choosing dimensions

$$D_0, \quad D_1 = D_0 + 1, \quad D_2 = D_0 + 2 \tag{3.28}$$

we find the amplitude to be,

$$A_{D_s}^{(2)} = \frac{(D_s - D_2)}{2} (D_s - D_1) A_{D_0}^{(2)} - (D_s - D_0)(D_s - D_2) A_{D_1}^{(2)} + \frac{(D_s - D_0)}{2} (D_s - D_1) A_{D_2}^{(2)}. \tag{3.29}$$

As a consistency check we can verify that for $D_s = D_0, D_1, D_2$ we obtain $A_{D_0}^{(2)}$, $A_{D_1}^{(2)}$ and $A_{D_2}^{(2)}$. As we now have two loop momenta ℓ_1, ℓ_2 , with the external momenta again four-dimensional, their $(D-4)$ -dimensional components $\tilde{\ell}_1, \tilde{\ell}_2$ can appear as $\tilde{\ell}_i^2 = \mu_i^2$ and $\tilde{\ell}_1 \cdot \tilde{\ell}_2 = \mu_{12}$. To properly represent the two loop momenta such that the μ_i^2 and μ_{12} are not linearly dependent, we need to

choose at least $D_0 = 6$, where the $\tilde{\ell}_i$ only have components in the fifth and sixth dimension. We set $D_1 = 7$ and $D_2 = 8$.

We again use Lorentz invariance to align the $(D - 4)$ -dimensional parts of the loop-momenta for $A_{D_0}^{(2)}$, $A_{D_1}^{(2)}$ and $A_{D_2}^{(2)}$. We can always pick a frame where the loop momenta take the form,

$$\begin{aligned} D_0 = 6 : \quad \ell_i &= (\bar{\ell}_i, \ell_i^{(4)}, \ell_i^{(5)}), \\ D_1 = 7 : \quad \ell_i &= (\bar{\ell}_i, \ell_i^{(4)}, \ell_i^{(5)}, 0), \\ D_2 = 8 : \quad \ell_i &= (\bar{\ell}_i, \ell_i^{(4)}, \ell_i^{(5)}, 0, 0). \end{aligned} \quad (3.30)$$

We can then use the same construction as in the one-loop case to see that the extra polarization states of $A_{D_1}^{(2)}$ and $A_{D_2}^{(2)}$ behave like scalars. The first $(D_0 - 2) = 4$ polarization states are the same for $A_{D_0}^{(2)}$, $A_{D_1}^{(2)}$ and $A_{D_2}^{(2)}$. For the fifth state in $A_{D_1}^{(2)}$ and $A_{D_2}^{(2)}$ we choose the polarization vector $\varepsilon_5^\mu = \delta_6^\mu$, while for the sixth state in $A_{D_2}^{(2)}$ we choose $\varepsilon_6^\mu = \delta_7^\mu$.

Due to the orthogonality of the additional polarization vectors ε_5 , ε_6 and the loop-momenta, we can express the amplitudes $A_{D_1}^{(2)}$ and $A_{D_2}^{(2)}$ in terms of amplitudes in dimension D_0 , where some of the loops carry an effective scalar degree of freedom. Such a decomposition would be of the form,

$$\begin{aligned} A_{D_1}^{(2)} &\rightarrow A_{D_0}^{(2)}, A_{D_0,1,0}^{(2)}, A_{D_0,2,0}^{(2)}, \\ A_{D_2}^{(2)} &\rightarrow A_{D_0}^{(2)}, A_{D_0,1,0}^{(2)}, A_{D_0,2,0}^{(2)}, A_{D_0,1,1}^{(2)}. \end{aligned} \quad (3.31)$$

We use the labelling conventions of ref. [107] for the scalar amplitudes. In $A_{D_0,1,0}^{(2)}$ only one closed loop carries a scalar, while the remaining propagators are of D_0 -dimensional gluons. In $A_{D_0,2,0}^{(2)}$ both loops carry a scalar degree of freedom, with the additional requirement that the two loops are connected via the exchange of a D_0 -dimensional gluon. In $A_{D_0,1,1}^{(2)}$ we also have two scalar loops, however they are connected via a four-scalar contact term which originates from the four-gluon vertex. Example diagrams contributing to these amplitudes are shown in Figures 3.1, 3.2a and 3.2b. Separating the gluon-exchange and contact-term contributions in $A_{D_2}^{(2)}$ will allow us to collect terms later on, as $A_{D_0,2,0}^{(2)}$ contributes to both the D_1 and D_2 amplitudes. Additionally, the contact term whose form we will derive next requires the scalar flavors in two loops to be different, such that one loop carries ε_5 while the other carries ε_6 . With a gluon exchange connecting the loops there is no such restriction.

To obtain the exact decomposition hinted at in eq. (3.31), we need to determine the Feynman rules for the scalars. For $A_{D_1}^{(1)}$ the rules are identical to the ones of the one-loop case in eq. (3.23). To obtain the rules for $D_2 = 8$ we repeat the procedure from the one-loop case, denoting $\varepsilon_5 \simeq \varphi$ and $\varepsilon_6 \simeq \varphi'$. As they can be treated identically, we will also refer to them as having different scalar “flavors”.

The Feynman rules for φ, φ' are again obtained from the three- and four-gluon vertices by setting Lorentz indices to $\mu = 6$ for φ and $\mu = 7$ for φ' . In addition to the Feynman rules of eq. (3.23), we now have two additional four-scalar contact terms,

$$V^4(1^\varphi 2^\varphi 3^{\varphi'} 4^{\varphi'}) = \text{diagram} = -\frac{i}{2}, \quad V^4(1^\varphi 2^{\varphi'} 3^\varphi 4^{\varphi'}) = \text{diagram} = i. \quad (3.32)$$

Cubic vertices coupling three scalars are absent, as at least one of their momenta would have to be

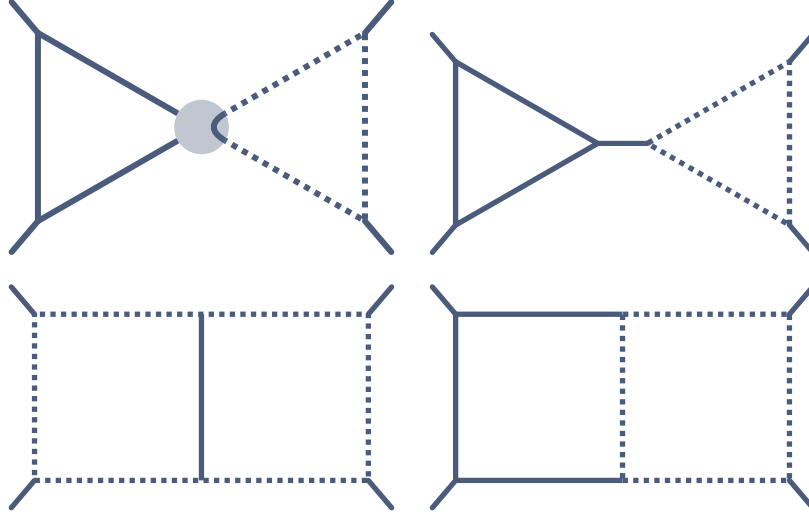


Figure 3.1: Representatives of graphs contributing to $A_{D_0,1,0}^{(2)}$. The grey circle is a quartic gluon-scalar vertex. The dashed lines represent propagators of massless six-dimensional scalars, while solid lines are associated to six-dimensional gluons.

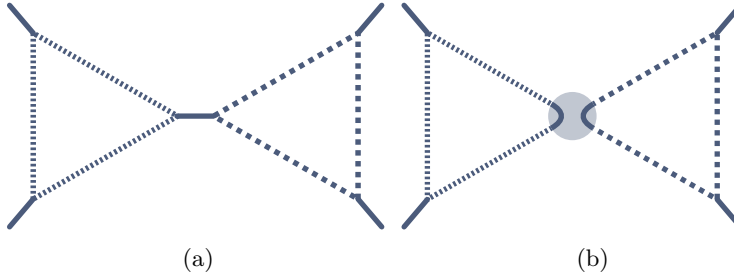


Figure 3.2: Representatives of graphs contributing to $A_{D_0,2,0}^{(2)}$ (a), and $A_{D_0,1,1}^{(2)}$ (b). Solid lines represent gluon propagators, while the dashed lines are associated to scalars. The different dashings represent the possibility of the two loops having different scalar flavors. In (a), the scalar flavors in the two loops can be the same, while the quartic scalar interaction represented in (b) requires the flavors to be different. The quartic interaction with all scalars having the same flavor vanishes. After summing over scalar flavors the diagrams in (a) and (b) therefore appear with prefactors of $(D_2 - D_0)^2$ and $(D_2 - D_0)(D_2 - D_0 - 1)$ respectively.

contracted with ε_5 or ε_6 . There are also no contact terms of four same-flavor scalars, as all three terms of the quartic gluon vertex would contribute, and end up cancelling each other. The rules of eqs.(3.23) and (3.32) are in agreement with those of ref. [115]².

Given our rules, we can now make the decomposition of eq. (3.31) explicit,

$$\begin{aligned} A_{D_1}^{(2)} &= A_{D_0}^{(2)} + (D_1 - D_0)A_{D_0,1,0}^{(2)} + (D_1 - D_0)^2 A_{D_0,2,0}^{(2)} \\ &= A_{D_0}^{(2)} + A_{D_0,1,0}^{(2)} + A_{D_0,2,0}^{(2)}, \\ A_{D_2}^{(2)} &= A_{D_0}^{(2)} + (D_2 - D_0)A_{D_0,1,0}^{(2)} + (D_2 - D_0)^2 A_{D_0,2,0}^{(2)} + (D_2 - D_0)(D_2 - D_0 - 1)A_{D_0,1,1}^{(2)} \\ &= A_{D_0}^{(2)} + 2A_{D_0,1,0}^{(2)} + 4A_{D_0,2,0}^{(2)} + 2A_{D_0,1,1}^{(2)}. \end{aligned} \quad (3.33)$$

When summing over the scalar-like degrees of freedom, each scalar loop in $A_{D_i,1,0}^{(2)}$ and $A_{D_i,2,0}^{(2)}$ leads to a prefactor of $(D_i - D_0)$. For $A_{D_2,1,1}^{(2)}$, the scalar contact term requires different scalars in the two loops, of which there are $(D_2 - D_0)(D_2 - D_0 - 1)$ combinations.

Applying eq. (3.33) to eq. (3.29), we finally obtain

$$A_{D_s}^{(2)} = A_{D_0}^{(2)} + (D_s - D_0)A_{D_0,1,0}^{(2)} + (D_s - D_0)^2 A_{D_0,2,0}^{(2)} + (D_s - D_0)(D_s - D_0 - 1)A_{D_0,1,1}^{(2)}. \quad (3.34)$$

As in ref. [107], we can compare the result in eq. (3.34) with similar approaches used for two-loop computations in the literature. As an example, we can consider the derivation of the four- and five-gluon all-plus amplitudes in ref. [115]. These were obtained by decomposing the integrand

$$\Delta_{D_s}^{(2)} = \Delta_6^{(2)} + (D_s - 6)\Delta_{6,s}^{(2)} + (D_s - 6)^2 \Delta_{6,ss}^{(2)}, \quad (3.35)$$

where $\Delta_6^{(2)}$ is the full integrand of the six-dimensional amplitude, while $\Delta_{6,s}^{(2)}$ and $\Delta_{6,ss}^{(2)}$ are integrands from diagrams involving the extra-dimensional scalars. In the case of the four-point amplitude, these scalar integrands correspond to contributions from the diagrams [115],

$$\Delta_{6,s}^{(2)} \simeq \text{[diagram 1]} + \text{[diagram 2]} + \text{[diagram 3]} + \text{[diagram 4]} + \text{[diagram 5]} + \text{[diagram 6]}, \quad (3.36)$$

and,

$$\Delta_{6,ss}^{(2)} \simeq \text{[diagram 7]} + \text{[diagram 8]}. \quad (3.37)$$

In the case of both loops carrying a scalar, $\Delta_{6,s}^{(2)}$ and $\Delta_{6,ss}^{(2)}$ distinguish between the scalar flavor conservation in the four-scalar vertex. The contractions in $\Delta_{6,s}^{(2)}$ require the scalars to be the same in both loops, while those in $\Delta_{6,ss}^{(2)}$ are independent, justifying the respective subscripts.

For consistency between eq. (3.34) and eq. (3.35) with $D_0 = 6$ we require after integration the

²Note that in ref. [115], the four-scalar contact-terms are defined with respect to the internal scalar flavor conservation, before summing over the flavor assignments. With this definition each of the contact terms is non-vanishing even in the case of all scalars being of the same flavor. However, one would also have to sum over the three internal flavor routings,

$$\text{[diagram 9]} + \text{[diagram 10]} + \text{[diagram 11]} = 0$$

causing such contributions to vanish as in our discussion.

correspondence,

$$\Delta_{6,s}^{(2)} \rightarrow A_{6,1,0}^{(2)} - A_{D_0,1,1}^{(2)}, \quad \Delta_{6,ss}^{(2)} \rightarrow A_{6,2,0}^{(2)} + A_{D_0,1,1}^{(2)}. \quad (3.38)$$

For $\Delta_{6,ss}^{(2)}$ we see that this is indeed the case, as the types of diagrams shown in eq. (3.37) match exactly the definitions of $A_{6,2,0}^{(2)}$ and $A_{D_0,1,1}^{(2)}$. For $\Delta_{6,s}^{(2)}$ we can obtain agreement by using the relation,

$$A_{6,1,1}^{(2)} \simeq \text{diagram 1} = - \text{diagram 2} - \text{diagram 3}, \quad (3.39)$$

which follows from the quartic scalar Feynman rules of eq. (3.32).

We can further rearrange eq. (3.34) to obtain relations between coefficients of different sampling dimensions. Collecting terms to turn eq. (3.34) into a polynomial in $(D_s - D'_0)$, we obtain

$$\begin{aligned} A_{D_s}^{(2)} = & \left[A_{D_0}^{(2)} + (D'_0 - D_0)A_{D_0,1,0}^{(2)} + (D'_0 - D_0)^2 A_{D_0,2,0}^{(2)} + (D'_0 - D_0)(D'_0 - D_0 - 1)A_{D_0,2,0}^{(2)} \right] \\ & + (D_s - D'_0) \left[A_{D_0,1,0}^{(2)} + 2(D'_0 - D_0)(A_{D_0,2,0}^{(2)} + A_{D_0,1,1}^{(2)}) \right] \\ & + (D_s - D'_0)^2 A_{D_0,2,0}^{(2)} + (D_s - D'_0)(D_s - D'_0 - 1)A_{D_0,1,1}^{(2)}. \end{aligned} \quad (3.40)$$

For $(D_s + L) \leq D'_0$, eq. (3.40) can be reinterpreted: the right hand side of the first line is just $A_{D'_0}^{(2)}$, so that

$$\begin{aligned} A_{D_s}^{(2)} = & A_{D'_0}^{(2)} + (D_s - D'_0) \left[A_{D_0,1,0}^{(2)} + 2(D'_0 - D_0)(A_{D_0,2,0}^{(2)} + A_{D_0,1,1}^{(2)}) \right] \\ & + (D_s - D'_0)^2 A_{D_0,2,0}^{(2)} + (D_s - D'_0)(D_s - D'_0 - 1)A_{D_0,1,1}^{(2)}. \end{aligned} \quad (3.41)$$

We can further make the identifications $A_{D_0,2,0}^{(2)} = A_{D'_0,2,0}^{(2)}$ and $A_{D_0,1,1}^{(2)} = A_{D'_0,1,1}^{(2)}$, since these amplitudes have no closed gluon loops and should therefore not depend on the specific value of space-time dimension. Lastly, we have to consider $A_{D_0,1,0}^{(2)}$. This amplitude contains closed gluon loops only through diagrams of the type,

$$\text{diagram 1}, \text{diagram 2}, \text{diagram 3}, \text{diagram 4} \in A_{D_0,1,0}^{(2)} \quad (3.42)$$

Since $D_0, D'_0 \geq (D_s + L)$, the additional term $2(D'_0 - D_0)(A_{D_0,2,0}^{(2)} + A_{D_0,1,1}^{(2)})$ adds or subtracts from the diagrams shown in eq. (3.42) scalar-like polarization states in the gluon loop. The factor 2 takes into account that the gluon can be in either one of the two loops. We therefore have,

$$A_{D'_0,1,0}^{(2)} = A_{D_0,1,0}^{(2)} + 2(D'_0 - D_0)(A_{D_0,2,0}^{(2)} + A_{D_0,1,1}^{(2)}), \quad (3.43)$$

and eq. (3.40) turns into,

$$A_{D_s}^{(2)} = A_{D'_0}^{(2)} + (D_s - D'_0)A_{D'_0,1,0}^{(2)} + (D_s - D'_0)^2 A_{D'_0,2,0}^{(2)} + (D_s - D'_0)(D_s - D'_0 - 1)A_{D'_0,1,1}^{(2)}. \quad (3.44)$$

3.3 Separability and Two-Loop Rational Terms

At leading color, refs. [11, 12] connect the finite polylogarithmic rational contributions of two-loop all-plus amplitudes to their representation as polynomials in power of $(D_s - 2)$.

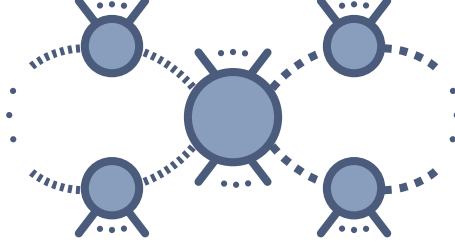


Figure 3.3: Generic example of two-loop cuts that have to be considered for $A_{ss}^{(2)}$ at leading color. The two loops are only connected by a central tree-amplitude, which does not contain any propagator carrying both loop-momenta.

Specifically, up to order ϵ^0 the finite polylogarithmic contributions $P_n^{(2)}$ arise entirely from the coefficient of $(D_s - 2)$, while the rational terms $R_n^{(2)}$ are entirely determined by the coefficient of $(D_s - 2)^2$,

$$F_{n:1}^{(2)}(1^+ \dots n^+) = \underbrace{(D_s - 2)\mathcal{P}^{(2)}(1^+ \dots n^+)}_{P_n^{(2)}} + \underbrace{(D_s - 2)^2\mathcal{R}^{(2)}(1^+ \dots n^+)}_{R_n^{(2)}} + \mathcal{O}(\epsilon). \quad (3.45)$$

This identification for $R^{(2)}(1^+ \dots n^+)$ was verified in ref. [12] for the five- and six-gluon leading color partial amplitudes by integrating those two-loop integrands proportional to $(D_s - 2)^2$. The resulting analytic expressions were then numerically checked against the known results of refs. [5, 6, 8, 9, 16].

We can connect the statement of ref. [12] for the finite contributions with the dimensional reconstruction picture of section 3.2. We choose as the base dimension $D_0 = 6$, and use the rearrangement of eq. (3.40) with $D'_0 = 2$. Comparing with eq. (3.45), we end up with the following relations for the finite polylogarithmic and rational contributions,

$$P^{(2)}(1^+ \dots n^+) = (D_s - 2)\mathcal{F} \left[A_{6,1,0}^{(2)} - 2 \times 4(A_{6,2,0}^{(2)} + A_{6,1,1}^{(2)}) - A_{6,1,1}^{(2)} \right] (1^+ \dots n^+), \quad (3.46)$$

$$R^{(2)}(1^+ \dots n^+) = (D_s - 2)^2\mathcal{F} \left[A_{6,2,0}^{(2)} + A_{6,1,1}^{(2)} \right] (1^+ \dots n^+), \quad (3.47)$$

where \mathcal{F} represents the operation of extracting the finite part, dropping terms of order ϵ .

Rephrasing the problem of computing $R^{(2)}(1^+ \dots n^+)$ in terms of $A_{6,2,0}^{(2)}$ and $A_{6,1,1}^{(2)}$ leads to a reduction in computational complexity. In $A_{6,1,1}^{(2)}$ the two scalar lines of the loops meet in a four-scalar contact term, while for $A_{6,2,0}^{(2)}$ the two loops are connected by an s-channel gluon exchange. Thus, for these amplitudes the two loop momenta can never appear in a shared propagator, and all two-loop integrals required for a complete integral basis factorize into a product of one-loop integrals. To determine the coefficients of such a basis from unitarity cuts we can proceed loop by loop. We first compute the coefficient of one of the loops using the usual one-loop unitarity techniques. Treating this coefficient as if it were a tree amplitude, we then proceed with the coefficient of the second loop in the same manner. The coefficient of the second loop ends up being the one of the full one-loop squared two-loop integral. Due to the separate treatment of the two loops, we call the described construction the separable approach. Note that this manner of computing the $A_{D_0,1,1}^{(2)}$ and $A_{D_0,2,0}^{(2)}$ also hints at the structure found for the finite polylogarithmic parts of two-loop all-plus amplitudes, where one of the loops can be separately integrated to give the one-loop all-plus amplitude. We will further discuss this similarity in chapter 4.

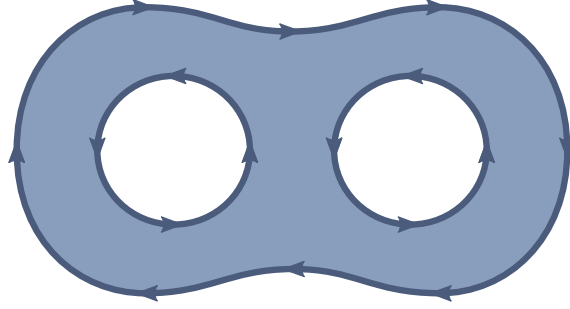


Figure 3.4: The partial amplitudes $A_{n:1}^{(2)}$, $A_{n:r}^{(2)}$ and $A_{n:r,k}^{(2)}$ can be interpreted as originating from open string amplitudes, in which the world-sheet takes the shape of a disc with two punctures. This genus-2 surface is orientable and has three boundaries, therefore providing three traces of color generators.

In ref. [12], the relation of eq. (3.47) was only discussed in reference to the leading-color partial amplitudes. In the following we loosen this restriction and assume that it also extends to rational contributions of all-plus amplitudes beyond leading color, more specifically those of non-planar partial amplitudes. In the rest of this chapter we will discuss the construction of the non-planar versions of $A_{6,2,0}^{(2)}$ and $A_{6,1,1}^{(2)}$ via color-dressed unitarity similar to the procedure for polylogarithmic contributions shown in refs. [4, 10, 18]. By direct computation of $A_{6,2,0}^{(2)}$ and $A_{6,1,1}^{(2)}$ for several subleading color-structures and subsequent comparison with results available in the literature [4, 10] we will see that eq. (3.47) does indeed appear to hold for all partial amplitudes in the color decomposition of all-plus amplitudes.

3.4 One-Loop Squared Cuts

3.4.1 Two-Loop Color Dressed Unitarity

We need to identify the two-loop cut topologies that contribute to the different trace structures in full-color all-plus amplitudes. As in section 2.4, it is again useful to consider the string-theoretic version of the amplitude, and use the origin of the color structures there as a guide for gauge theory. A similar analysis was carried out in ref. [18].

Two-loop amplitudes in gauge theory can be obtained from taking the infinite tension limit of amplitudes in open string theory, where the world-sheet is an orientable surface of genus 2 with at least one boundary. There are two such surfaces: the disc with two punctures, which has three boundaries, and the punctured torus, which has only a single boundary. Representations of these surfaces are shown in Figures 3.4 and 3.5.

We again associate to each boundary a trace of color generators. With empty traces simplifying to N_c , amplitudes with the topology of Figure 3.4 can therefore have color structures Tr^3 , $N_c \text{Tr}^2$ and $N_c^2 \text{Tr}$, while the topology of Figure 3.5 will always lead to a single trace Tr . These are again precisely the two-loop color structures introduced in the two-loop color decomposition in 1.4.2.2. The amplitudes $A_{n:1}^{(2)}$, $A_{n:r}^{(2)}$ and $A_{n:r,k}^{(2)}$ can be obtained from cuts following the shape of Figure 3.4. The three traces correspond to the two inner boundaries of the loops and the outer boundary.

We again use color algebra to convince us of this construction. We are mainly interested in

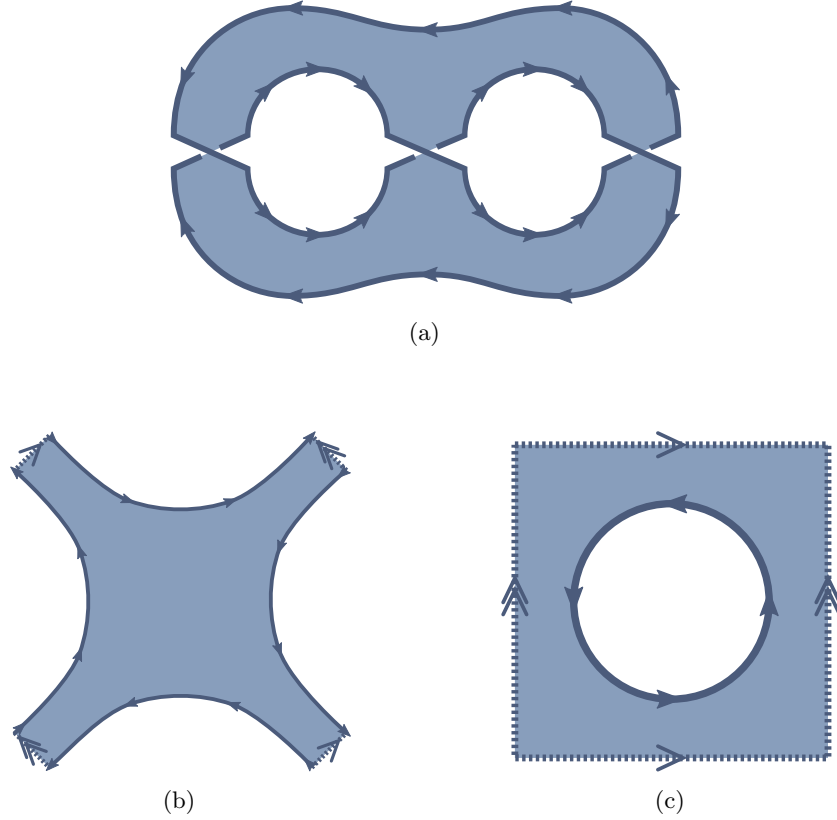


Figure 3.5: Three equivalent representations of the world-sheet of open string amplitudes, which lead to the field-theory partial amplitudes $A_{n;1B}^{(2)}$. This genus-2 surface is orientable, but has only one boundary, giving a single color trace. Its relation to the surface of Figure 3.4 is shown in (a). The representation in (b) will be useful for constructing the required unitarity cuts for the rational contributions to $A_{n;1B}^{(2)}$. Figure (c) shows the equivalence to the punctured torus. In (b) and (c) the dotted lines need to be sewn together according to their arrows.

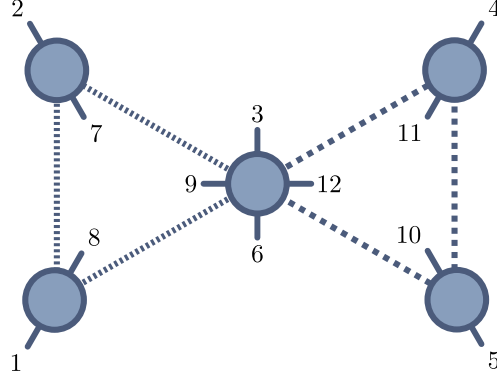


Figure 3.6: Sample one-loop squared cut to illustrate color routing. This cut belongs to the trace structure $\text{Tr}(T^1 \dots T^6) \text{Tr}(T^{10} T^{11} T^{12}) \text{Tr}(T^7 T^8 T^9)$

one-loop squared cuts, such as the one shown in Figure 3.6. Dressing the tree-amplitudes with color factors imposed by cyclic ordering, we obtain,

$$\text{Tr}(T^1 T^a T^8 T^f) \text{Tr}(T^a T^2 T^b T^7) \text{Tr}(T^b T^3 T^c T^{12} T^e T^6 T^f) \text{Tr}(T^c T^4 T^d T^{11}) \text{Tr}(T^d T^5 T^e T^{10}). \quad (3.48)$$

Using the $U(N_c)$ Fierz identities, we can rewrite this product as

$$\begin{aligned} & \text{Tr}(T^1 T^a T^8 T^f) \text{Tr}(T^a T^2 T^b T^7) \text{Tr}(T^b T^3 T^c T^{12} T^e T^6 T^f T^9) \text{Tr}(T^c T^4 T^d T^{11}) \text{Tr}(T^d T^5 T^e T^{10}), \\ &= \text{Tr}(T^1 T^2 T^b T^7 T^8 T^f) \text{Tr}(T^b T^3 T^c T^{12} T^e T^6 T^f T^9) \text{Tr}(T^c T^4 T^5 T^e T^{10} T^{11}) \\ &= \text{Tr}(T^1 T^2 T^3 T^c T^{12} T^e T^6 T^f T^9 T^7 T^8 T^f) \text{Tr}(T^c T^4 T^5 T^e T^{10} T^{11}) \\ &= \text{Tr}(T^1 T^2 T^3 T^c T^{12} T^e T^6) \text{Tr}(T^9 T^7 T^8) \text{Tr}(T^c T^4 T^5 T^e T^{10} T^{11}) \\ &= \text{Tr}(T^1 T^2 T^3 T^4 T^5 T^e T^{10} T^{11} T^{12} T^e T^6) \text{Tr}(T^7 T^8 T^9) \\ &= \text{Tr}(T^1 T^2 T^3 T^4 T^5 T^6) \text{Tr}(T^{10} T^{11} T^{12}) \text{Tr}(T^7 T^8 T^9), \end{aligned} \quad (3.49)$$

obtaining the three color traces expected for this graph. Note the direction of color flow, clockwise in the outer trace, and counter-clockwise in the two inner traces.

The partial amplitudes $A_{n:1B}^{(2)}$ on the other hand are constructed from unitarity cuts which adhere to the structure of the punctured torus shown in Figure 3.5. This illustrated at the one-loop squared cut shown in Figure 3.7. The dotted lines opposite of each other are connected. Whereas in $A_{n:1}^{(2)}, A_{n:r}^{(2)}$ and $A_{n:r,k}^{(2)}$ the loops were adjacent at the connecting vertex, they are now crossed. As the underlying surface has only one boundary, this cut produces a single color trace without factors of N_c . We again verify this explicitly: Dressing the amplitudes with color traces according to the shown ordering of particles, we obtain for the cut shown in Figure 3.7

$$\begin{aligned} & \text{Tr}(T^1 T^a T^8 T^f) \text{Tr}(T^a T^2 T^b T^7) \text{Tr}(T^6 T^b T^3 T^c T^{12} T^f T^9 T^e) \text{Tr}(T^c T^4 T^d T^{11}) \text{Tr}(T^d T^5 T^e T^{10}), \\ &= \text{Tr}(T^1 T^2 T^b T^7 T^8 T^f) \text{Tr}(T^6 T^b T^3 T^c T^{12} T^f T^9 T^e) \text{Tr}(T^c T^4 T^5 T^e T^{10} T^{11}) \\ &= \text{Tr}(T^1 T^2 T^3 T^c T^{12} T^f T^9 T^e T^6 T^b T^7 T^8 T^f) \text{Tr}(T^c T^4 T^5 T^e T^{10} T^{11}) \\ &= \text{Tr}(T^1 T^2 T^3 T^4 T^5 T^e T^{10} T^{11} T^{12} T^f T^9 T^e T^6 T^7 T^8 T^f) \\ &= \text{Tr}(T^1 T^2 T^3 T^4 T^5 T^6 T^7 T^8 T^f) \text{Tr}(T^{10} T^{11} T^{12} T^f T^9) \\ &= \text{Tr}(T^1 T^2 T^3 T^4 T^5 T^6 T^7 T^8 T^9 T^{10} T^{11} T^{12}). \end{aligned} \quad (3.50)$$

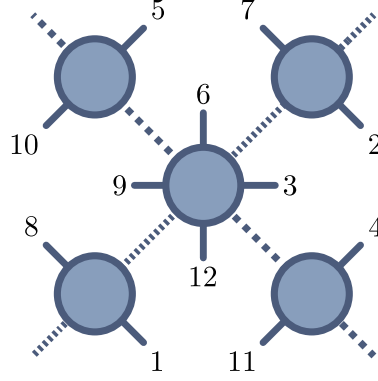


Figure 3.7: An example of a unitarity cut following the topology of Figure 3.5b. The open lines are connected according to the dashed, following Figure 3.5b. Dressing the amplitudes with the color structure according to the orderings shown gives us a single overall trace $\text{Tr}(T^1 T^2 \dots T^{11} T^{12})$. We can therefore identify such cuts as belonging to the subleading partial amplitude $A_{n:1B}^{(2)}$.

3.4.2 Generating Sets of Cuts

Now that know how to construct unitarity cuts belonging to the color structures in the two-loop color decomposition, we make the construction of the amplitudes $A_{6,2,0}^{(2)}$ and $A_{6,1,1}^{(2)}$ from such cuts explicit. We will then use this construction to verify the conjecture of section 3.3 about their connection to the rational contributions of all-plus amplitudes.

As discussed in section 3.3, the integral bases of $A_{6,2,0}^{(2)}$ and $A_{6,1,1}^{(2)}$ include all one-loop squared two-loop integrals, each of which can be factorized into a product of one-loop integrals. The partial amplitudes of the all-plus are symmetric under cyclic permutations of the particles in each of the color traces, and we choose to make these cyclic symmetries manifest in our computational approach. Instead of immediately summing over all cuts, we divide them into sets, which are related to each other by the permutations of the color structure. In analytic computations, we then only need to find the expression for one of the sets to recover the full amplitude. Due to this property, we call a reduced integral basis together with its coefficients a generating set $\tilde{R}^{(2)}$. In the following we will give the generic procedure for obtaining the generating sets $\tilde{R}^{(2)}$.

Due to the factorization of the required integrals, we only need to consider integral topologies where each loop is either a box, triangle, or bubble. As we are working Yang–Mills theory we can neglect tadpoles. In $A_{6,2,0}^{(2)}$ and $A_{6,1,1}^{(2)}$ both loops carry scalars, we are free to choose which loop’s coefficient to compute first. We can therefore impose an ordering in the integrals that enter $\tilde{R}^{(2)}$, such that the number of cuts in the left loop is always greater or equal to the number of cuts in the right. The opposite case will be obtained through the cyclic permutations once we compute $R^{(2)}$. We thus limit ourselves to the following classes of integrals

As described in section 2.4, the partial amplitudes fall into two different topologies, which need

to treated separately: the twice-punctured disk, and the punctured torus.

3.4.2.1 Twice Punctured Disk

First we will consider the twice-punctured disk topology. The associated partial amplitudes are $A_{n:1}^{(2)}$, $A_{n:k}^{(2)}$ and $A_{n:r,k}^{(2)}$, whose rational parts we denote by $R_{n:1}^{(2)}$, $R_{n:k}^{(2)}$, $R_{n:r,k}^{(2)}$. As discussed above, we define their generating sets $\tilde{R}_{n:1}^{(2)}$, $\tilde{R}_{n:k}^{(2)}$, $\tilde{R}_{n:r,k}^{(2)}$, such that,

$$R_{n:1}^{(2)}(1 \dots n) = \sum_{\sigma \in C_n} \tilde{R}_{n:1}^{(2)}(\sigma(1 \dots n)), \quad (3.52)$$

$$R_{n:k}^{(2)}(1 \dots k-1; k \dots n) = \sum_{\substack{\sigma_1 \in C_{k-1} \\ \sigma_2 \in C_{n-k-1}}} \tilde{R}_{n:k}^{(2)}(\sigma_1(1 \dots (k-1)); \sigma_2(k \dots n)), \quad (3.53)$$

$$R_{n:r,k}^{(2)}(1 \dots r; (r+1) \dots (r+k); (r+k+1) \dots n) = \sum_{\substack{\sigma_1 \in C_r, \sigma_2 \in C_k \\ \sigma_3 \in C_{n-r-k}}} \tilde{R}_{n:r,k}^{(2)}(\sigma_1(1 \dots r); \sigma_2((r+1) \dots (r+k)); \sigma_3((r+k+1) \dots n)). \quad (3.54)$$

Note that the sums do not include possible permutations of the traces themselves. Rather we include such permutations in our definition of the $\tilde{R}^{(2)}$. In the most general case, we have three traces of color generators, where each trace is the color structure of one of the boundaries in a cut, as described in section 3.4.1. We therefore have to separately account for all 6 possible assignments of the traces to these boundaries, treating each power of N_c as a trace without generators $\text{Tr}(\mathbb{1}_{N_c})$. For the leading-color case $R_{n:1}^{(2)}$, the single trace can only be associated to the outer boundary of the cut, consistent with refs. [11, 12] Any other assignment would turn one of the loops into a tadpole, and therefore would not contribute.

By choosing to construct the rational contributions through the generating sets $\tilde{R}^{(2)}$, we have to be make sure that every cut is only counted once when summing over cyclic permutations. If two different cuts are related by a permutation, we can avoid overcounting by including only one of them in the generating set. Figure 3.8 shows an example of such cyclicly related cuts of color structure $N_c \text{Tr}(T^1 T^2) \text{Tr}(T^3 T^4 T^5 T^6 T^7)$. Only one of the cuts would be kept in the generating set $\tilde{R}_{7:3}^{(2)}$.

For an even number of momenta, cuts exist that are related to themselves under cyclic permutation. For these it is not possible to avoid an overcounting, and we are forced to introduce symmetry factors. As an example, consider the cut contributing to $\tilde{R}_{6:1}^{(2)}$ shown in Figure 3.9. It is invariant under shifting all momenta by three positions, and therefore would contribute to $R_{6:1}^{(2)}$ twice. When adding this cut to $\tilde{R}_{6:1}^{(2)}$, we therefore need to dress it with a symmetry factor of $\frac{1}{2}$.

As mentioned in section 2.2, to obtain the full one-loop bubble coefficient we not only have to compute the bubble cut itself, but also need to include contributions from any triangle cuts obtained by cutting an additional propagator in the bubble. These triangle contributions to bubble coefficients have to be included in the generating sets as well, with the restriction that we cannot introduce cuts which separate both scalar pairs at once. Such cuts would belong to neither $A_{2,0}^{(2)}$ nor $A_{1,1}^{(2)}$ from the dimensional reconstruction point of view, and according to our premise should therefore not contribute to $R^{(2)}$.

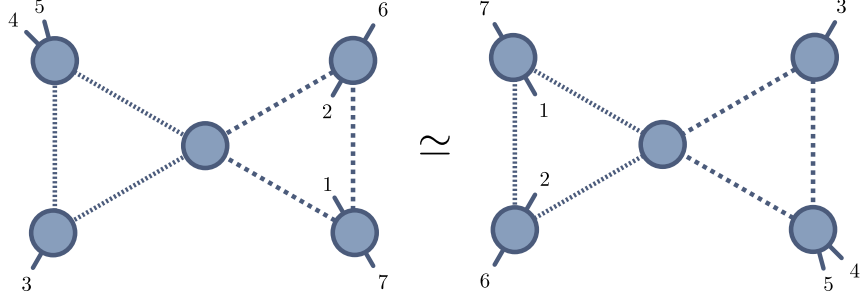


Figure 3.8: Example of overcounting after summing over cyclic permutations. The two cuts with color structure $N_c \text{Tr}(T^1 T^2) \text{Tr}(T^3 T^4 T^5 T^6 T^7)$ are related to each other by shifting the momenta of the traces by one and three places respectively. Therefore only one of the cuts should be added to $\tilde{R}_{7;3}^{(2)}$.

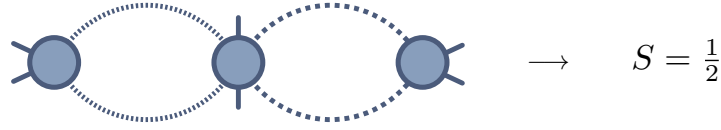
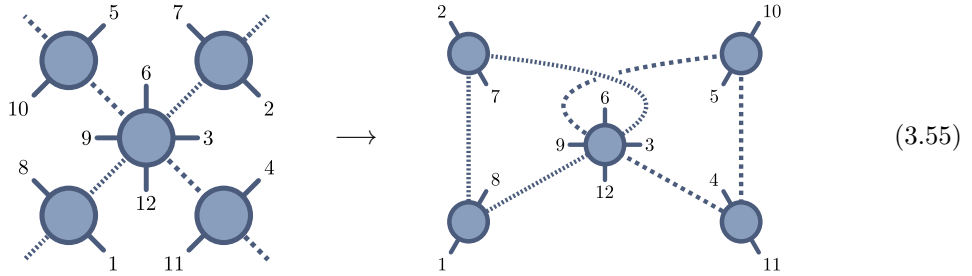


Figure 3.9: Example of symmetric cut for which overcounting cannot be avoided. Cuts of this type require a symmetry factor of $S = \frac{1}{2}$.

3.4.2.2 Punctured Torus

We now turn to the second topology, the punctured torus. Only one partial amplitude is associated to this topology, namely $A_{n:1B}^{(2)}$, with rational part $R_{n:1B}^{(2)}$. As described in section 2.4, we construct one-loop squared cuts belonging to this color structure by adhering to the topology shown in Figure 3.5b. One example of such a cut is shown in Figure 3.7.

By explicitly connecting the scalar lines of these cuts and flattening them,



we obtain the familiar one-loop squared form. From this point of view we can use the discussion of the previous section to construct generating sets of $R_{n:1B}^{(2)}$, i.e. building cuts according to the topologies of eq. (3.51). The main difference lies in the attachment of the scalar lines to the four-scalar vertex: while before the scalar lines did not intersect, they now cross each other in the central vertex.

A downside of working with the flattened version of 1B cuts is their tendency to hide the symmetries of the topology. While before the notion of particle attachments "inside" and "outside" the loops led to inclusions in different color traces, there is only a single trace in 1B partial amplitudes. The different attachments now only signify the relative ordering of the generators within the single trace, which is also less obvious than in the twice-punctured disk topology.

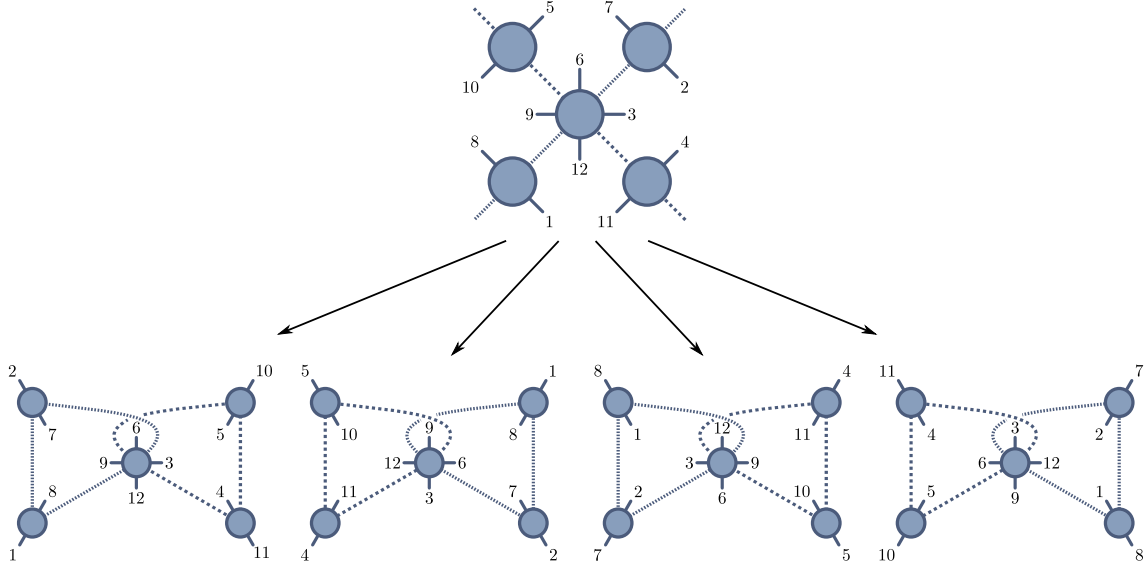


Figure 3.10: The cut at the top is the real contribution to $\mathcal{R}_{n:1B}$. Expressed in the usual one-loop squared layout it has four equally valid representations. When working cuts in the flattened layout, one has to ensure that only one is included in the generating set, as we would otherwise overcount the cut shown at the top.

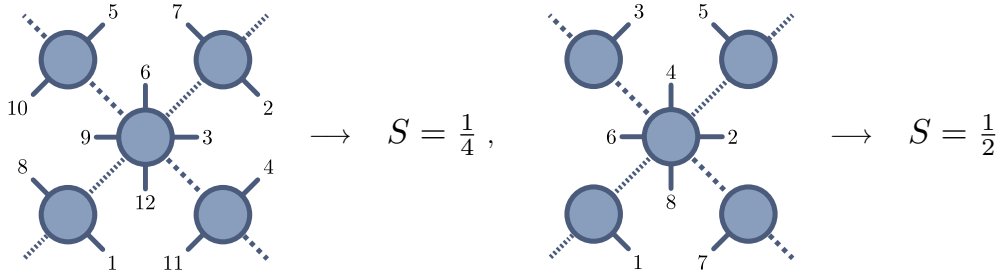


Figure 3.11: Examples of cuts that need to be included in the $\tilde{R}_{n:1B}^{(2)}$ with a symmetry factor S . The left cut requires $S = \frac{1}{4}$, as shifting all labels by four places amounts to a 90° rotation of the cut, causing it to appear four times in the permutation sum. Similarly, shifting all momenta in the right cut by four places is equivalent to a 180° rotation, such that $S = \frac{1}{2}$.

In addition, every 1B cut has four equivalent flattened representations, as shown in Figure 3.10. These representations appear unique at first glance as their two loops appear swapped or turned inside out, so particular care must be taken to ensure that no cut is included in $\tilde{R}_{n:1B}^{(2)}$ more than once. The four different representations also lead to new symmetry factors S . For an even number of momenta, some 1B cuts can be related to either two, or all of their representations under cyclic permutations. These cuts therefore need to be included in $\tilde{R}_{n:1B}^{(2)}$ with a symmetry factor of either $S = \frac{1}{2}$ or $S = \frac{1}{4}$ respectively.

The unflattened representation on the other hand does not distinguish between the sides of loops, and the overcounting and symmetry factor discussion simplifies, as they can be directly related to the rotational symmetry of the cuts, see Figure 3.11.

3.4.2.3 Mathematica Implementation

We automated the generation of cuts and symmetry factors required for the generating sets of the type $\tilde{R}_{n:1}^{(2)}$, $\tilde{R}_{n:i}^{(2)}$, $\tilde{R}_{n:r,k}^{(2)}$ and $\tilde{R}_{n:1B}^{(2)}$ in *Mathematica*. The code is completely generic and is able to obtain generating sets for an arbitrary number of gluons.

3.5 Six-Dimensional Amplitudes

To compute the amplitudes $A_{6,2,0}^{(2)}$ and $A_{6,1,1}^{(2)}$ from generalized unitarity we in principle require tree-amplitudes with six-dimensional states. While we keep the external momenta four-dimensional, all the momenta in the loops are generically six-dimensional, and in explicit sums over gluon polarizations we have to take into account the two additional states.

Fortunately, the loops of $A_{6,2,0}^{(2)}$ and $A_{6,1,1}^{(2)}$ carry only six-dimensional scalars, and the $(D-4)$ -dimensional components of the loop momenta are conserved within each loop. We can therefore treat the six-dimensional massless scalars as four-dimensional massive ones, allowing us to use the one-loop D -dimensional unitarity techniques presented in section 2.3. However, the resulting tree amplitudes require careful consideration, as they are in principle still six-dimensional. There are two classes of such amplitudes we need to consider: those amplitudes with a single scalar pair, appearing in each loop, and those with two scalar pairs, which connect the two loops.

While we could compute these tree amplitudes fully six-dimensionally using techniques laid down in refs. [125, 126], we can relate the required contributions to four-dimensional massive scalar QCD amplitudes, for which expressions partially exist in the literature. There are two key features that require special attention: the six-dimensional momentum components of the scalars, and the contact terms resulting from dimensional reduction, which are typically absent in scalar QCD. We will discuss the effects of these differences separately for amplitudes with one or two scalar lines.

3.5.1 Tree Amplitudes with One Scalar Pair

Let us first consider the single scalar-pair amplitudes,

$$A^{(0)}(1^\varphi 2^+ \dots (n-1)^+ n^\varphi). \quad (3.56)$$

As we only have one scalar line, the quartic scalar interactions do not play a role in this type of amplitude. Further, as the gluons only carry four-dimensional momenta, the $(D-4)$ -dimensional momentum components are conserved within the scalar pair. The only way these components can appear in the amplitude are contractions of the form

$$\mu^2 = (p_1^{(5)})^2 + (p_1^{(6)})^2 = (p_n^{(5)})^2 + (p_n^{(6)})^2. \quad (3.57)$$

As the six-dimensional scalars are massless, we have $\mu^2 = \bar{p}_1^2 = \bar{p}_n^2$, and we can interpret μ^2 as the squared mass of four-dimensional scalars. Thus, for four-dimensional gluon momenta the six-dimensional amplitudes $A^{(0)}(1^\varphi 2^+ \dots (n-1)^+ n^\varphi)$ are exactly those of four-dimensional massive scalar QCD, with squared scalar mass μ^2 . In computing these amplitudes using BCFW, gluonic

factorization channels will appear, and we would in principle have to include the two additional gluonic states in the polarization sum. However, the identification of the six-dimensional amplitudes with those scalar QCD shows us that we do not need to take these states into account, as their contribution is guaranteed to vanish.

Many results for the required scalar QCD tree-amplitudes already exist in the literature, so we will not discuss them any further here. In section B.1 we provide the expressions for the amplitudes used. In these and all following expressions we use six-dimensional Mandelstam invariants instead of four-dimensional ones, as they lead to more compact expressions.

3.5.2 Tree-Amplitudes with Two Scalar Pairs

In the case of the two scalar pair amplitudes, the situation is slightly more intricate. There exist two classes of amplitudes, differentiated by the manner in which the scalar lines interact. Amplitudes, where the scalar lines connect via the exchange of a gluon, we will denote by $A_{\text{gluon}}^{(0)}$, while those involving a four-scalar contact term we will call $A_{\text{contact}}^{(0)}$. Let us first consider such amplitudes without any external gluons. Three such amplitudes exist,³

$$A_{\text{gluon}}^{(0)}(1^\varphi 2^\varphi 3^{\varphi'} 4^{\varphi'}) \quad A_{\text{contact}}^{(0)}(1^\varphi 2^\varphi 3^{\varphi'} 4^{\varphi'}) \quad A_{\text{contact}}^{(0)}(1^\varphi 2^{\varphi'} 3^\varphi 4^{\varphi'}) \quad , \quad (3.58)$$

The first is required for $A_{6,2,0}^{(2)}$, while the second and third appear in cuts of $A_{6,1,1}^{(2)}$. Amplitudes of the type $A_{\text{contact}}^{(0)}(1^\varphi 2^{\varphi'} 3^\varphi 4^{\varphi'})$ will be required for subleading single trace partial amplitudes $A_{n:1B}^{(2)}$ as hinted at in section 2.4. If the scalar lines cross as shown in the third amplitude, the Feynman rules of eq. (3.32) do not allow for gluon exchange, hence the absence of $A_{\text{gluon}}^{(0)}(1^\varphi 2^{\varphi'} 3^\varphi 4^{\varphi'})$. If we include an additional four-dimensional gluon, we have the five distinct possibilities⁴

$$A_{\text{gluon}}^{(0)}(1^\varphi 2^\varphi 3^{\varphi+4^{\varphi'}} 5^{\varphi'}), \quad A_{\text{contact}}^{(0)}(1^\varphi 2^\varphi 3^{\varphi+4^{\varphi'}} 5^{\varphi'}), \quad A_{\text{gluon}}^{(0)}(1^\varphi 2^{\varphi+3^\varphi} 4^{\varphi'} 5^{\varphi'}), \quad (3.59)$$

$$A_{\text{contact}}^{(0)}(1^\varphi 2^{\varphi+3^\varphi} 4^{\varphi'} 5^{\varphi'}), \quad A_{\text{contact}}^{(0)}(1^\varphi 2^{\varphi+3^{\varphi'}} 4^\varphi 5^{\varphi'})$$

³Thanks to Ingrid Holm for suggesting the graphical representation of the scalar lines' internal connection. The absence of an internal border is meant to differentiate this representation from one-loop amplitudes.

⁴The external gluon in $A_{\text{gluon}}^{(0)}(1^\varphi 2^\varphi 3^{\varphi+4^{\varphi'}} 5^{\varphi'})$ can also be attached to the gluon propagator connecting the two scalar lines.

For amplitudes of both $A_{\text{gluon}}^{(0)}$ and $A_{\text{contact}}^{(0)}$ type, the $(D - 4)$ -dimensional momentum components are separately conserved for each scalar line. While the $A_{\text{gluon}}^{(0)}$ amplitudes are built using the same Feynman rules as scalar QCD, the gluon propagator contracts the momenta of the scalar lines, and particularly their $(D - 4)$ -dimensional components. These contractions are a feature of six-dimensional amplitudes and in principle we cannot obtain these contributions from purely four-dimensional techniques. Fortunately, for our purposes the four-dimensional parts of the amplitudes are sufficient. In the language of D -dimensional unitarity the missing terms will be proportional to μ_{12} . For one-loop squared topologies, μ_{12} integral coefficients are guaranteed to vanish by Lorentz invariance, and we can again use results from massive scalar QCD.

We use different methods to evaluate the four-scalar amplitudes. For simple cases, Feynman diagrams are a convenient choice to obtain compact expressions without spurious poles. The contact term amplitudes have a natural construction in terms of off-shell scalar currents that are sewn together at the contact term. For amplitudes where either of these methods becomes too complex we turn to massive BCFW recursion.

3.5.2.1 Feynman Diagrams

The four scalar amplitudes without external gluons shown in eq. (3.58) are each computed from a single Feynman diagram,

$$(3.60)$$

such that

$$A_{\text{gluon}}^{(0)}(1^\varphi 2^\varphi 3^{\varphi'} 4^{\varphi'}) = -\left(\frac{1}{2} + \frac{s_{23}}{s_{12}}\right), \quad (3.61)$$

$$A_{\text{contact}}^{(0)}(1^\varphi 2^\varphi 3^{\varphi'} 4^{\varphi'}) = -\frac{1}{2}, \quad (3.62)$$

$$A_{\text{contact}}^{(0)}(1^\varphi 2^{\varphi'} 3^\varphi 4^{\varphi'}) = 1. \quad (3.63)$$

The expression for $A_{\text{gluon}}^{(0)}(1^\varphi 2^\varphi 3^{\varphi'} 4^{\varphi'})$ is consistent with the one used in ref. [13], as well as the result of ref. [127]⁵.

In the presence of a single external gluon, Feynman diagrams are also a viable approach, as the analytic manipulations are still tractable. For the gluon-exchange amplitudes we again use

⁵The results in ref. [127] are defined up to prefactors, which in this case needs to be 2 for agreement with our expression

Feynman diagrams to obtain the compact expressions

$$A_{\text{gluon}}^{(0)}(1^\varphi 2^\varphi 3^+ 4^{\varphi'} 5^{\varphi'}) = -\frac{s_{24}(s_{23}[3|45|3] + s_{34}[3|12|3])}{2s_{12}s_{23}s_{34}s_{45}} - \frac{[3|24|3](s_{12}(s_{34} - s_{14}) + s_{45}(s_{23} - s_{25}) + 2s_{23}s_{34} - s_{12}s_{45})}{2s_{12}s_{23}s_{34}s_{45}} \quad (3.64)$$

$$A_{\text{gluon}}^{(0)}(1^\varphi 2^+ 3^\varphi 4^{\varphi'} 5^{\varphi'}) = -\frac{[2|13|2](s_{34} - s_{35}) + s_{12}[2|(4-5)3|2]}{2s_{12}s_{45}s_{23}} \quad (3.65)$$

The expression in eq. (3.64) was verified numerically using Berends–Giele recursion. It is also in agreement with the result of ref. [127]⁶.

3.5.2.2 Contact-Term Amplitudes from Off-Shell Scalar Currents

We obtain the contact-term amplitudes $A_{\text{contact}}^{(0)}$ from off-shell scalar currents. In these amplitudes, the two scalar lines are connected via a contact term. As these contact terms only amount to factors, we can construct the amplitudes from a Berends–Giele recursion [54], where we connect four off-shell scalar currents to the contact-term. The required currents contain a scalar line with a number of positive helicity gluons attached. Compared to the on-shell case there are two conditions that we have to loosen in our computations. By nature of an off-shell current, the mass and momentum square of the off-shell scalar are no longer connected. In addition, the current will no longer be gauge invariant, such that its form generally depends on the choice of reference momentum for the gluon polarization vectors.

The scalar current with only a single positive gluon matches exactly the on-shell amplitude, as it only consists of a single Feynman diagram,

$$J_\varphi(2^+ 3^\varphi) = -\frac{[2|3|q\rangle}{\langle 2q\rangle}. \quad (3.66)$$

Note that we define the currents J_φ to be the sum of Feynman diagrams normalized by a factor of $(-i)$, just as in the case of on-shell amplitudes. The scalar propagators sewing the currents to the contact term therefore have to be $\frac{-1}{s_{ijk\dots}}$. We can use this current to obtain the amplitude $A_{\text{contact}}^{(0)}(1^\varphi 2^\varphi 3^+ 4^{\varphi'} 5^{\varphi'})$,

$$\begin{aligned} A_{\text{contact}}^{(0)}(1^\varphi 2^\varphi 3^+ 4^{\varphi'} 5^{\varphi'}) &= V(\varphi\varphi\varphi'\varphi')\frac{-1}{s_{23}}J_\varphi(2^\varphi 3^+) \\ &\quad + V(\varphi\varphi\varphi'\varphi')\frac{-1}{s_{34}}J_{\varphi'}(3^+ 4^{\varphi'}) \\ &= \frac{1}{2s_{23}s_{34}\langle 3q\rangle}([3|2|q\rangle\langle 3|4|3] - [3|4|q\rangle\langle 3|2|3]) \\ &= \frac{1}{2s_{23}s_{34}\langle 3q\rangle}([3|2|3]\langle q|4|3] - [3|24|3]\langle 3q\rangle - [3|4|q\rangle\langle 3|2|3]) \\ &= -\frac{[3|24|3]}{2s_{23}s_{34}}. \end{aligned} \quad (3.67)$$

In the six-point case, *i.e.* amplitudes with two gluons, we generally require the two-gluon current

⁶As in the case of eq. (3.61), the result of ref. [127] requires a factor of 2 for agreement, due to it being defined only up to a prefactor.

$J_\varphi(2^+3^+4^\varphi)$ and $J_\varphi(2^+3^\varphi4^+)$. If we choose the reference momenta $q_2 = p_3$, $q_3 = p_2$, we obtain for $J_\varphi(2^+3^+4^\varphi)$,

$$J_\varphi(2^+3^+4^\varphi) = \frac{m_4^2 [23]}{s_{34} \langle 23 \rangle} + \frac{s_{234}}{2 \langle 23 \rangle^2}, \quad (3.68)$$

which closely resembles the on-shell result,

$$A^{(0)}(1^\varphi 2^+ 3^+ 4^\varphi) = \frac{m_4^2 [23]}{s_{34} \langle 23 \rangle}. \quad (3.69)$$

As we made a specific choice for the reference momenta, we have to make the same choice for the remaining currents. For $J_\varphi(2^+3^\varphi4^+)$ we get,

$$J_\varphi(2^+3^\varphi4^+) = -\frac{m_3^2 [24]^2}{s_{24}s_{34}} - \frac{s_{234} [2|3|4] [4|3|2]}{s_{23}s_{34} \langle 24 \rangle^2}, \quad (3.70)$$

where the first term again mirrors the on-shell amplitude,

$$A^{(0)}(1^\varphi 2^+ 3^\varphi 4^+) = -\frac{m_3^2 [24]^2}{s_{24}s_{34}}. \quad (3.71)$$

We can now construct the on-shell amplitudes. For $A_{\text{contact}}^{(0)}(1^\varphi 2^\varphi 3^+ 4^+ 5^{\varphi'} 6^{\varphi'})$ we obtain,

$$\begin{aligned} A_{\text{contact}}^{(0)}(1^\varphi 2^\varphi 3^+ 4^+ 5^{\varphi'} 6^{\varphi'}) &= V(\varphi\varphi\varphi'\varphi') \frac{-1}{s_{234}} J_\varphi(2^\varphi 3^+ 4^+) \\ &\quad + V(\varphi\varphi\varphi'\varphi') \frac{-1}{s_{345}} J_{\varphi'}(3^+ 4^+ 5^{\varphi'}) \\ &\quad + V(\varphi\varphi\varphi'\varphi') \left(\frac{-1}{s_{23}} J_\varphi(2^\varphi 3^+) \right) \times \left(\frac{-1}{s_{45}} J_{\varphi'}(4^+ 5^{\varphi'}) \right) \\ &= -\frac{1}{2 \langle 34 \rangle} \left[\frac{[3|25|4]}{s_{23}s_{45}} - [34] \left(\frac{m_2^2}{s_{23}s_{234}} + \frac{m_5^2}{s_{345}s_{45}} \right) \right]. \end{aligned} \quad (3.72)$$

Similarly, $A_{\text{contact}}^{(0)}(1^\varphi 2^\varphi 3^+ 4^{\varphi'} 5^{\varphi'} 6^+)$ and $A_{\text{contact}}^{(0)}(1^\varphi 2^+ 3^\varphi 4^{\varphi'} 5^+ 6^{\varphi'})$ evaluate to,

$$\begin{aligned} A_{\text{contact}}^{(0)}(1^\varphi 2^\varphi 3^+ 4^{\varphi'} 5^{\varphi'} 6^+) &= V(\varphi\varphi\varphi'\varphi') \\ &\quad \times \left(\frac{-1}{s_{23}} J_\varphi(2^\varphi 3^+) + \frac{-1}{s_{34}} J_{\varphi'}(3^+ 4^{\varphi'}) \right) \\ &\quad \times \left(\frac{-1}{s_{56}} J_{\varphi'}(5^{\varphi'} 6^+) + \frac{-1}{s_{61}} J_\varphi(6^+ 1^\varphi) \right) \\ &= -\frac{1}{2} \frac{[3|24|3]}{s_{23}s_{34}} \frac{[6|51|6]}{s_{56}s_{61}}, \end{aligned} \quad (3.73)$$

$$\begin{aligned} A_{\text{contact}}^{(0)}(1^\varphi 2^+ 3^\varphi 4^{\varphi'} 5^+ 6^{\varphi'}) &= V(\varphi\varphi\varphi'\varphi') \\ &\quad \times \left(\frac{-1}{s_{21}} J_\varphi(1^\varphi 2^+) + \frac{-1}{s_{23}} J_\varphi(2^+ 3^\varphi) \right) \\ &\quad \times \left(\frac{-1}{s_{45}} J_{\varphi'}(4^{\varphi'} 5^+) + \frac{-1}{s_{56}} J_{\varphi'}(5^+ 6^{\varphi'}) \right) \\ &= -\frac{1}{2} \frac{[2|13|2]}{s_{21}s_{23}} \frac{[5|46|5]}{s_{45}s_{56}}, \end{aligned} \quad (3.74)$$

where we used the same steps as in eq. (3.67). The sum over currents factorizes, as the gluons can never both appear in the same current. Note that in $A_{\text{contact}}^{(0)}(1^\varphi 2^\varphi 3^+ 4^{\varphi'} 5^{\varphi'} 6^+)$ the currents

in each factor belong to the same scalar line, while in $A_{\text{contact}}^{(0)}(1^\varphi 2^+ 3^\varphi 4^+ 5^{\varphi'} 6^{\varphi'})$ they do not.

Finally, we determine $A_{\text{contact}}^{(0)}(1^\varphi 2^+ 3^\varphi 4^+ 5^{\varphi'} 6^{\varphi'})$,

$$\begin{aligned}
A_{\text{contact}}^{(0)}(1^\varphi 2^+ 3^\varphi 4^+ 5^{\varphi'} 6^{\varphi'}) &= V(\varphi\varphi\varphi'\varphi') \times \left(\frac{-1}{s_{12}} J_\varphi(1^\varphi 2^+) \right) \times \left(\frac{-1}{s_{34}} J_\varphi(3^\varphi 4^+) \right) \\
&\quad + V(\varphi\varphi\varphi'\varphi') \times \left(\frac{-1}{s_{12}} J_\varphi(1^\varphi 2^+) \right) \times \left(\frac{-1}{s_{45}} J_{\varphi'}(4^+ 5^{\varphi'}) \right) \\
&\quad + V(\varphi\varphi\varphi'\varphi') \times \left(\frac{-1}{s_{23}} J_\varphi(2^+ 3^\varphi) \right) \times \left(\frac{-1}{s_{45}} J_{\varphi'}(4^+ 5^{\varphi'}) \right) \\
&\quad + V(\varphi\varphi\varphi'\varphi') \times \left(\frac{-1}{s_{234}} J_\varphi(2^+ 3^\varphi 4^+) \right) \\
&= -\frac{1}{2} \left[\frac{m_3^2 [24]^2}{s_{23}s_{234}s_{34}} - \frac{\langle 2|3|4\rangle \langle 4|1|2\rangle}{s_{12}s_{34} \langle 24\rangle^2} + \frac{\langle 2|5|4\rangle \langle 4|1|2\rangle}{s_{12}s_{45} \langle 24\rangle^2} \right. \\
&\quad \left. + \frac{\langle 2|3|4\rangle \langle 4|3|2\rangle}{s_{23}s_{34} \langle 24\rangle^2} - \frac{\langle 2|5|4\rangle \langle 4|3|2\rangle}{s_{23}s_{45} \langle 24\rangle^2} \right] \\
&= -\frac{1}{2} \left[\frac{m_3^2 [24]^2}{s_{23}s_{234}s_{34}} + \frac{[2|13|2][4|35|4]}{s_{12}s_{23}s_{34}s_{45}} \right]. \tag{3.75}
\end{aligned}$$

As the currents are agnostic as to the scalar type, we can summarize the results as follows,

$$A_{\text{contact}}^{(0)}(1^{\varphi_1} 2^{\varphi_2} 3^+ 4^{\varphi_3} 5^{\varphi_4}) = V(\varphi_1 \varphi_2 \varphi_3 \varphi_4) \times \left[\frac{[3|24|3]}{s_{23}s_{34}} \right], \tag{3.76}$$

$$A_{\text{contact}}^{(0)}(1^{\varphi_1} 2^{\varphi_2} 3^+ 4^+ 5^{\varphi_3} 6^{\varphi_4}) = V(\varphi_1 \varphi_2 \varphi_3 \varphi_4) \times \left[\frac{[3|25|4]}{s_{23}s_{45} \langle 34\rangle} - \frac{[34]}{\langle 34\rangle} \left(\frac{m_2^2}{s_{23}s_{234}} + \frac{m_5^2}{s_{345}s_{45}} \right) \right], \tag{3.77}$$

$$A_{\text{contact}}^{(0)}(1^{\varphi_1} 2^{\varphi_2} 3^+ 4^{\varphi_3} 5^{\varphi_4} 6^+) = V(\varphi_1 \varphi_2 \varphi_3 \varphi_4) \times \left[\frac{[3|24|3][6|51|6]}{s_{23}s_{34} s_{56}s_{61}} \right], \tag{3.78}$$

$$A_{\text{contact}}^{(0)}(1^{\varphi_1} 2^+ 3^{\varphi_2} 4^+ 5^{\varphi_3} 6^{\varphi_4}) = V(\varphi_1 \varphi_2 \varphi_3 \varphi_4) \times \left[\frac{m_3^2 [24]^2}{s_{23}s_{234}s_{34}} + \frac{[2|13|2][4|35|4]}{s_{12}s_{23}s_{34}s_{45}} \right]. \tag{3.79}$$

where the φ_i can be specified to be either φ or φ' .

3.5.2.3 Massive BCFW Recursion

For gluon-exchange amplitudes with more than one gluon, as well as contact-term amplitudes with more than two gluons we make use of BCFW recursion [59]. If such an amplitude has two adjacent gluons, we can use a standard BCFW gluon-gluon shift. We have verified using Berends–Giele recursion that the relevant amplitudes with up to three gluons scale as $\frac{1}{z}$ or better under such shifts. If an amplitude does not possess a pair of adjacent gluons, we can still use recursion, now shifting the momenta of an adjacent gluon and massive scalar pair. Such shifts have been used for example in refs. [128, 129] to compute tree-amplitudes with a single massive scalar line. In the case of four-scalar amplitudes, such shifts can also be used, provided that only the gluon’s angle spinor is shifted, and the shifted gluon and scalar are adjacent. We will demonstrate the method by recomputing $A_{\text{gluon}}^{(0)}(1^\varphi 2^\varphi 3^+ 4^{\varphi'} 5^{\varphi'})$ and $A_{\text{contact}}^{(0)}(1^\varphi 2^\varphi 3^+ 4^{\varphi'} 5^{\varphi'})$.

As in ref. [129], we choose to construct the shifted momenta using the massless projection of the massive momentum with respect to the massless one. For the amplitude in question, we use a

$\langle 3, 2^b \rangle$ -shift of the form,

$$\begin{aligned} p_2 \rightarrow \hat{p}_2 &= p_2 - \frac{z}{2} [3|\gamma|2^b], & p_3 \rightarrow \hat{p}_3 &= p_3 + \frac{z}{2} [3|\gamma|2^b], \\ \lambda_3 \rightarrow \lambda_3 &= \lambda_3 + z\lambda_2^b, & \tilde{\lambda}_3 \rightarrow \hat{\lambda}_3 &= \tilde{\lambda}_3. \end{aligned} \quad (3.80)$$

The momentum p_2^b is the massless projection of p_2 on p_3 [130],

$$p_2^b = p_2 - \frac{\mu_2^2}{2(p_2 \cdot p_3)} p_3. \quad (3.81)$$

From this definition we see that the shifted momenta \hat{p}_2, \hat{p}_3 satisfy all the requirements for a BCFW shift,

$$\begin{aligned} \hat{p}_2^2 &= \hat{p}_2 \cdot p_2 = p_2^2, & \hat{p}_3^2 &= \hat{p}_3 \cdot p_3 = p_3^2, \\ \hat{p}_2 \cdot \hat{p}_3 &= \hat{p}_2 \cdot p_3 = \hat{p}_3 \cdot p_2 = p_2 \cdot p_3. \end{aligned} \quad (3.82)$$

From these shifted momenta, the gluon-exchange amplitude can be computed via,

$$\begin{aligned} A_{\text{gluon}}^{(0)}(1^\varphi 2^\varphi 3^+ 4^{\varphi'} 5^{\varphi'}) &= - \sum_{h=\pm} A^{(0)}(\hat{2}^\varphi, \hat{K}^h, 1^\varphi) \frac{1}{s_{12}} A^{(0)}(5^{\varphi'}, (-\hat{K})^{-h}, \hat{3}^+, 4^{\varphi'}) \\ &\quad - A_{\text{gluon}}^{(0)}(1^\varphi, \hat{2}^\varphi, \hat{K}^{\varphi'}, 5^{\varphi'}) \frac{1}{s_{34}} A_3^{(0)}((- \hat{K})^{\varphi'}, \hat{3}^+, 4^{\varphi'}). \end{aligned} \quad (3.83)$$

Note that we are only summing over the four-dimensional polarization states. To compute the full six-dimensional amplitude, we would at this point also have to include the six-dimensional states⁷. However, for simplicity we discard these terms, as they would lead to cross-terms $\mu_{14}, \mu_{15}, \mu_{15}, \mu_{25}$, which will be irrelevant for our computations. Using the result for the four-scalar amplitude in eq. (3.61) as well as the two-scalar amplitudes in appendix B.1, we obtain,

$$A_{\text{gluon}}^{(0)}(1^\varphi 2^\varphi 3^+ 4^{\varphi'} 5^{\varphi'}) = \frac{1}{\Delta} \left(\frac{[3|45|3]^2 m_2^2 + [3|21|3]^2 m_4^2}{s_{12}s_{45}} - \frac{[3|42|3]^2 s_{15}}{s_{23}s_{34}} \right) - \frac{[3|42|3]}{2s_{23}s_{34}}, \quad (3.84)$$

where $\Delta = (s_{34} [3|12|3] + s_{12} [3|42|3])$ is a spurious pole. This expression numerically matches the Feynman diagram result of eq. (3.64).

For the contact-term amplitude, we have to discard in eq. (3.83) any channels corresponding to a gluon exchange between the scalar lines, and replace all appearances of $A_{\text{gluon}}^{(0)}$ with $A_{\text{contact}}^{(0)}$,

$$A_{\text{contact}}^{(0)}(1^\varphi 2^\varphi 3^+ 4^{\varphi'} 5^{\varphi'}) = -A_{\text{contact}}^{(0)}(1^\varphi \hat{2}^\varphi \hat{K}^{\varphi'} 5^{\varphi'}) \frac{1}{s_{34}} A_3^{(0)}((- \hat{K})^{\varphi'}, \hat{3}^+, 4^{\varphi'}). \quad (3.85)$$

Due to the simplicity of the tree amplitudes involved, the result is free of spurious poles, and agrees with the expression in eq. (3.76).

While recursion allows us to obtain analytic expressions tree-amplitudes with a arbitrary number of gluons, the results almost always suffer spurious poles which cancel non-trivially. In addition, as four-scalar amplitudes of previous steps appear in the recursion, these spurious poles propagate and lead to large expressions in denominators. For our purposes we only require these tree-amplitudes for up to three gluons, at which point the complexity of the expressions remains

⁷When summing over these states defined as in refs. [125, 126], they need to be accompanied by a relative sign compared to the four-dimensional states, as the polarization vectors in the completeness relation in eq.(33) of ref. [125] are contracted by anti-symmetric tensors

manageable.

3.6 Momentum Twistor Parametrization

To obtain analytic expressions for $R_{5:1}^{(2)}$ and $R_{5:3}^{(2)}$ we will use parametrized kinematics based on their representation in momentum twistor space. We therefore provide a short summary of momentum twistors and one possible choice of an n -momentum parametrization, which is the one used for the results of section 3.7.2.

Starting with an ordered set of massless four-dimensional momenta (p_1, \dots, p_n) satisfying $\sum p_i = 0$, one can associate to the p_i a set of elements y_i in dual momentum space, satisfying the relation $y_i - y_{i-1} = p_i$. The y_i are constructed explicitly as $y_i = \sum_{j=0}^i p_j$, where p_0 can be chosen arbitrarily. Since the momenta are massless we further have the property that $(y_i - y_{i-1})^2 = 0$. Ref. [131] details the construction of the twistor version of this dual momentum space, called projective momentum-twistor space. Momentum twistors are elements of \mathbb{CP}^3 , and for every momentum p_i in our set we can find an associated momentum twistor with homogeneous coordinates $Z_j^I = (\lambda_j^\alpha, \mu_j^{\dot{\alpha}})$. Here λ_i is the angle spinor of p_i defined as usual, while μ_i is a spinor transforming in the conjugate $SU(2)$ representation. The λ_i and μ_i satisfy the incidence relation

$$\mu_{i\dot{\alpha}} = \lambda_i^\alpha y_{i\alpha\dot{\alpha}}. \quad (3.86)$$

Under the usual little group transformation λ and μ scale equally, as can be seen from the incidence relation. This is consistent with the fact that the Z^I are homogeneous coordinates in \mathbb{CP}^3 , and a total rescaling of Z^I describes the same point in projective momentum-twistor space.

The bracket spinor $\tilde{\lambda}_i^{\dot{\alpha}}$ of a momentum p_i can be obtained via the relation [131],

$$\tilde{\lambda}_i^{\dot{\alpha}} = \frac{\langle i(i+1) \rangle \mu_{i-1}^{\dot{\alpha}} + \langle (i+1)(i-1) \rangle \mu_i^{\dot{\alpha}} + \langle (i-1)i \rangle \mu_{i+1}^{\dot{\alpha}}}{\langle i(i+1) \rangle \langle (i-1)i \rangle}. \quad (3.87)$$

Based on this relation, we can see that scaling λ^α and $\mu^{\dot{\alpha}}$ leads to the inverse behavior for $\tilde{\lambda}^{\dot{\alpha}}$ as expected.

A convenient way of expressing the momentum twistors Z_i^I of an n -momentum configuration is as a $(4 \times N)$ -matrix,

$$Z = (Z_1^I Z_2^I \dots Z_{n-1}^I Z_n^I) = \begin{pmatrix} \lambda_1^\alpha & \lambda_2^\alpha & \dots & \lambda_{n-1}^\alpha & \lambda_n^\alpha \\ \mu_1^{\dot{\alpha}} & \mu_2^{\dot{\alpha}} & \dots & \mu_{n-1}^{\dot{\alpha}} & \mu_n^{\dot{\alpha}} \end{pmatrix}. \quad (3.88)$$

In this representation all required spinor products can be obtained by computing appropriate minors of the matrix Z .

As masslessness and momentum conservation are manifest in kinematics defined through momentum twistors, any choice of values for the entries of Z represents a valid momentum configuration. This makes them a useful tool for generating numeric momentum configurations with elements in the rational numbers \mathbb{Q} or a finite field \mathbb{F}_p .

We can use symmetries of our kinematics to reduce the number of independent entries in Z . As mentioned before, the Z_i are homogeneous coordinates, allowing us to fix one element in each

column of Z . In choosing a frame, spatial rotations, Lorentz-boosts and shifts fix an additional 10 parameters. The remaining $(3n - 10)$ entries are free, and are sufficient to obtain any valid configuration of momenta by choosing their values appropriately. Momentum twistors therefore greatly simplify finding parametrizations of generic massless kinematics, as any choice of fixing entries leads to a different valid parametrization.

While spinors and Mandelstam invariants are linked by relations such as momentum conservation or Schouten identities, the momentum twistor parameters are independent of one another. Thus, parameterized momentum twistors allow us to express integral coefficients and rational parts of amplitudes as multivariate rational functions in the parameters, while encapsulating the full analytic dependence on the kinematics. In this representation, simplifications can be easier to carry out as there are no additional relations, and the simplification of multivariate rational expressions is a standard—though still challenging—problem.

When moving to momentum-twistor parameters we are removing the explicit spinorial dependence, and therefore any phase information. In fact, when we fix $(n + 10)$ entries of Z , we make a specific choice for the phases of the spinors. When evaluating expressions with non-zero phase-weight, such as helicity amplitudes, we therefore have to introduce a normalization factor that cancels the phase dependence, allowing us to restore it when necessary. In the case of all-plus partial amplitudes a convenient choice of normalization is to assign a Parke–Taylor factor to every color trace, so that in general

$$\text{Tr}(T^1 \dots T^{i-1}) \text{Tr}(T^i \dots T^{j-1}) \text{Tr}(T^j \dots T^n) \rightarrow \frac{1}{\text{PTF}(1 \dots i-1)} \frac{1}{\text{PTF}(i \dots j-1)} \frac{1}{\text{PTF}(j \dots n)}, \quad (3.89)$$

where

$$\text{PTF}(1 \dots n) = \langle 12 \rangle \dots \langle n1 \rangle. \quad (3.90)$$

As we are usually interested in obtaining a result in terms of spinors and Mandelstam invariants, we also need to find a solution to the momentum-twistor parameters in terms of these objects. Examples of parametrizations for four, five and six momenta together with such solutions can be found in refs. [115, 132]. In the following we give a parametrization of n -momentum kinematics, that extends the structure found in these examples. Other general parametrizations have been found in the past [133, 134], however the one presented below was discovered independently of these results.

Splitting the parameters into three sets a_p , b_q and c_r , with $p \in \{1, \dots, n-2\}$ and $q, r \in \{1, \dots, n-4\}$, we choose Z as follows,

$$Z = \begin{pmatrix} 1 & 0 & y_1 & y_2 & y_3 & \dots & y_{n-3} & y_{n-2} \\ 0 & 1 & 1 & 1 & 1 & \dots & 1 & 1 \\ 0 & 0 & 0 & \frac{b_{n-4}}{a_2} & \tilde{b}_{n-5} & \dots & \tilde{b}_1 & 1 \\ 0 & 0 & 1 & 1 & \tilde{c}_{n-4} & \dots & \tilde{c}_2 & \tilde{c}_1 \end{pmatrix}. \quad (3.91)$$

The y_k , \tilde{b}_k and \tilde{c}_k are defined recursively,

$$\begin{aligned} y_k &= \sum_{i=1}^k \prod_{j=1}^i \frac{1}{a_j}, \\ \tilde{b}_k &= \tilde{b}_{k-1} + a_{n-k}(\tilde{b}_{k-1} - \tilde{b}_{k-2}) + b_k, \\ \tilde{c}_k &= \tilde{c}_{k-1} + a_{n-k+1}(\tilde{c}_{k-1} - \tilde{c}_{k-2}) + \frac{b_{k-1}}{b_{n-4}}(c_k - 1), \end{aligned} \quad (3.92)$$

with $a_{k > (n-2)} = \tilde{b}_{k < 0} = \tilde{c}_{k \leq 0} = 0$ and $b_0 = \tilde{b}_0 = 1$. The associated solution in terms of spinors and Mandelstam invariants is then

$$\begin{aligned} a_1 &= s_{12} \\ a_{k>1} &= -\frac{\langle k, k+1 \rangle \langle k+2, 1 \rangle}{\langle 1, k \rangle \langle k+1, k+2 \rangle}, \\ b_{n-4} &= \frac{s_{23}}{s_{12}}, \\ b_k &= \frac{\langle n-k | n-k+1 | 2 \rangle}{\langle n-k | 1 | 2 \rangle}, \\ c_k &= -\frac{\langle 1 | 3 | n-k+2 \rangle}{\langle 1 | 2 | n-k+2 \rangle}, \end{aligned} \quad (3.93)$$

where in the solution for the c_k the spinor labels have to be taken mod n .

3.7 Results

3.7.1 The Four-Gluon Amplitude Analytically

To demonstrate the separable approach, we will give an analytic derivation of the rational parts $R_{4:1}^{(2)}$, $R_{4:3}^{(2)}$ and $R_{4:1B}^{(2)}$ of the four-gluon two-loop all-plus partial amplitudes $A_{4:1}^{(2)}$, $A_{4:3}^{(2)}$ and $A_{4:1B}^{(2)}$.

3.7.1.1 Leading Color $R_{4:1}^{(2)}$

For the leading-color contribution $R_{4:1}^{(2)}$ we can determine the required cuts to be those shown in Figure 3.12. As we have an even number of external particles, we have to include symmetry factors to avoid overcounting when summing over cyclic permutations, as described in section 3.4. Together with these symmetry factors the cuts form the generating set $\tilde{R}_{4:1}^{(2)}$, such that

$$R_{4:1}^{(2)}(1^+ 2^+ 3^+ 4^+) = \sum_{\sigma \in C_4} \tilde{R}_{4:1}^{(2)}(1^+ 2^+ 3^+ 4^+), \quad (3.94)$$

where $\tilde{R}^{(2)}$ is given by,

$$\begin{aligned} \tilde{R}_{4:1}^{(2)} &= (D_s - 2)^2 \left[\frac{1}{2} I_3^{[2]} I_3^{[2]} C^{(2)} \left[\text{Diagram 1} \right] + I_3^{[2]} I_2^{[2]} [s_{34}] C^{(2)} \left[\text{Diagram 2} \right] \right. \\ &\quad \left. + \frac{1}{2} I_2^{[2]} [s_{12}] I_2^{[2]} [s_{34}] C^{(2)} \left[\text{Diagram 3} \right] \right]. \end{aligned} \quad (3.95)$$

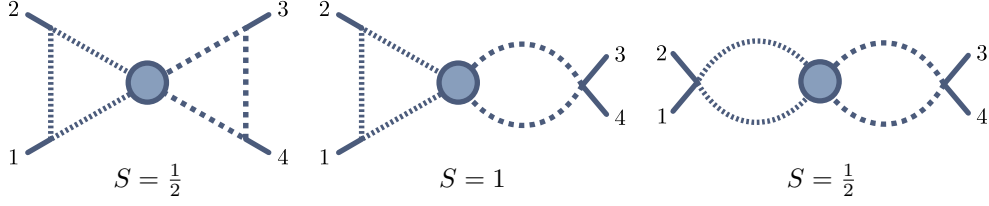
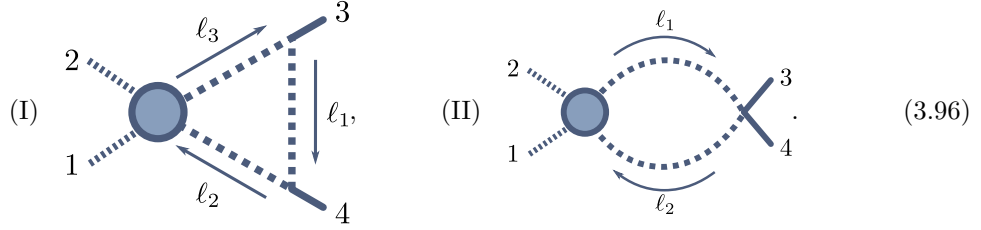


Figure 3.12: Cuts required for $R_{4,1}^{(2)}$, together with their symmetry factors S .

Due to separability, we can first focus our attention on the right-hand loop. There are only two distinct cuts, namely a triangle and a bubble with two gluons and two massive scalars,



For the triangle cut (I), we use the loop-momentum parametrization of eqs.(2.117), (2.119), which in this case simplifies to,

$$\begin{aligned}\ell_1^\mu &= \frac{1}{2} \left(t \langle 4 | \gamma^\mu | 3 \rangle - \frac{\mu^2}{s_{34}t} \langle 3 | \gamma^\mu | 4 \rangle \right), \\ \ell_1^{*\mu} &= \frac{1}{2} \left(t \langle 3 | \gamma^\mu | 4 \rangle - \frac{\mu^2}{s_{34}t} \langle 4 | \gamma^\mu | 3 \rangle \right).\end{aligned}\tag{3.97}$$

Using the expressions for the scalar tree amplitudes from Appendix B.1, a brief computation leads to

$$\begin{aligned}C_{\text{Tri},[2]}^{(1)} \left[\begin{array}{c} k_2^{\varphi} \\ k_1^{\varphi} \end{array} \right] &= \frac{1}{2} \sum_{\ell, \ell^*} \text{Inf}_{\mu^2, t} \left[A^{(0)}(k_1^{\varphi} k_2^{\varphi} \ell_3^{\varphi'} (-\ell_2)^{\varphi'}) \right. \\ &\quad \times A^{(0)}(3^+ \ell_1^{\varphi'} (-\ell_3)^{\varphi'}) A^{(0)}(4^+ \ell_2^{\varphi'} (-\ell_1)^{\varphi'}) \Big] \Big|_{\mu^2, t^0} \\ &= \frac{1}{2} \text{Inf}_{\mu^2, t} \left[\sum_{\ell, \ell^*} \frac{[3|\ell_1|4]}{\langle 34 \rangle} \frac{[4|\ell_1|3]}{\langle 43 \rangle} \frac{s_{k_1 \ell_3}}{s_{34}} \right] \Big|_{\mu^2, t^0} \\ &= \frac{1}{2} \text{Inf}_{\mu^2, t} \left[\frac{\mu^2}{\langle 34 \rangle^2} \left(2s_{k_1 3} + \left(t \langle 4 | k_1 | 3 \rangle - \frac{\mu^2}{s_{34}t} \langle 3 | k_1 | 4 \rangle \right) \right. \right. \\ &\quad \left. \left. + \left(t \langle 3 | k_1 | 4 \rangle - \frac{\mu^2}{s_{34}t} \langle 4 | k_1 | 3 \rangle \right) \right) \right] \Big|_{\mu^2, t^0} \\ &= \frac{s_{k_1 3}}{\langle 34 \rangle^2}.\end{aligned}\tag{3.98}$$

For the coefficient of the bubble integral associated to cut (II) in eq. (3.96) we would generally have to include a triangle contribution, where an additional cut is placed in the gluon vertex. However, by choosing the bubble reference momentum χ to be p_3 , the triangle contribution vanishes, and only the bubble cut itself is required. With this choice for χ , the generic bubble loop-momentum parametrization of eq. (2.122) simplifies to,

$$\ell_1^\mu = y p_4^\mu + (1-y) p_3^\mu + \frac{1}{2} \left(t \langle 4 | \gamma^\mu | 3 \rangle + \left(\frac{y(1-y)}{t} - \frac{\mu^2}{ts_{34}} \right) \langle 3 | \gamma^\mu | 4 \rangle \right), \tag{3.99}$$

and we obtain for the bubble coefficient,

$$\begin{aligned}
& C_{\text{Bub},[2]}^{(1)} \left[\begin{array}{c} k_2 \\ \text{---} \bullet \text{---} \\ k_1 \end{array} \begin{array}{c} 3 \\ \text{---} \times \text{---} \\ 4 \end{array} \right] \\
&= \text{Inf}_{\mu^2, y, t} \left[A^{(0)}(k_1^\varphi k_2^\varphi l_1^{\varphi'} (-l_2)^{\varphi'}) \times A^{(0)}(3^+ 4^+ \ell_2^{\varphi'} (-\ell_1)^{\varphi'}) \right] \Big|_{t^0, y^i \rightarrow Y_i, \mu^2} \\
&= - \text{Inf}_{\mu^2, y, t} \left[\frac{s_{k_1 \ell_1}}{s_{34}} \frac{\mu^2}{s_{3 \ell_1}} \frac{[34]}{\langle 34 \rangle} \right] \Big|_{t^0, y^i \rightarrow Y_i, \mu^2} \\
&= \text{Inf}_{\mu^2, y, t} \left[\frac{\mu^2}{y \langle 34 \rangle^2 s_{34}} \right. \\
&\quad \times \left[y s_{k_1 4} + (1-y) s_{k_1 3} + t [3|k_1|4] + \frac{y(1-y)s_{34} - \mu^2}{s_{34}t} [4|k_1|3] \right] \Big|_{t^0, y^i \rightarrow Y_i, \mu^2} \\
&= \frac{s_{k_1 4} - s_{k_1 3}}{\langle 34 \rangle^2 s_{34}}.
\end{aligned} \tag{3.100}$$

In this case the Inf_y operation only leads to a y^0 term, whose parameter integral Y_i is 1.

We can now use these results to compute the cuts of Figure 3.12 by evaluating the left-hand side loops,

$$\text{(I)} \quad \begin{array}{c} 2 \\ \text{---} \ell_2 \\ \text{---} \bullet \text{---} \\ \text{---} \ell_3 \\ 1 \end{array} \begin{array}{c} 3 \\ \text{---} \times \text{---} \\ 4 \end{array}, \quad \text{(II)} \quad \begin{array}{c} 2 \\ \text{---} \ell_2 \\ \text{---} \bullet \text{---} \\ \text{---} \ell_1 \\ 1 \end{array} \begin{array}{c} 3 \\ \text{---} \times \text{---} \\ 4 \end{array}. \tag{3.101}$$

For the triangle cut (I), we use the loop-momentum parametrization,

$$\begin{aligned}
\ell_1^\mu &= \frac{1}{2} \left(t \langle 2|\gamma^\mu|1] - \frac{\mu^2}{s_{12}t} \langle 1|\gamma^\mu|2] \right), \\
\ell_1^{*\mu} &= \frac{1}{2} \left(t \langle 1|\gamma^\mu|2] - \frac{\mu^2}{s_{12}t} \langle 2|\gamma^\mu|1] \right).
\end{aligned} \tag{3.102}$$

The coefficients of the first two cuts in Figure 3.12 evaluate to,

$$\begin{aligned}
C_{[1]}^{(2)} \left[\begin{array}{c} 2 \\ \text{---} \text{---} \text{---} \\ 1 \end{array} \begin{array}{c} 3 \\ \text{---} \text{---} \text{---} \\ 4 \end{array} \right] &= C_{\text{Tri}}^{(1)} \left[\begin{array}{c} 2 \\ \text{---} \text{---} \text{---} \\ 1 \end{array} \right] \times C_{\text{Tri}}^{(1)} \left[\begin{array}{c} 3 \\ \text{---} \text{---} \text{---} \\ 4 \end{array} \right] \\
&= \frac{1}{2} \sum_{\ell_1, \ell_1^*} \text{Inf}_{\mu^2, t} \left[A^{(0)}((-\ell_3)^\varphi 1^+ \ell_1^\varphi) A^{(0)}((-\ell_1)^\varphi 2^+ \ell_2^\varphi) C_{\text{Tri}}^{(1)} \left[\begin{array}{c} 3 \\ \text{---} \text{---} \text{---} \\ 4 \end{array} \right] \right] \Big|_{t^0, \mu^2} \\
&= \frac{1}{2} \frac{s_{12}}{\langle 12 \rangle^2 \langle 34 \rangle^2} \sum_{\ell_1, \ell_1^*} \text{Inf}_{\mu^2, t} \left[s_{\ell_3 3} \right] \Big|_{t^0, \mu^2} \\
&= \frac{1}{2} \frac{s_{12}}{\langle 12 \rangle^2 \langle 34 \rangle^2} \text{Inf}_{\mu^2, t} \left[\mu^2 \left(2s_{13} + \left(t \langle 2|3|1] - \frac{\mu^2}{s_{12}t} \langle 1|3|2] \right) \right. \right. \\
&\quad \left. \left. + \left(t \langle 1|3|2] - \frac{\mu^2}{s_{12}t} \langle 2|3|1] \right) \right) \right] \Big|_{\mu^2, t^0} \\
&= \frac{s_{12} s_{13}}{\langle 12 \rangle^2 \langle 34 \rangle^2},
\end{aligned} \tag{3.103}$$

$$\begin{aligned}
C^{(2)} \left[\begin{array}{c} 2 \\ 1 \end{array} \right] &= C_{\text{Tri}}^{(1)} \left[\begin{array}{c} 2 \\ 1 \end{array} \right] \times C_{\text{Bub}}^{(1)} \left[\begin{array}{c} 3 \\ 4 \end{array} \right] \\
&= \frac{1}{2} \sum_{\ell_1, \ell_1^*} \text{Inf}_{\mu^2, t} \left[A^{(0)}((- \ell_3)^\varphi 1^+ \ell_1^\varphi) A^{(0)}((- \ell_1)^\varphi 2^+ \ell_2^\varphi) C_{\text{Bub}}^{(1)} \left[\begin{array}{c} 3 \\ 4 \end{array} \right] \right] \Big|_{t^0, \mu^2} \\
&= \frac{1}{2} \frac{s_{12}}{\langle 12 \rangle^2 \langle 34 \rangle^2} \sum_{\ell_1, \ell_1^*} \text{Inf}_{\mu^2, t} \left[s_{\ell_3 4} - s_{\ell_3 3} \right] \Big|_{t^0, \mu^2} \\
&= \frac{s_{14} - s_{13}}{\langle 12 \rangle^2 \langle 34 \rangle^2}.
\end{aligned} \tag{3.104}$$

For the third cut in Figure 3.12, we choose $\chi = p_1$ as the reference momentum for the loop momentum of the left bubble, so that no triangles contribute to its coefficient,

$$\ell_1^\mu = y p_2^\mu + (1-y) p_1^\mu + \frac{1}{2} \left(t \langle 2 | \gamma^\mu | 1 \rangle + \left(\frac{y(1-y)}{t} - \frac{\mu^2}{t s_{12}} \right) \langle 1 | \gamma^\mu | 2 \rangle \right). \tag{3.105}$$

The double-bubble coefficient therefore evaluates to,

$$\begin{aligned}
C^{(2)} \left[\begin{array}{c} 2 \\ 1 \end{array} \right] &= C_{\text{Bub}}^{(1)} \left[\begin{array}{c} 2 \\ 1 \end{array} \right] \times C_{\text{Bub}}^{(1)} \left[\begin{array}{c} 3 \\ 4 \end{array} \right] \\
&= -\text{Inf}_{\mu^2, t, y} \left[A^{(0)}(1^+ 2^+ \ell_2^\varphi (- \ell_1)^\varphi) C_{\text{Bub}}^{(1)} \left[\begin{array}{c} 3 \\ 4 \end{array} \right] \right] \Big|_{y^i \rightarrow Y^i, t^0, \mu^2} \\
&= -\text{Inf}_{\mu^2, t, y} \left[\frac{[12]}{\langle 12 \rangle} \frac{\mu^2}{s_{1 \ell_1}} \frac{s_{4 \ell_1} - s_{3 \ell_1}}{\langle 34 \rangle^2 s_{34}} \right] \Big|_{y^i \rightarrow Y^i, t^0, \mu^2} \\
&= 2 \frac{s_{13} - s_{14}}{\langle 12 \rangle^2 \langle 34 \rangle^2 s_{12}}.
\end{aligned} \tag{3.106}$$

With the integrals in eq. (2.104), we can now evaluate $\tilde{R}_{4;1}^{(2)}$ according to eq. (3.95),

$$\tilde{R}_{4;1}^{(2)}(1^+ 2^+, 3^+ 4^+) = \frac{5 s_{12} s_{23} + s_{23}^2}{18 \langle 12 \rangle \langle 23 \rangle \langle 34 \rangle \langle 41 \rangle}. \tag{3.107}$$

After summing over cyclic permutations of the external kinematics we obtain,

$$\begin{aligned}
R_{4;1}^{(2)}(1^+ 2^+ 3^+ 4^+) &= \sum_{C_4} \tilde{R}_{4;1}^{(2)}(\sigma(1)^+ \sigma(2)^+ \sigma(3)^+ \sigma(4)^+) \\
&= \frac{s_{13}^2 + 8 s_{12} s_{23}}{9 \langle 12 \rangle \langle 23 \rangle \langle 34 \rangle \langle 41 \rangle},
\end{aligned} \tag{3.108}$$

which agrees with the result of refs. [13, 15].

3.7.1.2 Subleading Color $R_{4;3}^{(2)}$

The four-gluon partial amplitude $A_{4;3}^{(2)}$ is the simplest example subleading in color for which we can demonstrate the separable approach. The color structure associated to this amplitude is of the type $N_c \text{Tr}(T^1 T^2) \text{Tr}(T^3 T^4)$, meaning that we construct the generating set such that we obtain the full rational contribution after separately summing over the cyclic permutations of momenta

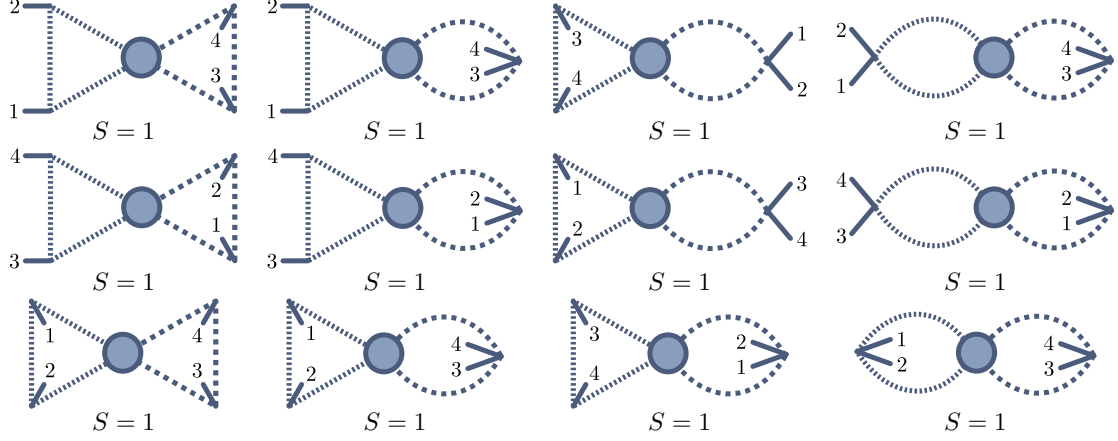


Figure 3.13: Cuts required for $R_{4;3}^{(2)}$. As none of the cuts are self-similar under cyclic permutations of the traces, all the symmetry factors S are one.

in each of the traces,

$$R_{4;3}^{(2)}(1^+2^+; 3^+4^+) = \sum_{\substack{\sigma_1 \in C_2(\{12\}) \\ \sigma_2 \in C_2(\{34\})}} \tilde{R}_{4;3}^{(2)}(\sigma_1(1)^+ \sigma_1(2)^+; \sigma_2(1)^+ \sigma_2(2)^+). \quad (3.109)$$

The method laid out in section 3.4 leads us to a generating set that includes 12 cuts, shown in Figure 3.13. The cuts are each distinct under cyclic permutations of the traces, such that no symmetry factors are required here. The generating set of the rational term $R_{4;3}^{(2)}$ can therefore be constructed as follows,

$$\begin{aligned} \tilde{R}_{4;3}^{(2)}(1^+2^+; 3^+4^+) = & (D_s - 2)^2 \left[I_3^{[2]} I_3^{[2]} C^{(2)} \left[\begin{array}{c} 2 \\ 1 \end{array} \right] \right] + I_3^{[2]} I_2^{[2]} [s_{34}] C^{(2)} \left[\begin{array}{c} 2 \\ 1 \end{array} \right] \\ & + I_3^{[2]} I_2^{[2]} [s_{34}] C^{(2)} \left[\begin{array}{c} 3 \\ 4 \end{array} \right] + I_2^{[2]} [s_{12}] I_2^{[2]} [s_{34}] C^{(2)} \left[\begin{array}{c} 2 \\ 1 \end{array} \right] + I_3^{[2]} I_3^{[2]} C^{(2)} \left[\begin{array}{c} 4 \\ 3 \end{array} \right] \\ & + I_3^{[2]} I_2^{[2]} [s_{34}] C^{(2)} \left[\begin{array}{c} 4 \\ 3 \end{array} \right] + I_3^{[2]} I_2^{[2]} [s_{34}] C^{(2)} \left[\begin{array}{c} 1 \\ 2 \end{array} \right] + I_2^{[2]} [s_{12}] I_2^{[2]} [s_{34}] C^{(2)} \left[\begin{array}{c} 4 \\ 3 \end{array} \right] \\ & + I_3^{[2]} I_3^{[2]} C^{(2)} \left[\begin{array}{c} 1 \\ 2 \end{array} \right] + I_3^{[2]} I_2^{[2]} [s_{34}] C^{(2)} \left[\begin{array}{c} 1 \\ 2 \end{array} \right] + I_3^{[2]} I_2^{[2]} [s_{34}] C^{(2)} \left[\begin{array}{c} 3 \\ 4 \end{array} \right] \\ & + I_2^{[2]} [s_{12}] I_2^{[2]} [s_{34}] C^{(2)} \left[\begin{array}{c} 2 \\ 1 \end{array} \right] \right]. \quad (3.110) \end{aligned}$$

As the tree amplitudes have at most two external gluons attached, we can relate the coefficients of the cuts in eq. (3.110) to the ones already found for $\tilde{R}_{4;1}^{(2)}$. From the relations,

$$A^{(0)}(1^\varphi 2^+ 3^\varphi) = -A^{(0)}(3^\varphi 2^+ 1^\varphi), \quad A^{(0)}(1^\varphi 2^+ 3^+ 4^\varphi) = A^{(0)}(4^\varphi 3^+ 2^+ 1^\varphi), \quad (3.111)$$

we find that the cuts for $\tilde{R}_{4:3}^{(2)}$ can be obtained from the expressions (3.103), (3.104), and (3.106) by appropriate exchanges of the momenta. We thus obtain

$$\begin{aligned}
C^{(2)} \left[\begin{array}{c} 2 \\ 1 \end{array} \left[\begin{array}{c} 4 \\ 3 \end{array} \right] \right] &= \frac{s_{12}s_{14}}{\langle 12 \rangle^2 \langle 34 \rangle^2}, & C^{(2)} \left[\begin{array}{c} 2 \\ 1 \end{array} \left[\begin{array}{c} 4 \\ 3 \end{array} \right] \right] &= \frac{s_{13} - s_{14}}{\langle 12 \rangle^2 \langle 34 \rangle^2}, \\
C^{(2)} \left[\begin{array}{c} 3 \\ 4 \end{array} \left[\begin{array}{c} 1 \\ 2 \end{array} \right] \right] &= \frac{s_{42} - s_{41}}{\langle 12 \rangle^2 \langle 34 \rangle^2}, & C^{(2)} \left[\begin{array}{c} 2 \\ 1 \end{array} \left[\begin{array}{c} 4 \\ 3 \end{array} \right] \right] &= 2 \frac{s_{14} - s_{13}}{\langle 12 \rangle^2 \langle 34 \rangle^2 s_{12}}, \\
C^{(2)} \left[\begin{array}{c} 4 \\ 3 \end{array} \left[\begin{array}{c} 1 \\ 2 \end{array} \right] \right] &= \frac{s_{34}s_{32}}{\langle 12 \rangle^2 \langle 34 \rangle^2}, & C^{(2)} \left[\begin{array}{c} 4 \\ 3 \end{array} \left[\begin{array}{c} 1 \\ 2 \end{array} \right] \right] &= \frac{s_{31} - s_{32}}{\langle 12 \rangle^2 \langle 34 \rangle^2}, \\
C^{(2)} \left[\begin{array}{c} 1 \\ 2 \end{array} \left[\begin{array}{c} 3 \\ 4 \end{array} \right] \right] &= \frac{s_{24} - s_{23}}{\langle 12 \rangle^2 \langle 34 \rangle^2}, & C^{(2)} \left[\begin{array}{c} 4 \\ 3 \end{array} \left[\begin{array}{c} 1 \\ 2 \end{array} \right] \right] &= 2 \frac{s_{32} - s_{31}}{\langle 12 \rangle^2 \langle 34 \rangle^2 s_{12}}, \\
C^{(2)} \left[\begin{array}{c} 1 \\ 2 \end{array} \left[\begin{array}{c} 3 \\ 4 \end{array} \right] \right] &= \frac{s_{12}s_{24}}{\langle 12 \rangle^2 \langle 34 \rangle^2}, & C^{(2)} \left[\begin{array}{c} 1 \\ 2 \end{array} \left[\begin{array}{c} 3 \\ 4 \end{array} \right] \right] &= \frac{s_{23} - s_{24}}{\langle 12 \rangle^2 \langle 34 \rangle^2}, \\
C^{(2)} \left[\begin{array}{c} 3 \\ 4 \end{array} \left[\begin{array}{c} 1 \\ 2 \end{array} \right] \right] &= \frac{s_{41} - s_{42}}{\langle 12 \rangle^2 \langle 34 \rangle^2}, & C^{(2)} \left[\begin{array}{c} 1 \\ 2 \end{array} \left[\begin{array}{c} 3 \\ 4 \end{array} \right] \right] &= 2 \frac{s_{24} - s_{23}}{\langle 12 \rangle^2 \langle 34 \rangle^2 s_{12}}.
\end{aligned} \tag{3.112}$$

Evaluating eq. (3.110) with these coefficients gives us,

$$\tilde{R}_{4:3}^{(2)}(1^+2^+; 3^+4^+) = -\frac{1}{9} \frac{s_{12}}{\langle 12 \rangle^2 \langle 34 \rangle^2} (14s_{12} + s_{13}). \tag{3.113}$$

After summing over the permutations of the particles in the two traces, some algebra leads to the final result,

$$\begin{aligned}
R_{4:3}^{(2)}(1^+2^+; 3^+4^+) &= \sum_{\substack{\sigma_1 \in C_2(\{12\}) \\ \sigma_2 \in C_2(\{34\})}} \tilde{R}_{4:3}^{(2)}(\sigma_1(1)^+ \sigma_1(2)^+; \sigma_2(1)^+ \sigma_2(2)^+) \\
&= -6 \frac{[12]^2}{\langle 34 \rangle^2}.
\end{aligned} \tag{3.114}$$

This result is in agreement with ref. [15].

3.7.1.3 Subleading Color $R_{4:1B}^{(2)}$

Finally, we can obtain the subleading single trace rational part $R_{4:1B}^{(2)}$ of the four-gluon amplitude using the separable approach as well. A possible set of cuts for $\tilde{R}_{4:1B}^{(2)}$ is given in Figure 3.14. The first and third cuts in the top row are invariant under all cyclic permutations of the external momenta, as these permutations are just the different representations of the real non-planar contribution (cf. Figure 3.10 and the associated discussion in section 3.4). As such, these cuts require a symmetry factor of $\frac{1}{4}$. In addition there are two cuts that are invariant under shifting all momenta by two positions, and that therefore have to be included with a factor of $\frac{1}{2}$.

As these cuts contain the twisted scalar amplitude, we cannot reuse the previous results. We again begin with the right hand loops, of which there are now three distinct types,

$$\begin{aligned}
\text{(I)} \quad & \begin{array}{c} \ell_3 \\ \nearrow \\ k_2 \text{ (dotted)} \\ \searrow \\ k_1 \text{ (dotted)} \end{array} \quad \begin{array}{c} \text{---} 3 \\ \downarrow \ell_1 \\ \text{---} 4 \end{array} \\
\text{(II)} \quad & \begin{array}{c} \ell_1 \\ \nearrow \\ k_2 \text{ (dotted)} \\ \searrow \\ k_1 \text{ (dotted)} \end{array} \quad \begin{array}{c} \text{---} 3 \\ \downarrow \ell_2 \\ \text{---} 4 \end{array} \\
\text{(III)} \quad & \begin{array}{c} \ell_1 \\ \nearrow \\ k_2 \text{ (dotted)} \\ \searrow \\ k_1 \text{ (dotted)} \end{array} \quad \begin{array}{c} \text{---} 3 \\ \downarrow \ell_2 \\ \text{---} 4 \end{array} \cdot \tag{3.115}
\end{aligned}$$

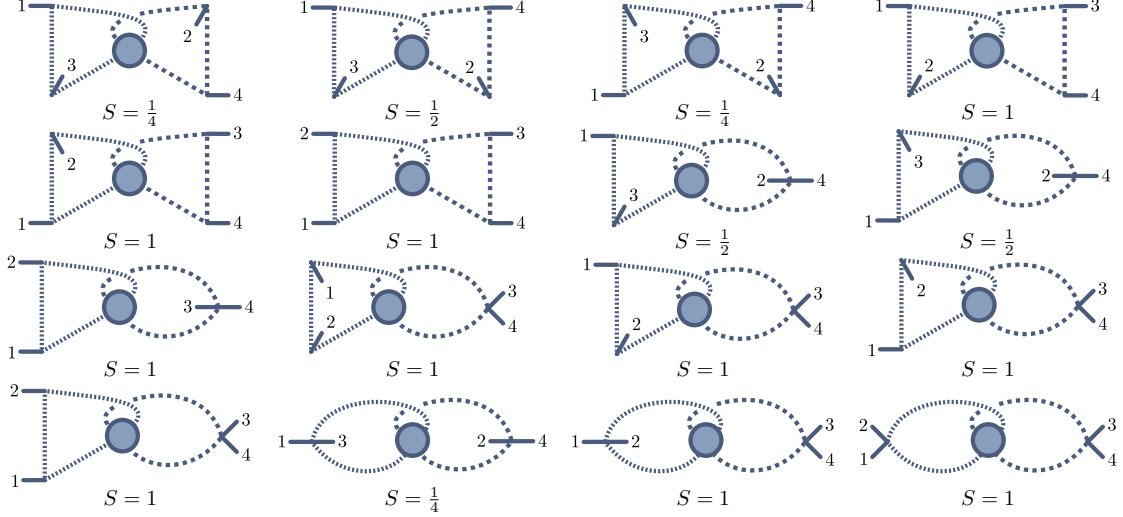


Figure 3.14: Cuts required for $R_{4:1B}^{(2)}$, together with the required symmetry factors S .

Using the same loop-momentum parametrization as in eqs. (3.97) and (3.99), we obtain for these cuts,

$$\begin{aligned}
 C_{\text{Tri},[2]}^{(1)} \left[\text{Diagram} \right] &= \frac{1}{2} \sum_{\ell, \ell^*} \text{Inf}_{\mu^2, t} \left[A^{(0)}(k_1^\varphi \ell_3^{\varphi'} k_2^\varphi (-\ell_2)^{\varphi'}) A^{(0)}(3^+ \ell_1^{\varphi'} (-\ell_3)^{\varphi'}) \right. \\
 &\quad \left. \times A^{(0)}(4^+ \ell_2^{\varphi'} (-\ell_1)^{\varphi'}) \right] \Big|_{\mu^2, t^0} \\
 &= -\frac{1}{2} \text{Inf}_{\mu^2, t} \left[\sum_{\ell, \ell^*} \frac{[3|\ell_1|4]}{\langle 34 \rangle} \frac{[4|\ell_1|3]}{\langle 43 \rangle} \right] \Big|_{\mu^2, t^0} \\
 &= -\text{Inf}_{\mu^2, t} \left[\frac{\mu^2 s_{34}}{\langle 34 \rangle^2} \right] \Big|_{\mu^2, t^0} = \frac{[34]}{\langle 34 \rangle},
 \end{aligned} \tag{3.116}$$

$$\begin{aligned}
 C_{\text{Bub},[2]}^{(1)} \left[\text{Diagram} \right] &= \text{Inf}_{\mu^2, y, t} \left[A^{(0)}(k_1^\varphi l_1^{\varphi'} k_2^\varphi (-l_2)^{\varphi'}) A^{(0)}(3^+ 4^+ \ell_2^{\varphi'} (-\ell_1)^{\varphi'}) \right] \Big|_{t^0, y^i \rightarrow Y_i, \mu^2} \\
 &= -\text{Inf}_{\mu^2, y, t} \left[\frac{\mu^2}{s_{3\ell_1}} \frac{[34]}{\langle 34 \rangle} \right] \Big|_{t^0, y^i \rightarrow Y_i, \mu^2} = \text{Inf}_{\mu^2, y, t} \left[\frac{\mu^2}{y \langle 34 \rangle^2} \right] \Big|_{t^0, y^i \rightarrow Y_i, \mu^2} \\
 &= 0,
 \end{aligned} \tag{3.117}$$

$$\begin{aligned}
 C_{\text{Bub},[2]}^{(1)} \left[\text{Diagram} \right] &= \text{Inf}_{\mu^2, y, t} \left[A^{(0)}(k_1^\varphi l_1^{\varphi'} k_2^\varphi (-l_2)^{\varphi'}) A^{(0)}(3^+ (-\ell_1)^{\varphi'} 4^+ \ell_2^{\varphi'}) \right] \Big|_{t^0, y^i \rightarrow Y_i, \mu^2} \\
 &= \text{Inf}_{\mu^2, y, t} \left[\frac{\mu^2 [34]^2}{s_{3\ell_1} s_{3\ell_2}} \right] \Big|_{t^0, y^i \rightarrow Y_i, \mu^2} = -\text{Inf}_{\mu^2, y, t} \left[\frac{\mu^2}{y(1-y) \langle 34 \rangle^2} \right] \Big|_{t^0, y^i \rightarrow Y_i, \mu^2} \\
 &= 0.
 \end{aligned} \tag{3.118}$$

Because the bubble cuts vanish, most of the cuts in Figure 3.14 vanish, and only the double-triangle cuts give a non-zero contribution to $\tilde{R}_{4:1B}^{(2)}$. It is again sufficient to compute only one of the double-triangle cuts, as they are all related to each other by appropriate signs and exchanges of momenta

due to the reversal identity of eq. (3.111). Picking one specific cut, we obtain

$$\begin{aligned}
C^{(2)} \left[\text{Diagram 1} \right] &= C_{\text{Tri}}^{(1)} \left[\text{Diagram 2} \right] \times C_{\text{Tri}}^{(1)} \left[\text{Diagram 3} \right] \\
&= \frac{1}{2} \sum_{\ell_1, \ell_1^*} \text{Inf}_{\mu^2, t} \left[A^{(0)}((- \ell_3)^\varphi 1^+ \ell_1^\varphi) A^{(0)}((- \ell_1)^\varphi 2^+ \ell_2^\varphi) C_{\text{Tri}}^{(1)} \left[\text{Diagram 4} \right] \right] \Big|_{t^0, \mu^2} \\
&= \frac{1}{2} \sum_{\ell_1, \ell_1^*} \text{Inf}_{\mu^2, t} \left[\frac{[1|\ell_1|2]}{\langle 12 \rangle} \frac{[2|\ell_1|1]}{\langle 21 \rangle} \frac{[34]}{\langle 34 \rangle} \right] \Big|_{t^0, \mu^2} \\
&= \frac{[12][34]}{\langle 12 \rangle \langle 34 \rangle}.
\end{aligned} \tag{3.119}$$

The remaining five cuts are then,⁸

$$\begin{aligned}
C^{(2)} \left[\text{Diagram 5} \right] &= C^{(2)} \left[\text{Diagram 6} \right] = C^{(2)} \left[\text{Diagram 7} \right] = C^{(2)} \left[\text{Diagram 8} \right] = \frac{[12][34]}{\langle 12 \rangle \langle 34 \rangle}, \\
C^{(2)} \left[\text{Diagram 9} \right] &= C^{(2)} \left[\text{Diagram 10} \right] = -\frac{[12][34]}{\langle 12 \rangle \langle 34 \rangle}.
\end{aligned} \tag{3.120}$$

Combining these coefficients with their associated symmetry factors, we obtain

$$\begin{aligned}
\tilde{R}_{4:1B}^{(2)}(1^+ 2^+ 3^+ 4^+) &= (D_s - 2)^2 \left[\frac{1}{4} I_3^{[2]} I_3^{[2]} C^{(2)} \left[\text{Diagram 11} \right] + \frac{1}{2} I_3^{[2]} I_3^{[2]} C^{(2)} \left[\text{Diagram 12} \right] \right. \\
&\quad + \frac{1}{4} I_3^{[2]} I_3^{[2]} C^{(2)} \left[\text{Diagram 13} \right] + I_3^{[2]} I_3^{[2]} C^{(2)} \left[\text{Diagram 14} \right] \\
&\quad \left. + I_3^{[2]} I_3^{[2]} C^{(2)} \left[\text{Diagram 15} \right] + I_3^{[2]} I_3^{[2]} C^{(2)} \left[\text{Diagram 16} \right] \right] \\
&= \frac{[12][34]}{\langle 12 \rangle \langle 34 \rangle} \left[\frac{1}{4} + \frac{1}{2} + \frac{1}{4} - 1 - 1 + 1 \right] = 0,
\end{aligned} \tag{3.121}$$

and as a consequence,

$$R_{4:1B}^{(2)}(1^+ 2^+ 3^+ 4^+) = \sum_{\sigma \in C_4} \tilde{R}_{4:1B}^{(2)}(\sigma(1)^+ \sigma(2)^+ \sigma(3)^+ \sigma(4)^+) = 0. \tag{3.122}$$

This is again consistent with the result of ref. [14, 15]

3.7.2 The Five-Gluon Amplitude Analytically

In the color decomposition of the five-gluon amplitude we require three partial amplitudes $A_{5:1}^{(2)}$, $A_{5:3}^{(2)}$ and $A_{5:1B}^{(2)}$, whose rational parts we label $R_{5:1}^{(2)}$, $R_{5:3}^{(2)}$ and $R_{5:1B}^{(2)}$. Following the discussion of section 3.4, we create generating sets $\tilde{R}_{5:1}^{(2)}$, $\tilde{R}_{5:3}^{(2)}$ and $\tilde{R}_{5:1B}^{(2)}$, which require 12, 62 and 133 unitarity cuts respectively. The topologies for the cuts of $\tilde{R}_{5:1}^{(2)}$, $\tilde{R}_{5:3}^{(2)}$ are shown in Figures 3.15 and 3.16, while those of $\tilde{R}_{5:1B}^{(2)}$ are omitted for brevity. As we have an odd number of momenta, none of the cuts are related by cyclic permutations, and no symmetry factors are required.

Beginning with five-gluon amplitudes, we rely on our implementation in *Mathematica* to compute the unitarity cuts due to their increased number and complexity. As our code is able to

⁸Keeping in mind that $\frac{[12][34]}{\langle 12 \rangle \langle 34 \rangle} = \frac{[13][24]}{\langle 13 \rangle \langle 24 \rangle}$

	$n = 4$	$n = 5$	$n = 6$	$n = 7$
$\tilde{R}_{n:1}^{(2)}$	3(7)	12(33)	47(149)	126(413)
$\tilde{R}_{n:3}^{(2)}$	12(27)	62(171)	242(729)	773(2440)
$\tilde{R}_{n:4}^{(2)}$	—	—	240(735)	768(2422)
$\tilde{R}_{n:2,2}^{(2)}$	—	—	1023(3168)	3300(10760)
$\tilde{R}_{n:1B}^{(2)}$	16(42)	133(385)	847(2678)	3909(12751)

Table 3.1: A table showing the number of cuts in the generating sets for partial amplitudes up to seven gluons. In each case the first number excludes the triangle contributions to bubble coefficients, while for the number in parenthesis they are included.

perform computations symbolically, we evaluated the cuts using parametrized kinematics obtained from the momentum twistor parametrization of section 3.6, giving us analytic results. As an example, an analytic expression of the generating set $\tilde{R}_{5:1}^{(2)}$ derived with this approach is provided in appendix B.2.

We verify our approach using the known results for the three partial amplitudes of refs. [4, 6, 18], which were obtained from augmented recursion. Our expressions are in numerical agreement with these results⁹ and satisfy the color relations of ref. [135]¹⁰. We further notice that only double-triangle cuts contribute to $\tilde{R}_{5:1B}^{(2)}$.

3.7.3 The Six- and Seven-Gluon Amplitudes: Numeric Results

An analytic expression for the leading-color rational part $R_{6:1}^{(2)}$ of the six-gluon two-loop all-plus was first presented in ref. [5]. Ref. [10] further provides analytic expressions for the rational parts of all six-gluon partial amplitudes, namely $R_{6:3}^{(2)}$, $R_{6:4}^{(2)}$, $R_{6:2,2}^{(2)}$ and $R_{6:1B}^{(2)}$. We are therefore able to verify the one-loop squared approach for the full color six-gluon amplitudes.

Due to the increased number of parameters in fully parametrized six-gluon kinematics, we limit ourselves to numerical checks. Using the automated routines in *Mathematica* we find generating sets $\tilde{R}_{6:1}^{(2)}$, $\tilde{R}_{6:3}^{(2)}$, $\tilde{R}_{6:4}^{(2)}$, $\tilde{R}_{6:2,2}^{(2)}$ and $\tilde{R}_{6:1B}^{(2)}$. The number of cuts involved in these sets is shown in Table 3.1. For numerical evaluations we have to perform the sum over permutations before evaluation. For $R_{6:1}^{(2)}$, $R_{6:3}^{(2)}$, $R_{6:4}^{(2)}$, $R_{6:2,2}^{(2)}$ and $R_{6:1B}^{(2)}$ we therefore have to evaluate a total of 894, 5832, 6615, 25344 and 16068 cuts respectively. For all partial amplitudes we find complete numerical agreement with the expressions of refs. [5, 10]. As in the five-gluon partial amplitude $R_{5:1B}^{(2)}$, we find for $R_{6:1B}^{(2)}$ that the only non-zero cuts are of the double-triangle type.

Further, we compute the seven-gluon leading-color rational part $R_{7:1}^{(2)}$ numerically. Its generating set $\tilde{R}_{7:1}^{(2)}$ contains 126 unique cuts, which increases to 413 when including all triangle cuts required for bubble coefficients. For numerical evaluations we need to perform the cyclic sum explicitly, such that we have to compute 2891 one-loop squared cuts in total. We compared our result with the evaluation of the analytic expression of ref. [8], which was obtained using augmented recursion. We find our result to be in exact numerical agreement.

⁹We compared with the expressions of the published version.

¹⁰The equivalent expression given in ref. [4] is missing an overall sign.

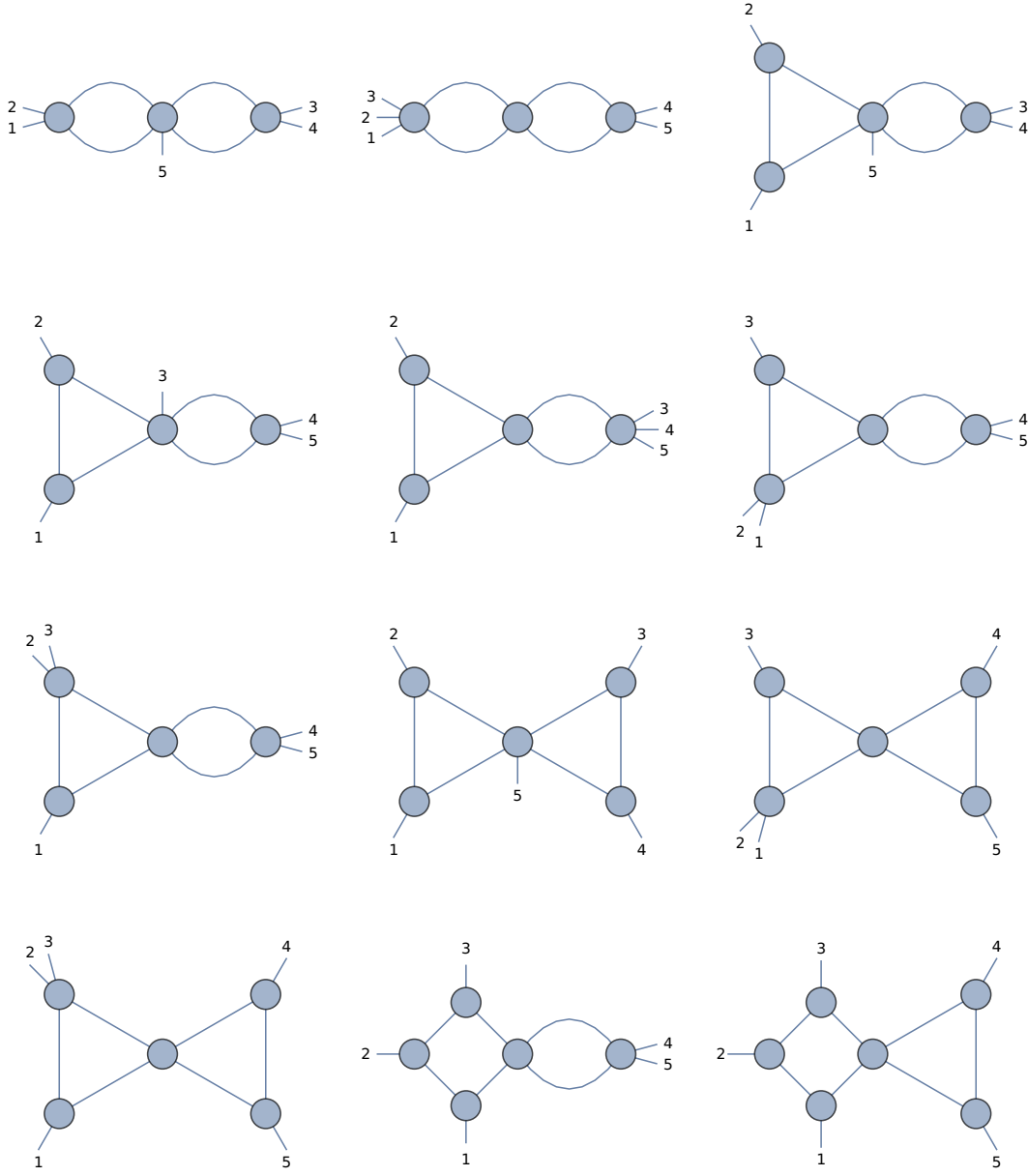


Figure 3.15: One-loop squared cuts for $\tilde{R}_{5;1}^{(2)}$. The full set of cuts can be obtained by summing over cyclic permutations. As the number of particles is odd, no symmetry factors are required.

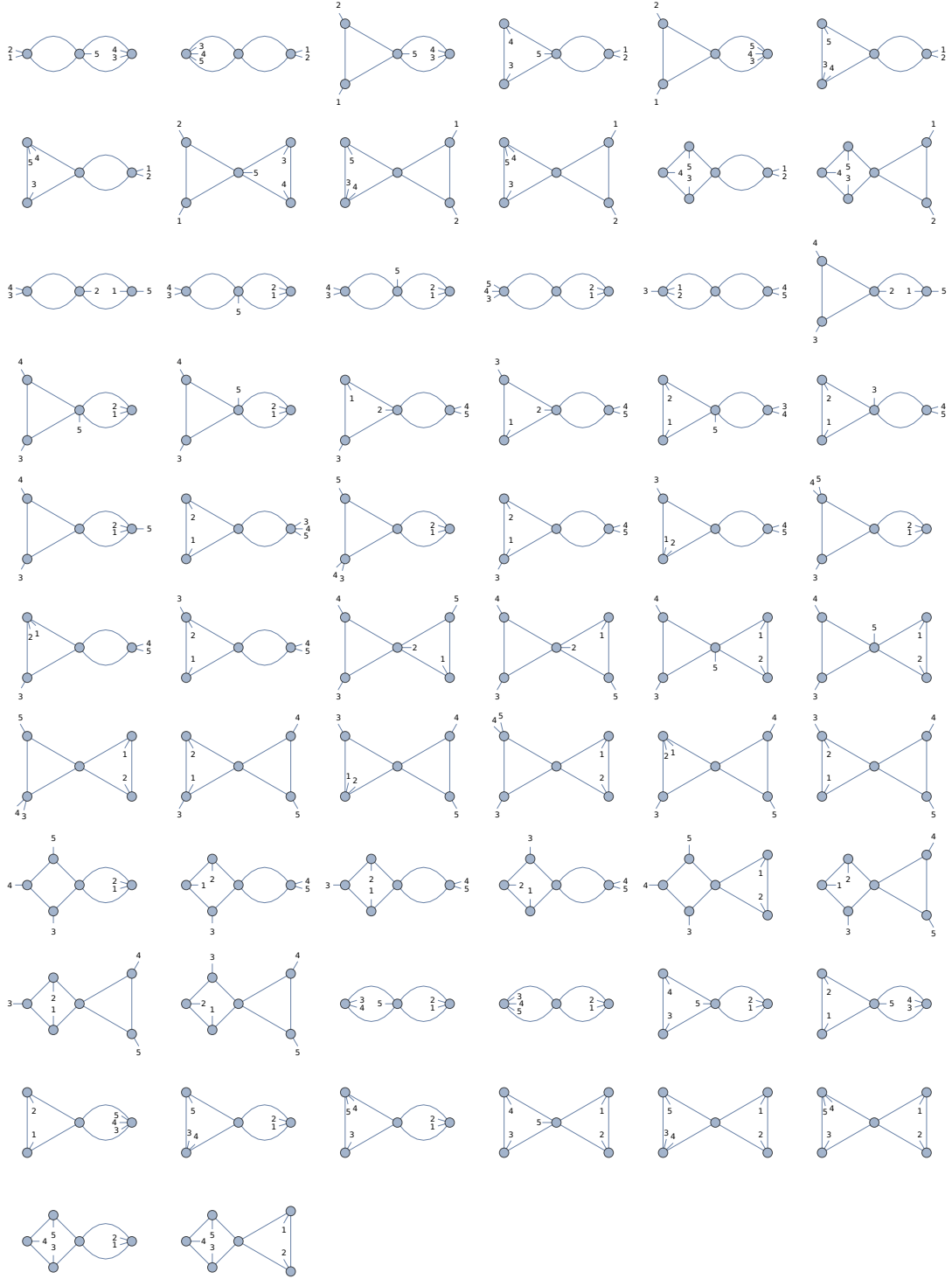


Figure 3.16: One-loop squared cuts for $\tilde{R}_{5;1}^{(2)}$. The full set of cuts can be obtained by separately summing over cyclic permutations of (12) and (345). As the number of particles is odd again, we also do require symmetry here.

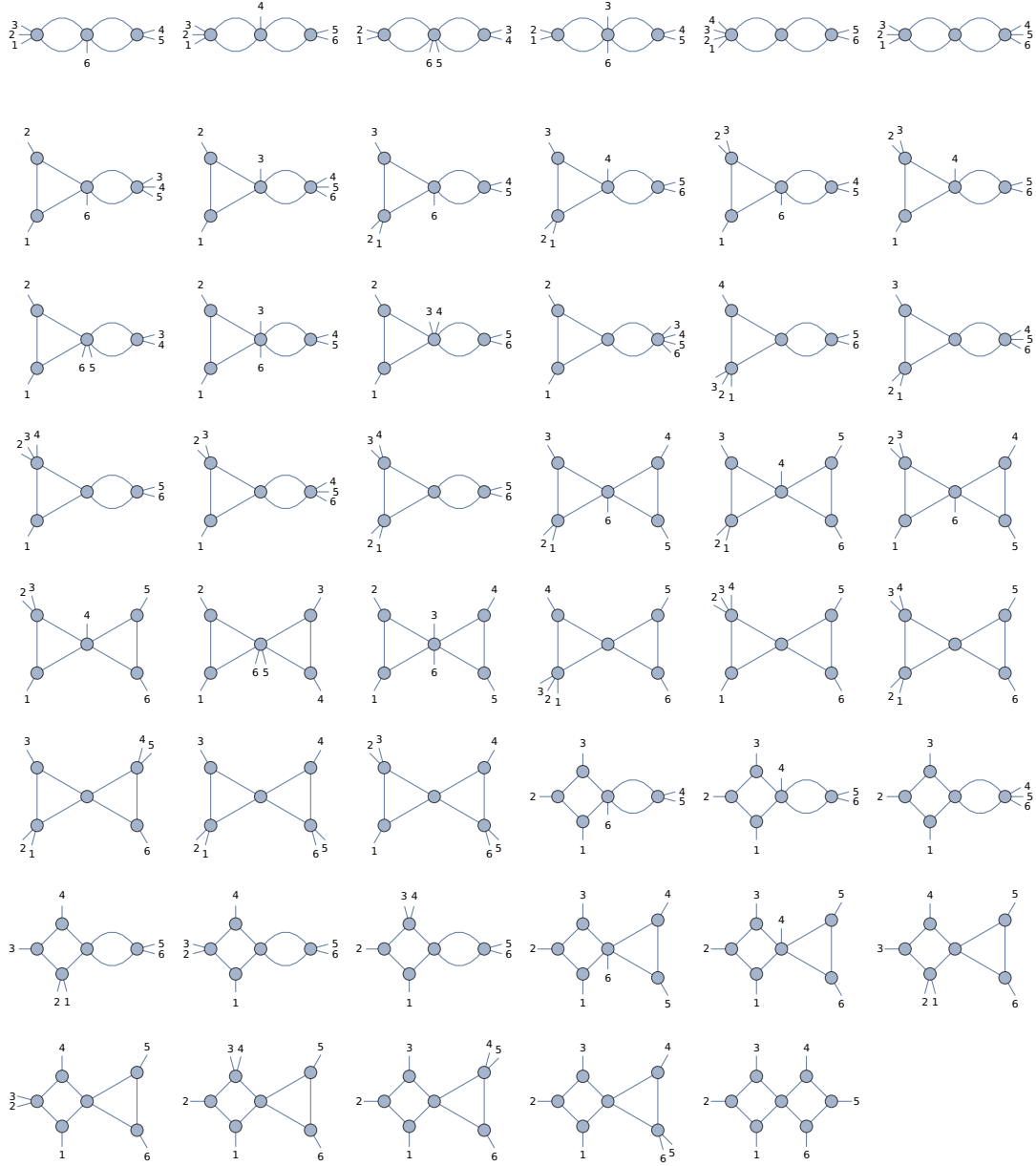


Figure 3.17: Unitarity cuts required for $\tilde{R}_{6;1}^{(2)}$. The full set of cuts can be obtained by summing over cyclic permutations. As the number of momenta is even, a symmetry factor of $\frac{1}{2}$ is necessary to avoid overcounting of symmetric cuts.

3.7.4 Agreement with Seven-Gluon $R_{7:1B}^{(2)}$ Conjecture

The simple factorization behavior of the subleading partial amplitudes $\tilde{R}_{n:1B}^{(2)}$ made it possible to formulate a conjecture for a closed analytic all- n form of $\tilde{R}_{n:1B}^{(2)}$ [18]. While the five- and six-gluon rational terms $R_{5:1B}^{(2)}$, $R_{6:1B}^{(2)}$ are known from explicit computations in refs. [4, 10], the seven-gluon case $R_{7:1B}^{(2)}$ is only known as part of the all- n conjecture. As the conjecture was based solely on requiring the correct two-particle collinear factorization behavior, we can use the separable approach to provide an independent cross-check of this result. Finding agreement would provide evidence for both the correctness of the conjecture of ref. [18], while at the same time validating the use of the separable approach in the computation of the rational contributions $R_{n:1B}^{(2)}$.

Specializing the all- n form of ref. [18] to $n = 7$ we obtain

$$R_{7:1B}^{(2)} = R_{7:1B,1}^{(2)} + R_{7:1B,2}^{(2)}, \quad (3.123)$$

with¹¹

$$\begin{aligned} R_{7:1B,1}^{(2)} &= 2 \frac{\sum_{1 \leq i < j < k < l \leq 7} \text{tr}_5(ijkl)}{\langle 12 \rangle \langle 23 \rangle \langle 34 \rangle \langle 45 \rangle \langle 56 \rangle \langle 67 \rangle \langle 71 \rangle} \\ R_{7:1B,2}^{(2)} &= -4 \left[C_{3745} \text{tr}_5[(1+2+3)547] - C_{3746} \text{tr}_5[(1+2+3)647] + C_{3756} \text{tr}_5[(1+2+3)657] \right. \\ &\quad + C_{2634} \text{tr}_5[(1+2)43(6+7)] + C_{2734} \text{tr}_5[(1+2)437] - C_{2635} \text{tr}_5[(1+2)53(6+7)] \\ &\quad - C_{2735} \text{tr}_5[(1+2)537] + C_{2645} \text{tr}_5[(1+2)54(6+7)] + C_{2745} \text{tr}_5[(1+2)547] \\ &\quad + C_{2736} \text{tr}_5[(1+2)637] - C_{2746} \text{tr}_5[(1+2)647] + C_{2756} \text{tr}_5[(1+2)657] \\ &\quad + C_{1523} \text{tr}_5[132(5+6+7)] + C_{1623} \text{tr}_5[132(6+7)] + C_{1723} \text{tr}_5[1327] \\ &\quad - C_{1524} \text{tr}_5[142(5+6+7)] - C_{1624} \text{tr}_5[142(6+7)] - C_{1724} \text{tr}_5[1427] \\ &\quad + C_{1534} \text{tr}_5[143(5+6+7)] + C_{1634} \text{tr}_5[143(6+7)] + C_{1734} \text{tr}_5[1437] \\ &\quad + C_{1625} \text{tr}_5[152(6+7)] + C_{1725} \text{tr}_5[1527] - C_{1635} \text{tr}_5[153(6+7)] \\ &\quad - C_{1735} \text{tr}_5[1537] + C_{1645} \text{tr}_5[154(6+7)] + C_{1745} \text{tr}_5[1547] - C_{1726} \text{tr}_5[1627] \\ &\quad \left. + C_{1736} \text{tr}_5[1637] - C_{1746} \text{tr}_5[1647] + C_{1756} \text{tr}_5[1657] \right]. \end{aligned} \quad (3.124)$$

The C_{rsij} are sums over terms with a Parke–Taylor like structure,

$$C_{rsij} = \sum_{\alpha \in S_{rsij}} \text{CPT}(1, \dots, r, j, \{\alpha\}, i, s, \dots, 7), \quad (3.125)$$

where,

$$\text{CPT}(a_1, \dots, a_7) = \frac{1}{\langle a_1 a_2 \rangle \langle a_2 a_3 \rangle \dots \langle a_6 a_7 \rangle \langle a_7 a_1 \rangle}. \quad (3.126)$$

Further defining the sets S_1 , S_2 and S_3 by splitting $\{1, \dots, 7\}$ according to,

$$\{1, \dots, 7\} = \{1, \dots, r\} \cup S_1 \cup \{i\} \cup S_2 \cup \{j\} \cup S_3 \cup \{s, \dots, 7\}, \quad (3.127)$$

¹¹Defining $\text{tr}_5(ijkl) = \text{tr}_-(ijkl) - \text{tr}_+(ijkl)$, $\text{tr}_-(ijkl) = \langle i|jkl|i \rangle$ and $\text{tr}_+(ijkl) = [i|jkl|i]$.

the sets S_{rsij} are obtained via the shuffle product,

$$S_{rsij} = S_1 \sqcup S_2^T \sqcup S_3. \quad (3.128)$$

The transposition denotes the reversal of the elements in S_2 .

The form of the conjecture slightly obscures the final form in terms of spinor products. After evaluation of the C_{rsij} and applications of the Schouten identity we find,

$$\begin{aligned} R_{7:1B,2}^{(2)} = & \frac{4}{\langle 12 \rangle \langle 23 \rangle \langle 34 \rangle \langle 45 \rangle \langle 56 \rangle \langle 67 \rangle \langle 71 \rangle} \times \\ & \left[\frac{\langle 12 \rangle \langle 23 \rangle \langle 45 \rangle}{\langle 13 \rangle \langle 24 \rangle \langle 25 \rangle} \text{tr}_5(1325) + \frac{\langle 12 \rangle \langle 23 \rangle \langle 46 \rangle}{\langle 13 \rangle \langle 24 \rangle \langle 26 \rangle} \text{tr}_5(1326) + \frac{\langle 12 \rangle \langle 23 \rangle \langle 47 \rangle}{\langle 13 \rangle \langle 24 \rangle \langle 27 \rangle} \text{tr}_5(1327) \right. \\ & + \frac{\langle 12 \rangle \langle 45 \rangle}{\langle 14 \rangle \langle 25 \rangle} \text{tr}_5(1425) + \frac{\langle 12 \rangle \langle 46 \rangle}{\langle 14 \rangle \langle 26 \rangle} \text{tr}_5(1426) + \frac{\langle 12 \rangle \langle 47 \rangle}{\langle 14 \rangle \langle 27 \rangle} \text{tr}_5(1427) \\ & + \frac{\langle 12 \rangle \langle 34 \rangle \langle 45 \rangle}{\langle 14 \rangle \langle 24 \rangle \langle 35 \rangle} \text{tr}_5(1435) + \frac{\langle 34 \rangle (\langle 12 \rangle \langle 36 \rangle \langle 45 \rangle + \langle 13 \rangle \langle 24 \rangle \langle 56 \rangle)}{\langle 14 \rangle \langle 24 \rangle \langle 35 \rangle \langle 36 \rangle} \text{tr}_5(1436) \\ & + \frac{\langle 34 \rangle (\langle 12 \rangle \langle 37 \rangle \langle 45 \rangle + \langle 13 \rangle \langle 24 \rangle \langle 57 \rangle)}{\langle 14 \rangle \langle 24 \rangle \langle 35 \rangle \langle 37 \rangle} \text{tr}_5(1437) + \frac{\langle 12 \rangle \langle 56 \rangle}{\langle 15 \rangle \langle 26 \rangle} \text{tr}_5(1526) \\ & + \frac{\langle 12 \rangle \langle 57 \rangle}{\langle 15 \rangle \langle 27 \rangle} \text{tr}_5(1527) + \frac{\langle 13 \rangle \langle 56 \rangle}{\langle 15 \rangle \langle 36 \rangle} \text{tr}_5(1536) + \frac{\langle 13 \rangle \langle 57 \rangle}{\langle 15 \rangle \langle 37 \rangle} \text{tr}_5(1537) \\ & + \frac{\langle 13 \rangle \langle 45 \rangle \langle 56 \rangle}{\langle 15 \rangle \langle 35 \rangle \langle 46 \rangle} \text{tr}_5(1546) + \frac{\langle 45 \rangle (\langle 13 \rangle \langle 47 \rangle \langle 56 \rangle + \langle 14 \rangle \langle 35 \rangle \langle 67 \rangle)}{\langle 15 \rangle \langle 35 \rangle \langle 46 \rangle \langle 47 \rangle} \text{tr}_5(1547) \\ & + \frac{\langle 12 \rangle \langle 67 \rangle}{\langle 16 \rangle \langle 27 \rangle} \text{tr}_5(1627) + \frac{\langle 13 \rangle \langle 67 \rangle}{\langle 16 \rangle \langle 37 \rangle} \text{tr}_5(1637) + \frac{\langle 14 \rangle \langle 67 \rangle}{\langle 16 \rangle \langle 47 \rangle} \text{tr}_5(1647) \\ & + \frac{\langle 14 \rangle \langle 56 \rangle \langle 67 \rangle}{\langle 16 \rangle \langle 46 \rangle \langle 57 \rangle} \text{tr}_5(1657) + \frac{\langle 23 \rangle \langle 34 \rangle \langle 56 \rangle}{\langle 24 \rangle \langle 35 \rangle \langle 36 \rangle} \text{tr}_5(2436) + \frac{\langle 23 \rangle \langle 34 \rangle \langle 57 \rangle}{\langle 24 \rangle \langle 35 \rangle \langle 37 \rangle} \text{tr}_5(2437) \\ & + \frac{\langle 23 \rangle \langle 56 \rangle}{\langle 25 \rangle \langle 36 \rangle} \text{tr}_5(2536) + \frac{\langle 23 \rangle \langle 57 \rangle}{\langle 25 \rangle \langle 37 \rangle} \text{tr}_5(2537) + \frac{\langle 23 \rangle \langle 45 \rangle \langle 56 \rangle}{\langle 25 \rangle \langle 35 \rangle \langle 46 \rangle} \text{tr}_5(2546) \\ & + \frac{\langle 45 \rangle (\langle 23 \rangle \langle 47 \rangle \langle 56 \rangle + \langle 24 \rangle \langle 35 \rangle \langle 67 \rangle)}{\langle 25 \rangle \langle 35 \rangle \langle 46 \rangle \langle 47 \rangle} \text{tr}_5(2547) + \frac{\langle 23 \rangle \langle 67 \rangle}{\langle 26 \rangle \langle 37 \rangle} \text{tr}_5(2637) \\ & + \frac{\langle 24 \rangle \langle 67 \rangle}{\langle 26 \rangle \langle 47 \rangle} \text{tr}_5(2647) + \frac{\langle 24 \rangle \langle 56 \rangle \langle 67 \rangle}{\langle 26 \rangle \langle 46 \rangle \langle 57 \rangle} \text{tr}_5(2657) + \frac{\langle 34 \rangle \langle 45 \rangle \langle 67 \rangle}{\langle 35 \rangle \langle 46 \rangle \langle 47 \rangle} \text{tr}_5(3547) \\ & + \frac{\langle 34 \rangle \langle 67 \rangle}{\langle 36 \rangle \langle 47 \rangle} \text{tr}_5(3647) + \frac{\langle 34 \rangle \langle 56 \rangle \langle 67 \rangle}{\langle 36 \rangle \langle 46 \rangle \langle 57 \rangle} \text{tr}_5(3657) \Big]. \quad (3.129) \end{aligned}$$

We build the generating set $\tilde{R}_{7:1B}^{(2)}$ from 3909 unitarity cuts, which expand to 12751 cuts when including all triangle contributions to bubble coefficients. After summing over permutations, we have to compute a total of 89257 one-loop squared cuts. For each permutation, there exist only 416 non-vanishing cuts. These again all belong to the double-triangle topology.

To ensure a reliable comparison we evaluate the cuts semi-analytically on a univariate kinematic

slice, parameterized by a variable δ ,

$$\begin{aligned}
\begin{pmatrix} \langle 1| \\ [1] \end{pmatrix} &= \begin{pmatrix} \frac{439436}{7631} \\ -38 \\ -\frac{31698(285029\delta^2-7419)}{1865571745\delta^2-8709906} \\ \frac{44612(285029\delta^2-7419)}{1865571745\delta^2-8709906} \end{pmatrix}, \quad \begin{pmatrix} \langle 2| \\ [2] \end{pmatrix} = \begin{pmatrix} \frac{40}{13} \left(\frac{22991}{8689\delta^2+2348} + 15 \right) \\ -50 \\ \frac{(8689\delta^2+2348)(216723227\delta^2-704805)}{43549530-9327858725\delta^2} \\ \frac{(8689\delta^2+2348)(264559501\delta^2-370950)}{1865571745\delta^2-87099060} \end{pmatrix}, \\
\begin{pmatrix} \langle 3| \\ [3] \end{pmatrix} &= \begin{pmatrix} 36 \\ -39 \\ \frac{10094}{39} \\ -\frac{6161}{39} \end{pmatrix}, \quad \begin{pmatrix} \langle 4| \\ [4] \end{pmatrix} = \begin{pmatrix} 66 \\ -97 \\ -72 \\ 19 \end{pmatrix}, \quad \begin{pmatrix} \langle 5| \\ [5] \end{pmatrix} = \begin{pmatrix} 36 \\ -52 \\ -1 \\ 19 \end{pmatrix}, \\
\begin{pmatrix} \langle 6| \\ [6] \end{pmatrix} &= \begin{pmatrix} -\frac{4}{5}(27\delta-38) \\ \frac{3}{5}(39\delta-88) \\ -\frac{2}{65}(5047\delta+52) \\ \frac{6161\delta}{65} + \frac{84}{5} \end{pmatrix}, \quad \begin{pmatrix} \langle 7| \\ [7] \end{pmatrix} = \begin{pmatrix} \frac{6}{5}(24\delta+19) \\ -\frac{6}{5}(26\delta+33) \\ \frac{40376\delta}{195} - \frac{6}{5} \\ \frac{63}{5} - \frac{24644\delta}{195} \end{pmatrix}.
\end{aligned} \tag{3.130}$$

We chose the slice such that the limit $\delta \rightarrow 0$ probes the collinear momentum configuration $6||7$. Due to the symbolic approach of our code, we preserve the full analytic dependence of our result on δ during the computation. Choosing all remaining kinematic degrees of freedom to be rational, we can perform an exact comparison with the conjectured form on the entire slice.

We evaluate all 89257 cuts on these parameterized kinematics. We find that the resulting expression and the conjectured form as rational functions of δ are in full analytic agreement. We also explicitly verify that the result has the correct collinear behavior,

$$R_{7:1B}^{(2)}(1^+2^+3^+4^+5^+6^+7^+) \xrightarrow{6||7} R_{6:1B}^{(2)}(1^+2^+3^+4^+5^+K^+) \times \text{Split}_-^{(0)}(6^+7^+), \tag{3.131}$$

which is to be expected, as the conjecture of ref. [18] was based on demanding the correct two-particle collinear limits.

Chapter 4

Integrating A Loop: The Effective One-Loop Picture

In the previous chapter we have seen that two-loop rational terms can be obtained using only one-loop techniques due to the separability of the computation. However, as discussed in section 3.1, the finite polylogarithmic contributions possess an even more explicit one-loop structure. They can be constructed in a one-loop four-dimensional unitarity computation, where one of the amplitudes is itself a one-loop all-plus amplitude. Based on the previous chapter, it appears reasonable to attempt a similar construction for the rational contributions. We may expect them to be constructible from a one-loop D -dimensional unitarity computation, where one of the amplitudes is a one-loop all-plus amplitude with a massive scalar pair,

$$R^{(2)}(1^+ \dots n^+) = \text{[Diagram 1]} + \text{[Diagram 2]} + \text{[Diagram 3]} .$$

We can justify such a construction by interpreting it as a reorganization of the one-loop square cut approach of the previous chapter. Given a specific cut of one of the loops we collect all cuts belonging to second loop, which then sum to an object resembling a one-loop amplitude,

$$\text{[Diagram 1]} + \text{[Diagram 2]} + \text{[Diagram 3]} + \dots \longrightarrow \text{[Diagram 4]} .$$

As the rules for computing these one-loop vertices are exactly those of computing the rational part of an amplitude with two massive scalars and a gluon running in the loop, we will call them massive-scalar one-loop amplitudes.

We will first demonstrate explicitly that, for the rational parts of all two-loop four-gluon all-plus amplitudes, such a rearrangement can be done consistently. As we have computed the one-loop squared cuts explicitly in section 3.7.1 we will also be able to easily derive analytic forms for the

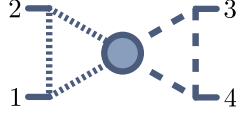
so the right hand side of eq. (4.1) is,

$$\begin{aligned}
 & 2 \times \sum_{C_4} \left[C_{\text{Tri},[2]}^{(1)} \left[\begin{array}{c} 2 \\ 1 \end{array} \right] \begin{array}{c} 3 \\ 4 \end{array} \right] I_3^D[\mu^2] + C_{\text{Bub},[2]}^{(1)} \left[\begin{array}{c} 2 \\ 1 \end{array} \right] \begin{array}{c} 3 \\ 4 \end{array} \right] I_2^D[\mu^2] \right] \\
 &= \sum_{C_4} \left[\frac{1}{3} \frac{s_{12}(s_{13} - s_{12})}{\langle 12 \rangle^2 \langle 34 \rangle^2} + \frac{1}{9} \frac{s_{12}(s_{23} - s_{13})}{\langle 12 \rangle^2 \langle 34 \rangle^2} \right] = \sum_{C_4} \left[-\frac{s_{12}(5s_{12} + s_{23})}{9 \langle 12 \rangle^2 \langle 34 \rangle^2} \right].
 \end{aligned} \tag{4.5}$$

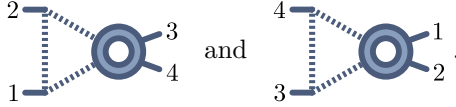
We can check numerically that this is the two-loop rational part $R_{4;1}^{(2)}$ multiplied by a factor of 2. This allows us to make the relation in eq. (4.1) precise,

$$R_{4;1}^{(2)}(1^+2^+3^+4^+) = \frac{1}{2} \times 2 \sum_{C_4} \left[C_{\text{Tri},[2]}^{(1)} \left[\begin{array}{c} 2 \\ 1 \end{array} \right] \begin{array}{c} 3 \\ 4 \end{array} \right] I_3^D[\mu^2] + C_{\text{Bub},[2]}^{(1)} \left[\begin{array}{c} 2 \\ 1 \end{array} \right] \begin{array}{c} 3 \\ 4 \end{array} \right] I_2^D[\mu^2] \right] \tag{4.6}$$

To understand the origin of the additional factor of $\frac{1}{2}$ that is required, consider the one-loop square cut



As the two loops are indistinguishable, this cut has to be counted only once in the one-loop squared computation. In fact, we had to introduce a symmetry factor of $\frac{1}{2}$ in the generating set $\tilde{R}_{4;1}^{(2)}$ to ensure this. In the present computation we single out one of the loops, while still summing over all cyclic permutations. The cut above will therefore appear two times, once for each of,



The same argument holds for all other cuts, and we require an overall symmetry factor of $\frac{1}{2}$. As it is linked to the indistinguishability of the loops in the one-loop squared approach, we expect this factor to be also required when constructing the two-loop rational parts of amplitudes with more than four gluons.

In chapter 3 we saw that the one-loop squared construction is also applicable to rational parts of amplitudes subleading in color. We can therefore attempt an effective one-loop construction for these partial amplitudes as well. We first discuss $R_{4;3}^{(2)}(1^+2^+; 3^+3^+)$. From color dressed unitarity,

we expect the following one-loop cuts to contribute to the color structure $N_c \text{Tr}(T^1 T^2) \text{Tr}(T^3 T^4)$

$$\begin{aligned}
 R_{4:3}^{(2)}(1^+ 2^+; 3^+ 4^+) = & \sum_{C_2(\{1,2\})} \left[C_{\text{Tri},[2]}^{(1)} \left[\text{Diagram 1} \right] I_3^D[\mu^2] + C_{\text{Bub},[2]}^{(1)} \left[\text{Diagram 2} \right] I_2^D[\mu^2] \right. \\
 & \left. + C_{\text{Tri},[2]}^{(1)} \left[\text{Diagram 3} \right] I_3^D[\mu^2] + C_{\text{Bub},[2]}^{(1)} \left[\text{Diagram 4} \right] I_2^D[\mu^2] \right] \\
 & + \sum_{C_2(\{3,4\})} \left[C_{\text{Tri},[2]}^{(1)} \left[\text{Diagram 5} \right] I_3^D[\mu^2] + C_{\text{Bub},[2]}^{(1)} \left[\text{Diagram 6} \right] I_2^D[\mu^2] \right. \\
 & \left. + C_{\text{Tri},[2]}^{(1)} \left[\text{Diagram 7} \right] I_3^D[\mu^2] + C_{\text{Bub},[2]}^{(1)} \left[\text{Diagram 8} \right] I_2^D[\mu^2] \right] \\
 & + \sum_{\substack{C_2(\{1,2\}) \\ C_2(\{3,4\})}} \left[C_{\text{Tri},[2]}^{(1)} \left[\text{Diagram 9} \right] I_3^D[\mu^2] + C_{\text{Bub},[2]}^{(1)} \left[\text{Diagram 10} \right] I_2^D[\mu^2] \right. \\
 & \left. + C_{\text{Tri},[2]}^{(1)} \left[\text{Diagram 11} \right] I_3^D[\mu^2] + C_{\text{Bub},[2]}^{(1)} \left[\text{Diagram 12} \right] I_2^D[\mu^2] \right] \quad (4.7)
 \end{aligned}$$

Here we already included the symmetry factor of $\frac{1}{2}$. We see that we need an additional one-loop massive scalar amplitude $R_{4:3}^{(1)}(k_1^\varphi k_2^\varphi; 3^+ 4^+)$, associated to the color structure $\text{Tr}(T^{k_1} T^{k_2}) \text{Tr}(T^3 T^4)$. Again requiring that the two scalars be attached to the same tree amplitude, this one-loop amplitude can be computed from unitarity cuts via,

$$R_{4:3}^{(1)}(k_1^\varphi k_2^\varphi; 3^+ 4^+) = 2 \sum_{C_2(\{3,4\})} \left[C_{\text{Tri},[2]}^{(1)} \left[\text{Diagram 13} \right] I_3^D[\mu^2] + C_{\text{Bub},[2]}^{(1)} \left[\text{Diagram 14} \right] I_2^D[\mu^2] \right]. \quad (4.8)$$

The two cuts evaluate to the expression in eq. (4.3), which after the summation over the two assignments of labels 3 and 4 turns into,

$$R_{4:3}^{(1)}(k_1^\varphi k_2^\varphi; 3^+ 4^+) = \sum_{C_2(\{3,4\})} \left[-\frac{1}{3} \frac{s_{k_1 3} - s_{34}}{\langle 34 \rangle^2} \right] = \frac{s_{34}}{\langle 34 \rangle^2}. \quad (4.9)$$

Using this as a vertex in the cuts of eq. (4.7) we find

$$\begin{aligned}
 C_{\text{Bub},[2]}^{(1)} \left[\text{Diagram 15} \right] &= C_{\text{Bub},[2]}^{(1)} \left[\text{Diagram 16} \right] \\
 &= C_{\text{Bub},[2]}^{(1)} \left[\text{Diagram 17} \right] = C_{\text{Bub},[2]}^{(1)} \left[\text{Diagram 18} \right] = 0, \quad (4.10)
 \end{aligned}$$

$$\begin{aligned}
 C_{\text{Tri},[2]}^{(1)} \left[\text{Diagram 19} \right] &= C_{\text{Tri},[2]}^{(1)} \left[\text{Diagram 20} \right] \\
 &= C_{\text{Tri},[2]}^{(1)} \left[\text{Diagram 21} \right] = C_{\text{Tri},[2]}^{(1)} \left[\text{Diagram 22} \right] = \frac{s_{12} s_{34}}{\langle 12 \rangle^2 \langle 34 \rangle^2}. \quad (4.11)
 \end{aligned}$$

The remaining cuts of eq. (4.7) can be related to the leading color ones of eq. (4.4), such that eq. (4.7) evaluates to

$$R_{4:3}^{(2)}(1^+2^+; 3^+4^+) = \sum_{C_2(\{1,2\})} \left[-\frac{s_{12}s_{34}}{\langle 12 \rangle^2 \langle 34 \rangle^2} \right] + \sum_{C_2(\{3,4\})} \left[-\frac{s_{12}s_{34}}{\langle 12 \rangle^2 \langle 34 \rangle^2} \right] + \sum_{\substack{C_2(\{1,2\}) \\ C_2(\{3,4\})}} \left[-\frac{s_{12}(5s_{12} + s_{13})}{9 \langle 12 \rangle^2 \langle 34 \rangle^2} \right]. \quad (4.12)$$

After carrying out the permutation sums, we can verify that this matches the result for $R_{4:3}^{(1)}$ we found in section 3.7.1. Furthermore, we can alternatively expand the cuts of eq. (4.7) into one-loop squared cuts using the unitarity construction of the one-loop vertices. We find that we obtain every one-loop squared cut of section 3.7.1 exactly twice, justifying the inclusion of the symmetry factor of $\frac{1}{2}$.

Lastly, we can attempt to find a one-loop construction of the $R_{4:1B}^{(2)}$ rational terms. We can use the flattened representation of the one-loop squared 1B cuts introduced in chapter 3 to find the associated one-loop cuts. To obtain the single trace of color generators without any factors of N_c we require one-loop vertices where the scalars are distributed between the two traces. For the moment it is convenient to assume the gauge group to be $U(N_c)$. For two scalars φ_1, φ_2 and two gluons 3, 4 there then exist two unique color structures of this type, $\text{Tr}(T^{\varphi_1}) \text{Tr}(T^{\varphi_2} T^3 T^4)$ and $\text{Tr}(T^{\varphi_1} T^3) \text{Tr}(T^{\varphi_2} T^4)$. All other structures can be obtained from permutations of the scalars and the gluons. We denote the associated one-loop vertices as $R_{4:2}^{(1)}(k_1^\varphi; k_2^\varphi 3^+ 4^+)$ and $R_{4:2}^{(1)}(k_1^\varphi 3^+; k_2^\varphi 4^+)$, and we can compute them using the expressions for the cuts found in section 3.7.1.

$$R_{4:2}^{(1)}(k_1^\varphi; k_2^\varphi 3^+ 4^+) = 2 C_{\text{Tri},[2]}^{(1)} \left[\text{Diagram} \right] I_3^D[\mu^2] = -\frac{[34]}{\langle 34 \rangle} \quad (4.13)$$

$$R_{4:3}^{(1)}(k_1^\varphi 3^+; k_2^\varphi 4^+) = 2 \left[C_{\text{Tri},[2]}^{(1)} \left[\text{Diagram} \right] I_3^D[\mu^2] + C_{\text{Tri},[2]}^{(1)} \left[\text{Diagram} \right] I_3^D[\mu^2] \right] = 2 \frac{[34]}{\langle 34 \rangle} \quad (4.14)$$

We did not include the bubble contributions explicitly as they vanish.

To obtain the one-loop cuts of $R_{4:1B}^{(2)}$ from color-dressed unitarity, the second loop is sewn into both of the traces. Up to cyclic permutation, the one-loop cuts compatible with the $R_{4:1B}^{(2)}$ structure are then

$$\text{Set (I)} \left\{ \begin{array}{ccc} \text{Diagram 1} & \text{Diagram 2} & \text{Diagram 3} \\ \text{Diagram 4} & \text{Diagram 5} & \text{Diagram 6} \end{array} \right. \quad (4.15)$$

$$\text{Set (II)} \left\{ \begin{array}{ccc} \begin{array}{c} \text{Diagram 1} \\ \text{Diagram 2} \end{array} & \begin{array}{c} \text{Diagram 3} \\ \text{Diagram 4} \end{array} & \begin{array}{c} \text{Diagram 5} \\ \text{Diagram 6} \end{array} \end{array} \right. \quad (4.16)$$

We again include only triangle cuts. We found in the one-loop squared construction of $R_{n:1B}^{(2)}$ with at least up to seven gluons that all one-loop squared cuts involving either a box or a bubble vanish, such that we can expect the construction of $R_{n:1B}^{(2)}$ purely from triangle cuts to hold in general. We also split the cuts into two sets, which are mirror images of each other. When we expand the one-loop cuts into one-loop squared ones we can see that the two sets are in fact the same cuts, related by the symmetry of the punctured torus topology. To avoid overcounting we therefore limit ourselves to computing set (I). Note that even after removing the redundant set (II) we will still overcount cuts when summing over cyclic permutations. This is the same redundancy we found in the one-loop construction of $R_{4:1}^{(2)}$ and $R_{4:3}^{(2)}$ above, and again makes the inclusion of a symmetry factor of $\frac{1}{2}$ necessary. The redundancy of sets (I) and (II) in addition to the one of the permutation sum are the realization of the four-fold symmetry we found for one-loop squared cuts of $R_{n:1B}^{(2)}$ in section 3.4. We therefore expect,

$$\begin{aligned} R_{4:1B}^{(2)}(1^+2^+3^+4^+) &= \sum_{C_4} \left[C_{\text{Tri},[2]}^{(1)} \left[\begin{array}{c} \text{Diagram 1} \\ \text{Diagram 2} \end{array} \right] I_3^D[\mu^2] + C_{\text{Tri},[2]}^{(1)} \left[\begin{array}{c} \text{Diagram 3} \\ \text{Diagram 4} \end{array} \right] I_3^D[\mu^2] \right. \\ &+ C_{\text{Tri},[2]}^{(1)} \left[\begin{array}{c} \text{Diagram 5} \\ \text{Diagram 6} \end{array} \right] I_3^D[\mu^2] + C_{\text{Tri},[2]}^{(1)} \left[\begin{array}{c} \text{Diagram 7} \\ \text{Diagram 8} \end{array} \right] I_3^D[\mu^2] \\ &\left. + C_{\text{Tri},[2]}^{(1)} \left[\begin{array}{c} \text{Diagram 9} \\ \text{Diagram 10} \end{array} \right] I_3^D[\mu^2] + C_{\text{Tri},[2]}^{(1)} \left[\begin{array}{c} \text{Diagram 11} \\ \text{Diagram 12} \end{array} \right] I_3^D[\mu^2] \right]. \end{aligned} \quad (4.17)$$

Evaluation of these coefficients as in section 3.7.1 leads to following expressions for the coefficients,

$$\begin{aligned} C_{\text{Tri},[2]}^{(1)} \left[\begin{array}{c} \text{Diagram 1} \\ \text{Diagram 2} \end{array} \right] &= -\frac{[12][34]}{\langle 12 \rangle \langle 34 \rangle}, & C_{\text{Tri},[2]}^{(1)} \left[\begin{array}{c} \text{Diagram 3} \\ \text{Diagram 4} \end{array} \right] &= 2\frac{[12][34]}{\langle 12 \rangle \langle 34 \rangle}, \\ C_{\text{Tri},[2]}^{(1)} \left[\begin{array}{c} \text{Diagram 5} \\ \text{Diagram 6} \end{array} \right] &= -\frac{[12][34]}{\langle 12 \rangle \langle 34 \rangle}, & C_{\text{Tri},[2]}^{(1)} \left[\begin{array}{c} \text{Diagram 7} \\ \text{Diagram 8} \end{array} \right] &= \frac{[12][34]}{\langle 12 \rangle \langle 34 \rangle}, \\ C_{\text{Tri},[2]}^{(1)} \left[\begin{array}{c} \text{Diagram 9} \\ \text{Diagram 10} \end{array} \right] &= -2\frac{[13][24]}{\langle 13 \rangle \langle 24 \rangle}, & C_{\text{Tri},[2]}^{(1)} \left[\begin{array}{c} \text{Diagram 11} \\ \text{Diagram 12} \end{array} \right] &= \frac{[14][23]}{\langle 14 \rangle \langle 23 \rangle}. \end{aligned} \quad (4.18)$$

Even before summing over the cyclic permutations the sum over cuts in eq. (4.17) vanishes¹, such that we recover the expected result,

$$R_{4:1B}^{(2)}(1^+2^+3^+4^+) = 0 \quad (4.19)$$

¹Using $\frac{[12][34]}{\langle 12 \rangle \langle 34 \rangle} = \frac{[13][24]}{\langle 13 \rangle \langle 24 \rangle} = \frac{[14][23]}{\langle 14 \rangle \langle 23 \rangle}$.

We have thus shown that the rational parts of all four-gluon two-loop partial amplitudes with all-plus helicity are constructible from a one-loop unitarity computation. The results of this construction are given in eqs.(4.19), (4.12) and (4.6). The cuts involve vertices reminiscent of rational parts of one-loop amplitudes, which include a massive scalar pair. From unitarity we derived analytic expressions for these in eqs. (4.3), (4.9), (4.13) and (4.14). In the next section we will build on this interpretation, and describe how to use one-loop amplitude techniques to compute the vertices for additional gluons. We will then show explicitly that the leading color five-gluon rational term is constructible via one-loop unitarity as well.

4.2 One-Loop Massive Scalar Amplitudes

In this section we will discuss the origin and the computation of the one-loop vertices in more detail.

A natural interpretation for the one-loop vertices derives from their dimensional reconstruction origins in the one-loop squared picture. As a reminder, we used the one-loop squared cuts to compute the six-dimensional amplitudes $A_{6,2,0}^{(1)}$ and $A_{6,1,1}^{(1)}$, which together formed the coefficient of $(D_s - 2)^2$. These two-loop amplitudes are associated to the Lagrangian [107],

$$\mathcal{L}_{6D,\text{scalar}} = +\frac{1}{2}D_\mu\varphi^a D^\mu\varphi^a + \frac{1}{2}D_\mu\varphi'^a D^\mu\varphi'^a - \frac{g^2}{2}f^{abc}f^{ade}\varphi^b\varphi'^c\varphi^d\varphi'^e, \quad (4.20)$$

describing two massless six-dimensional scalar fields in the adjoint representation of the gauge group. In $A_{6,2,0}^{(1)}$ and $A_{6,1,1}^{(1)}$, each loop carries such a scalar, and the loops are connected via gluon exchange or a four-scalar contact term respectively.

We can therefore identify the one-loop vertices used in the construction of the previous section as six-dimensional one-loop amplitudes, with a six-dimensional massless external scalar, and a massless scalar running in the loop. As the scalars are the only external particles carrying six-dimensional momentum, the arguments used for the scalar tree-amplitudes in section 3.5, and we can compute the relevant cuts via massive four-dimensional methods.

Considering the one-loop squared construction of two-loop rational contributions subleading in color, we require subleading one-loop partial amplitudes as well. In the language of the one-loop color decomposition, we require the rational parts of the amplitudes,

$$\begin{aligned} \text{Tr}(1^\varphi 2^g \dots i^\varphi \dots n^g) &\rightarrow R_{n:1}^{(1)}(1^\varphi 2^+ \dots i^\varphi \dots n^+), \\ \text{Tr}(1^\varphi 2^g \dots i^\varphi \dots (r-1)^g) \text{Tr}(r^g \dots n^g) &\rightarrow R_{n:r}^{(1)}(1^\varphi 2^+ \dots i^\varphi \dots (r-1)^+; r^+ \dots n^+), \\ \text{Tr}(1^\varphi 2^g \dots (r-1)^g) \text{Tr}(r^\varphi \dots n^g) &\rightarrow R_{n:r}^{(1)}(1^\varphi 2^+ \dots (r-1)^+; r^\varphi (r+1)^+ \dots n^+), \end{aligned} \quad (4.21)$$

for both the gluon-exchange and contact-term contributions. As for tree amplitudes, we distinguish the two via a subscript, *i.e.* $R_{\text{gluon}}^{(1)}$ and $R_{\text{contact}}^{(1)}$. In the first two cases, the two external scalars φ appear in the same trace. As in the four-gluon example, these amplitudes will be required for the twice punctured disk topology. Both gluon-exchange and contact-term versions of these amplitudes exist. In the third case, the two external scalars are distributed across the two traces, and are required for the punctured torus topology, *i.e.* $R_{n:1B}^{(2)}$. As the external scalar line crosses the loop, only contact-term amplitudes can contribute.

4.2.1 One-Loop BCFW

To compute the rational part of the one-loop massive scalar amplitudes, we will use a hybrid approach of BCFW recursion and unitarity.

As the BCFW construction makes use of the analyticity of scattering amplitudes it can also be used to determine rational parts of loop amplitudes. In the presence of loops, there are new features in the BCFW computations that require special consideration. For one, not all poles can be associated to on-shell propagators. We are also not limited to single poles anymore; in one-loop amplitudes we will generally encounter double poles in the shift parameter z . While the double poles follow from the universal collinear behavior, there exist single poles that cannot be obtained from on-shell factorization. In refs. [112, 136], BCFW shifts were used to define a recursive construction of one-loop single-minus amplitudes, as well as all-plus amplitudes with a massless fermion pair. In these, the missing pole contributions were found by experimentation, and turn out to be related to a product of soft functions. As a more general procedure, ref. [19] introduced the augmented recursion procedure, which allows one to determine these missing poles from off-shell currents. This method has been successfully applied in a number of one-loop computations [20–22], and was used to determine the rational contributions to two-loop all-plus helicity amplitudes in refs. [4–10]. For our computation, we will choose a different approach for the missing pole terms. We will see that both the double- and missing single-pole terms originate from a limited number of unitarity cuts. In the leading-color case only two cuts are generally required, which have a particularly simple form. Contrary to the augmented-recursion procedure, we only require on-shell tree-amplitudes in this approach.

As a warm up, we will review the computation of the five-gluon single-minus amplitude, as it was presented in ref. [112]. We then show that the missing pole pieces are obtainable from two unitarity cuts, which we compute explicitly. We will then apply this method to the massive scalar amplitudes required for our effective one-loop approach to the two-loop rational terms.

4.2.1.1 The One-Loop Single-Minus Amplitude from BCFW

Just as in the case of tree amplitudes, we can use analyticity to construct the rational parts of loop amplitudes recursively in the BCFW spirit. However, the analytic structure is slightly more complicated, as propagators going on-shell are now not the only source of poles.

To explore the peculiarities involved in using BCFW recursion to compute one-loop amplitudes, we review the BCFW construction of the amplitude,

$$A^{(1)}(1^- 2^+ 3^+ 4^+ 5^+) = \frac{1}{3 \langle 34 \rangle^2} \left[\frac{\langle 14 \rangle^3 \langle 35 \rangle [45]}{\langle 12 \rangle \langle 23 \rangle \langle 45 \rangle^2} + \frac{\langle 13 \rangle^3 \langle 24 \rangle [23]}{\langle 15 \rangle \langle 23 \rangle^2 \langle 45 \rangle} + \frac{[25]^3}{[12][15]} \right]. \quad (4.22)$$

We will follow the discussion of ref. [112]. As a one-loop single-minus amplitude, it is purely rational, and has all relevant features required for later discussions.

We use a $[1, 2]$ -shift, which has the form,

$$\begin{aligned} [\hat{1}] &= [1] - z[2], & \langle \hat{1} \rangle &= \langle 1 \rangle, \\ \langle \hat{2} \rangle &= \langle 2 \rangle + z \langle 1 \rangle, & [\hat{2}] &= [2]. \end{aligned} \quad (4.23)$$

We see from the expression (4.22) that $A^{(1)}(1^- 2^+ 3^+ 4^+ 5^+)$ scales as $\frac{1}{z}$ at worst. We would therefore expect to reconstruct the amplitude from its finite poles in z . At tree level, such poles stem entirely from propagators going on-shell, and we would naively expect to obtain the amplitude via,

$$\begin{aligned} A^{(1)}(1^- 2^+ 3^+ 4^+ 5^+) \sim & - \sum_{h=\pm} A^{(0)}(\hat{1}^- \hat{K}^h 5^+) \frac{1}{s_{15}} A^{(1)}(\hat{2}^+ 3^+ 4^+ (-\hat{K})^{\bar{h}}) \\ & - A^{(1)}(\hat{1}^- \hat{K}^+ 4^+ 5^+) \frac{1}{s_{34}} A^{(0)}(\hat{2}^+ 3^+ (-\hat{K})^-) \end{aligned} \quad (4.24)$$

Using the results for the one-loop all-plus and single-minus amplitudes of eqs.(3.5) and (A.9), these channels result in,

$$\begin{aligned} -A^{(0)}(\hat{1}^- \hat{K}^- 5^+) \frac{1}{s_{15}} A^{(1)}(\hat{2}^+ 3^+ 4^+ (-\hat{K})^+) &= -\frac{1}{3} \frac{\langle 1\hat{K} \rangle^3}{\langle \hat{K}5 \rangle \langle 51 \rangle} \frac{1}{s_{15}} \frac{[34] [\hat{K}2]}{\langle 34 \rangle \langle \hat{K}\hat{2} \rangle} \\ &= \frac{1}{3} \frac{1}{\langle 34 \rangle^2} \frac{[25]^3}{[15] [12]}, \end{aligned} \quad (4.25)$$

$$-A^{(0)}(\hat{1}^- \hat{K}^+ 5^+) \frac{1}{s_{15}} A^{(1)}(\hat{2}^+ 3^+ 4^+ (-\hat{K})^-) = -\frac{1}{3} \frac{[\hat{1}\hat{K}]^3}{[\hat{K}5] [5\hat{1}]} \frac{1}{s_{15}} \frac{\langle \hat{2}4 \rangle [24]^3}{\langle \hat{2}3 \rangle \langle 34 \rangle [\hat{K}2] [\hat{K}4]} = 0, \quad (4.26)$$

$$\begin{aligned} -A^{(1)}(\hat{1}^- \hat{K}^+ 4^+ 5^+) \frac{1}{s_{23}} A^{(0)}(\hat{2}^+ 3^+ (-\hat{K})^-) &= \frac{1}{3} \frac{\langle \hat{K}5 \rangle [\hat{K}5]^3}{\langle \hat{K}4 \rangle \langle 45 \rangle [\hat{1}\hat{K}] [\hat{1}5]} \frac{1}{s_{23}} \frac{[23]^3}{[3\hat{K}] [\hat{K}2]} \\ &= \frac{1}{3} \frac{\langle 14 \rangle^2 [45]}{\langle 23 \rangle \langle 45 \rangle^2 \langle 12 \rangle \langle 34 \rangle [\hat{1}5]} \frac{s_{5\hat{K}}}{[\hat{1}5]} \\ &= \frac{1}{3} \frac{\langle 14 \rangle^3 \langle 35 \rangle [45]}{\langle 34 \rangle^2 \langle 12 \rangle \langle 23 \rangle \langle 45 \rangle^2}. \end{aligned} \quad (4.27)$$

We recover the first and last term of eq. (4.22), but are missing the second. When we evaluate this term on the shifted kinematics we can spot the root of the problem. It contains the troubling factor,

$$\frac{[23]}{\langle \hat{2}3 \rangle^2} = \frac{[23]}{(\langle 23 \rangle + z \langle 13 \rangle)^2}, \quad (4.28)$$

that is a double pole in the s_{23} channel. This is a feature we have not accounted for in the construction of eq. (4.24). This factor generates a double pole only for complex momenta, as spinor products $\langle 23 \rangle$ and $[23]$ are then independent. For real momenta they are linked by complex conjugation, and we recover the expected physical single pole $1/\langle 23 \rangle$ in this term, up to a phase.

The source of the double pole can be understood from the behavior of the amplitude in the collinear region $2||3$. Besides the factorization involving the tree-level splitting function,

$$A^{(1)} \times \text{Split}^{(0)} \rightarrow \text{Diagram 1} \times \text{Diagram 2}, \quad (4.29)$$

we also need to consider contributions from the one-loop splitting function $\text{Split}^{(1)}$. It can be

thought of diagrammatically as,

$$A^{(0)} \times \text{Split}^{(1)} \rightarrow \begin{array}{c} 1^- \\ \diagup \quad \diagdown \\ \text{---} \bigcirc \text{---} \\ \diagdown \quad \diagup \\ 4^+ \end{array} \times \begin{array}{c} 2^+ \\ \diagup \quad \diagdown \\ \text{---} \bigcirc \text{---} \\ \diagdown \quad \diagup \\ 3^+ \end{array}. \quad (4.30)$$

The splitting function $\text{Split}_h^{(1)}(i^+, j^+)$ receives contributions from diagrams of the form [55, 56, 137, 138],

$$\text{Split}_h^{(1)}(i^+, j^+) \simeq \frac{1}{s_{ij}} \left[h \begin{array}{c} i^+ \\ \diagup \quad \diagdown \\ \text{---} \triangle \text{---} \\ \diagdown \quad \diagup \\ j^+ \end{array} + h \begin{array}{c} i^+ \\ \diagup \quad \diagdown \\ \text{---} \bigcirc \text{---} \\ \diagdown \quad \diagup \\ j^+ \end{array} \right]. \quad (4.31)$$

and evaluates to [56],

$$\text{Split}_+^{(1)}(i^+ j^+) = -\frac{i}{6} \frac{\varepsilon_K^+ \cdot (p_i - p_j)}{\sqrt{2} p_i \cdot p_j} \left[\varepsilon_i^+ \cdot \varepsilon_j^+ - \frac{\varepsilon_i^+ \cdot p_j \varepsilon_j^+ \cdot p_i}{p_i \cdot p_j} \right] + \mathcal{O}(\epsilon), \quad (4.32)$$

with $K = -(p_i + p_j)$. We removed a factor of $i/(4\pi)^2$ to align $\text{Split}^{(1)}$ with our definition of one-loop amplitudes given in eq. (1.98).

Assuming all momenta to be complex, we can express $\text{Split}_+^{(1)}(i^+ j^+)$ in terms of spinor products. As there are only three on-shell momenta, all invariants have to vanish. Furthermore, all angle spinor products are proportional to one another, as are all the bracket products, causing either all angle or all bracket spinor products to vanish. Similar to the three-gluon $\overline{\text{MHV}}$ amplitude, we assume the products $\langle Ki \rangle$, $\langle jK \rangle$ and $\langle ij \rangle$ to be zero. Starting from the expression in eq. (4.32), we then obtain

$$\begin{aligned} \text{Split}^{(1)}(i^+ j^+) &= -\frac{1}{6} \frac{\varepsilon_K^+ \cdot (p_i - p_j)}{\sqrt{2} p_i \cdot p_j} \left[\varepsilon_i^+ \cdot \varepsilon_j^+ - \frac{\varepsilon_i^+ \cdot p_j \varepsilon_j^+ \cdot p_i}{p_i \cdot p_j} \right] \\ &= \frac{1}{3} \frac{1}{s_{ij}^2} \frac{[Ki] \langle iq \rangle [ij] \langle jq \rangle [ji] \langle iq \rangle}{\langle Kq \rangle \langle iq \rangle \langle jq \rangle} \\ &= -\frac{1}{3} \frac{[Ki] [ij] [jK]}{s_{ij}^2}. \end{aligned} \quad (4.33)$$

Here we chose the reference momenta of the three polarization vectors to be the same arbitrary momentum q . The double pole is manifest, and when the momenta i and j —now assumed to be real—become collinear we obtain,

$$\text{Split}^{(1)}(i^+ j^+) \stackrel{i||j}{\propto} \frac{[ij]}{\langle ij \rangle^2}, \quad (4.34)$$

as expected. The $\langle 23 \rangle$ double pole in our example is generated by the collinear factorization²

$$A^{(1)}(1^- 2^+ 3^+ 4^+ 5^+) \xrightarrow{2||3} -A^{(0)}(1^- K^- 4^+ 5^+) \times \text{Split}_+^{(1)}(2^+ 3^+) + \text{other}, \quad (4.35)$$

where we have neglected contributions from the tree-level splitting functions.

We can use this splitting function to explicitly add the double pole contribution in the BCFW

²The sign is the result of having normalized all amplitudes and splitting functions by a factor of $-i$

computation of eq. (4.24). As in ref. [112] we define,

$$V^{(1)}(i^+ j^+ k^+) = -\frac{1}{3} [ij] [jk] [ki]. \quad (4.36)$$

as the factorizable part of the one-loop splitting function without its denominator. We can see that the term

$$-A^{(0)}(\hat{1}^- \hat{K}^- 4^+ 5^+) \frac{1}{s_{34}^2} V^{(1)}(\hat{K}^+ \hat{2}^+ 3^+) \quad (4.37)$$

in the $2||3$ limit exactly reproduces the behavior predicted by the one-loop splitting function. In other words, using the shifted kinematics, we can probe the $2||3$ limit by taking the limit $z \rightarrow z_{23} = -\frac{\langle 23 \rangle}{\langle 13 \rangle}$. In this case the term in eq. (4.37) is the required contribution to the universal factorization behavior.

Evaluating eq. (4.37) we get,

$$\begin{aligned} -A^{(0)}(\hat{1}^- \hat{K}^- 4^+ 5^+) \frac{1}{s_{34}^2} V^{(1)}(\hat{K}^+ \hat{2}^+ 3^+) &= -\frac{\langle 1\hat{K}^3 \rangle}{\langle \hat{K}4 \rangle \langle 45 \rangle \langle 51 \rangle} \frac{1}{s_{23}^2} \frac{1}{3} [\hat{K}2] [23] [3\hat{K}] \\ &= \frac{1}{3} \frac{\langle 13 \rangle^2 \langle 12 \rangle [23]}{\langle 34 \rangle \langle 45 \rangle \langle 15 \rangle \langle 23 \rangle^2}, \end{aligned} \quad (4.38)$$

which does not match the middle term in eq. (4.22). To see why, we evaluate the amplitude of eq. (4.22) on shifted kinematics and make the z_{23} poles of the $\langle \hat{2}3 \rangle$ denominators manifest. We can then write the amplitude in the form,

$$A^{(1)}(z) = \frac{f(z)}{(z - z_{23})^2} + \frac{g(z)}{z - z_{23}} + h(z). \quad (4.39)$$

where the functions

$$f(z) = \frac{1}{3} \frac{\langle 13 \rangle \langle \hat{2}4 \rangle [23]}{\langle 34 \rangle^2 \langle 15 \rangle \langle 45 \rangle}, \quad g(z) = \frac{1}{3} \frac{\langle 14 \rangle^3 \langle 35 \rangle [45]}{\langle 34 \rangle^2 \langle 13 \rangle \langle 12 \rangle \langle 45 \rangle^2}, \quad h(z) = \frac{1}{3} \frac{[25]^3}{\langle 34 \rangle^2 [\hat{1}2] [\hat{1}5]}, \quad (4.40)$$

are free of z_{23} poles. In the BCFW construction we have to determine the residue of $-A^{(1)}(z)/z$ at z_{23} , which given the form for $A^{(1)}(z)$ turns into

$$-\text{Res}_{z=z_{23}} \left[\frac{A^{(1)}(z)}{z} \right] = - \left[-\frac{f(z_{23})}{z_{23}^2} + \frac{1}{z_{23}} \frac{df}{dz} \Big|_{z=z_{23}} + \frac{g(z_{23})}{z_{23}} \right]. \quad (4.41)$$

We already obtained the last term from the $A^{(1)} \times A^{(0)}$ factorization, and indeed we recover

$$-\frac{g(z_{23})}{z_{23}} = \frac{1}{3} \frac{\langle 14 \rangle^3 \langle 35 \rangle [45]}{\langle 34 \rangle^2 \langle 23 \rangle \langle 12 \rangle \langle 45 \rangle^2}. \quad (4.42)$$

The first term is exactly the one we obtained from requiring the universal collinear behavior, as

$$\frac{f(z_{23})}{z_{23}^2} = \frac{1}{3} \frac{\langle 13 \rangle^2 (\langle 24 \rangle \langle 13 \rangle - \langle 14 \rangle \langle 23 \rangle) [23]}{\langle 34 \rangle^2 \langle 15 \rangle \langle 45 \rangle \langle 23 \rangle^2} = \frac{1}{3} \frac{\langle 13 \rangle^2 \langle 12 \rangle [23]}{\langle 34 \rangle \langle 15 \rangle \langle 45 \rangle \langle 23 \rangle^2} \quad (4.43)$$

matches eq. (4.38). We are however missing the middle term involving the derivative of $f(z)$, which

evaluates to

$$-\frac{1}{z_{23}} \frac{df}{dz} \Big|_{z=z_{23}} = \frac{1}{3} \frac{\langle 13 \rangle^2 \langle 14 \rangle [23]}{\langle 34 \rangle^2 \langle 15 \rangle \langle 45 \rangle \langle 23 \rangle}. \quad (4.44)$$

These single-pole contributions descend from the double-pole piece, and are in some sense hidden underneath the double pole. For this reason they have been coined *pole-under-pole* contributions in ref. [19], or PUP terms for short. Currently no universal construction in terms of products of amplitudes is known for these types of contributions, and they have to be obtained by other means. In the specific case of one-loop single-minus amplitudes, an all- n construction in terms of soft factors was proposed in ref. [112]. By adding to the usual BCFW poles and universal double pole contributions the term,

$$-A^{(0)}(\hat{1}^- \hat{K}^- 4^+ \dots n^+) \frac{1}{s_{23}} V^{(1)}(-\hat{K}^+ \hat{2}^+ 3^+) \times \text{Soft}^{(0)}(\hat{1}_g \hat{K}^+ 4_g) \text{Soft}^{(0)}(3_g (-\hat{K})^- \hat{2}_g) \quad (4.45)$$

the n -gluon one-loop single-minus amplitude can be constructed recursively. In ref. [139] it was shown that gauge- and Lorentz-invariance are sufficient to derive this all- n form for the PUP terms. The soft functions $\text{Soft}^{(0)}$,

$$\text{Soft}^{(0)}(i_g s^+ j_g) = \frac{\langle ij \rangle}{\langle is \rangle \langle sj \rangle}, \quad \text{Soft}^{(0)}(i_g s^+ j_g) = -\frac{[ij]}{[is][sj]}, \quad (4.46)$$

specify the universal behavior of a tree amplitude when one of the particle momenta vanishes,

$$A^{(0)}(\dots i_g s^h j_g \dots) \xrightarrow{p_s \rightarrow 0} A^{(0)}(\dots i_g j_g \dots) \times \text{Soft}^{(0)}(i_g s^h j_g). \quad (4.47)$$

The subscript g is meant to indicate that the particle is a (massless) gluon. In appendix A.3 we derive the form of the soft functions shown above, and also provide expressions in the case that one or both of the momenta are massive scalars.

Specializing this construction to our five-gluon amplitude, we obtain

$$\begin{aligned} & -A^{(0)}(\hat{1}^- \hat{K}^- 4^+ 5^+) \frac{1}{s_{23}} V^{(1)}(-\hat{K}^+ \hat{2}^+ 3^+) \\ & \quad \times \text{Soft}^{(0)}(\hat{1}_g \hat{K}^+ 4_g) \text{Soft}^{(0)}(3_g (-\hat{K})^- \hat{2}_g) \\ & = -\frac{\langle 1\hat{K} \rangle^3}{\langle \hat{K}4 \rangle \langle 45 \rangle \langle 51 \rangle} \frac{1}{s_{34}} \frac{1}{3} [\hat{K}2] [23] [3\hat{K}] \frac{\langle 14 \rangle}{\langle \hat{1}\hat{K} \rangle \langle \hat{K}4 \rangle} \frac{[32]}{[3\hat{K}] [\hat{K}2]} \\ & = \frac{1}{3} \frac{1}{\langle 23 \rangle} \frac{\langle 13 \rangle^2 \langle 14 \rangle [23]}{\langle 34 \rangle^2 \langle 45 \rangle \langle 15 \rangle}, \end{aligned} \quad (4.48)$$

which is precisely the missing contribution of eq. (4.44).

A similar construction in terms of soft functions also exists for two-fermion amplitudes [136], and in the case of gravity amplitudes partial results are known [140].

4.2.1.2 Pole-under-pole Terms from Unitarity

We now describe a method to obtain the pole-under-pole terms via generalized unitarity methods. While the augmented recursion procedure provides a path for their derivation, we would have to work with off-shell currents. By instead using unitarity, we are able to reuse the results for scalar

on-shell amplitudes we derived in the previous chapter.

As a reminder, we would like to obtain the pole-under-pole contributions of $A^{(1)}(1^-2^+3^+4^+5^+)$ under a $\langle 2, 1 \rangle$ -shift. As discussed in section 4.2.1, the double pole contributions originate from the one-loop factorizing splitting function $\text{Split}^{(1)}$. For the amplitude in question, the diagrams contributing to universal behavior described by the splitting function are of the form,

$$(4.49)$$

where the hatched disks represent the sum of all Feynman diagrams. The double-pole and pole-under-pole terms therefore belong to the s_{23} -channel, where

$$s_{23} = 0 \Rightarrow z_{23} = -\frac{\langle 23 \rangle}{\langle 13 \rangle}. \quad (4.50)$$

Considering the Feynman diagrams above, we might expect the double pole and pole-under-pole terms to be related to the unitarity cuts,

$$(4.51)$$

The third cut is the contribution of the tensor triangle integral to the bubble coefficient. The fine dashing represents the third propagator cut in addition to the bubble cut shown in the center. As we are interested in rational contributions, we replaced the gluon loop with a scalar one, and use D -dimensional unitarity techniques. We will see that after evaluating these cuts on BCFW kinematics, their combined single and double poles in z_{23} are exactly the double pole and pole-under-pole terms, for which we found expressions in eqs.(4.38) and (4.44) of section 4.2.1.

Let us first evaluate the triangle cut in eq. (4.51). The triangle loop-momentum parametrization of eq. (2.51) takes the form,

$$\ell_1^\mu = \frac{1}{2} \left(t \langle 3 | \gamma^\mu | 2 \rangle - \frac{\mu^2}{s_{23}t} \langle 2 | \gamma^\mu | 3 \rangle \right), \quad \ell_1^{*\mu} = \frac{1}{2} \left(t \langle 2 | \gamma^\mu | 3 \rangle - \frac{\mu^2}{s_{23}t} \langle 3 | \gamma^\mu | 2 \rangle \right). \quad (4.52)$$

We obtain the associated integral coefficient via,

$$\begin{aligned} C_{\text{Tri},[2]}^{(1)} \left[\begin{array}{c} 1^- \\ 5^+ \\ 4^+ \end{array} \begin{array}{c} 2^+ \\ 3^+ \end{array} \right] &= \frac{1}{2} \sum_{\ell, \ell^*} \text{Inf}_{\mu^2 t} \left[A^{(0)} \left((-\ell_2)^\varphi 4^+ 5^+ 1^- \ell_3^\varphi \right) \right. \\ &\quad \times A^{(0)} \left((-\ell_3)^\varphi 2^+ \ell_1^\varphi \right) A^{(0)} \left((-\ell_1)^\varphi 3^+ \ell_2^\varphi \right) \Big]_{t^0, \mu^2} \\ &= -\frac{1}{2} \frac{[23]}{\langle 23 \rangle} \sum_{\ell, \ell^*} \text{Inf}_{\mu^2 t} \left[A^{(0)} \left((-\ell_2)^\varphi 4^+ 5^+ 1^- \ell_3^\varphi \right) \right]_{t^0, \mu^0}. \end{aligned} \quad (4.53)$$

Here we used,

$$A^{(0)} \left((-\ell_3)^\varphi 2^+ \ell_1^\varphi \right) A^{(0)} \left((-\ell_1)^\varphi 3^+ \ell_2^\varphi \right) = -\mu^2 \frac{[23]}{\langle 23 \rangle}, \quad (4.54)$$

which is true for both ℓ and ℓ^* in the parametrization of eq. (4.52). Using the expression for the amplitude in eq. (B.4), the cut becomes,

$$C_{\text{Tri},[2]}^{(1)} \left[\begin{array}{c} 1^- \\ 5^+ \\ 4^+ \end{array} \begin{array}{c} \bullet \\ \bullet \\ \bullet \end{array} \begin{array}{c} 2^+ \\ 3^+ \end{array} \right] = -\frac{1}{2} \frac{[23]}{\langle 23 \rangle} \sum_{\ell, \ell^*} \text{Inf}_{\mu^2 t} \left[-\frac{\mu^2 [45]^3}{s_{\ell_3(-\ell_2)} [51] [1|(4+5)(-\ell_2)|5]} \right. \\ \left. + \frac{\langle 1|\ell_3(4+5)(-\ell_2)|4\rangle^2}{s_{(\ell_3)4} s_{\ell_3 1} \langle 45 \rangle \langle 51 \rangle [1|(4+5)(-\ell_2)|4]} \right]_{t^0, \mu^0}. \quad (4.55)$$

Extracting the t^0 and μ^0 part of the $\text{Inf}_{\mu^2, t}$ expansion, we obtain

$$C_{\text{Tri},[2]}^{(1)} \left[\begin{array}{c} 1^- \\ 5^+ \\ 4^+ \end{array} \begin{array}{c} \bullet \\ \bullet \\ \bullet \end{array} \begin{array}{c} 2^+ \\ 3^+ \end{array} \right] = -\frac{\langle 12 \rangle [23] \left(2 \langle 13 \rangle^2 \langle 24 \rangle^2 - \langle 14 \rangle^2 \langle 23 \rangle^2 \right)}{2 \langle 15 \rangle \langle 23 \rangle^2 \langle 24 \rangle^2 \langle 34 \rangle \langle 45 \rangle}, \quad (4.56)$$

giving the contribution to the amplitude,

$$\begin{array}{c} 1^- \\ 5^+ \\ 4^+ \end{array} \begin{array}{c} \bullet \\ \bullet \\ \bullet \end{array} \begin{array}{c} 2^+ \\ 3^+ \end{array} = 2 C_{\text{Tri},[2]}^{(1)} \left[\begin{array}{c} 1^- \\ 5^+ \\ 4^+ \end{array} \begin{array}{c} \bullet \\ \bullet \\ \bullet \end{array} \begin{array}{c} 2^+ \\ 3^+ \end{array} \right] I_{3,[2]}^D \left[\begin{array}{c} 1^- \\ 5^+ \\ 4^+ \end{array} \begin{array}{c} \bullet \\ \bullet \\ \bullet \end{array} \begin{array}{c} 2^+ \\ 3^+ \end{array} \right] = \frac{\langle 12 \rangle [23] \left(2 \langle 13 \rangle^2 \langle 24 \rangle^2 - \langle 14 \rangle^2 \langle 23 \rangle^2 \right)}{2 \langle 15 \rangle \langle 23 \rangle^2 \langle 24 \rangle^2 \langle 34 \rangle \langle 45 \rangle}. \quad (4.57)$$

We now evaluate this expression on the BCFW kinematics of eq. (4.23). The cut only contains a double pole in z_{23} , which we easily determine as

$$\begin{array}{c} 1^- \\ 5^+ \\ 4^+ \end{array} \begin{array}{c} \bullet \\ \bullet \\ \bullet \end{array} \begin{array}{c} 2^+ \\ 3^+ \end{array} \Big|_{z_{23}\text{-double pole}} = \frac{\langle 12 \rangle \langle 13 \rangle^2 [23]}{\langle 15 \rangle \langle 23 \rangle^2 \langle 34 \rangle \langle 45 \rangle} \quad (4.58)$$

Next, we need to determine the bubble and tensor triangle cut of eq. (4.51). For the loop momentum parametrization of eq. (2.122) we choose the reference momentum χ to be p_3 for convenience, meaning that

$$K = p_2 + p_3, \quad K^\flat = K - \frac{s_{23}}{2(K \cdot p_3)} p_3 = p_2, \quad \gamma = s_{23}. \quad (4.59)$$

The loop momentum therefore takes the form

$$\ell^\mu = y p_2^\mu + (1-y) p_3^\mu + \frac{1}{2} \left(t \langle 2|\gamma^\mu|3 \rangle + \frac{y(1-y)s_{23} - \mu^2}{t s_{23}} \langle 3|\gamma^\mu|2 \rangle \right). \quad (4.60)$$

Besides resulting in a simple loop-momentum parametrization, choosing p_3 as reference momentum further eliminates the tensor triangle cut contribution on the right of eq. (4.51). Evaluating eq. (4.60) at the two values y^\pm associated with the extra on-shell propagator leads to the two triangle solutions of eq. (4.52). The contributions to the bubble coefficient are related to integrals over positive powers of t , which we know vanish for the parametrization of eq. (4.52). Alternatively we can see that the t -integrals of eq. (2.127) vanish explicitly, as they are proportional to $[K^\flat|p_2|\chi\rangle$ for the cut in question.

The bubble cut of eq. (4.51) does not specify the bubble integral coefficient entirely, as we are missing additional tensor triangle contributions. These do not belong to the graph topologies of eq. (4.49), and are therefore not relevant for our computation. We determine the bubble-cut part

$\tilde{C}_{\text{Bub},[2]}^{(1)}$ of the coefficient $C_{\text{Bub},[2]}^{(1)}$ by

$$\begin{aligned} \tilde{C}_{\text{Bub},[2]}^{(1)} \left[\begin{array}{c} 1^- \\ 5^+ \text{---} \text{---} 2^+ \\ 4^+ \text{---} \text{---} 3^+ \end{array} \right] &= \text{Inf}_{\mu^2, t, y} \left[A^{(0)} \left((-\ell_2)^\varphi 4^+ 5^+ 1^- \ell_1^\varphi \right) A^{(0)} \left((-\ell_1)^\varphi 2^+ 3^+ \ell_2^\varphi \right) \right]_{y^i \rightarrow Y^i, t^0, \mu^2} \\ &= -\frac{[23]}{s_{23} \langle 23 \rangle} \text{Inf}_{\mu^2, t, y} \left[\frac{1}{y} A^{(0)} \left((-\ell_1)^\varphi 4^+ 5^+ 1^- \ell_2^\varphi \right) \right]_{y \rightarrow Y^i, t^0, \mu^0}, \end{aligned} \quad (4.61)$$

where we used

$$A^{(0)} \left((-\ell_1)^\varphi 2^+ 3^+ \ell_2^\varphi \right) = -\frac{\mu^2 [23]}{y s_{23} \langle 23 \rangle}. \quad (4.62)$$

Only the y^0 coefficient in the Inf_y expansion is non-zero, and we end up with

$$C_{\text{Tri},[2]}^{(1)} \left[\begin{array}{c} 1^- \\ 5^+ \text{---} \text{---} 2^+ \\ 4^+ \text{---} \text{---} 3^+ \end{array} \right] = \frac{\langle 13 \rangle^2 (\langle 13 \rangle \langle 24 \rangle - 3 \langle 12 \rangle \langle 34 \rangle)}{\langle 15 \rangle \langle 23 \rangle^3 \langle 34 \rangle^2 \langle 45 \rangle}, \quad (4.63)$$

making the contribution to the amplitude

$$\begin{aligned} \begin{array}{c} 1^- \\ 5^+ \text{---} \text{---} 2^+ \\ 4^+ \text{---} \text{---} 3^+ \end{array} &= 2 \tilde{C}_{\text{Bub},[2]}^{(1)} \left[\begin{array}{c} 1^- \\ 5^+ \text{---} \text{---} 2^+ \\ 4^+ \text{---} \text{---} 3^+ \end{array} \right] I_{2,[2]}^D \left[\begin{array}{c} 1^- \\ 5^+ \text{---} \text{---} 2^+ \\ 4^+ \text{---} \text{---} 3^+ \end{array} \right] \\ &= \frac{\langle 13 \rangle^2 [23] (\langle 13 \rangle \langle 24 \rangle - 3 \langle 12 \rangle \langle 34 \rangle)}{3 \langle 15 \rangle \langle 23 \rangle^2 \langle 34 \rangle^2 \langle 45 \rangle}. \end{aligned} \quad (4.64)$$

Evaluating on the BCFW shift kinematics, we first extract the double pole via

$$\begin{aligned} \left. \begin{array}{c} 1^- \\ 5^+ \text{---} \text{---} 2^+ \\ 4^+ \text{---} \text{---} 3^+ \end{array} \right|_{z_{23}\text{-double pole}} &= \frac{1}{\langle 23 \rangle^2} \left[\frac{\langle 13 \rangle^2 [23] (\langle 13 \rangle \langle \hat{2}4 \rangle - 3 \langle 12 \rangle \langle 34 \rangle)}{3 \langle 15 \rangle \langle 34 \rangle^2 \langle 45 \rangle} \right] \Big|_{z=z_{23}} \\ &= -\frac{2 \langle 13 \rangle^2 [23] \langle 12 \rangle}{3 \langle 15 \rangle \langle 34 \rangle \langle 45 \rangle \langle 23 \rangle^2}. \end{aligned} \quad (4.65)$$

Combining this with the double pole of the triangle cut of eq. (4.58),

$$\left. \begin{array}{c} 1^- \\ 5^+ \text{---} \text{---} 2^+ \\ 4^+ \text{---} \text{---} 3^+ \end{array} \right|_{z_{23}\text{-double pole}} + \left. \begin{array}{c} 1^- \\ 5^+ \text{---} \text{---} 2^+ \\ 4^+ \text{---} \text{---} 3^+ \end{array} \right|_{z_{23}\text{-double pole}} = \frac{\langle 13 \rangle^2 [23] \langle 12 \rangle}{3 \langle 15 \rangle \langle 34 \rangle \langle 45 \rangle \langle 23 \rangle^2}, \quad (4.66)$$

reproduces the double pole we found in eq. (4.38).

Following the procedure shown in section 4.2.1, we can extract the pole-under-pole term via

$$\begin{aligned} \left. \begin{array}{c} 1^- \\ 5^+ \text{---} \text{---} 2^+ \\ 4^+ \text{---} \text{---} 3^+ \end{array} \right|_{z_{23}\text{-PUP}} &= -\frac{1}{z_{23}} \frac{d}{dz} \left[\frac{1}{\langle 13 \rangle^2} \frac{\langle 13 \rangle^2 [23] (\langle 13 \rangle \langle \hat{2}4 \rangle - 3 \langle 12 \rangle \langle 34 \rangle)}{3 \langle 15 \rangle \langle 34 \rangle^2 \langle 45 \rangle} \right] \Big|_{z=z_{23}} \\ &= \frac{\langle 13 \rangle}{\langle 23 \rangle} \frac{d}{dz} \left[\frac{[23] (\langle 13 \rangle \langle \hat{2}4 \rangle - 3 \langle 12 \rangle \langle 34 \rangle)}{3 \langle 15 \rangle \langle 34 \rangle^2 \langle 45 \rangle} \right] \Big|_{z=z_{23}} \\ &= \frac{\langle 13 \rangle^3 [23] \langle 14 \rangle}{3 \langle 15 \rangle \langle 23 \rangle \langle 34 \rangle^2 \langle 45 \rangle}, \end{aligned} \quad (4.67)$$

which matches eq. (4.44). The factor of $1/\langle 13 \rangle^2$ inside the derivative stems from removing the $(z - z_{23})^2$ denominator, as

$$\langle \hat{2}3 \rangle = \langle 13 \rangle (z - z_{23}) \quad (4.68)$$

We can thus see that by using both BCFW recursion and generalized unitarity we can compute the one-loop amplitude $A^{(1)}(1^-2^+3^+4^+5^+)$ from a small number of cuts using only on-shell quantities. In the following we will apply this approach in computing massive-scalar amplitudes.

4.2.2 Contact Term Amplitudes

We will focus first on the rational contributions $R_{\text{contact}}^{(1)}$, as these end up being particularly simple.

Requiring the four-scalar contact term to appear forces the external scalar line to be directly attached to the scalar loop. Thus neither class of Feynman diagram generating the double pole can exist, and we expect $R_{\text{contact}}^{(1)}$ to be free of complex double poles. However, this does not mean that all single poles have to originate from a factorization into a product of tree amplitudes. To give a heuristic argument, let us consider the two classes of Feynman diagrams which led to such double poles,

(4.69)

The hatched disks are off-shell currents to which the remaining gluons are attached. Due to the required appearance of the contact term in $R_{\text{contact}}^{(1)}$, the center propagator usually providing one of the two complex poles in these diagram classes is absent. The remaining pole in the bubble diagrams shown on the right is now related to a factorization channel, and should therefore be obtainable from a factorization into a one-loop amplitude and a three-gluon tree vertex. In the case of the triangle diagrams, one of the complex poles is due to the triangle integral itself. These types of poles are still present in $R_{\text{contact}}^{(1)}$, and are non-factorizable. However, due to their connection to the triangle integral, we will be able to obtain these poles from the associated triangle cut.

For the computations we choose to shift one of the massive scalar momenta and an adjacent gluon. We are able to numerically verify our results using the *Mathematica* one-loop generalized unitarity implementation discussed in section 2.5. We are also able to carry out the unitarity computation semi-analytically on the shifted kinematics, keeping the full z -dependence. By considering the large- z behavior this allows us to verify apriori the validity of our choice of shift.

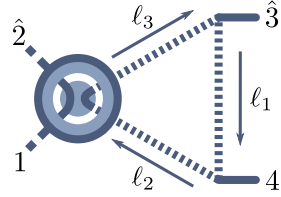
For one-loop amplitudes of two massive scalars and two gluons, there exist six rational parts of amplitudes,

$$\begin{aligned}
 & R_{4:1}^{(1)}(1^\varphi 2^\varphi 3^+ 4^+), \quad R_{4:3}^{(1)}(1^\varphi 2^\varphi; 3^+ 4^+), \quad R_{4:2}^{(1)}(1^\varphi 2^+ 3^+; 4^\varphi), \quad R_{4:3}^{(1)}(1^\varphi 2^+; 3^\varphi 4^+), \\
 & R_{4:1}^{(1)}(1^\varphi 2^+ 3^\varphi 4^+), \quad R_{4:2}^{(1)}(1^\varphi 2^\varphi 3^+; 4^+).
 \end{aligned}
 \tag{4.70}$$

The four amplitudes in the top row we already encountered in the four-gluon example computation. For the amplitudes in the bottom row there exist no unitarity cuts, consequently they have to be zero. Focusing on $R_{\text{contact}}^{(1)}(1^\varphi 2^\varphi 3^+ 4^+)$, we use a massive BCFW shift of the form

$$\begin{aligned} p_2 \rightarrow \hat{p}_2 &= p_2 - \frac{z}{2} [3|\gamma|2^\flat], & p_3 \rightarrow \hat{p}_3 &= p_3 + \frac{z}{2} [3|\gamma|2^\flat], \\ \lambda_3 \rightarrow \lambda_3 &= \lambda_3 + z\lambda_2^\flat, & \tilde{\lambda}_3 \rightarrow \hat{\lambda}_3 &= \tilde{\lambda}_3. \end{aligned} \quad (4.71)$$

Under this shift, there are no standard factorization channels. Nonetheless, we can check numerically via unitarity that this amplitude is non-zero. The reason for this discrepancy is the non-factorizable z_{34} pole, which in this particular case makes up the entire amplitude. We can compute this pole from the cut



(4.72)

With the triangle loop momentum parametrization

$$\ell_1^\mu = \frac{1}{2} \left(t \langle 4|\gamma^\mu|3 \rangle - \frac{\mu^2}{s_{34}t} \langle \hat{3}|\gamma^\mu|4 \rangle \right), \quad \ell_1^{*\mu} = \frac{1}{2} \left(t \langle \hat{3}|\gamma^\mu|4 \rangle - \frac{\mu^2}{s_{34}t} \langle 4|\gamma^\mu|3 \rangle \right), \quad (4.73)$$

we determine the cut coefficient to be

$$\begin{aligned} C_{\text{Tri},[2]}^{(1)} \left[\text{Diagram} \right] &= \frac{1}{2} \sum_{\ell, \ell^*} \text{Inf} \left[A_{\text{contact}}^{(0)}(1^\varphi \hat{2}^\varphi \ell_3^{\varphi'} (-\ell_2^{\varphi'})) \right. \\ &\quad \times A^{(0)}((- \ell_2)^{\varphi'} \hat{3}^+ \ell_1^{\varphi'}) A^{(0)}((- \ell_1)^{\varphi'} 4^+ \ell_3^{\varphi'}) \Big]_{t^0, \mu^2} \\ &= \frac{1}{4} \sum_{\ell, \ell^*} \frac{[34]}{\langle \hat{3}4 \rangle} = \frac{1}{2} \frac{[34]}{\langle \hat{3}4 \rangle}. \end{aligned} \quad (4.74)$$

We again used,

$$A^{(0)}((- \ell_2)^{\varphi'} \hat{3}^+ \ell_1^{\varphi'}) A^{(0)}((- \ell_1)^{\varphi'} 4^+ \ell_3^{\varphi'}) = -\mu^2 \frac{[34]}{\langle \hat{3}4 \rangle}. \quad (4.75)$$

Including the triangle integral $I_3^{(1)}[\mu^2]$ we obtain for the cut,

$$\text{Diagram} = 2I_3^{(1)}[\mu^2] C_{\text{Tri},[2]}^{(1)} \left[\text{Diagram} \right] = -\frac{1}{2} \frac{[34]}{\langle \hat{3}4 \rangle}. \quad (4.76)$$

Following the four-gluon example computations, we also include a factor of two. The step of extracting the z_{34} residue is trivial in this case. The non-factorizable pole-term that we need to add to the $[2^\flat, 3]$ -shift construction of $R_{\text{contact}}^{(1)}(1^\varphi 2^\varphi 3^+ 4^+)$ is,

$$R_{\text{contact}}^{(1), \text{non-fact } z_{34}}(1^\varphi 2^\varphi 3^+ 4^+) = \frac{1}{-z_{34}} \text{Res}_{z=z_{34}} \left[\text{Diagram} \right]. \quad (4.77)$$

Instead of explicitly calculating the residue, it is in practice slightly simpler to determine the entire

right-hand side of eq. (4.77) at once via,

$$\frac{1}{-z_{34}} \operatorname{Res}_{z=z_{34}} \left[\text{Diagram} \right] = \frac{1}{\langle 34 \rangle} \left[\langle \hat{3}4 \rangle \times \text{Diagram} \right] \Big|_{z=z_{34}} = -\frac{1}{2} \frac{[34]}{\langle 34 \rangle}. \quad (4.78)$$

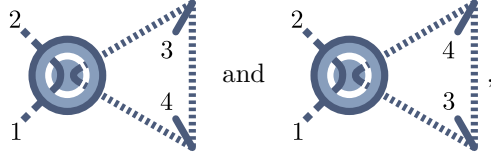
As there are no factorizable poles, we therefore have

$$R_{\text{contact}}^{(1)}(1^\varphi 2^\varphi 3^+ 4^+) = R_{\text{contact}}^{(1), \text{non-fact } z_{34}}(1^\varphi 2^\varphi 3^+ 4^+) = -\frac{1}{2} \frac{[34]}{\langle 34 \rangle}. \quad (4.79)$$

We can apply the same construction to the remaining non-vanishing amplitudes shown in eq. (4.70),

$$\begin{aligned} R_{4:3, \text{contact}}^{(1)}(1^\varphi 2^\varphi; 3^+ 4^+) &= -\frac{[34]}{\langle 34 \rangle}, \\ R_{4:2, \text{contact}}^{(1)}(1^\varphi; 2^\varphi 3^+ 4^+) &= \frac{[34]}{\langle 34 \rangle}, \\ R_{4:3, \text{contact}}^{(1)}(1^\varphi 2^+; 3^\varphi 4^+) &= -2 \frac{[24]}{\langle 24 \rangle}. \end{aligned} \quad (4.80)$$

In the case of $R_{\text{contact}}^{(1)}(1^\varphi 2^\varphi; 3^+ 4^+)$ there exists no adjacent scalar-gluon pair to shift. However we can verify via unitarity that shifting any scalar-gluon pair causes the amplitude to scale as $\frac{1}{z}$ in the large- z limit. We can therefore apply the approach above to all rational parts of eq. (4.70). For each of these we need to compute two triangle cuts. For example, in $R_{4:3, \text{contact}}^{(1)}(1^\varphi 2^\varphi; 3^+ 4^+)$, both the cuts,



$$\quad \text{and} \quad (4.81)$$

belong to triangle integrals that contain non-factorizing poles. We also find that the forms of $R_{4:3, \text{contact}}^{(1)}(1^\varphi 2^\varphi; 3^+ 4^+)$ already matches that of $R_{4:3}^{(1)}(1^\varphi 2^\varphi; 3^+ 4^+)$ found in eq. (4.9). The corresponding gluon amplitude is therefore expected to vanish.

Furthermore we can attempt to find a BCFW construction for the non-factorizing contributions of $R_{\text{contact}}^{(1)}(1^\varphi 2^\varphi 3^+ 4^+)$ based on soft factors. As the contact-term amplitudes do not possess complex double poles we neglect the term that explicitly generates them. We could expect the non-factorizing pole to originate from,

$$-A^{(0)}(1^\varphi \hat{2}^\varphi \hat{K}^-) \frac{1}{s_{34}} V^{(1)}((- \hat{K})^+ \hat{3}^+ 4^+) \times \mathcal{S}_{\text{contact}}(1^\varphi \hat{2}^\varphi \hat{3}^+ 4^+ | K) \times \text{Soft}^{(0)}(4_g (- \hat{K})^- \hat{3}_g) \quad (4.82)$$

where $\mathcal{S}_{\text{contact}}(1^\varphi \hat{2}^\varphi \hat{3}^+ 4^+ | K)$ is the equivalent of the soft function $\text{Soft}^{(0)}(* K^+ *)$ in eq. (4.45). Indeed, we find the concise form

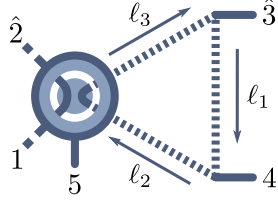
$$\mathcal{S}_{\text{contact}}(1^\varphi \hat{2}^\varphi \hat{3}^+ 4^+ | \hat{K}^-) = -\frac{3}{2} \frac{[\hat{K} q]}{\langle \hat{K} | 1 | q \rangle}. \quad (4.83)$$

Moving on to a slightly more complicated example, we compute $R_{\text{contact}}^{(1)}(1^\varphi 2^\varphi 3^+ 4^+ 5^+)$. We

again use a $[2^b, 3]$ -shift. There now exists a factorizable contribution, which we determine as follows

$$\begin{aligned}
 R_{\text{contact}}^{(1), \text{fact}}(1^\varphi 2^\varphi 3^+ 4^+ 5^+) &= -R_{\text{contact}}^{(1)}(1^\varphi \hat{2}^\varphi \hat{K}^+ 5^+) \frac{1}{s_{34}} A^{(0)}((- \hat{K})^- \hat{3}^+ 4^+) \\
 &= \frac{1}{2} \frac{[\hat{K}5]}{\langle \hat{K}5 \rangle} \frac{1}{s_{34}} \frac{[34]^3}{[4\hat{K}][\hat{K}3]} \\
 &= -\frac{1}{2} \left[\frac{[35]}{\langle 34 \rangle \langle 45 \rangle} + \frac{[3|24|5]}{\langle 34 \rangle \langle 45 \rangle s_{23}} \right].
 \end{aligned} \tag{4.84}$$

To obtain the non-factorizable pole we compute the unitarity cut,


(4.85)

After determining the coefficient,

$$\begin{aligned}
 C_{\text{Tri}, [2]}^{(1)} \left[\begin{array}{c} \text{Diagram} \\ \text{with lines } 1, 2, 3, 4, 5 \end{array} \right] &= \frac{1}{2} \sum_{\ell, \ell^*} \text{Inf}_{\mu^2, t} \left[A_{\text{contact}}^{(0)}(1^\varphi \hat{2}^\varphi \ell_3^{\varphi'} (-\ell_2^{\varphi'})) \right. \\
 &\quad \times A^{(0)}((- \ell_2)^{\varphi'} \hat{3}^+ \ell_1^{\varphi'}) A^{(0)}((- \ell_1)^{\varphi'} 4^+ \ell_2^{\varphi'}) \left. \right]_{t^0, \mu^2} \\
 &= + \frac{1}{2} \sum_{\ell, \ell^*} \text{Inf} \left[\mu^2 \frac{[34]}{\langle \hat{3}4 \rangle} \frac{[5](-\ell_2)1[5]}{2s_{15}s(-\ell_2)5} \right]_{t^0, \mu^2} \\
 &= + \frac{1}{4} \frac{[34]}{\langle \hat{3}4 \rangle s_{15}} \left(\frac{[53] \langle 4|1|5 \rangle}{\langle 4|5|3 \rangle} + \frac{[54] \langle \hat{3}|1|5 \rangle}{\langle \hat{3}|5|4 \rangle} \right) \\
 &= + \frac{1}{\langle \hat{3}4 \rangle} \frac{1}{4s_{15}} \left(\frac{[3|41|5]}{\langle 45 \rangle} - \frac{[4|\hat{3}1|5]}{\langle \hat{3}5 \rangle} \right),
 \end{aligned} \tag{4.86}$$

and including the triangle integral and factor of 2,

$$\begin{array}{c} \text{Diagram} \\ \text{with lines } 1, 2, 3, 4, 5 \end{array} = 2I_3^{(1)}[\mu^2] C_{\text{Tri}, [2]}^{(1)} \left[\begin{array}{c} \text{Diagram} \\ \text{with lines } 1, 2, 3, 4, 5 \end{array} \right] = -\frac{1}{\langle \hat{3}4 \rangle} \frac{1}{4s_{15}} \left(\frac{[3|41|5]}{\langle 45 \rangle} - \frac{[4|\hat{3}1|5]}{\langle \hat{3}5 \rangle} \right), \tag{4.87}$$

the non-factorizable pole contribution evaluates to,

$$\begin{aligned}
 R_{\text{contact}}^{(1), \text{non-fact}} z_{34}(1^\varphi 2^\varphi 3^+ 4^+ 5^+) &= \frac{1}{-z_{34}} \text{Res}_{z=z_{34}} \left[\begin{array}{c} \text{Diagram} \\ \text{with lines } 1, 2, 3, 4, 5 \end{array} \right] = \frac{1}{\langle 34 \rangle} \left[\langle \hat{3}4 \rangle \times \begin{array}{c} \text{Diagram} \\ \text{with lines } 1, 2, 3, 4, 5 \end{array} \right]_{z=z_{34}=-\frac{\langle 34 \rangle}{\langle 2^b 4 \rangle}} \\
 &= -\frac{1}{4s_{15} \langle 34 \rangle} \left(\frac{[3|41|5]}{\langle 45 \rangle} - \frac{[4|31|5] - s_{34} \frac{[3|21|5]}{[3|2|4]}}{\langle 35 \rangle - \langle 34 \rangle \frac{[3|2|5]}{[3|2|4]}} \right) \\
 &= -\frac{1}{4s_{15} \langle 34 \rangle} \left(\frac{[3|41|5]}{\langle 45 \rangle} - \frac{[4|31|5] [3|2|4] - s_{34} [3|21|5]}{s_{23} \langle 45 \rangle} \right) \\
 &= -\frac{[3|41|5]}{2s_{15} \langle 34 \rangle \langle 45 \rangle}.
 \end{aligned} \tag{4.88}$$

We therefore get for the full rational part

$$R_{\text{contact}}^{(1)}(1^\varphi 2^\varphi 3^+ 4^+ 5^+) = -\frac{1}{2} \left[\frac{[35]}{\langle 34 \rangle \langle 45 \rangle} + \frac{[3|24|5]}{\langle 34 \rangle \langle 45 \rangle s_{23}} + \frac{[3|41|5]}{\langle 34 \rangle \langle 45 \rangle s_{15}} \right]. \quad (4.89)$$

We have verified this expression against a numerical unitarity computation.

As in the case of $R_{\text{contact}}^{(1)}(1^\varphi 2^\varphi 3^+ 4^+)$, we can attempt to find a BCFW construction, where the non-factorizable terms are obtained from a product of soft factors. We find,

$$\begin{aligned} R_{5:1,\text{contact}}^{(1)}(1^\varphi 2^\varphi 3^+ 4^+ 5^+) &= -R_{4:1,\text{contact}}^{(1)}(1^\varphi \hat{2}^\varphi \hat{K}^+ 5^+) \frac{1}{s_{34}} A^{(0)}((- \hat{K})^- \hat{3}^+ 4^+) \\ &\quad - A^{(0)}(1^\varphi \hat{2}^\varphi \hat{K}^- 5^+) \frac{1}{s_{34}} V^{(1)}((- \hat{K})^+ \hat{3}^+ 4^+) \\ &\quad \times \mathcal{S}_{\text{contact}}(1^\varphi \hat{2}^\varphi \hat{3}^+ 4^+ 5^+ | K) \text{Soft}^{(0)}(4, (- \hat{K})^-, \hat{3}), \end{aligned} \quad (4.90)$$

where the would-be soft function closely resembles the one found for $R_{\text{contact}}^{(1)}(1^\varphi 2^\varphi 3^+ 4^+)$,

$$\mathcal{S}_{\text{contact}}(1^\varphi \hat{2}^\varphi \hat{3}^+ 4^+ 5^+ | \hat{K}) = -\frac{3}{2} \frac{[\hat{K}5]}{\langle \hat{K} | 1 | 5 \rangle}. \quad (4.91)$$

Interestingly, in the limit of vanishing scalar mass, this turns into a proper soft factor, as

$$-\frac{[\hat{K}5]}{\langle \hat{K} | 1 | 5 \rangle} = -\frac{\langle \hat{2} | \hat{K} | 5 \rangle}{[15]} \frac{1}{\langle \hat{K} 1 \rangle \langle \hat{2} \hat{K} \rangle} = \frac{\langle \hat{2} 1 \rangle}{\langle \hat{K} \hat{2} \rangle \langle 1 \hat{K} \rangle} = \text{Soft}^{(0)}(\hat{2}_\varphi \hat{K}^+ 1_g) \Big|_{m \rightarrow 0}. \quad (4.92)$$

Repeating this computation for $R_{5:2,\text{contact}}^{(1)}(1^\varphi 2^+ 3^+ 4^+; 5^\varphi)$ we find

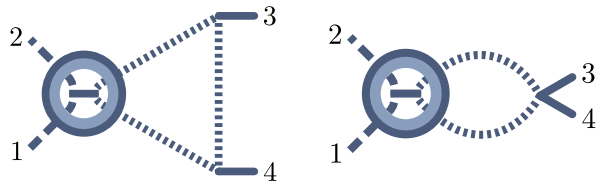
$$R_{5:2,\text{contact}}^{(1)}(1^\varphi 2^+ 3^+ 4^+; 5^\varphi) = \frac{[24]}{\langle 23 \rangle \langle 34 \rangle} + \frac{[2|53|4]}{s_{25} \langle 23 \rangle \langle 34 \rangle} + \frac{[2|35|4]}{s_{45} \langle 23 \rangle \langle 34 \rangle}. \quad (4.93)$$

The similarity with the expression of eq. (4.89) can be understood from the form of the four-scalar contact-term tree-amplitudes given in eq. (3.76): these amplitudes can be expressed in terms of a universal kinematic factor together with the relevant four-scalar contact-term. The amplitudes $R_{\text{contact}}^{(1)}(1^\varphi 2^+ 3^+ 4^+; 5^\varphi)$ and $R_{\text{contact}}^{(1)}(1^\varphi 2^\varphi 3^+ 4^+ 5^+)$ thus differ only in the choice of contact term and relabeling of momenta.

At the time of writing we have not determined the remaining three gluon $R_{\text{contact}}^{(1)}$ amplitudes.

4.2.3 One-Loop Gluon-Exchange Amplitudes

Next we consider amplitudes with a gluon exchange between the external scalar line and the internal scalar line of the loop. These are more complicated to compute due to the appearance of double poles, which will generally require determining a bubble coefficient as well. For $R_{\text{gluon}}^{(1)}(1^\varphi 2^\varphi 3^+ 4^+)$ we require the cuts,



$$(4.94)$$

As the procedure is the same as the one shown in section 4.2.1, we will not show the computation explicitly here, and only present the result. Casting the pole-under-pole term into the form of a product of soft factors, we find the BCFW construction,

$$R_{4:1}^{(1)}(1^\varphi 2^\varphi 3^+ 4^+) = -A^{(0)}(1^\varphi \hat{2}^\varphi \hat{K}^-) \frac{1}{s_{34}^2} V^{(1)}(-\hat{K}^+ \hat{3}^+ 4^+) \times \left(1 + s_{34} \text{Soft}^{(0)}(4_g (-K)^- \hat{3}_g) \mathcal{S}_{\text{gluon}}(1^\varphi \hat{2}^\varphi \hat{3}^+ 4^+ | \hat{K})\right), \quad (4.95)$$

where

$$\mathcal{S}_{\text{gluon}}(1^\varphi \hat{2}^\varphi \hat{3}^+ 4^+ | \hat{K}) = -\frac{[\hat{K}q]}{2 \langle \hat{K} | 1 | q \rangle}. \quad (4.96)$$

After evaluation we find the compact form,

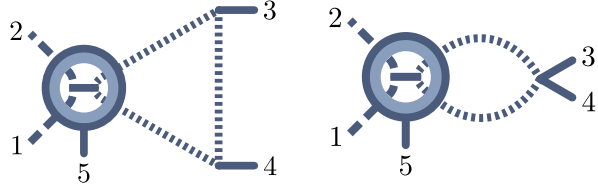
$$R_{\text{gluon}}^{(1)}(1^\varphi 2^\varphi 3^+ 4^+) = \frac{1}{6} \frac{s_{23} - s_{13}}{\langle 34 \rangle^2}. \quad (4.97)$$

From unitarity we find numerically that,

$$R_{4:3, \text{gluon}}^{(1)}(1^\varphi 2^\varphi; 3^+ 4^+) = 0, \quad (4.98)$$

as expected.

For the pole-under-pole terms of $R_{5:1, \text{gluon}}^{(1)}(1^\varphi 2^\varphi 3^+ 4^+ 5^+)$ we compute the cuts,



$$(4.99)$$

From these we find the BCFW construction,

$$\begin{aligned} R_{5:1, \text{gluon}}^{(1)}(1^\varphi 2^\varphi 3^+ 4^+ 5^+) = & -R_{4:1, \text{gluon}}^{(1)}(1^\varphi \hat{2}^\varphi \hat{K}^+ 5^+) \frac{1}{s_{34}} A^{(0)}((-\hat{K})^- \hat{3}^+ 4^+) \\ & - A^{(0)}(1^\varphi \hat{2}^\varphi \hat{K}^+) \frac{1}{s_{12}} A^{(1)}(-\hat{K}^- \hat{3}^+ 4^+ 5^+) \\ & - A^{(0)}(1^\varphi \hat{2}^\varphi \hat{K}^-) \frac{1}{s_{12}} A^{(1)}(-\hat{K}^+ \hat{3}^+ 4^+ 5^+) \\ & - A^{(0)}(1^\varphi \hat{2}^\varphi \hat{K}^- 5^+) \frac{1}{s_{34}} V^{(1)}((-\hat{K})^+ \hat{3}^+ 4^+) \\ & \times \mathcal{S}_{\text{contact}}(1^\varphi \hat{2}^\varphi \hat{3}^+ 4^+ 5^+ | K) \text{Soft}^{(0)}(4, (-\hat{K})^-, \hat{3}), \end{aligned} \quad (4.100)$$

where,

$$\begin{aligned} \mathcal{S}_{\text{gluon}}(1^\varphi \hat{2}^\varphi \hat{3}^+ 4^+ 5^+ | \hat{K}) = & \text{Soft}^{(0)}(\hat{2}_\varphi \hat{K}^+ 5_g) + \frac{1}{2} \frac{[\hat{K}5]}{\langle \hat{K} | 1 | 5 \rangle} \\ & + m^2 \left[\frac{[\hat{K}5]}{\langle \hat{K} | 1 | 5 \rangle s_{15}} + \frac{s_{15} [35]^2 [45]}{\langle \hat{K} | 1 | 5 \rangle^2 \langle \hat{K} | 2 | 3 \rangle [34] [\hat{K}5]} \right]. \end{aligned} \quad (4.101)$$

4.2.4 Combining $R_{\text{contact}}^{(1)}$ and $R_{\text{gluon}}^{(1)}$ Amplitudes

Just as in the one-loop squared computations, we will require the sum of both $R_{\text{contact}}^{(1)}$ and $R_{\text{gluon}}^{(1)}$ to derive the two-loop rational parts $R^{(2)}$.

In the case of the leading color $R_{4:1}^{(1)}$, we combine the results of eqs.(4.79) and (4.97),

$$R_{4:1}^{(1)}(1^\varphi 2^\varphi 3^+ 4^+) = R_{4:1,\text{contact}}^{(1)}(1^\varphi 2^\varphi 3^+ 4^+) + R_{4:1,\text{gluon}}^{(1)}(1^\varphi 2^\varphi 3^+ 4^+) = -\frac{1}{3} \frac{s_{13} - s_{34}}{\langle 34 \rangle^2}, \quad (4.102)$$

which agrees with the result we previously found from unitarity cuts in eq. (4.3).

In general we expect the leading-color scalar rational part $R_{n:1}^{(1)}$ to be constructed via

$$\begin{aligned} R_{n:1}^{(1)}(1^\varphi 2^\varphi 3^+ \dots n^+) &= -R_{n-1:1}^{(1)}(1^\varphi \hat{2}^\varphi \hat{K}^+ 5^+ \dots n^+) \frac{1}{s_{34}} A^{(0)}(-\hat{K}^- \hat{3}^+ 4^+) \\ &\quad - \sum_{i=5}^n \sum_{h=\pm} A^{(0)}(1^\varphi \hat{2}^\varphi \hat{K}^h (i+1)^+ \dots n^+) \frac{1}{s_{3\dots i}} A^{(1)}(-\hat{K}^{\bar{h}} \hat{3}^+ 4^+ \dots i^+) \\ &\quad - A^{(0)}(1^\varphi \hat{2}^\varphi \hat{K}^- 5^+ \dots n^+) \frac{1}{s_{34}^2} V^{(1)}(-\hat{K}^+ \hat{3}^+ 4^+) \\ &\quad - A^{(0)}(1^\varphi \hat{2}^\varphi \hat{K}^- 5^+ \dots n^+) \frac{1}{s_{34}^2} V^{(1)}(-\hat{K}^+ \hat{3}^+ 4^+) \\ &\quad \times \text{Soft}^{(0)}(4_g (-K)^{-\hat{3}_g} \mathcal{S}(1^\varphi \hat{2}^\varphi \hat{3}^+ \dots n^+ | \hat{K})), \end{aligned} \quad (4.103)$$

where \mathcal{S} needs to be determined. In the case of massless external scalars we are able to find through experimentation that both for five and six gluons \mathcal{S} is just the sum of two soft factors

$$\begin{aligned} \mathcal{S}_{\text{massless}}(1^\varphi \hat{2}^\varphi \hat{3}^+ 4^+ 5^+ | \hat{K}) &= \left[\text{Soft}^{(0)}(\hat{2}_\varphi \hat{K}^+ 5_g) + \text{Soft}^{(0)}(\hat{2}_\varphi \hat{K}^+ 1_\varphi) \right] \Big|_{m \rightarrow 0}, \\ \mathcal{S}_{\text{massless}}(1^\varphi \hat{2}^\varphi \hat{3}^+ 4^+ 5^+ 6^+ | \hat{K}) &= \left[\text{Soft}^{(0)}(\hat{2}_\varphi \hat{K}^+ 5_g) + \text{Soft}^{(0)}(\hat{2}_\varphi \hat{K}^+ 1_\varphi) \right] \Big|_{m \rightarrow 0}. \end{aligned} \quad (4.104)$$

$\text{Soft}^{(0)}(*_\varphi \hat{K}^+ *_g)$ and $\text{Soft}^{(0)}(*_\varphi \hat{K}^+ *_\varphi)$ are respectively the soft factors for \hat{K} adjacent to a massive and a massless particle, or two massive particles. We derive the form of these soft function in appendix A.3. In the massless limit they both reduce to the function $\text{Soft}^{(0)}(*_g \hat{K}^+ *_g)$. We verified this form of the pole-under-pole terms by numerically comparing the resulting amplitudes against a unitarity computation.

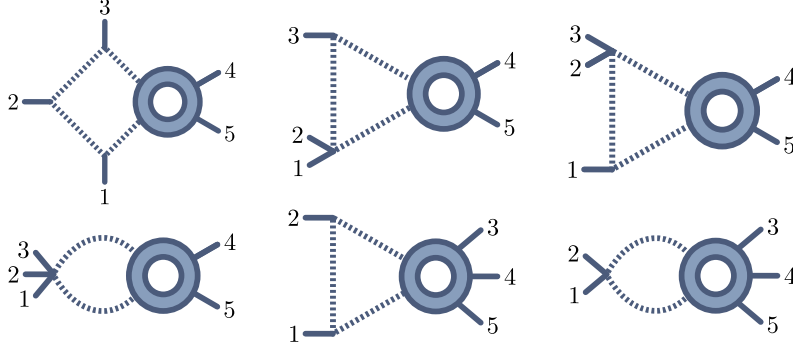
In the leading color three gluon case with massive scalars, we combine the expressions of eqs. (4.91) and (4.101) to find,

$$\mathcal{S}(1^\varphi \hat{2}^\varphi \hat{3}^+ 4^+ 5^+ | \hat{K}) = \text{Soft}^{(0)}(\hat{2}_\varphi \hat{K}^+ 5_g) - \frac{[\hat{K}5]}{\langle \hat{K} | 1 | 5 \rangle} + m^2 \left[\frac{[\hat{K}5]}{\langle \hat{K} | 1 | 5 \rangle s_{15}} + \frac{s_{15} [35]^2 [45]}{\langle \hat{K} | 1 | 5 \rangle^2 \langle \hat{K} | 2 | 3 \rangle [34] [\hat{K}5]} \right]. \quad (4.105)$$

While we can check numerically that,

$$\mathcal{S}(1^\varphi \hat{2}^\varphi \hat{3}^+ 4^+ 5^+ | \hat{K}) \neq \text{Soft}^{(0)}(\hat{2}_\varphi \hat{K}^+ 5_g) + \text{Soft}^{(0)}(\hat{2}_\varphi \hat{K}^+ 1_\varphi), \quad (4.106)$$

we can use the relation of eq. (4.92) to see that for vanishing m we do reproduce this sum of soft

Figure 4.1: Cuts required for the one-loop construction of $R_{5:1}^{(2)}$.

factors. Evaluating eq. (4.103) for $R_{5:1}^{(1)}$ leads to,

$$\begin{aligned}
 R_{5:1}^{(1)}(1^\varphi 2^\varphi 3^+ 4^+ 5^+) &= \frac{1}{3} \left[- \frac{m^2 \langle 35 \rangle [3|12|3] [35]^3}{s_{12} \langle 45 \rangle [3|2(3+4)|5] (s_{12} \langle 4|2|3] - \langle 34 \rangle [3|12|3])} \right. \\
 &+ \frac{m^2 \langle 5|2|3] [35]^3}{\langle 45 \rangle [3|2(3+4)|5] (s_{12} \langle 4|2|3] - \langle 34 \rangle [3|12|3])} - \frac{m^2 \langle 4|1|5] [3|2(3+4)|5] [34]}{s_{15}^2 \langle 34 \rangle \langle 45 \rangle [3|(1+2)1|5]} \\
 &- \frac{m^2 [3|42|3] [35]^2 [45]}{\langle 34 \rangle \langle 45 \rangle [3|(1+2)1|5] [3|2(3+4)|5] [34]} + \frac{2s_{12} [34] [3|42|3]}{s_{23} \langle 34 \rangle \langle 5|4|3]^2} \\
 &- \frac{[3|21|3] [3|2(3+4)|5] [34]}{s_{12} \langle 5|4|3] (s_{12} \langle 4|2|3] - \langle 34 \rangle [3|12|3])} - \frac{s_{23} \langle 4|1|5]^2 [34]}{s_{15} \langle 34 \rangle^2 \langle 45 \rangle [3|(1+2)1|5]} + \frac{s_{15} [34] [3|42|3]}{s_{23} \langle 34 \rangle \langle 5|4|3]^2} \\
 &+ \frac{\langle 4|1|5]^2 \langle 5|1(3+4)2|3] [34]^2}{s_{15}^2 \langle 34 \rangle \langle 45 \rangle \langle 5|4|3] [3|(1+2)1|5]} + \frac{\langle 4|1|5] [3|2(3+4)|5] [34]}{s_{15} \langle 34 \rangle \langle 45 \rangle [3|(1+2)1|5]} - \frac{2 [3|12|3] [34]^2}{s_{23} \langle 5|4|3]^2} \Big].
 \end{aligned} \tag{4.107}$$

We were also able to derive an expression for $\mathcal{S}(1^\varphi \hat{2}^\varphi \hat{3}^+ 4^+ 5^+ 6^+ | \hat{K})$ in the massive case, which currently only exists in an unsimplified form, and is not present here.

4.3 One Loop Construction of $R^{(2)}(1^+2^+3^+4^+5^+)$

In section 4.1 we saw that the rational contributions to the four-gluon all-plus partial amplitudes are derivable from a one-loop unitarity computation. While it seems plausible that this construction generalizes to amplitudes with additional gluons, it warrants further verification. As the one-loop squared construction holds at least up to seven gluons, an initial cross-check involves comparing the sets of one-loop squared cuts with those obtained from expanding the loop vertex in the one-loop construction. We have verified by hand that this is indeed the case for $R_{5:1}^{(2)}$. As we have derived a closed-form expression for the three-gluon two-scalar amplitude $R^{(1)}(1^\varphi 2^\varphi 3^+ 4^+ 5^+)$, we can also verify the one-loop construction of $R_{5:1}^{(2)}$ explicitly. Such a unitarity construction consists of six cuts, shown in Figure 4.1, only two of which require the three-gluon one-loop amplitude. Numerically evaluating these cuts in the manner of the four-gluon computations, we indeed recover the value expected from the known analytic form. In particular, we need to include the symmetry of $\frac{1}{2}$ to obtain the correct result.

Moving on to non-planar partial amplitudes, or additional gluons, the number of cuts grows

rapidly. We have not carried out a systematic comparison of cuts between the one-loop squared and effective one-loop approaches for additional partial amplitudes, though we fully expect the two to agree.

Chapter 5

BCJ-Like Relations for Two-Loop All-Plus Amplitudes

In this last chapter we briefly discuss new relations between the two-loop partial amplitudes of the all-plus configuration. We focus mainly on amplitudes of five gluons, for which ref. [135] provides a universal set of relations. These relations are solely based on the gauge-group structure, and therefore have to hold for any two-loop amplitudes in gauge theories. An example of such relations are the U(1) decoupling identities we encountered in chapter 1.

A further class of relations between gauge-theory amplitudes that we will touch on are the BCJ relations, first presented in ref. [141] and later proven in refs. [142–146]. At tree level, these relate color ordered amplitudes multiplied by Mandelstam invariants. For example, for five gluons the BCJ relations provide the two identities [141],

$$\begin{aligned}(s_{12} + s_{45})A^{(0)}(12345) &= s_{24}A^{(0)}(12435) - s_{14}A^{(0)}(12354) \\ s_{34}s_{15}A^{(0)}(12345) &= -s_{24}s_{13}A^{(0)}(12453) - s_{14}(s_{13} + s_{35})A^{(0)}(12354)\end{aligned}\tag{5.1}$$

For loop amplitudes, the BCJ relations usually do not directly link partial amplitudes. Rather they manifest themselves as relations between loop integrands.

We present relations between the two-loop all-plus partial amplitudes of five gluons, which were found numerically. We find four additional linear relations beyond what is expected from group theory, which can be expressed in terms of the partial amplitudes $R_{5,3}^{(2)}$. Furthermore, we encounter additional relations which involve one or two powers of Mandelstams. This type of structure is well known from BCJ relations. However, in our case the relations do not apply to the integrand but to the rational part of the integrated partial amplitudes.

5.1 Linear Relations

The colour decomposition of a five-gluon two-loop amplitude $\mathcal{A}_5^{(2)}$ with gauge group $SU(N_c)$ takes the form,

$$\begin{aligned} \mathcal{A}_5^{(2)} = g^3 & \left[N_c^2 \sum_{S_5/C_5} \text{Tr}(T^{a_1} T^{a_2} T^{a_3} T^{a_4} T^{a_5}) A_{5:1}^{(2)}(a_1, a_2, a_3, a_4, a_5) \right. \\ & + N_c \sum_{S_5/C_2 \times C_3} \text{Tr}(T^{a_1} T^{a_2}) \text{Tr}(T^{a_3} T^{a_4} T^{a_5}) A_{5:3}^{(2)}(a_1, a_2; a_3, a_4, a_5) \\ & \left. + \sum_{S_5/C_5} \text{Tr}(T^{a_1} T^{a_2} T^{a_3} T^{a_4} T^{a_5}) A_{5:1B}^{(2)}(a_1, a_2, a_3, a_4, a_5) \right]. \end{aligned} \quad (5.2)$$

In the case of all-plus amplitudes, the cyclic symmetry of each of the traces reduces the number of independent $A_{5:1}$ and $A_{5:1B}^{(2)}$ amplitudes to $|S_5/C_5| = \frac{5!}{5} = 24$, while for the amplitudes $A_{5:3}^{(2)}$ there exist $|S_5/(C_2 \times C_3)| = \frac{5!}{2 \times 3} = 20$.

The single trace amplitudes are antisymmetric under reversal, thereby reducing the number of each from 24 to 12. For five gluons, ref. [135] showed that the subleading single trace amplitudes $A_{5:1B}^{(2)}$ are entirely determined in terms of the $A_{5:1}^{(2)}$ and $A_{5:3}^{(2)}$, via the,

$$\begin{aligned} A_{5:1B}^{(2)}(1, 2, 3, 4, 5) = & - \left[-A_{5:1}^{(2)}(1, 2, 4, 3, 5) + 2A_{5:1}^{(2)}(1, 2, 5, 3, 4) + A_{5:1}^{(2)}(1, 2, 5, 4, 3) \right. \\ & - A_{5:1}^{(2)}(1, 3, 2, 4, 5) + 2A_{5:1}^{(2)}(1, 3, 4, 2, 5) - 5A_{5:1}^{(2)}(1, 3, 5, 2, 4) \\ & - 2A_{5:1}^{(2)}(1, 3, 5, 4, 2) + 2A_{5:1}^{(2)}(1, 4, 2, 3, 5) + A_{5:1}^{(2)}(1, 4, 3, 2, 5) \\ & + 2A_{5:1}^{(2)}(1, 4, 5, 2, 3) + A_{5:1}^{(2)}(1, 4, 5, 3, 2) \\ & \left. - \frac{1}{2} \sum_{Z_5} \left(A_{5:3}^{(2)}(1, 2; 3, 4, 5) - A_{5:3}^{(2)}(1, 3; 2, 4, 5) \right) \right]. \end{aligned} \quad (5.3)$$

and permutations thereof.

While the $A_{5:1B}^{(2)}$ are completely determined by the $A_{5:1}^{(2)}$ and $A_{5:3}^{(2)}$, they themselves are related by more identities than those expected from $U(1)$ decoupling. After picking a 12 element basis of $A_{5:1B}^{(2)}$, constructed by removing cyclic and reversal symmetry, there are 6 additional linear relations. These have been previously discovered as part of L -loop identities of five-point amplitudes [135], or Kleiss–Kuijff style relations [147]. The latter appear to continue trivially at seven, and non-trivially at eight points, and may be interesting to look at, considering that there now exists a conjecture for the n -point form of $A_{n:1B}^{(2)}$ [18]. In the five-point case the Kleiss–Kuijff-like relations described by ref. [147] can be written as

$$A_{5:1B}^{(2)}(1, \{\alpha\}, 5, \{\beta\}) = (-1)^{|\beta|} \sum_{\sigma \in \text{OP}(\{\alpha\} \cup \{\beta^T\})} A_{5:1B}^{(2)}(1, \sigma(2, 3, 4), 5). \quad (5.4)$$

Taking into account cyclic- and reversal symmetry, this expression describes six unique identities, as expected. Note that these are expressly included in the twelve two-loop relations of ref. [135].

Let us now consider the amplitudes $A_{5:3}^{(2)}$. These are related by five $U(1)$ decoupling identities [4]

$$0 = A_{5:3}^{(2)}(2, 3; 1, 4, 5) + A_{5:3}^{(2)}(2, 3; 1, 5, 4) + A_{5:3}^{(2)}(4, 5; 1, 2, 3) + A_{5:3}^{(2)}(4, 5; 1, 3, 2) \quad (5.5)$$

reducing the number of independent $A_{5:3}^{(2)}$ to 15. Besides these, we also observe that the $A_{5:3}^{(2)}$ are generally antisymmetric under reversal of the three generator traces, which would provide us with 10 additional constraints, one for each $A_{5:3}^{(2)}(i, j; \dots)$, $j > i$. However, this antisymmetry trivializes the $U(1)$ decoupling identity, as it implies separately

$$\begin{aligned} 0 &= A_{5:3}^{(2)}(2, 3; 1, 4, 5) + A_{5:3}^{(2)}(2, 3; 1, 5, 4), \\ 0 &= A_{5:3}^{(2)}(4, 5; 1, 2, 3) + A_{5:3}^{(2)}(4, 5; 1, 3, 2). \end{aligned} \quad (5.6)$$

The $U(1)$ -identities are therefore included in the antisymmetry relations, such that we are left with a total of 10 independent $A_{5:3}^{(2)}$.

We now specialize to the rational parts $R_{5:1}^{(2)}$, $R_{5:3}^{(2)}$ and $R_{5:1B}^{(2)}$, for which explicit forms are given in [4]. We find four additional relations that are independent of the ones discussed so far. These were found through numeric evaluations, and take the form

$$\begin{aligned} R_{5:3}^{(2)}(21; 345) &= R_{5:3}^{(2)}(23; 451) + R_{5:3}^{(2)}(24; 531) + R_{5:3}^{(2)}(25; 341), \\ R_{5:3}^{(2)}(31; 245) &= R_{5:3}^{(2)}(32; 451) + R_{5:3}^{(2)}(34; 251) + R_{5:3}^{(2)}(35; 241), \\ R_{5:3}^{(2)}(41; 235) &= R_{5:3}^{(2)}(42; 351) + R_{5:3}^{(2)}(43; 521) + R_{5:3}^{(2)}(45; 231), \\ R_{5:3}^{(2)}(51; 234) &= R_{5:3}^{(2)}(52; 341) + R_{5:3}^{(2)}(53; 421) + R_{5:3}^{(2)}(54; 231), \end{aligned} \quad (5.7)$$

or, expressed more compactly,

$$R_{5:3}^{(2)}(i1; jkl) = \sum_{C_3(jkl)} R_{5:3}^{(2)}(ij; kl1) \quad i \in \{2, 3, 4, 5\}. \quad (5.8)$$

These are not part of the group theory relations of ref. [135], and appear to be previously unknown. Including these relations, we are left with 6 linearly independent $R_{5:3}^{(2)}$. One possible choice of basis would be

$$\begin{aligned} &R_{5:3}^{(2)}(35; 124), \quad R_{5:3}^{(2)}(25; 134), \quad R_{5:3}^{(2)}(24; 135), \\ &R_{5:3}^{(2)}(15; 234), \quad R_{5:3}^{(2)}(14; 235), \quad R_{5:3}^{(2)}(13; 245). \end{aligned} \quad (5.9)$$

5.2 Relations Involving Mandelstam Invariants

There exist further relations beyond the linear ones we just described. Inspired by the BCJ relations [141] relating amplitudes at tree-level and numerators at loop-level via factors of Mandelstams, we look for relations between structures of the form $R^{(2)}s_{ij}^l$. We focus for now on $R_{5:1}^{(2)}$, for which

a linearly independent basis contains twelve elements, for example:

$$\hat{R}_{5:1}^{(2)} = \begin{pmatrix} R_{5:1}^{(2)}(12345) \\ R_{5:1}^{(2)}(12354) \\ R_{5:1}^{(2)}(12435) \\ R_{5:1}^{(2)}(12453) \\ R_{5:1}^{(2)}(12534) \\ R_{5:1}^{(2)}(12543) \\ R_{5:1}^{(2)}(13245) \\ R_{5:1}^{(2)}(13254) \\ R_{5:1}^{(2)}(13425) \\ R_{5:1}^{(2)}(13524) \\ R_{5:1}^{(2)}(14235) \\ R_{5:1}^{(2)}(14325) \end{pmatrix} \quad (5.10)$$

For $l = 1$, we pick a linearly independent basis S_5^1 of s_{ij} ,

$$\hat{S}_5^1 = \{s_{12}, s_{23}, s_{34}, s_{45}, s_{51}\} \quad (5.11)$$

We find numerically that there exist no linear relations between the 60 products,

$$\hat{S}_5^1 \otimes \hat{R}_{5:1}^{(2)} = \left\{ s_{12} R_{5:1}^{(2)}(12345), \dots, s_{51} R_{5:1}^{(2)}(14325) \right\}. \quad (5.12)$$

For $l = 2$, there are 15 linearly independent products $s_{ij}s_{pq}$, for example:

$$S_5^2 = \{s_{12}^2, s_{12}s_{23}, s_{12}s_{34}, s_{12}s_{45}, s_{12}s_{15}, s_{23}^2, s_{23}s_{34}, s_{23}s_{45}, s_{15}s_{23}, s_{34}^2, s_{34}s_{45}, \\ s_{15}s_{34}, s_{45}^2, s_{15}s_{45}, s_{15}^2\} \quad (5.13)$$

In this case we do find linear relations between the 180 combinations,

$$S_5^2 \otimes \hat{R}_{5:1}^{(2)} = (s_{12}^2 R_{5:1}^{(2)}(12345), s_{12}s_{23} R_{5:1}^{(2)}(12345), \dots, s_{51}^2 R_{5:1}^{(2)}(14325)). \quad (5.14)$$

There exist five such relations, which expressed in the basis of eq. (5.10) take the form,

$$0 = v_{5:1;i} \cdot \hat{R}_{5:1}^{(2)}, \quad i = 1, 2, 3, 4, 5, \quad (5.15)$$

with the $v_{5:1;i}$ defined as follows:

$$v_{5:1;1} = \begin{pmatrix} 0 \\ -((s_{12} - s_{23})(s_{12} - s_{15} + s_{23} - s_{34} - 3s_{45})) \\ (s_{12} - s_{15})(s_{12} + s_{15} - s_{23} - 3s_{34} - s_{45}) \\ -((2s_{12} + s_{23} - s_{34} - 2s_{45})(s_{12} - s_{15} + s_{23} + s_{34} + s_{45})) \\ (2s_{12} + s_{15} - 2s_{34} - s_{45})(s_{12} + s_{15} - s_{23} + s_{34} + s_{45}) \\ -((s_{34} - s_{45})(3s_{12} + s_{15} + s_{23} - s_{34} - s_{45})) \\ (s_{15} - s_{45})(-s_{12} + s_{15} - 3s_{23} - s_{34} + s_{45}) \\ -((s_{12} - s_{15} + 2s_{23} - 2s_{45})(s_{12} + s_{15} + s_{23} - s_{34} + s_{45})) \\ -((s_{12} + 2s_{15} - s_{23} - 2s_{34})(s_{12} + s_{15} + s_{23} + s_{34} - s_{45})) \\ 0 \\ -((2s_{15} - 2s_{23} - s_{34} + s_{45})(s_{12} - s_{15} - s_{23} - s_{34} - s_{45})) \\ (s_{23} - s_{34})(-s_{12} - 3s_{15} + s_{23} + s_{34} - s_{45}) \end{pmatrix}, \quad (5.16)$$

$$v_{5:1;2} = \begin{pmatrix} s_{12}(-s_{15} + s_{23} - 2s_{34} + 2s_{45}) + (s_{15} + s_{23})(s_{34} - s_{45}) \\ (s_{15} - s_{23} + 2s_{45})(-2s_{12} + s_{23} + s_{34} + s_{45}) \\ (s_{15} - s_{23} - 2s_{34})(-2s_{12} + s_{15} + s_{34} + s_{45}) \\ (s_{12} + s_{23} - s_{45})(-s_{15} + s_{23} + 2(s_{34} + s_{45})) \\ -((s_{12} + s_{15} - s_{34})(s_{15} - s_{23} + 2(s_{34} + s_{45}))) \\ s_{12}(s_{15} - s_{23} - 2s_{34} + 2s_{45}) \\ s_{12}(3s_{15} - 3s_{23} - 2(s_{34} + s_{45})) + s_{15}(3s_{23} - s_{34} - 4s_{45}) + s_{15}^2 - 3s_{23}s_{34} - 4s_{23}^2 + 2s_{34}s_{45} + 2s_{45}^2 \\ (s_{15} - s_{23} + 2s_{45})(2s_{12} + s_{15} + 2s_{23} - s_{34} - s_{45}) \\ -((s_{15} - s_{23} - 2s_{34})(2s_{12} + 2s_{15} + s_{23} - s_{34} - s_{45})) \\ (s_{12} - s_{34} - s_{45})(3s_{15} - 3s_{23} - 2s_{34} + 2s_{45}) \\ s_{12}(5s_{15} - 5s_{23} - 2s_{34} + 2s_{45}) - 2(s_{15}(2s_{34} + 3s_{45}) + s_{15}^2 - s_{34}(3s_{23} + s_{34}) - 2s_{23}s_{45} - s_{23}^2 + s_{45}^2) \\ -s_{12}(3s_{15} - 3s_{23} + 2(s_{34} + s_{45})) - s_{45}(3s_{15} + s_{23} - 2s_{34}) + 3s_{15}s_{23} - 4s_{15}^2 - 4s_{23}s_{34} + s_{23}^2 + 2s_{34}^2 \end{pmatrix}, \quad (5.17)$$

$$v_{5:1;3} = \begin{pmatrix} (s_{23} - s_{34})(s_{12} - s_{15} + s_{45}) \\ -((s_{12} - s_{34} - 2s_{45})(s_{12} + s_{15} - 2s_{23} + s_{45})) \\ -((s_{12} - s_{15} + s_{23} + s_{34})(s_{12} - s_{15} - 2s_{34} - s_{45})) \\ 0 \\ (3s_{12} + s_{15} - 2s_{34} - s_{45})(s_{15} - s_{23} + s_{34} + s_{45}) \\ (2s_{12} + s_{23} - s_{45})(s_{12} + s_{15} - 2s_{34} + s_{45}) \\ (s_{12} + s_{15} + 2s_{23} - s_{45})(s_{15} - s_{23} - s_{34} - s_{45}) \\ -((s_{12} + s_{15} + s_{23} - s_{34})(s_{12} - s_{15} + 2s_{23} - 3s_{45})) \\ (s_{12} + 2s_{15} - s_{34})(s_{12} - s_{15} + 2(s_{23} + s_{34}) - s_{45}) \\ (2s_{12} + s_{23} - s_{34} - 2s_{45})(s_{12} + 3s_{15} - 2(s_{23} + s_{34}) + s_{45}) \\ (2s_{15} - s_{23} + s_{45})(s_{12} + s_{15} - 2(s_{23} + s_{34}) - s_{45}) \\ 0 \end{pmatrix}, \quad (5.18)$$

$$\begin{aligned}
v_{5:1;4} = & \left(\begin{array}{c} s_{23}(-s_{12} + s_{15} + s_{34} - s_{45}) \\ s_{12}(-s_{12} + s_{15} + s_{34} + 3s_{45}) \\ (s_{12} - s_{15} + s_{23} + 2s_{34})(s_{12} - s_{15} - s_{34} - s_{45}) \\ s_{12}(-2s_{23} + 3s_{34} + 8s_{45}) - 4s_{12}^2 - (s_{34} + 2s_{45})(s_{15} - 2s_{23} - s_{34} + s_{45}) \\ -((s_{15} - s_{23} + s_{45})(3s_{12} + s_{15} - 3s_{34} - s_{45})) \\ -((s_{12} + s_{15} - s_{34} + s_{45})(2s_{12} + s_{23} + s_{34} - s_{45})) \\ -s_{12}(s_{15} + s_{23} - s_{45}) - s_{15}(5s_{23} + s_{34}) + s_{15}^2 + s_{45}(5s_{23} + s_{34}) + s_{23}s_{34} - s_{45}^2 \\ -((s_{12} - s_{15} + 3s_{23} - 2s_{45})(s_{12} + s_{15} - s_{34} + s_{45})) \\ -s_{12}(s_{15} + 2s_{23} + 3s_{34} - s_{45}) - s_{12}^2 + 2(s_{15}(-2s_{23} - 4s_{34} + s_{45}) + s_{15}^2 + s_{34}(s_{23} + 2s_{34})) \\ s_{12}(-6s_{15} + 9s_{23} - 8s_{45}) + 2s_{12}^2 + s_{15}(5s_{23} + 8s_{34}) - 4s_{15}^2 - 9s_{23}s_{34} - 5s_{23}s_{45} + 6s_{34}s_{45} - 2s_{34}^2 + 4s_{45}^2 \\ -((s_{12} - s_{15} - s_{34} - s_{45})(2s_{15} - 3s_{23} - s_{34} + s_{45})) \\ s_{34}(s_{12} + 3s_{15} - s_{34} + s_{45}) \end{array} \right), \quad (5.19) \\
v_{5:1;5} = & \left(\begin{array}{c} -s_{45}(s_{12} + s_{15} - 2s_{23} + s_{34}) + 2s_{12}s_{15} + s_{12}s_{23} - 3s_{15}s_{23} + 2s_{15}s_{34} - s_{23}s_{34} \\ s_{12}(-3s_{15} + 4s_{23} + s_{34} - 3s_{45}) - s_{12}^2 + 2(s_{15} - s_{23})(s_{23} + s_{34}) + 3s_{45}(s_{15} + s_{34}) + 4s_{45}^2 \\ s_{12}(4s_{15} - 3(s_{23} + s_{34}) + s_{45}) - s_{12}^2 + s_{15}(s_{23} - 3(s_{34} + s_{45})) - s_{15}^2 + s_{45}(2s_{23} + 3s_{34}) + s_{34}(3s_{23} + 4s_{34}) \\ s_{12}(-6s_{15} + 8s_{23} + 3s_{34} - 5s_{45}) + 4s_{12}^2 + s_{15}(-2s_{23} + 3s_{34} + 7s_{45}) - s_{45}(8s_{23} + 7s_{34}) - 2s_{23}s_{34} + 2s_{23}^2 - 3s_{34}^2 \\ s_{12}(5s_{15} - 3s_{23} - 8s_{34}) + 4s_{12}^2 - s_{15}(s_{23} + 7s_{34} + 2s_{45}) + s_{15}^2 + 2s_{45}(s_{23} - 2s_{34}) + s_{34}(5s_{23} + 2s_{34}) - 2s_{45}^2 \\ s_{12}(4s_{15} + 5s_{23} + s_{34} - 4s_{45}) + 6s_{12}^2 + 2s_{45}(-2s_{15} + s_{23} + 3s_{34}) + 3(s_{15} - s_{34})(s_{23} + s_{34}) - 2s_{45}^2 \\ s_{12}(s_{15} + s_{23}) + s_{15}(5s_{23} + s_{34}) - s_{15}^2 - s_{23}(s_{34} + 2s_{45}) \\ s_{12}(-4s_{15} + s_{23} + s_{34} - 5s_{45}) - s_{12}^2 + s_{15}(-5s_{23} + s_{34} + s_{45}) - s_{15}^2 + s_{23}s_{34} - 10s_{23}s_{45} + 4s_{23}^2 + s_{34}s_{45} + 4s_{45}^2 \\ (s_{12} + s_{15} - s_{34})(s_{12} + 2(s_{23} + s_{34}) - s_{45}) \\ s_{12}(-6s_{15} + 3s_{23} + 8s_{34} + 3s_{45}) - 2s_{12}^2 + s_{15}(-7s_{23} + 2s_{34} + 9s_{45}) + 2s_{15}^2 - 3s_{45}(2s_{23} + 3s_{34}) + 3s_{23}s_{34} + 4s_{23}^2 - 4s_{34}^2 \\ s_{12}(-2s_{15} + s_{23} + s_{34}) + s_{15}(s_{23} + s_{34} + 2s_{45}) - (s_{23} + s_{34})(s_{34} + 2s_{45}) \\ (s_{12} - s_{34})(-2s_{23} + s_{34} + s_{45}) + 3s_{15}(-2s_{23} + s_{34} + s_{45}) + 2s_{15}^2 \end{array} \right). \quad (5.20)
\end{aligned}$$

We have verified these relations numerically.

We can repeat this process for $R_{5:3}^{(2)}$, using the six-element basis of eq. (5.9), *i.e.*

$$\hat{R}_{5:3}^{(2)} = \begin{pmatrix} R_{5:3}^{(2)}(35; 124) \\ R_{5:3}^{(2)}(25; 134) \\ R_{5:3}^{(2)}(24; 135) \\ R_{5:3}^{(2)}(15; 234) \\ R_{5:3}^{(2)}(14; 235) \\ R_{5:3}^{(2)}(13; 245) \end{pmatrix}. \quad (5.21)$$

We can find numerically that there exist no linear relations for,

$$\hat{S}_5^1 \otimes \hat{R}_{5:3}^{(2)}, \quad \hat{S}_5^2 \otimes \hat{R}_{5:3}^{(2)}. \quad (5.22)$$

Next we combine the bases $\hat{R}_{5:1}^{(2)}$ and $\hat{R}_{5:3}^{(2)}$,

$$\hat{R}_5^{(2)} = \hat{R}_{5:1}^{(2)} \oplus \hat{R}_{5:3}^{(2)}. \quad (5.23)$$

The elements of $\hat{R}_5^{(2)}$ are linearly independent, and due to the $R_{5:1B}^{(2)}$ being determined by $R_{5:1}^{(2)}$ and $R_{5:3}^{(2)}$, constitute a basis for all five-gluon all-plus two-loop partial amplitudes. There exist 10 linear relations between the 90 elements of,

$$\hat{S}_5^1 \otimes \hat{R}_5^{(2)}, \quad (5.24)$$

which can be expressed in terms of $\hat{R}^{(2)}$ as

$$0 = v_{5;i} \cdot \hat{R}^{(2)}, \quad i = 1, \dots, 10, \quad (5.25)$$

with

$$v_{5;1} = \begin{pmatrix} s_{45} - s_{15} \\ -s_{12} + s_{34} + 2s_{45} \\ s_{12} - s_{34} \\ -s_{15} - s_{45} \\ -2s_{12} - s_{15} + 2s_{34} + s_{45} \\ s_{34} - s_{12} \\ s_{12} - s_{34} \\ s_{15} + s_{45} \\ s_{15} + s_{45} \\ s_{12} - s_{34} \\ s_{15} + s_{45} \\ s_{12} + 2s_{15} - s_{34} \\ \frac{1}{2}(s_{12} + s_{15} - s_{34} - s_{45}) \\ 0 \\ \frac{1}{2}(-s_{12} - s_{15} + s_{34} - s_{45}) \\ \frac{1}{2}(s_{12} + s_{15} - s_{34} - s_{45}) \\ 0 \\ \frac{1}{2}(-s_{12} + s_{15} + s_{34} + s_{45}) \end{pmatrix}, \quad v_{5;2} = \begin{pmatrix} s_{34} - s_{12} \\ s_{23} - s_{45} \\ s_{23} + s_{34} \\ s_{34} + s_{45} \\ 0 \\ s_{12} + s_{23} \\ 0 \\ s_{12} + s_{23} - s_{34} - s_{45} \\ -s_{12} - s_{15} \\ s_{12} + s_{15} - s_{34} - s_{45} \\ -s_{12} - s_{15} + s_{23} + s_{34} \\ s_{23} - s_{15} \\ \frac{1}{2}(-s_{23} - s_{34}) \\ \frac{1}{2}(-s_{12} - s_{15} + s_{23} + 2s_{34} + s_{45}) \\ \frac{1}{2}(s_{12} + s_{15} - s_{23} - s_{34}) \\ \frac{1}{2}(2s_{12} + s_{15} - 2s_{34} - s_{45}) \\ \frac{1}{2}(-s_{12} - s_{15} + s_{34} + s_{45}) \\ \frac{1}{2}(s_{12} + s_{23} - s_{34} - s_{45}) \end{pmatrix}, \quad (5.26)$$

$$v_{5;3} = \begin{pmatrix} s_{34} - s_{15} \\ 0 \\ s_{34} + s_{45} \\ -s_{12} - s_{15} + s_{34} + s_{45} \\ -s_{12} - s_{15} \\ s_{45} - s_{12} \\ s_{45} - s_{23} \\ s_{15} - s_{23} - s_{34} + s_{45} \\ 0 \\ s_{12} + s_{15} - s_{23} - s_{34} \\ s_{23} + s_{34} \\ s_{15} + s_{45} \\ \frac{1}{2}(s_{12} + s_{15} - s_{34} - s_{45}) \\ \frac{1}{2}(-s_{12} - s_{15} + s_{23} + 2s_{34} + s_{45}) \\ \frac{1}{2}(-s_{34} - s_{45}) \\ \frac{1}{2}(s_{12} + 2s_{15} - s_{23} - 2s_{34}) \\ \frac{1}{2}(-s_{12} - s_{15} + s_{34} + s_{45}) \\ \frac{1}{2}(s_{15} - s_{34}) \end{pmatrix}, \quad v_{5;4} = \begin{pmatrix} s_{23} - s_{45} \\ -s_{34} - s_{45} \\ 0 \\ s_{12} + s_{23} \\ s_{12} + s_{23} - s_{34} - s_{45} \\ s_{12} - s_{34} \\ s_{23} + s_{34} \\ 0 \\ -s_{15} + s_{23} + s_{34} - s_{45} \\ -s_{12} + s_{15} - s_{23} + s_{45} \\ -s_{15} - s_{45} \\ s_{34} - s_{15} \\ \frac{1}{2}(-s_{12} - s_{23} + s_{34} + s_{45}) \\ \frac{1}{2}(s_{12} - s_{15} + s_{23} - s_{45}) \\ \frac{1}{2}(s_{15} - s_{23} - s_{34} + s_{45}) \\ \frac{1}{2}(-s_{12} + s_{15} - 2s_{23} + 2s_{45}) \\ \frac{1}{2}(s_{12} - s_{15} + 2s_{23} + s_{34} - s_{45}) \\ \frac{1}{2}(-s_{23} - s_{34}) \end{pmatrix}, \quad (5.27)$$

$$v_{5;5} = \begin{pmatrix} s_{12} - s_{15} + s_{23} - s_{45} \\ -s_{12} - s_{15} \\ s_{12} - s_{15} \\ s_{12} - s_{15} + s_{23} - s_{45} \\ -s_{12} - s_{15} + s_{23} - s_{45} \\ -s_{12} - s_{15} \\ s_{12} + s_{15} \\ -s_{12} + s_{15} - s_{23} + s_{45} \\ s_{12} + s_{15} + s_{23} - s_{45} \\ -s_{12} + s_{15} - 2s_{23} + 2s_{45} \\ s_{12} - s_{15} + s_{23} - s_{45} \\ s_{12} + s_{15} \\ \frac{1}{2}(2s_{15} - s_{23} + s_{45}) \\ s_{12} - s_{15} + s_{23} - s_{45} \\ \frac{1}{2}(-2s_{12} - s_{23} + s_{45}) \\ -s_{12} + s_{15} - \frac{3}{2}(s_{23} - s_{45}) \\ s_{12} + s_{23} - s_{45} \\ \frac{1}{2}(-2s_{12} - s_{23} + s_{45}) \end{pmatrix}, \quad v_{5;6} = \begin{pmatrix} s_{12} + 2s_{15} + s_{34} - 4s_{45} \\ -s_{12} + 2s_{15} + 2s_{23} + s_{34} + 2s_{45} \\ -s_{12} + 2s_{15} + 2s_{23} + 5s_{34} + 4s_{45} \\ 3s_{12} + 2s_{15} - s_{34} - 2s_{45} \\ 3s_{12} + 2s_{15} - 5s_{34} - 4s_{45} \\ s_{12} + 2s_{15} + 2s_{23} - s_{34} + 4s_{45} \\ -s_{12} - 4s_{15} - 2s_{23} + s_{34} + 6s_{45} \\ -3s_{12} - 4s_{15} + s_{34} - 6s_{45} \\ 3s_{12} + 4s_{15} - 5s_{34} - 4s_{45} \\ 11s_{12} + 8s_{15} - 2s_{23} - 11s_{34} - 6s_{45} \\ 3s_{12} - 8s_{15} + 4s_{23} - s_{34} - 6s_{45} \\ s_{12} + 4s_{15} + 2s_{23} - s_{34} + 4s_{45} \\ -s_{12} - 2s_{15} - s_{23} \\ 2(s_{23} + s_{34} + s_{45}) \\ -s_{12} - s_{23} \\ -s_{12} - s_{23} + 2s_{45} \\ 0 \\ s_{23} - s_{12} \end{pmatrix}, \quad (5.28)$$

$$v_{5;7} = \begin{pmatrix} -s_{12} + s_{15} + 2s_{23} - 2s_{45} \\ 5s_{12} + 5s_{15} - 6s_{23} + 6s_{45} \\ -5s_{12} + 5s_{15} - 4s_{23} + 4s_{45} \\ 7s_{12} - s_{15} + 4s_{23} - 4s_{45} \\ -s_{12} - s_{15} + 2s_{23} - 2s_{45} \\ -5s_{12} + 3s_{15} - 4s_{23} + 4s_{45} \\ -5s_{12} - 5s_{15} - 6s_{23} + 6s_{45} \\ s_{12} - s_{15} + 4s_{23} - 4s_{45} \\ s_{12} + s_{15} + 2s_{23} - 2s_{45} \\ 5s_{12} - 5s_{15} + 6s_{23} - 6s_{45} \\ s_{12} - 7s_{15} + 4s_{23} - 4s_{45} \\ -3s_{12} + 5s_{15} - 4s_{23} + 4s_{45} \\ -2s_{15} + s_{23} - s_{45} \\ -2(s_{12} - s_{15} + s_{23} - s_{45}) \\ 2s_{12} + s_{23} - s_{45} \\ s_{45} - s_{23} \\ -2s_{12} \\ 2s_{15} - s_{23} + s_{45} \end{pmatrix}, \quad v_{5;8} = \begin{pmatrix} -5s_{12} + 5s_{15} + s_{23} - s_{45} \\ s_{12} + s_{15} - 3s_{23} + 3s_{45} \\ s_{12} - s_{15} - s_{23} + s_{45} \\ 5s_{12} + 3s_{15} + s_{23} - s_{45} \\ 5s_{12} + 5s_{15} - s_{23} + s_{45} \\ -7s_{12} - s_{15} - 3s_{23} + 3s_{45} \\ -s_{12} - s_{15} - 3s_{23} + 3s_{45} \\ 5s_{12} - 5s_{15} + 11(s_{23} - s_{45}) \\ -5s_{12} - 5s_{15} - s_{23} + s_{45} \\ -s_{12} + s_{15} - 3s_{23} + 3s_{45} \\ -3s_{12} - 5s_{15} + s_{23} - s_{45} \\ s_{12} + 7s_{15} - 3s_{23} + 3s_{45} \\ -2s_{15} + s_{23} - s_{45} \\ -2(s_{12} - s_{15} + s_{23} - s_{45}) \\ 2s_{12} + s_{23} - s_{45} \\ 2s_{12} - 2s_{15} + s_{23} - s_{45} \\ 2s_{15} \\ -2s_{15} + s_{23} - s_{45} \end{pmatrix}, \quad (5.29)$$

$$v_{5;9} = \begin{pmatrix} -3s_{12} + s_{15} + 3s_{23} - s_{34} \\ s_{12} - 3s_{15} - s_{23} + 3s_{34} \\ s_{12} - 5s_{15} + s_{23} + 5s_{34} \\ 3s_{12} - s_{15} + 3s_{23} + s_{34} \\ 3s_{12} + s_{15} + s_{23} - s_{34} \\ -11s_{12} - 5s_{15} - s_{23} + 5s_{34} \\ -s_{12} + 5s_{15} - 11s_{23} - 5s_{34} \\ 3s_{12} + s_{15} + 3s_{23} - s_{34} \\ -3s_{12} - 7s_{15} + 3s_{23} + 7s_{34} \\ -s_{12} - 5s_{15} + s_{23} + 5s_{34} \\ -s_{12} + s_{15} - 3s_{23} - s_{34} \\ s_{12} + 5s_{15} + s_{23} - 5s_{34} \\ s_{12} + 2s_{15} - s_{23} - 2s_{34} \\ -2s_{12} \\ s_{12} + s_{23} \\ s_{12} - s_{23} \\ 2(s_{15} - s_{34}) \\ -s_{12} - 2s_{15} + s_{23} + 2s_{34} \end{pmatrix}, \quad v_{5;10} = \begin{pmatrix} 3(s_{12} - s_{15} - s_{34} + s_{45}) \\ 3(s_{12} - s_{15} - s_{34} - 3s_{45}) \\ -3s_{12} - s_{15} + 3s_{34} - s_{45} \\ 3s_{12} - s_{15} - 3s_{34} - 7s_{45} \\ -9s_{12} - 3s_{15} + 9s_{34} + 3s_{45} \\ 3s_{12} - s_{15} - 3s_{34} - s_{45} \\ -s_{12} + 3s_{15} + s_{34} - 3s_{45} \\ -s_{12} + 3s_{15} + s_{34} + 3s_{45} \\ 3s_{12} + 7s_{15} - 3s_{34} + s_{45} \\ -7s_{12} - 3s_{15} + 7s_{34} + 3s_{45} \\ s_{12} + 3s_{15} - s_{34} + 3s_{45} \\ -3(s_{12} + 3s_{15} - s_{34} + s_{45}) \\ 2(s_{15} + s_{45}) \\ 2(s_{12} - s_{15} - s_{34} - s_{45}) \\ 0 \\ 2s_{34} - 2s_{12} \\ 0 \\ 0 \end{pmatrix}. \quad (5.30)$$

We have again verified all of these relations numerically.

In addition, we have verified that there further exist 53 relations between the 270 elements of

$$\hat{S}_5^2 \otimes \hat{R}_5^{(2)}, \quad (5.31)$$

which include the five relations of eq. (5.15). At least five of the remaining 48 are instances of the $\hat{S}_5^1 \otimes \hat{R}_5^{(2)}$ relations in disguise. At this point, we have not determined how many of these relations are distinct from the ones we found previously.

Conclusion

Let us summarize the main results presented in this thesis:

In chapter 3, we saw that one-loop generalized unitarity techniques are sufficient to compute the rational parts of the full-color two-loop all-plus amplitude. We started from the conjecture by Badger, Mogull and Peraro [11, 12], relating the $(D_s - 2)^2$ coefficient of the leading-color amplitude to its rational part. We extended the scope of this conjecture to include partial amplitudes subleading in color as well. Through dimensional reconstruction we saw that this coefficient can be constructed from cuts of six-dimensional amplitudes with massless scalars circulating in both loops. These amplitudes do not allow propagators to be shared between the two loops. They can therefore be expressed in terms of a basis of two-loop integrals that factorize into a product of one-loop integrals. We are able to determine the coefficients of such integrals loop-by-loop using one-loop generalized unitarity cuts. The factorization of the integrals further allowed us to use four-dimensional amplitudes of massive scalars, instead of six-dimensional massless scalar amplitudes, further solidifying the similarity to one-loop computations. A necessary ingredient for the computation of the cuts are four-dimensional tree amplitudes involving two massive scalar lines, for which we derived new analytic expressions. For the computation of analytic expressions, we also found a new parametrization of momentum twistors, valid for an arbitrary number of momenta, whose parameters have simple solutions in terms of spinors. Via explicit analytic and numerical computations we were able to reproduce all previously known analytic results for rational terms of two-loop all-plus amplitudes up to seven gluons. In particular, we saw that this construction reproduces all four-, five-, and six-gluon results subleading in color. For seven gluons we were also able to find agreement with the conjectured form of the subleading single trace rational part.

In chapter 4, we saw that construction in terms of one-loop squared integrals of chapter 3 can be reformulated as an effective D -dimensional one-loop generalized unitarity computation. This reformulation introduced rational parts of one-loop amplitudes, which could be identified as six-dimensional amplitudes with a two external massless scalars, and a scalar running in the loop. We saw that all four-gluon rational parts could be derived from such a computation. We further discussed the computation of the one-loop rational parts required for such computations from complex recursion. The subleading and non-factorizing single poles in this recursion were shown to arise from a small set of unitarity cuts. We further saw that these pole terms can be expressed in a form resembling the product of soft factors found for one-loop single-minus and two-fermion all-plus amplitudes in refs. [112, 136]. Having derived the one-loop rational term for two scalars and three gluons, we were then able to verify that the leading color five-gluon rational term can be derived from an effective one-loop computation as well.

Finally, in chapter 5 we saw that there exist non-trivial relations for two-loop all-plus partial

amplitudes of five gluons. After finding a linearly independent basis of partial amplitudes, the new relations were found by allowing such basis elements to be multiplied by powers of Mandelstam invariants. They therefore follow the structure of BCJ relations, which usually only apply at the integrand level for loop amplitudes.

There are several future research directions that could be followed based on the results presented in this thesis:

- As we saw in chapter 4, the rational terms of the two-loop all-plus allow for a natural one-loop computational approach. Precisely such an approach has led to the derivation of general results for the leading-color polylogarithmic parts in ref. [8], and the hope is that this construction opens the door for finding an all- n form of the leading-color rational parts as well. Finding such a derivation from unitarity directly would certainly be more challenging as we require box, triangle, and bubble contributions for the rational parts, whereas for the polylogarithms only two-mass easy boxes were needed. As an alternative, one might be able to use the one-loop construction of chapter 4 as an aid in the determining the rational terms from complex recursion.
- In ref. [148], it was proven that one-loop all-plus amplitudes are conformally invariant. The two-loop amplitudes can be verified not to be conformally invariant as a whole, however the breaking of conformal symmetry may be constrained. A first hint of such behavior can be seen in the case of the finite polylogarithmic parts of the two-loop leading-color amplitude. These are given by the product of truncated two-mass easy box integral and a rational prefactor. This prefactor on its own was shown to be conformally invariant in ref. [148]. The construction of the rational terms in chapter 4 is similar to that of the polylogarithmic terms. It may therefore present a route to better understand the behavior of the two-loop rational contributions under conformal transformations.
- In ref. [149], Dunbar, Jehu and Perkins further explored the application of the one-loop approach to two-loop all-plus graviton amplitudes in pure gravity. They found for four and five gravitons, that the polylogarithmic part also allows for a one-loop construction involving a one-loop all-plus graviton amplitudes. This again follows the pattern found for the polylogarithmic part of all-plus amplitudes in Yang–Mills. Based on the one-loop construction of the rational terms presented in this thesis, it would be natural to ask, whether a similar pattern exists for the rational parts of two-loop all-plus graviton amplitudes.
- In a more speculative direction, it would be interesting to see, whether an extension of the one-loop squared construction exists for single-minus amplitudes. These are the second class of amplitudes that are finite at one-loop level, and as such may also have simpler properties at two-loop level.
- Finally, the relations between the rational parts of the five-gluon amplitudes presented in chapter 5 are only the result of a preliminary analysis that needs to be carried out more systematically. Right away there exist two main question, which beg to be answered: Do there exist manifestations of such relations for one-loop all-plus amplitudes? And do such relations extend to two-loop amplitudes with more than five gluons? Furthermore, as we have found these relations numerically it would be interesting to investigate whether their origin can be understood from general principles.

Appendix A

A.1 The Vanishing of $A^{(0)}(1^\pm 2 + \dots n^+)$

We can prove that the $A^{(0)}(1^\pm 2 + \dots n^+)$ amplitudes vanish by dimensional arguments and making appropriate choices for the reference momenta of the gluon polarization vectors. This section follows the arguments of ref. [47].

First we have to determine the mass dimension of a scattering amplitude $A_n^{(0)}$, which can be inferred from the number of cubic vertices and propagators. We limit ourselves to amplitudes in Yang–Mills, though the dimension has to be the same in all renormalizable theories. The number of vertices V , edges E and faces F of a planar graph are related by,

$$V - E + F = 2. \quad (\text{A.1})$$

At tree-level, $F = 1$, such that $V - E = 1$. V and E still include the external particles, which are irrelevant for the dimension counting. Removing them by introducing the reduced variables,

$$v = v_3 + v_4 = V - n, \quad e = E - n, \quad (\text{A.2})$$

we still obtain,

$$e - v = 1. \quad (\text{A.3})$$

v_3 and v_4 represent the number of internal three- and four-gluon vertices. Next we relate the number of internal edges to the number of vertices and external particles,

$$e = \frac{1}{2}(3v_3 + 4v_4 - n) = n - v_4 - 3. \quad (\text{A.4})$$

Each vertex contributes with either three or four edges. Each of the edges belongs to two vertices, leading to the factors of $\frac{1}{2}$, and the term $(-\frac{n}{2})$ removes the external edges in this counting. Using,

$$\begin{aligned} (v_3 + v_4) - e &= 1 \\ \Rightarrow v_3 &= n - 2v_4 - 2, \end{aligned} \quad (\text{A.5})$$

we obtain,

$$e = \frac{1}{2}(3v_3 + 4v_4 - n) = n - v_4 - 3. \quad (\text{A.6})$$

Each v_3 vertex has mass dimension one, while every edge e reduces the dimension by two powers

due to the propagator. Therefore, the total mass dimension of an n -point amplitude tree-amplitude is

$$\left[A_n^{(0)} \right]_{\text{mass}} = v_3 - 2e = 4 - n. \quad (\text{A.7})$$

This statement ends up being true for loop amplitudes as well, as they have to be of the same mass dimension as the tree-level amplitudes (assuming dimensionless couplings).

Now consider the case, where n gluons of the same helicity, for example $+$, interact via a tree-level diagram. Each external gluon is accompanied by a polarization vector ε_{i+}^μ . Choosing all reference momenta to be the same, any product $(\varepsilon_+ \cdot \varepsilon_+)$ vanishes. For the all-plus amplitude to not vanish, every polarization vector needs to be contracted with one of the external momenta. These however only appear in the numerator due to the cubic gluon vertices, of which there are $v_3 = (n - 2v_4 - 2)$ (c.f. eq. (A.5)). In the best case scenario there are no quartic vertices, meaning that $v_3 = n - 2$. However, even in this case we do not have a sufficient number of momenta to contract all polarization vectors. Thus, there must exist a contraction of the form $(\varepsilon_+ \cdot \varepsilon_+)$, and the amplitude has to vanish.

We can find a similar argument to show that single-minus amplitudes vanish. If we choose all reference spinors of the positive helicity gluons to be the momentum of the negative helicity gluon, all products $(\varepsilon_+ \cdot \varepsilon_-)$ and $(\varepsilon_+ \cdot \varepsilon_+)$ vanish. The amplitude must therefore be zero due to the same lack of momenta for the contraction of the polarization vectors. This argument of course excludes the three-point amplitudes $A^{(0)}(1^- 2^- 3^+)$, where we cannot choose the reference momenta to be any of the gluon momenta.

The vanishing properties of these tree-level amplitudes can therefore be concisely summarized as,

$$A^{(0)}(1^\pm 2^+ \dots n^+) = A^{(0)}(1^\mp 2^- \dots n^-) = 0. \quad (\text{A.8})$$

A.2 Single-Minus One-Loop Amplitudes

Single-minus amplitudes at one loop were first computed for four and five gluons in refs. [119, 150, 151]. In addition there exist general forms of for this helicity configuration for an arbitrary number of positive helicity gluons [2, 112]. For up to six-gluons these amplitudes are,

$$A^{(1)}(1^- 2^+ 3^+ 4^+) = -\frac{\langle 24 \rangle [24]^3}{3 \langle 23 \rangle \langle 34 \rangle [12], [14]} + \mathcal{O}(\epsilon) \quad (\text{A.9})$$

$$A^{(1)}(1^- 2^+ 3^+ 4^+ 5^+) = \frac{1}{3 \langle 34 \rangle^2} \left[\frac{\langle 14 \rangle^3 \langle 35 \rangle [45]}{\langle 12 \rangle \langle 23 \rangle \langle 45 \rangle^2} + \frac{\langle 13 \rangle^3 \langle 24 \rangle [23]}{\langle 15 \rangle \langle 23 \rangle^2 \langle 45 \rangle} + \frac{[25]^3}{[12] [15]} \right] + \mathcal{O}(\epsilon), \quad (\text{A.10})$$

$$\begin{aligned}
A^{(1)}(1^- 2^+ 3^+ 4^+ 5^+ 6^+) = & \frac{1}{3} \left(\frac{\langle 1|2+3|6\rangle^3}{s_{123} \langle 12 \rangle \langle 23 \rangle \langle 45 \rangle^2 \langle 3|1+2|6 \rangle} - \frac{\langle 1|3+4|2\rangle^3}{s_{234} \langle 16 \rangle \langle 34 \rangle^2 \langle 56 \rangle \langle 5|3+4|2 \rangle} \right. \\
& - \frac{[26]^3}{s_{345} [12] [16]} \left(\frac{[35]}{\langle 34 \rangle \langle 45 \rangle} - \frac{[45] [56]}{\langle 34 \rangle \langle 3|1+2|6 \rangle} + \frac{[23] [34]}{\langle 45 \rangle \langle 5|3+4|2 \rangle} \right) \\
& + \frac{\langle 14 \rangle^3 \langle 35 \rangle \langle 1|2+3|4 \rangle}{\langle 12 \rangle \langle 16 \rangle \langle 23 \rangle \langle 34 \rangle^2 \langle 45 \rangle^2 \langle 56 \rangle} + \frac{\langle 15 \rangle^3 \langle 46 \rangle [56]}{\langle 12 \rangle \langle 23 \rangle \langle 34 \rangle \langle 45 \rangle^2 \langle 56 \rangle^2} \\
& \left. + \frac{\langle 13 \rangle^3 \langle 24 \rangle [23]}{\langle 16 \rangle \langle 23 \rangle^2 \langle 34 \rangle^2 \langle 45 \rangle \langle 56 \rangle} \right) + \mathcal{O}(\epsilon). \quad (\text{A.11})
\end{aligned}$$

A.3 Tree-Level Soft Functions

Here we would like to derive the form of the tree-level soft-functions $\text{Soft}^{(0)}$. We use these in the construction of pole-under-pole contributions in one-loop BCFW computations. The soft functions specify the leading behavior of tree-amplitudes in the limit of vanishing momentum of a massless particle. In a color-ordered amplitude, the form of the soft function depends on the momenta of the particles adjacent to the soft one, as well as on the soft particles helicity. The soft function is generally defined via,

$$A^{(0)}(\dots i \ s^h \ j \dots) \xrightarrow{p_s \rightarrow 0} A^{(0)}(\dots i \ j \dots) \times \text{Soft}^{(0)}(i, s^h, j) \quad (\text{A.12})$$

While in the single-minus amplitude of section 4.2.1 we only required the soft functions for a gluon adjacent to two other gluons becoming soft, the discussion of chapter 4 requires the generalization to one or two of the adjacent particles to be massive scalars.

For a massless particle becoming soft, the leading behavior of an amplitude is given by the diagrams,

$$\text{Diagram with lines } i, s, j \text{ meeting at a vertex} \longrightarrow \text{Hatched diagram with lines } i, s, j + \text{Hatched diagram with lines } i, s, j \quad (\text{A.13})$$

We will always assume that the soft particle is a gluon. Let us first assume that particles i and j are gluons, such that the vertices in the right hand diagrams are cubic gluon interactions. The hatching represents the sum over Feynman diagrams. The diagrams are divergent in the limit $p_s \rightarrow 0$, as the propagators $1/(p_i + p_s)^2$ and $1/(p_s + p_j)^2$ will go on-shell. In this limit these diagrams evaluate to

$$\begin{aligned}
A^{(0)}(\dots i_g \ s^h \ j_g \dots) \xrightarrow{p_s \rightarrow 0} & \mathcal{M}_\mu(\dots (p_i + p_s)_g \ j_g \dots) \frac{(-i)}{s_{is}} \frac{i}{\sqrt{2}} [\varepsilon_i^\mu \varepsilon_s \cdot (-2p_i - p_s) + \varepsilon_s^\mu \varepsilon_i \cdot (2p_s + p_i) + (p_i - p_s)^\mu \varepsilon_i \cdot \varepsilon_s] \\
& + \mathcal{M}_\mu(\dots i_g \ (p_j + p_s)_g \dots) \frac{(-i)}{s_{sj}} \frac{i}{\sqrt{2}} [\varepsilon_j^\mu \varepsilon_s \cdot (2p_j + p_s) + \varepsilon_s^\mu \varepsilon_j \cdot (-2p_s - p_i) + (p_s - p_j)^\mu \varepsilon_j \cdot \varepsilon_s]. \quad (\text{A.14})
\end{aligned}$$

With the help of the Ward identity, we can see that the second and third term in each of the brackets are subleading for $p_s \rightarrow 0$. Contracting the \mathcal{M}_μ with $\varepsilon_{i,j}^\mu$ just returns the amplitude $A^{(0)}(\dots ij \dots)$. Choosing p_j as reference momentum for the soft gluon the first term of the third

bracket vanishes as well, so that we end up with,

$$A^{(0)}(\dots i_g s^h j_g \dots) \xrightarrow{p_s \rightarrow 0} A^{(0)}(\dots i_g j_g \dots) \frac{-\sqrt{2}(\varepsilon_s \cdot p_i)}{s_{is}} \quad (\text{A.15})$$

When the soft gluon has positive and negative helicity we get respectively,

$$A^{(0)}(\dots i_g s^h j_g \dots) \xrightarrow{p_s \rightarrow 0} A^{(0)}(\dots i_g j_g \dots) \begin{cases} \frac{\langle ij \rangle}{\langle is \rangle \langle sj \rangle} & , h = +, \\ -\frac{[ij]}{[is][sj]} & , h = -, \end{cases} \quad (\text{A.16})$$

so that we can identify the soft functions,

$$\text{Soft}^{(0)}(i_g s^+ j_g) = \frac{\langle ij \rangle}{\langle is \rangle \langle sj \rangle}, \quad \text{Soft}^{(0)}(i_g s^- j_g) = -\frac{[ij]}{[is][sj]}. \quad (\text{A.17})$$

Let us now assume that particle i is a massive scalar φ , whose massive propagator $1/s_{is}$ vanishes in the soft limit. For the massive propagators we use the compact six-dimensional Mandelstam notation as a short hand to include the mass term. Expanded, s_{is} is the usual $(p_i + p_s)^2 - m^2$, where m is the scalar mass. The two leading diagrams evaluate to,

$$\begin{aligned} & A^{(0)}(\dots i_\varphi s^h j_g \dots) \xrightarrow{p_s \rightarrow 0} \\ & \mathcal{M}(\dots (p_i + p_s)_\varphi j_g \dots) \frac{-i}{s_{is}} \frac{i}{\sqrt{2}} [\varepsilon_s \cdot (-2p_i - p_s)] \\ & + \mathcal{M}_\mu(\dots i_\varphi (p_j + p_s)_g \dots) \frac{-i}{s_{sj}} \frac{i}{\sqrt{2}} [\varepsilon_j^\mu \varepsilon_s \cdot (2p_j + p_s) + \varepsilon_s^\mu \varepsilon_j \cdot (-2p_s - p_i) + (p_s - p_j)^\mu \varepsilon_j \cdot \varepsilon_s]. \end{aligned} \quad (\text{A.18})$$

Again choosing p_j as reference momentum for the soft gluon, the entire second bracket vanishes, and we end up with,

$$A^{(0)}(\dots i_\varphi s^h j_g \dots) \xrightarrow{p_s \rightarrow 0} A^{(0)}(\dots i_\varphi j_g \dots) \begin{cases} \frac{[s|j|i]}{s_{is} \langle sj \rangle} & , h = +, \\ -\frac{\langle s|i|j \rangle}{s_{is} [sj]} & , h = -. \end{cases} \quad (\text{A.19})$$

When j is a massive scalar, we instead have,

$$\begin{aligned} & A^{(0)}(\dots i_g s^h j_\varphi \dots) \xrightarrow{p_s \rightarrow 0} \\ & \mathcal{M}_\mu(\dots (p_i + p_s)_g j_\varphi \dots) \frac{(-i)}{s_{is}} \frac{i}{\sqrt{2}} [\varepsilon_i^\mu \varepsilon_s \cdot (-2p_i - p_s) + \varepsilon_s^\mu \varepsilon_i \cdot (2p_s + p_i) + (p_i - p_s)^\mu \varepsilon_i \cdot \varepsilon_s] \\ & + \mathcal{M}(\dots i_g (p_j + p_s)_\varphi \dots) \frac{(-i)}{s_{sj}} \frac{i}{\sqrt{2}} [\varepsilon_s \cdot (2p_j + p_s)]. \end{aligned} \quad (\text{A.20})$$

Now choosing p_i as reference momentum, we obtain,

$$A^{(0)}(\dots i_g s^h j_\varphi \dots) \xrightarrow{p_s \rightarrow 0} A^{(0)}(\dots i_g j_\varphi \dots) \begin{cases} -\frac{[s|j|i]}{s_{js} \langle si \rangle} & , h = +, \\ \frac{\langle s|j|i \rangle}{s_{js} [si]} & , h = -. \end{cases} \quad (\text{A.21})$$

In summary we have the following soft functions for a gluon becoming soft while adjacent to a

massive and a massless particle

$$\begin{aligned} \text{Soft}^{(0)}(i_\varphi s^+ j_g) &= \frac{[s|i|j]}{s_{is} \langle sj \rangle}, & \text{Soft}^{(0)}(i_g s^+ j_\varphi) &= -\frac{[s|j|i]}{s_{js} \langle si \rangle}, \\ \text{Soft}^{(0)}(i_\varphi s^- j_g) &= -\frac{\langle s|i|j \rangle}{s_{is} [sj]}, & \text{Soft}^{(0)}(i_g s^- j_\varphi) &= \frac{\langle s|j|i \rangle}{s_{js} [si]}, \end{aligned} \quad (\text{A.22})$$

In the massless limit these reduce to the massless soft functions of eq. (A.17).

Lastly, we can consider the case of the soft gluon being adjacent to two massive scalars. In this case, the leading Feynman diagrams lead to,

$$\begin{aligned} A^{(0)}(\dots i_\varphi s^h j_\varphi \dots) &\xrightarrow{p_s \rightarrow 0} \mathcal{M}(\dots (p_i + p_s)_\varphi j_\varphi \dots) \frac{(-i)}{s_{is}} \frac{i}{\sqrt{2}} [\varepsilon_s \cdot (-2p_i - p_s)] \\ &+ \mathcal{M}(\dots i_\varphi (p_j + p_s)_\varphi \dots) \frac{(-i)}{s_{sj}} \frac{i}{\sqrt{2}} [\varepsilon_s \cdot (2p_j + p_s)]. \end{aligned} \quad (\text{A.23})$$

In this case we have no obvious choice for reference momentum, so we will use an arbitrary momentum q . For a positive helicity gluon the expression above then becomes,

$$A^{(0)}(\dots i_\varphi s^+ j_\varphi \dots) \xrightarrow{p_s \rightarrow 0} A^{(0)}(\dots i_\varphi j_\varphi \dots) \left[-\frac{[s|i|q]}{s_{is} \langle sq \rangle} + \frac{[s|j|q]}{s_{js} \langle sq \rangle} \right]. \quad (\text{A.24})$$

Using the Schouten identity, this can be simplified to,

$$\begin{aligned} -\frac{[s|i|q]}{s_{is} \langle sq \rangle} + \frac{[s|j|q]}{s_{js} \langle sq \rangle} &= \frac{1}{s_{is} s_{js} \langle sq \rangle} (-[s|i|q] \langle s|j|s \rangle + [s|j|q] \langle s|i|s \rangle) \\ &= \frac{[s|i|j|s]}{s_{is} s_{js}}, \end{aligned} \quad (\text{A.25})$$

eliminating the dependence on the reference momentum. We therefore have,

$$A^{(0)}(\dots i_\varphi s^+ j_\varphi \dots) \xrightarrow{p_s \rightarrow 0} A^{(0)}(\dots i_\varphi j_\varphi \dots) \times \frac{[s|i|j|s]}{s_{is} s_{js}}. \quad (\text{A.26})$$

Repeating this procedure in the negative helicity case leads to,

$$A^{(0)}(\dots i_\varphi s^- j_\varphi \dots) \xrightarrow{p_s \rightarrow 0} A^{(0)}(\dots i_\varphi j_\varphi \dots) \times \left[-\frac{\langle s|i|j|s \rangle}{s_{is} s_{js}} \right]. \quad (\text{A.27})$$

The soft functions for massive adjacent scalars are therefore,

$$\text{Soft}^{(0)}(i_\varphi s^+ j_\varphi) = \frac{[s|i|j|s]}{s_{is} s_{js}}, \quad \text{Soft}^{(0)}(i_\varphi s^- j_\varphi) = -\frac{\langle s|i|j|s \rangle}{s_{is} s_{js}}. \quad (\text{A.28})$$

In addition, by setting one or both of the masses to zero we recover the soft functions of eq. (A.22) and eq. (A.17).

A.4 Computing One-Loop μ^2 Integrals

In D -dimensional unitarity, we generally need to include basis integrals with powers of μ^2 in the numerator. For Yang–Mills power counting we have argued in section 2.3.1 that for a one-loop

basis in $D = (4 - 2\epsilon)$ only three integrals are required, namely,

$$\begin{aligned} I_4[\mu^4] &= -\frac{1}{6} + \mathcal{O}(\epsilon), \\ I_3[\mu^2] &= -\frac{1}{2} + \mathcal{O}(\epsilon), \\ I_2[\mu^2] &= -\frac{s}{2} + \mathcal{O}(\epsilon). \end{aligned} \quad (\text{A.29})$$

Box integrals with μ^2 numerator do not contribute, as they are of order ϵ . If we were to instead consider amplitudes in gravitational theories, the power counting doubles, and we would have to also include the integrals

$$I_4[\mu^8], \quad I_4[\mu^6], \quad I_3[\mu^6], \quad I_3[\mu^4], \quad I_2[\mu^4]. \quad (\text{A.30})$$

For these integrals partial results can be found in the literature [152].

The essential ingredient in the computation of one-loop μ^2 integrals are the so-called dimension shifting identities. These allow us to reduce the degree of the μ in the numerator by increasing the dimension of the loop momentum that is integrated over, thereby allowing us to reduce every μ integral to a Feynman integral without such a numerator. For an integral,

$$\mathcal{I}_m^{4-2\epsilon}[\mu^{2r}] = \int \frac{d^4\ell}{(2\pi)^4} \frac{d^{-\epsilon}\mu^2}{(2\pi)^{-2\epsilon}} \frac{\mu^{2r}}{(\ell^2 - \mu^2)((\ell - K_1)^2 - \mu^2) \dots ((\ell^2 - \sum_{i=1}^{m-1} K_i)^2 - \mu^2)}, \quad (\text{A.31})$$

the dimension shifting identity takes the form [152],

$$\mathcal{I}_m^{4-2\epsilon}[\mu^{2r}] = -\epsilon(1-\epsilon) \dots (r-1-\epsilon)(4\pi)^r \mathcal{I}_m^{D=4+2r-2\epsilon}. \quad (\text{A.32})$$

To obtain the rational parts of the integral $\mathcal{I}_m[\mu^{2r}]$, we first extract all divergent parts by manipulating the integrand, and then apply the dimension shifting identities. This will cancel the $\frac{1}{\epsilon}$ poles, leaving us with the desired result up to terms of order ϵ . We will see that using this method we only ever need to compute (higher dimensional) tadpole diagrams of both the scalar and tensor kind, which are however relatively trivial.

The general expression for the massive tadpole in arbitrary dimension [42, 153] is,

$$\int \frac{d^D\ell}{(2\pi)^D} \frac{1}{(\ell^2 - M^2)^\alpha} = i(-1)^\alpha \frac{(M^2)^{\frac{D}{2}-\alpha}}{(4\pi)^{\frac{D}{2}}} \frac{\Gamma(\alpha - \frac{D}{2})}{\Gamma(\alpha)}. \quad (\text{A.33})$$

For higher powers in μ^2 we will need to perform Passarino–Veltman reduction of high tensor ranks. Here I would like to document some identities that will prove to be useful. We will need to deal with reduction of tensor integrals of the form

$$\frac{\ell^{\mu_1} \dots \ell^{\mu_{2n}}}{(\ell^2 - M^2)^\alpha} = g^{(\mu_1 \mu_2 \dots \mu_{2n-1} \mu_{2n})} A_{2n} \quad (\text{A.34})$$

where $g^{(\mu_1 \dots \mu_{2n})}$ is the symmetrization

$$g^{(\mu_1 \dots \mu_{2n})} = \frac{1}{n!2^n} \sum_{\sigma \in S_{2n}} g^{\mu_{\sigma(1)} \mu_{\sigma(2)} \dots \mu_{\sigma(2n-1)} \mu_{\sigma(2n)}} \quad (\text{A.35})$$

The number $N(n)$ of *unique* combinations of the $g^{\mu_i \mu_j}$ in this sum is given recursively by,

$$N(n) = (2n - 1)N(n - 1), \quad N(2) = 3. \quad (\text{A.36})$$

For example, in the case of $n = 2$ the three combinations are,

$$\{g^{\mu_1 \mu_2} g^{\mu_3 \mu_4}, g^{\mu_1 \mu_3} g^{\mu_2 \mu_4}, g^{\mu_1 \mu_4} g^{\mu_2 \mu_3}\}. \quad (\text{A.37})$$

Solving the recursion using *Mathematica*, we obtain,

$$N(n) = 2^{n-1} \left(\frac{3}{2}\right)_{n-1} = 2^{n-1} \frac{\Gamma(\frac{1}{2} + n)}{\Gamma(\frac{3}{2})} = \frac{(2n)!}{n! 2^n} \quad (\text{A.38})$$

which is defined using the Pochhammer symbol,

$$(x)_n = x(x+1)(x+2) \dots (x+n-1) = \frac{\Gamma(x+n)}{\Gamma(x)}. \quad (\text{A.39})$$

The first few values are,

$$N(2) = 3, \quad N(3) = 15, \quad N(4) = 105, \quad N(5) = 945, \quad N(6) = 10395 \quad (\text{A.40})$$

Next, we would like to contract $g^{(\mu_1 \mu_2 \dots \mu_{2n-1} \mu_{2n})}$ with a given ordering of $g_{\mu_i \mu_j}$, that is,

$$g_{\mu_1 \mu_2} \dots g_{\mu_{2n-1} \mu_{2n}} g^{(\mu_1 \dots \mu_{2n})} \equiv G(n). \quad (\text{A.41})$$

Depending on how the indices in these contractions match up, we will get chains of contracted $g^{\mu\nu}$ and factors of $g_\mu^\mu = D$. In the end, $G(n)$ will be a polynomial in D , where the coefficients have to add up to $N(n)$. Using the fact that,

$$g^{(\mu_1 \dots \mu_{2n})} = \sum_{i=2}^{2n} g^{\mu_1 \mu_i} g^{(\mu_2 \dots \mu_{i-1} \mu_{i+1} \dots \mu_{2n})}, \quad (\text{A.42})$$

and the fact that $g^{(\dots)}$ is symmetrized, we can write down a recursion relation for $G(n)$,

$$G(n) = DG(n-1) + (2n-1)G(n-1), \quad G(1) = D, \quad (\text{A.43})$$

which we again solve using *Mathematica*,

$$G(n) = 2^{n-1} D \left(1 + \frac{D}{2}\right)_{n-1} = 2^n \frac{\Gamma(\frac{D}{2} + n)}{\Gamma(\frac{D}{2})}. \quad (\text{A.44})$$

The first few values of $G(n)$ are,

$$\begin{aligned}
G(1) &= D, \\
G(2) &= D^2 + 2D, \\
G(3) &= D^3 + 6D^2 + 8D, \\
G(4) &= D^4 + 12D^3 + 44D^2 + 48D, \\
G(5) &= D^5 + 20D^4 + 120D^3 + 400D^2 + 384D, \\
G(6) &= D^6 + 30D^5 + 340D^4 + 1800D^3 + 4384D^2 + 3840D.
\end{aligned} \tag{A.45}$$

Adding up the coefficients in each case yields exactly the associated value of $N(n)$, as expected.

As a warm up, let us Passarino–Veltman-reduce the rank-2 massive tensor tadpole integral. As there are no four-momenta involved, we know it has to be expressible as

$$\frac{\ell^\mu \ell^\nu}{(\ell^2 - M^2)^4} = g^{\mu\nu} A, \tag{A.46}$$

where A needs to be determined. Contracting with $g_{\mu\nu}$ we obtain,

$$A = \frac{1}{D} \left(\frac{1}{(\ell^2 - M^2)^3} + \frac{M^2}{(\ell^2 - M^2)^4} \right). \tag{A.47}$$

We can further simplify this via the IBP relation,

$$\begin{aligned}
0 &= \int d^D \ell \frac{\partial}{\partial \ell^\mu} \left(\ell^\mu \frac{1}{(\ell^2 - M^2)^\alpha} \right) \\
&= D \int d^D \ell \frac{1}{(\ell^2 - M^2)^\alpha} - 2\alpha \int d^D \ell \frac{\ell^2}{(\ell^2 - M^2)^{\alpha+1}} \\
&\Leftrightarrow \int d^D \ell \frac{M^2}{(\ell^2 - M^2)^{\alpha+1}} = \left(\frac{D}{2\alpha} - 1 \right) \int d^D \ell \frac{1}{(\ell^2 - M^2)^\alpha},
\end{aligned} \tag{A.48}$$

allowing us to make the identification

$$A = \frac{1}{6} \frac{1}{(\ell^2 - M^2)^3}. \tag{A.49}$$

The integral therefore becomes,

$$\frac{\ell^\mu \ell^\nu}{(\ell^2 - M^2)^4} = \frac{g^{\mu\nu}}{6} \frac{1}{(\ell^2 - M^2)^3}, \tag{A.50}$$

which is notably independent of D .

Now consider the reduction of the general integral,

$$\frac{\ell^{\mu_1} \ell^{\mu_2} \dots \ell^{\mu_{2n}}}{(\ell^2 - M^2)^{\alpha+n}} = g^{(\mu_1 \dots \mu_{2n})} A_{2n}. \tag{A.51}$$

Contracting with metric tensors and repeatedly using the IBP identity of eq. (A.48), we obtain,

$$\begin{aligned} A_{2n} &= \frac{1}{G(n)} \frac{(\ell^2)^n}{(\ell^2 - M^2)^{\alpha+n}} \\ &= \frac{1}{G(n)} \frac{1}{(\ell^2 - M^2)^\alpha} \underbrace{\left(\sum_{i=0}^n \binom{n}{i} \prod_{j=0}^{n-i} \left(\frac{D}{2(\alpha + (n-i) - j)} - 1 \right) \right)}_{\tilde{G}(n)}. \end{aligned} \quad (\text{A.52})$$

The expression of $\tilde{G}(n)$ is automatically simplified by *Mathematica* to,

$$\tilde{G}(n) = \frac{\Gamma(\frac{D}{2} + n)}{\Gamma(\frac{D}{2})} \left(\frac{\Gamma(\alpha + n)}{\Gamma(\alpha)} \right)^{-1} = G(n) \left(2^n \frac{\Gamma(\alpha + n)}{\Gamma(\alpha)} \right)^{-1}. \quad (\text{A.53})$$

Substituting this back into A_{2n} we obtain for the Passarino–Veltman decomposition,

$$\frac{\ell^{\mu_1} \ell^{\mu_2} \dots \ell^{\mu_{2n}}}{(\ell^2 - M^2)^{\alpha+n}} = g^{(\mu_1 \dots \mu_{2n})} \frac{1}{G_{2\alpha}(n)} \frac{1}{(\ell^2 - M^2)^\alpha}, \quad (\text{A.54})$$

which is defined in terms of $G_a(n)$,

$$G_a(n) \equiv G(n)|_{D \rightarrow a}. \quad (\text{A.55})$$

Extracting the UV divergent parts of the integral we expanding the propagators around large loop-momentum configurations¹. This will introduce larger powers of $\frac{1}{\ell^2}$, which will eventually lead to (spurious) IR divergences. Since we know that these divergences cancel in the end, and we are not really interested in them anyway, we can add a fictitious mass to each propagator, which will end up being irrelevant for the UV-divergent contribution. Note that in the large $\frac{1}{\ell^2}$ expansion of the propagators we make the integral more and more UV convergent, while introducing terms that are IR divergent. The only terms that are both UV divergent and (spuriously) IR divergent are the order zero terms in the loop momentum power counting, *i.e.* the logarithmically divergent terms, and these are the ones we have to regulate with the fictitious mass. The terms of the expansion that are quadratically or worse UV divergent are IR convergent and scaleless. Their UV contribution has to be zero, as in dimensional regularization, the UV and IR divergent parts of scaleless integrals cancel each other. Therefore, in the end the logarithmically divergent terms in the expansion contain the entire information about the UV divergence of the original integral.

The μ^2 triangle $\mathcal{I}_3[\mu^2]$ and the μ^4 box $\mathcal{I}_4[\mu^4]$ are simple to compute, as they are already logarithmically divergent. To extract the logarithmically divergent pieces, we therefore only have to replace each propagator with $\frac{1}{\ell^2 - M^2}$, and then use the dimension shift identity. In practice this means,

$$\begin{aligned} \mathcal{I}_3[\mu^2] &= -\epsilon(4\pi) \int \frac{d^{6-2\epsilon}\ell}{(2\pi)^{6-2\epsilon}} \frac{1}{(\ell^2 - M^2)^3} + \mathcal{O}(\epsilon) \\ &= \epsilon \frac{i}{(4\pi)^{2-\epsilon}} M^{-\epsilon} \frac{\Gamma(\epsilon)}{\Gamma(3)} + \mathcal{O}(\epsilon) \\ &= \frac{1}{2} \frac{i}{(4\pi)^2} + \mathcal{O}(\epsilon), \end{aligned} \quad (\text{A.56})$$

¹I would like to thank Ben Page for showing me this method.

$$\begin{aligned}
\mathcal{I}_4[\mu^4] &= -\epsilon(1-\epsilon)(4\pi)^2 \int \frac{d^{8-2\epsilon}\ell}{(2\pi)^{8-2\epsilon}} \frac{1}{(\ell^2 - M^2)^4} + \mathcal{O}(\epsilon) \\
&= -\epsilon \frac{i}{(4\pi)^{2-\epsilon}} M^{-\epsilon} \frac{\Gamma(\epsilon)}{\Gamma(4)} + \mathcal{O}(\epsilon) \\
&= -\frac{1}{6} \frac{i}{(4\pi)^2} + \mathcal{O}(\epsilon).
\end{aligned} \tag{A.57}$$

With the normalization of eq. (2.1), we therefore obtain the expected result,

$$I_4[\mu^4] = -\frac{1}{6} + \mathcal{O}(\epsilon), \quad I_3[\mu^2] = -\frac{1}{2} + \mathcal{O}(\epsilon). \tag{A.58}$$

A more complicated case is the bubble integral with a μ^2 numerator $\mathcal{I}_2[\mu^2]$. Just focusing on the integrand, we can effectively perform the expansion by repeatedly using the identity,

$$\frac{1}{(\ell + p)^2} = \frac{1}{\ell^2} \left(1 - \frac{2(\ell \cdot p) + p^2}{(\ell + p)^2} \right). \tag{A.59}$$

Note that the extra terms have better UV convergence behavior than the original term. Applying this identity to the integrand, we obtain,

$$\begin{aligned}
\frac{\mu^2}{\ell^2(\ell + p)^2} &= \frac{\mu^4}{(\ell^2)^2} - \frac{(2(\ell \cdot p) + p^2) \mu^2}{(\ell^2)^2(\ell + p)^2} \\
&= \frac{\mu^4}{(\ell^2)^2} - \frac{p^2 \mu^2}{(\ell^2)^6} + \frac{4(\ell \cdot p)^2 \mu^2}{(\ell^2)^4} + (\text{UV convergent terms}).
\end{aligned} \tag{A.60}$$

Only the last two terms are non-vanishing in dimensional regularization as they are logarithmically UV divergent. They are also IR divergent, though as the original integral was IR convergent we know that this divergence is spurious. These divergences must therefore be compensated by contributions from the remaining UV convergent terms. To remove these IR divergences and extract only the UV behavior we can now make the propagators massive, so that,

$$\begin{aligned}
\frac{\mu^2}{\ell^2(\ell + p)^2} &= -\frac{p^2 \mu^2}{(\ell^2 - M^2)^3} + \frac{4(\ell \cdot p)^2 \mu^2}{(\ell^2 - M^2)^4} + (\text{UV/IR convergent terms}) \\
&= -\frac{p^2 \mu^2}{(\ell^2 - M^2)^3} + \frac{4}{6} \frac{p^2 \mu^2}{(\ell^2 - M^2)^3} + (\text{UV/IR convergent terms}) \\
&= -\frac{1}{3} \frac{p^2 \mu^2}{(\ell^2 - M^2)^3} + (\text{UV/IR convergent terms}).
\end{aligned} \tag{A.61}$$

Using the dimension shift identity we obtain,

$$\begin{aligned}
\mathcal{I}_2[\mu^2] &= -\epsilon(4\pi)^2 \left(-\frac{p^2}{3} \int \frac{d^{6-2\epsilon}\ell}{(2\pi)^{6-2\epsilon}} \frac{1}{(\ell^2 - M^2)^3} \right) + \mathcal{O}(\epsilon) \\
&= -\epsilon \frac{(-i)}{(4\pi)^{2-\epsilon}} \left(-\frac{p^2}{3} M^{-\epsilon} \frac{\Gamma(\epsilon)}{\Gamma(3)} \right) + \mathcal{O}(\epsilon) \\
&= -\frac{1}{6} \frac{i}{(4\pi)^2} p^2 + \mathcal{O}(\epsilon),
\end{aligned} \tag{A.62}$$

such that we again obtain the expected result,

$$I_2^D[\mu^2] = -\frac{p^2}{6} + \mathcal{O}(\epsilon). \tag{A.63}$$

This agrees with the result in ref. [96]. That reference also provides the result for the case of massive propagators in the bubble, namely,

$$I_2^D[\mu^2] = -\frac{1}{6}(p^2 - 3(m_1^2 + m_2^2)) + \mathcal{O}(\epsilon), \quad (\text{A.64})$$

where m_1 and m_2 are the masses of the two propagators. We can reproduce this result by using modified relations for the expansion,

$$\begin{aligned} \frac{1}{\ell^2 - m_1^2} &= \frac{1}{\ell^2} \left(1 + \frac{m_1^2}{\ell^2 - m_1^2} \right), \\ \frac{1}{(\ell + p)^2 - m_2^2} &= \frac{1}{\ell^2} \left(1 - \frac{2(\ell \cdot p) + p^2 - m_2^2}{(\ell + p)^2 - m_2^2} \right). \end{aligned} \quad (\text{A.65})$$

The integrand then becomes

$$\begin{aligned} \frac{\mu^2}{(\ell^2 - m_1^2)((\ell + p)^2 - m_2^2)} &= -\frac{(p^2 - (m_1^2 + m_2^2))\mu^2}{(\ell^2 - M^2)^3} + \frac{4}{6} \frac{p^2 \mu^2}{(\ell^2 - M^2)^4} + (\text{UV/IR convergent terms}) \\ &= -\frac{1}{3} \frac{p^2 \mu^2}{(\ell^2 - M^2)^3} + \frac{(m_1^2 + m_2^2)\mu^2}{(\ell^2 - M^2)^3} + (\text{UV/IR convergent terms}) \\ &= -\frac{1}{3} \frac{\mu^2 (p^2 - 3(m_1^2 + m_2^2))}{(\ell^2 - M^2)^3} + (\text{UV/IR convergent terms}), \end{aligned} \quad (\text{A.66})$$

leading us to the expected result,

$$\mathcal{I}_2[\mu^2] = -\frac{1}{6} \frac{i}{(4\pi)^2} (p^2 - 3(m_1^2 + m_2^2)) + \mathcal{O}(\epsilon). \quad (\text{A.67})$$

We can automate the series expansion approach in *Mathematica*. Using the general results for the Passarino–Veltman reduction of tadpole integrals in eq. (A.54), we can obtain generic results for an arbitrary power of μ^2 in the numerator. Using the *Mathematica* method `FindSequenceFunction` and explicit values of $I_2[\mu^{2r}]$ up to $r = 40$, we find the following fitted form,

$$I_2[\mu^{2r}] = -\frac{1}{3} \frac{1}{2^{2r-1}} \frac{\Gamma(r)}{(\frac{5}{2})_{r-1}} (p^2)^r + \mathcal{O}(\epsilon). \quad (\text{A.68})$$

The denominator again contains the Pochhammer symbol from eq. (A.39). This expression correctly reproduces the result of eq. (A.63), while for μ^4 , μ^6 and μ^8 it evaluates to

$$\begin{aligned} I_2[\mu^4] &= -\frac{1}{60} (p^2)^2 + \mathcal{O}(\epsilon), \\ I_2[\mu^6] &= -\frac{1}{420} (p^2)^3 + \mathcal{O}(\epsilon), \\ I_2[\mu^8] &= -\frac{1}{2520} (p^2)^4 + \mathcal{O}(\epsilon). \end{aligned} \quad (\text{A.69})$$

Moving on to triangles and bubbles, deriving a general form becomes more complicated as the result will be a polynomial of multiple kinematic variables. Extending the automation in *Mathematica*,

we obtain for the triangles $I_3^D[\mu^4]$, $I_3^D[\mu^6]$ the forms,

$$\begin{aligned} I_3^D[\mu^4] &= -\frac{1}{24}(p_1^2 + p_2^2 + s_{12}) + \mathcal{O}(\epsilon), \\ I_3^D[\mu^6] &= -\frac{1}{180}((p_1^2)^2 + (p_2^2)^2 + p_1^2 p_2^2 + s_{12}(p_1^2 + p_2^2) + s_{12}^2) + \mathcal{O}(\epsilon). \end{aligned} \tag{A.70}$$

For the boxes $I_4^D[\mu^6]$, $I_4^D[\mu^8]$ we get,

$$\begin{aligned} I_4^D[\mu^6] &= -\frac{1}{60} \frac{i}{(4\pi)^2} (2s_{12} + 2s_{23} + s_{13}) + \mathcal{O}(\epsilon) \\ &= -\frac{1}{60} \frac{i}{(4\pi)^2} (p_1^2 + p_2^2 + p_3^2 + p_4^2 + s_{12} + s_{23}) + \mathcal{O}(\epsilon), \\ I_4^D[\mu^8] &= -\frac{1}{840} \frac{i}{(4\pi)^2} \left[2((p_1^2)^2 + (p_2^2)^2 + (p_3^2)^2 + (p_4^2)^2) \right. \\ &\quad + 2(p_1^2 p_2^2 + p_2^2 p_3^2 + p_3^2 p_4^2 + p_4^2 p_1^2) + 2(s_{12}^2 + s_{23}^2) \\ &\quad \left. + 2(s_{12} + s_{23})(p_1^2 + p_2^2 + p_3^2 + p_4^2) + p_1^2 p_3^2 + p_2^2 p_4^2 + s_{12} s_{23} \right] + \mathcal{O}(\epsilon). \end{aligned} \tag{A.71}$$

As a cross-check we can use the result for the easy two-mass box $I_4^D[\mu^8]$ from ref. [154], which the result above matches exactly for $p_2^2 = p_4^2 = 0$. As we go from bubbles to triangles to boxes we can also see a pattern emerging in the arrangement of the kinematic variables.

Appendix B

B.1 Scalar Tree Amplitudes

For unitarity cuts, in addition to the four-scalar tree amplitudes section 3.5.2 we require amplitudes with a single massive scalar pair. These are well known, and below we collect the ones relevant for the computations in this paper. For adjacent scalars and up to four gluons, we obtain these expressions from ref. [128]. Arbitrary-multiplicity expressions exist as well for the all-plus [155–158] and single-minus [155] helicity configurations. In the case of tree amplitudes with non-adjacent scalars we use Kleiss–Kuijf relations [57] to obtain them from adjacent-scalar ones.

We numerically verified all tree-amplitudes via Berends–Giele recursion.

$$A^{(0)}(1^\varphi 2^+ 3^+ 4^\varphi) = \frac{m^2}{s_{12}} \frac{[23]}{\langle 23 \rangle}, \quad (\text{B.1})$$

$$A^{(0)}(1^\varphi 2^+ 3^- 4^\varphi) = -\frac{\langle 3|1|2 \rangle \langle 3|4|2 \rangle}{s_{12}s_{23}}, \quad (\text{B.2})$$

$$A^{(0)}(1^\varphi 2^+ 3^+ 4^+ 5^\varphi) = -\frac{m^2 [4|(2+3)1|2]}{s_{12}s_{45} \langle 23 \rangle \langle 34 \rangle}, \quad (\text{B.3})$$

$$A^{(0)}(1^\varphi 2^+ 3^+ 4^- 5^\varphi) = -\frac{m^2 [23]^3}{s_{15} [34] [4|(2+3)1|2]} + \frac{\langle 4|5(2+3)1|2 \rangle^2}{s_{12}s_{45} \langle 23 \rangle \langle 34 \rangle [4|(2+3)1|2]}, \quad (\text{B.4})$$

$$A^{(0)}(1^\varphi 2^+ 3^- 4^+ 5^\varphi) = -\frac{m^2 [24]^4}{s_{15} [23] [34] [4|(2+3)1|2]} + \frac{\langle 3|1|2 \rangle^2 \langle 3|5|4 \rangle^2}{s_{12}s_{45} \langle 23 \rangle \langle 34 \rangle [4|(2+3)1|2]}, \quad (\text{B.5})$$

$$A^{(0)}(1^\varphi 2^+ 3^+ 4^+ 5^+ 6^\varphi) = -\frac{m^2 [5|6(4+5)(2+3)1|2]}{s_{12}s_{123}s_{56} \langle 23 \rangle \langle 34 \rangle \langle 45 \rangle}. \quad (\text{B.6})$$

For $A^{(0)}(1^\varphi 2^+ 3^+ 4^+ 5^- 6^\varphi)$ we have to flip the sign of the second term in the result of ref. [128] to match our own BCFW result, such that,

$$\begin{aligned} A^{(0)}(1^\varphi 2^+ 3^+ 4^+ 5^- 6^\varphi) &= \frac{(s_{123} \langle 5|6(2+3+4)1|2 \rangle - m^2 \langle 5|643|2 \rangle)^2}{s_{12}s_{123}s_{1234} \langle 23 \rangle \langle 34 \rangle \langle 45 \rangle [5|6(4+5)(2+3)1|2]} \\ &\quad - \frac{m^2 [4|(2+3)1|2]^3}{s_{12} \langle 23 \rangle \langle 3|(4+5)(1+6)1|2 \rangle [45] [5|6(4+5)(2+3)1|2]} \\ &\quad - \frac{m^2 \langle 5|(3+4)2 \rangle^3}{s_{2345}s_{345} \langle 34 \rangle \langle 45 \rangle \langle 3|(4+5)(1+6)1|2 \rangle}. \end{aligned} \quad (\text{B.7})$$

For $A^{(0)}(1^\varphi 2^+ 3^+ 4^- 5^+ 6^\varphi)$, we were not able to align the expression in eq.(3.21) of ref. [128] with our numerical result. While the last two lines of eq.(3.21) could be separately verified, as

they belong to the s_{234} and s_{16} channels in the BCFW computation, the first two lines belonging to the s_{23} channel do not match. We therefore replace these lines with our less compact result for this channel,

$$\begin{aligned}
A^{(0)}(1^\varphi 2^+ 3^+ 4^- 5^+ 6^\varphi) = & \\
& \frac{[23]}{s_{12} \langle 23 \rangle \left(\frac{s_{23} [2|1(1+2+3)(2+3)1|2][25]}{[2|13|2]} + [5|(2+3+4)(1+2+3)(2+3)1|2] \right)} \\
& \times \left[\frac{m^2 [5|(2+3)1|2]^4}{[4|(2+3)1|2][45](s_{16}[2|31|2] + s_{23}[2|61|2])} + \frac{\langle 4|(1+2+3)(2+3)1|2 \rangle^2 \langle 4|6|5 \rangle^2}{s_{123}s_{56} \langle 45 \rangle \langle 4|3|2]} \right] \\
& - \frac{m^2 \langle 4|(3+5)|2 \rangle^4}{s_{61}s_{345} \langle 34 \rangle \langle 45 \rangle \langle 3|(4+5)(1+6)1|2 \rangle \langle 5|(3+4)|2 \rangle} \\
& - \frac{m^2 [23]^3 [5|(1+6)1|2]}{s_{56}s_{234} \langle 5|(3+4)|2 \rangle [34] [4|(2+3)1|2]}. \tag{B.8}
\end{aligned}$$

For the seven-gluon rational contributions we also require scalar amplitudes with five positive helicity gluons. We obtained the adjacent scalar amplitude using the all-multiplicity form of ref. [158],

$$\begin{aligned}
A^{(0)}(1^\varphi 2^+ 3^+ 4^+ 5^+ 6^+ 7^\varphi) = & \\
& \frac{m^2 (-s_{23} [2|1(5+6+7)(5+6)7|6] + [2|1(2+3)1(2+3+4)(5+6)7|6])}{s_{12}s_{123}s_{567}s_{67} \langle 23 \rangle \langle 34 \rangle \langle 45 \rangle \langle 56 \rangle}, \tag{B.9}
\end{aligned}$$

while the non-adjacent scalar amplitudes are again obtained using Kleiss–Kuijf relations.

B.2 Analytic Expressions for $R_{5:1}^{(2)}$

Here we present the unsimplified result for $\tilde{R}_{5:1}^{(2)}$, obtained from the automated analytic computation described in section 3.7.2. The full two-loop rational part $R_{5:1}^{(2)}$ can be obtained from summing the expression over all cyclic permutations of the external momenta. For evaluation of the one-loop

squared cuts the momentum twistor parametrization of section 3.6 was used.

$$\begin{aligned}
& \tilde{R}_{5:1}^{(2)}(1^+2^+3^+4^+5^+) \\
&= -\frac{1}{18(s_{12}+s_{13})(s_{13}+s_{23})\langle 12 \rangle^3 \langle 13 \rangle^4 \langle 23 \rangle^2 \langle 25 \rangle^2 \langle 34 \rangle^2 \langle 35 \rangle^2 \langle 45 \rangle^3 \langle 51 \rangle} \\
&\times \left[-s_{12}(s_{12}+s_{13})(s_{13}+s_{23})\langle 15 \rangle^3 (\langle 13 \rangle^2 \langle 45 \rangle^2 ((s_{13}+s_{23})(11\langle 15 \rangle \langle 34 \rangle + 12\langle 13 \rangle \langle 45 \rangle)) \right. \\
&\quad - s_{12}\langle 15 \rangle \langle 34 \rangle) - 2s_{45}\langle 15 \rangle^2 \langle 34 \rangle^2 (7\langle 15 \rangle \langle 34 \rangle + 12\langle 13 \rangle \langle 45 \rangle) \langle 23 \rangle^5 \\
&\quad + s_{12}\langle 12 \rangle \langle 15 \rangle^2 \langle 35 \rangle (2(s_{13}+s_{23})(2s_{23}^2 + 31(s_{12}+s_{13})s_{23} \\
&\quad + (s_{12}+s_{13})(28s_{12}+29s_{13})) \langle 15 \rangle^3 \langle 34 \rangle^3 \\
&\quad + 2(s_{13}+s_{23})(2s_{23}^2 + 47(s_{12}+s_{13})s_{23} + (s_{12}+s_{13})(44s_{12}+45s_{13})) \langle 13 \rangle \langle 15 \rangle^2 \langle 45 \rangle \langle 34 \rangle^2 \\
&\quad + (s_{12}+s_{13})(-19s_{13}^2 - 58s_{23}s_{13} - 39s_{23}^2 + s_{12}(5s_{13}+9s_{23})) \langle 13 \rangle^2 \langle 15 \rangle \langle 45 \rangle^2 \langle 34 \rangle \\
&\quad - 12(s_{12}+s_{13})(s_{13}+s_{23})(2s_{13}+3s_{23}) \langle 13 \rangle^3 \langle 45 \rangle^3 \langle 23 \rangle^4 \\
&\quad + \langle 12 \rangle^2 \langle 15 \rangle \langle 35 \rangle^2 ((s_{13}+s_{23})((19s_{12}+11s_{13})s_{23}^2 + (s_{12}+s_{13})(111s_{12}+25s_{13})s_{23} \\
&\quad + 2(s_{12}+s_{13})(42s_{12}^2 + 51s_{13}s_{12} + 7s_{13}^2)) \langle 15 \rangle^3 \langle 34 \rangle^3 + 2(s_{13}+s_{23})(60s_{12}^3 \\
&\quad + 9s_{23}(8s_{12}+s_{23})s_{12} + 8s_{13}^3 + 13s_{13}^2(6s_{12}+s_{23}) \\
&\quad + 5s_{13}(26s_{12}^2 + 17s_{23}s_{12} + s_{23}^2)) \langle 13 \rangle \langle 15 \rangle^2 \langle 45 \rangle \langle 34 \rangle^2 + s_{12}(s_{12}+s_{13})(s_{12}(7s_{13}+15s_{23}) \\
&\quad - 2(s_{13}^2 + 25s_{23}s_{13} + 24s_{23}^2)) \langle 13 \rangle^2 \langle 15 \rangle \langle 45 \rangle^2 \langle 34 \rangle \\
&\quad - 6s_{12}(s_{12}+s_{13})(s_{13}^2 + 6s_{23}s_{13} + 5s_{23}^2) \langle 13 \rangle^3 \langle 45 \rangle^3 \langle 23 \rangle^3 \\
&\quad + \langle 12 \rangle^3 \langle 35 \rangle^3 (2(s_{13}+s_{23})((15s_{12}+13s_{13})s_{23}^2 + 7(s_{12}+s_{13})(7s_{12}+4s_{13})s_{23} \\
&\quad + (s_{12}+s_{13})(28s_{12}^2 + 43s_{13}s_{12} + 14s_{13}^2)) \langle 15 \rangle^3 \langle 34 \rangle^3 + 2(s_{13}+s_{23})(2(6s_{12}+5s_{13})s_{23}^2 \\
&\quad + (s_{12}+s_{13})(51s_{12}+26s_{13})s_{23} \\
&\quad + (s_{12}+s_{13})(36s_{12}^2 + 53s_{13}s_{12} + 16s_{13}^2)) \langle 13 \rangle \langle 15 \rangle^2 \langle 45 \rangle \langle 34 \rangle^2 \\
&\quad + s_{12}(s_{12}+s_{13})(-23s_{23}^2 + (7s_{12}-17s_{13})s_{23} + 3s_{13}(s_{12}+2s_{13})) \langle 13 \rangle^2 \langle 15 \rangle \langle 45 \rangle^2 \langle 34 \rangle \\
&\quad - 6s_{12}(s_{12}+s_{13})s_{23}(s_{13}+s_{23}) \langle 13 \rangle^3 \langle 45 \rangle^3 \langle 23 \rangle^2 \\
&\quad + (s_{12}+s_{13})(s_{13}+s_{23}) \langle 12 \rangle^4 \langle 34 \rangle \langle 35 \rangle^4 ((14(s_{12}+s_{13})^2 + 19s_{23}^2 \\
&\quad + (41s_{12}+37s_{13})s_{23}) \langle 15 \rangle^2 \langle 34 \rangle^2 + 2(8(s_{12}+s_{13})^2 + 5s_{23}^2 \\
&\quad + (14s_{12}+13s_{13})s_{23}) \langle 13 \rangle \langle 15 \rangle \langle 45 \rangle \langle 34 \rangle - 3s_{12}s_{23} \langle 13 \rangle^2 \langle 45 \rangle^2) \langle 23 \rangle \\
&\quad \left. + 2(s_{12}+s_{13})s_{23}(s_{13}+s_{23})(3s_{12}+3s_{13}+2s_{23}) \langle 12 \rangle^5 \langle 15 \rangle \langle 34 \rangle^3 \langle 35 \rangle^5 \right]
\end{aligned}
\tag{B.10}$$

Bibliography

- [1] Z. Bern et al. “One-Loop N Gluon Amplitudes with Maximal Helicity Violation via Collinear Limits”. In: *Physical Review Letters* 72.14 (Apr. 4, 1994), pp. 2134–2137. ISSN: 0031-9007. DOI: 10.1103/PhysRevLett.72.2134. arXiv: hep-ph/9312333.
- [2] Gregory Mahlon. “Multigluon Helicity Amplitudes Involving a Quark Loop”. In: *Physical Review D* 49.9 (May 1, 1994), pp. 4438–4453. ISSN: 0556-2821. DOI: 10.1103/PhysRevD.49.4438. arXiv: hep-ph/9312276.
- [3] Stefano Catani. “The Singular Behaviour of QCD Amplitudes at Two-Loop Order”. In: *Physics Letters B* 427.1-2 (May 1998), pp. 161–171. ISSN: 03702693. DOI: 10.1016/S0370-2693(98)00332-3. arXiv: hep-ph/9802439.
- [4] David C. Dunbar et al. “Color Dressed Unitarity and Recursion for Yang-Mills Two-Loop All-Plus Amplitudes”. In: *Physical Review D* 101.1 (Jan. 13, 2020), p. 016009. ISSN: 2470-0010, 2470-0029. DOI: 10.1103/PhysRevD.101.016009. arXiv: 1911.06547.
- [5] David C. Dunbar and Warren B. Perkins. “Two-Loop Six Gluon All plus Helicity Amplitude”. In: *Physical Review Letters* 117.6 (Aug. 4, 2016), p. 061602. ISSN: 0031-9007, 1079-7114. DOI: 10.1103/PhysRevLett.117.061602. arXiv: 1605.06351.
- [6] David C. Dunbar and Warren B. Perkins. “Two-Loop Five-Point All plus Helicity Yang-Mills Amplitude”. In: *Physical Review D* 93.8 (Apr. 21, 2016), p. 085029. ISSN: 2470-0010, 2470-0029. DOI: 10.1103/PhysRevD.93.085029. arXiv: 1603.07514.
- [7] David C. Dunbar, Guy R. Jehu, and Warren B. Perkins. “The Two-Loop n-Point All-plus Helicity Amplitude”. In: *Physical Review D* 93.12 (June 6, 2016), p. 125006. ISSN: 2470-0010, 2470-0029. DOI: 10.1103/PhysRevD.93.125006. arXiv: 1604.06631.
- [8] David C. Dunbar et al. “Analytic All-plus-Helicity Gluon Amplitudes in QCD”. In: *Physical Review D* 96.11 (Dec. 19, 2017), p. 116013. ISSN: 2470-0010, 2470-0029. DOI: 10.1103/PhysRevD.96.116013. arXiv: 1710.10071.
- [9] David C. Dunbar et al. *Analytic Results for Two-Loop Yang-Mills*. Dec. 14, 2017. arXiv: 1712.05312 [hep-ph]. URL: <http://arxiv.org/abs/1712.05312> (visited on 06/28/2021).
- [10] Adam R. Dalgleish et al. *The Full Color Two-Loop Six-Gluon All-Plus Helicity Amplitude*. Feb. 28, 2020. arXiv: 2003.00897 [hep-ph]. URL: <http://arxiv.org/abs/2003.00897> (visited on 04/15/2020).
- [11] Simon Badger, Gustav Mogull, and Tiziano Peraro. “Local Integrands for Two-Loop QCD Amplitudes”. In: *PoS LL2016* (July 1, 2016), p. 006. DOI: 10.22323/1.260.0006.

- [12] Simon Badger, Gustav Mogull, and Tiziano Peraro. “Local Integrands for Two-Loop All-plus Yang-Mills Amplitudes”. In: *Journal of High Energy Physics* 2016.8 (Aug. 2016), p. 63. ISSN: 1029-8479. DOI: 10.1007/JHEP08(2016)063. arXiv: 1606.02244.
- [13] Z. Bern, L. Dixon, and D. A. Kosower. “A Two-Loop Four-Gluon Helicity Amplitude in QCD”. In: *Journal of High Energy Physics* 2000.01 (Jan. 20, 2000), pp. 027–027. ISSN: 1029-8479. DOI: 10.1088/1126-6708/2000/01/027. arXiv: hep-ph/0001001.
- [14] E. W. N. Glover, C. Oleari, and M. E. Tejeda-Yeomans. “Two-Loop QCD Corrections to Gluon-Gluon Scattering”. In: *Nuclear Physics B* 605.1-3 (July 2001), pp. 467–485. ISSN: 05503213. DOI: 10.1016/S0550-3213(01)00210-3. arXiv: hep-ph/0102201.
- [15] Zvi Bern, Abilio De Freitas, and Lance Dixon. “Two-Loop Helicity Amplitudes for Gluon-Gluon Scattering in QCD and Supersymmetric Yang-Mills Theory”. Version 2. In: *Journal of High Energy Physics* 2002.03 (Mar. 8, 2002), pp. 018–018. ISSN: 1029-8479. DOI: 10.1088/1126-6708/2002/03/018. arXiv: hep-ph/0201161.
- [16] T. Gehrmann, J. M. Henn, and N. A. Lo Presti. “Analytic Form of the Two-Loop Planar Five-Gluon All-plus-Helicity Amplitude in QCD”. In: *Physical Review Letters* 116.6 (Feb. 8, 2016), p. 062001. ISSN: 0031-9007, 1079-7114. DOI: 10.1103/PhysRevLett.116.062001. arXiv: 1511.05409.
- [17] S. Badger et al. “Analytic Form of the Full Two-Loop Five-Gluon All-plus Helicity Amplitude”. In: *Physical Review Letters* 123.7 (Aug. 13, 2019), p. 071601. ISSN: 0031-9007, 1079-7114. DOI: 10.1103/PhysRevLett.123.071601. arXiv: 1905.03733.
- [18] David C. Dunbar, Warren B. Perkins, and Joseph M. W. Strong. “An n -Point QCD Two-Loop Amplitude”. In: *Physical Review D* 101.7 (Apr. 2, 2020), p. 076001. ISSN: 2470-0010, 2470-0029. DOI: 10.1103/PhysRevD.101.076001. arXiv: 2001.11347.
- [19] David C. Dunbar, James H. Eftle, and Warren B. Perkins. “Augmented Recursion For One-Loop Gravity Amplitudes”. In: *Journal of High Energy Physics* 2010.6 (June 2010), p. 27. ISSN: 1029-8479. DOI: 10.1007/JHEP06(2010)027. arXiv: 1003.3398.
- [20] Sam D. Alston, David C. Dunbar, and Warren B. Perkins. “Complex Factorisation and Recursion for One-Loop Amplitudes”. In: *Physical Review D* 86.8 (Oct. 10, 2012), p. 085022. ISSN: 1550-7998, 1550-2368. DOI: 10.1103/PhysRevD.86.085022. arXiv: 1208.0190.
- [21] David C. Dunbar and Warren B. Perkins. “The $\mathcal{N}=4$ Supergravity NMHV Six-Point One-Loop Amplitude”. In: *Physical Review D* 94.12 (Dec. 29, 2016), p. 125027. ISSN: 2470-0010, 2470-0029. DOI: 10.1103/PhysRevD.94.125027. arXiv: 1601.03918.
- [22] Sam D. Alston, David C. Dunbar, and Warren B. Perkins. “ n -Point Amplitudes with a Single Negative-Helicity Graviton”. In: *Physical Review D* 92.6 (Sept. 24, 2015), p. 065024. ISSN: 1550-7998, 1550-2368. DOI: 10.1103/PhysRevD.92.065024. arXiv: 1507.08882.
- [23] Z. Bern et al. “One-Loop n -Point Gauge Theory Amplitudes, Unitarity and Collinear Limits”. In: *Nuclear Physics B* 425.1-2 (Aug. 1994), pp. 217–260. ISSN: 05503213. DOI: 10.1016/0550-3213(94)90179-1. arXiv: hep-ph/9403226.
- [24] Z. Bern et al. “Fusing Gauge Theory Tree Amplitudes Into Loop Amplitudes”. In: *Nuclear Physics B* 435.1-2 (Feb. 1995), pp. 59–101. ISSN: 05503213. DOI: 10.1016/0550-3213(94)00488-Z. arXiv: hep-ph/9409265.

- [25] Ruth Britto, Freddy Cachazo, and Bo Feng. “Generalized Unitarity and One-Loop Amplitudes in N=4 Super-Yang-Mills”. In: *Nuclear Physics B* 725.1-2 (Oct. 2005), pp. 275–305. ISSN: 05503213. DOI: 10.1016/j.nuclphysb.2005.07.014. arXiv: hep-th/0412103.
- [26] Charalampos Anastasiou et al. “D-Dimensional Unitarity Cut Method”. In: *Physics Letters B* 645.2-3 (Feb. 2007), pp. 213–216. ISSN: 03702693. DOI: 10.1016/j.physletb.2006.12.022. arXiv: hep-ph/0609191.
- [27] R. E. Cutkosky. “Singularities and Discontinuities of Feynman Amplitudes”. In: *Journal of Mathematical Physics* 1.5 (Sept. 1, 1960), pp. 429–433. ISSN: 0022-2488. DOI: 10.1063/1.1703676.
- [28] C. F. Berger et al. “One-Loop Calculations with BlackHat”. In: *Nuclear Physics B - Proceedings Supplements* 183 (Oct. 2008), pp. 313–319. ISSN: 09205632. DOI: 10.1016/j.nuclphysbps.2008.09.123. arXiv: 0807.3705.
- [29] Z. Bern et al. *The BlackHat Library for One-Loop Amplitudes*. Oct. 16, 2013. DOI: 10.1088/1742-6596/523/1/012051. arXiv: 1310.2808 [hep-ph]. URL: <http://arxiv.org/abs/1310.2808> (visited on 11/23/2020).
- [30] Giovanni Ossola, Costas G. Papadopoulos, and Roberto Pittau. “Reducing Full One-Loop Amplitudes to Scalar Integrals at the Integrand Level”. In: *Nucl.Phys.B763:147-169,2007* (Sept. 1, 2006). DOI: 10.1016/j.nuclphysb.2006.11.012. arXiv: hep-ph/0609007v2.
- [31] Giovanni Ossola, Costas G. Papadopoulos, and Roberto Pittau. “CutTools: A Program Implementing the OPP Reduction Method to Compute One-Loop Amplitudes”. In: *Journal of High Energy Physics* 2008.03 (Mar. 13, 2008), pp. 042–042. ISSN: 1029-8479. DOI: 10.1088/1126-6708/2008/03/042. arXiv: 0711.3596.
- [32] W. T. Giele and G. Zanderighi. *On the Numerical Evaluation of One-Loop Amplitudes: The Gluonic Case*. June 19, 2008. DOI: 10.1088/1126-6708/2008/06/038. arXiv: 0805.2152 [hep-ph]. URL: <http://arxiv.org/abs/0805.2152> (visited on 11/23/2020).
- [33] A. van Hameren, C. G. Papadopoulos, and R. Pittau. “Automated One-Loop Calculations: A Proof of Concept”. In: *Journal of High Energy Physics* 2009.09 (Sept. 25, 2009), pp. 106–106. ISSN: 1029-8479. DOI: 10.1088/1126-6708/2009/09/106. arXiv: 0903.4665.
- [34] Fabio Cascioli, Philipp Maierhöfer, and Stefano Pozzorini. “Scattering Amplitudes with Open Loops”. In: *Physical Review Letters* 108.11 (Mar. 12, 2012), p. 111601. ISSN: 0031-9007, 1079-7114. DOI: 10.1103/PhysRevLett.108.111601. arXiv: 1111.5206.
- [35] Federico Buccioni et al. “OpenLoops 2”. In: *The European Physical Journal C* 79.10 (Oct. 2019), p. 866. ISSN: 1434-6044, 1434-6052. DOI: 10.1140/epjc/s10052-019-7306-2. arXiv: 1907.13071.
- [36] Simon Badger et al. “Numerical Evaluation of Virtual Corrections to Multi-Jet Production in Massless QCD”. In: *Computer Physics Communications* 184.8 (Aug. 2013), pp. 1981–1998. ISSN: 00104655. DOI: 10.1016/j.cpc.2013.03.018. arXiv: 1209.0100.
- [37] S. Abreu et al. “Planar Two-Loop Five-Parton Amplitudes from Numerical Unitarity”. In: *Journal of High Energy Physics* 2018.11 (Nov. 2018), p. 116. ISSN: 1029-8479. DOI: 10.1007/JHEP11(2018)116. arXiv: 1809.09067.

- [38] Samuel Abreu et al. “Planar Two-Loop Five-Gluon Amplitudes from Numerical Unitarity”. In: *Physical Review D* 97.11 (June 20, 2018), p. 116014. ISSN: 2470-0010, 2470-0029. DOI: 10.1103/PhysRevD.97.116014. arXiv: 1712.03946.
- [39] S. Abreu et al. “Two-Loop Four-Gluon Amplitudes with the Numerical Unitarity Method”. In: *Physical Review Letters* 119.14 (Oct. 5, 2017), p. 142001. ISSN: 0031-9007, 1079-7114. DOI: 10.1103/PhysRevLett.119.142001. arXiv: 1703.05273.
- [40] S. Abreu et al. *Leading-Color Two-Loop QCD Corrections for Three-Jet Production at Hadron Colliders*. Apr. 21, 2021. arXiv: 2102.13609 [hep-ph]. URL: <http://arxiv.org/abs/2102.13609> (visited on 06/27/2021).
- [41] C. N. Yang and R. L. Mills. “Conservation of Isotopic Spin and Isotopic Gauge Invariance”. In: *Physical Review* 96.1 (Oct. 1, 1954), pp. 191–195. DOI: 10.1103/PhysRev.96.191.
- [42] Michael E. Peskin and Daniel V. Schroeder. *An Introduction to Quantum Field Theory*. Addison-Wesley, Reading, USA, 1995. ISBN: 978-0-201-50397-5 0-201-50397-2.
- [43] A. Zee. *Quantum Field Theory in a Nutshell*. 2003. ISBN: 978-0-691-14034-6.
- [44] M. Srednicki. *Quantum Field Theory*. Cambridge University Press, Jan. 2007. ISBN: 978-0-521-86449-7 978-0-511-26720-8.
- [45] Matthew D. Schwartz. *Quantum Field Theory and the Standard Model*. Cambridge University Press, Mar. 2014. ISBN: 978-1-107-03473-0.
- [46] L. D. Faddeev and V. N. Popov. “Feynman Diagrams for the Yang-Mills Field”. In: *Physics Letters B* 25.1 (July 24, 1967), pp. 29–30. ISSN: 0370-2693. DOI: 10.1016/0370-2693(67)90067-6.
- [47] Henriette Elvang and Yu-tin Huang. *Scattering Amplitudes*. Aug. 7, 2013. arXiv: 1308.1697.
- [48] Johannes M. Henn and Jan C. Plefka. *Scattering Amplitudes in Gauge Theories*. Vol. 883. Lecture Notes in Physics. Berlin, Heidelberg: Springer Berlin Heidelberg, 2014. ISBN: 978-3-642-54021-9 978-3-642-54022-6. DOI: 10.1007/978-3-642-54022-6.
- [49] Zhan Xu, Da-Hua Zhang, and Lee Chang. “Helicity Amplitudes for Multiple Bremsstrahlung in Massless Non-Abelian Gauge Theories”. In: *Nuclear Physics B* 291 (Jan. 1, 1987), pp. 392–428. ISSN: 0550-3213. DOI: 10.1016/0550-3213(87)90479-2.
- [50] Paolo Benincasa and Freddy Cachazo. *Consistency Conditions on the S-Matrix of Massless Particles*. Jan. 17, 2008. arXiv: 0705.4305 [hep-th]. URL: <http://arxiv.org/abs/0705.4305> (visited on 08/02/2021).
- [51] Nima Arkani-Hamed, Tzu-Chen Huang, and Yu-tin Huang. *Scattering Amplitudes For All Masses and Spins*. Sept. 14, 2017. arXiv: 1709.04891 [hep-th]. URL: <http://arxiv.org/abs/1709.04891> (visited on 05/21/2020).
- [52] Stephen J. Parke and T. R. Taylor. “An Amplitude for n Gluon Scattering”. In: *Phys. Rev. Lett.* 56 (1986), p. 2459. DOI: 10.1103/PhysRevLett.56.2459.
- [53] Michelangelo L. Mangano, Stephen J. Parke, and Zhan Xu. “Duality and Multi - Gluon Scattering”. In: *Nucl. Phys. B* 298 (1988), pp. 653–672. DOI: 10.1016/0550-3213(88)90001-6.
- [54] Frits A. Berends and W. T. Giele. “Recursive Calculations for Processes with n Gluons”. In: *Nucl. Phys. B* 306 (1988), pp. 759–808. DOI: 10.1016/0550-3213(88)90442-7.

- [55] Zvi Bern, Vittorio Del Duca, and Carl R. Schmidt. “The Infrared Behavior of One-Loop Gluon Amplitudes at Next-to-Next-to-Leading Order”. In: *Physics Letters B* 445.1-2 (Dec. 1998), pp. 168–177. ISSN: 03702693. DOI: 10.1016/S0370-2693(98)01495-6. arXiv: hep-ph/9810409.
- [56] Z. Bern et al. *The Infrared Behavior of One-Loop QCD Amplitudes at Next-to-Next-to-Leading Order*. Dec. 27, 1999. DOI: 10.1103/PhysRevD.60.116001. arXiv: hep-ph/9903516. URL: <http://arxiv.org/abs/hep-ph/9903516> (visited on 03/09/2021).
- [57] Ronald Kleiss and Hans Kuijf. “Multigluon Cross Sections and 5-Jet Production at Hadron Colliders”. In: *Nuclear Physics B* 312.3 (Jan. 1989), pp. 616–644. ISSN: 05503213. DOI: 10.1016/0550-3213(89)90574-9.
- [58] Ruth Britto, Freddy Cachazo, and Bo Feng. “New Recursion Relations for Tree Amplitudes of Gluons”. In: *Nuclear Physics B* 715.1-2 (May 2005), pp. 499–522. ISSN: 05503213. DOI: 10.1016/j.nuclphysb.2005.02.030. arXiv: hep-th/0412308.
- [59] Ruth Britto et al. “Direct Proof Of Tree-Level Recursion Relation In Yang-Mills Theory”. In: *Physical Review Letters* 94.18 (May 10, 2005), p. 181602. ISSN: 0031-9007, 1079-7114. DOI: 10.1103/PhysRevLett.94.181602. arXiv: hep-th/0501052.
- [60] Carola F. Berger et al. “Bootstrapping One-Loop QCD Amplitudes with General Helicities”. In: *Physical Review D* 74.3 (Aug. 31, 2006), p. 036009. ISSN: 1550-7998, 1550-2368. DOI: 10.1103/PhysRevD.74.036009. arXiv: hep-ph/0604195.
- [61] C. Itzykson and J. B. Zuber. *Quantum Field Theory*. International Series In Pure and Applied Physics. New York: McGraw-Hill, 1980. ISBN: 978-0-486-44568-7 0-486-44568-2.
- [62] Christian Bogner and Stefan Weinzierl. “Feynman Graph Polynomials”. In: *International Journal of Modern Physics A* 25.13 (May 20, 2010), pp. 2585–2618. ISSN: 0217-751X, 1793-656X. DOI: 10.1142/S0217751X10049438. arXiv: 1002.3458.
- [63] L. D. Landau. “On Analytic Properties of Vertex Parts in Quantum Field Theory”. In: *Nuclear Physics* 13.1 (Oct. 1, 1959), pp. 181–192. ISSN: 0029-5582. DOI: 10.1016/0029-5582(59)90154-3.
- [64] T. Kinoshita. “Mass Singularities of Feynman Amplitudes”. In: *J. Math. Phys.* 3 (1962), pp. 650–677. DOI: 10.1063/1.1724268.
- [65] Charalampos Anastasiou and George Sterman. “Removing Infrared Divergences from Two-Loop Integrals”. In: *Journal of High Energy Physics* 2019.7 (July 2019), p. 56. ISSN: 1029-8479. DOI: 10.1007/JHEP07(2019)056. arXiv: 1812.03753.
- [66] Yuri L. Dokshitzer et al. *Basics of Perturbative QCD*. 1991.
- [67] T. D. Lee and M. Nauenberg. “Degenerate Systems and Mass Singularities”. In: *Phys. Rev.* 133 (1964), B1549–B1562. DOI: 10.1103/PhysRev.133.B1549.
- [68] K. G. Chetyrkin and F. V. Tkachov. “Integration by Parts: The Algorithm to Calculate Beta Functions in 4 Loops”. In: *Nucl. Phys.* B192 (1981), pp. 159–204. DOI: 10.1016/0550-3213(81)90199-1.
- [69] S. Laporta. “High-Precision Calculation of Multi-Loop Feynman Integrals by Difference Equations”. In: *International Journal of Modern Physics A* 15 (2000), p. 5087. ISSN: 0217751X. DOI: 10.1016/S0217-751X(00)00215-7. arXiv: hep-ph/0102033.

- [70] Janusz Gluza, Krzysztof Kajda, and David A. Kosower. “Towards a Basis for Planar Two-Loop Integrals”. In: *Physical Review D* 83.4 (Feb. 15, 2011), p. 045012. ISSN: 1550-7998, 1550-2368. DOI: 10.1103/PhysRevD.83.045012. arXiv: 1009.0472.
- [71] R. N. Lee. “Group Structure of the Integration-by-Part Identities and Its Application to the Reduction of Multiloop Integrals”. In: *Journal of High Energy Physics* 2008.07 (July 8, 2008), pp. 031–031. ISSN: 1029-8479. DOI: 10.1088/1126-6708/2008/07/031. arXiv: 0804.3008.
- [72] C. Studerus. “Reduze - Feynman Integral Reduction in C++”. In: *Computer Physics Communications* 181.7 (July 2010), pp. 1293–1300. ISSN: 00104655. DOI: 10.1016/j.cpc.2010.03.012. arXiv: 0912.2546.
- [73] A. von Manteuffel and C. Studerus. *Reduze 2 - Distributed Feynman Integral Reduction*. Jan. 20, 2012. arXiv: 1201.4330 [hep-ph, physics:hep-th, physics:physics]. URL: <http://arxiv.org/abs/1201.4330> (visited on 07/28/2021).
- [74] C. Anastasiou and A. Lazopoulos. “Automatic Integral Reduction for Higher Order Perturbative Calculations”. In: *Journal of High Energy Physics* 2004.07 (July 21, 2004), pp. 046–046. ISSN: 1029-8479. DOI: 10.1088/1126-6708/2004/07/046. arXiv: hep-ph/0404258.
- [75] Philipp Maierhoefer, Johann Usovitsch, and Peter Uwer. “Kira - A Feynman Integral Reduction Program”. In: *Computer Physics Communications* 230 (Sept. 2018), pp. 99–112. ISSN: 00104655. DOI: 10.1016/j.cpc.2018.04.012. arXiv: 1705.05610.
- [76] Jonas Klappert et al. “Integral Reduction with Kira 2.0 and Finite Field Methods”. In: *Computer Physics Communications* 266 (Sept. 2021), p. 108024. ISSN: 00104655. DOI: 10.1016/j.cpc.2021.108024. arXiv: 2008.06494.
- [77] Philipp Maierhöfer and Johann Usovitsch. *Kira 1.2 Release Notes*. Dec. 4, 2018. arXiv: 1812.01491 [hep-ph]. URL: <http://arxiv.org/abs/1812.01491> (visited on 07/28/2021).
- [78] A. V. Smirnov. “An Algorithm to Construct Groebner Bases for Solving Integration by Parts Relations”. In: *Journal of High Energy Physics* 2006.04 (Apr. 13, 2006), pp. 026–026. ISSN: 1029-8479. DOI: 10.1088/1126-6708/2006/04/026. arXiv: hep-ph/0602078.
- [79] A. V. Smirnov. “Algorithm FIRE – Feynman Integral REduction”. In: *Journal of High Energy Physics* 2008.10 (Oct. 29, 2008), pp. 107–107. ISSN: 1029-8479. DOI: 10.1088/1126-6708/2008/10/107. arXiv: 0807.3243.
- [80] A. V. Smirnov and V. A. Smirnov. “FIRE4, LiteRed and Accompanying Tools to Solve Integration by Parts Relations”. In: *Computer Physics Communications* 184.12 (Dec. 2013), pp. 2820–2827. ISSN: 00104655. DOI: 10.1016/j.cpc.2013.06.016. arXiv: 1302.5885.
- [81] A. V. Smirnov and F. S. Chukharev. “FIRE6: Feynman Integral REduction with Modular Arithmetic”. In: *Computer Physics Communications* 247 (Feb. 2020), p. 106877. ISSN: 00104655. DOI: 10.1016/j.cpc.2019.106877. arXiv: 1901.07808.
- [82] Zvi Bern and David A. Kosower. “Color Decomposition of One-Loop Amplitudes in Gauge Theories”. In: *Nuclear Physics B* 362.1 (Sept. 16, 1991), pp. 389–448. ISSN: 0550-3213. DOI: 10.1016/0550-3213(91)90567-H.
- [83] Z. Bern, L. Dixon, and D. A. Kosower. “One-Loop Corrections to Two-Quark Three-Gluon Amplitudes”. In: *Nuclear Physics B* 437.2 (Mar. 1995), pp. 259–304. ISSN: 05503213. DOI: 10.1016/0550-3213(94)00542-M. arXiv: hep-ph/9409393.

- [84] Z. Bern, L. Dixon, and D. A. Kosower. “Dimensionally Regulated Pentagon Integrals”. In: *Nuclear Physics B* 412.3 (Jan. 1994), pp. 751–816. ISSN: 05503213. DOI: 10.1016/0550-3213(94)90398-0. arXiv: hep-ph/9306240.
- [85] G. Passarino and M. J. G. Veltman. “One Loop Corrections for e^+e^- Annihilation Into $\mu^+\mu^-$ in the Weinberg Model”. In: *Nucl. Phys.* B160 (1979), pp. 151–207. DOI: 10.1016/0550-3213(79)90234-7.
- [86] A. Denner and S. Dittmaier. “Reduction Schemes for One-Loop Tensor Integrals”. In: *Nuclear Physics B* 734.1-2 (Jan. 2006), pp. 62–115. ISSN: 05503213. DOI: 10.1016/j.nuclphysb.2005.11.007. arXiv: hep-ph/0509141.
- [87] J. Ohnemus and J. F. Owens. “Order- α_s Calculation of Hadronic ZZ Production”. In: *Physical Review D* 43.11 (June 1, 1991), pp. 3626–3639. DOI: 10.1103/PhysRevD.43.3626.
- [88] A. Denner, U. Nierste, and R. Scharf. “A Compact Expression for the Scalar One-Loop Four-Point Function”. In: *Nuclear Physics B* 367.3 (Dec. 30, 1991), pp. 637–656. ISSN: 0550-3213. DOI: 10.1016/0550-3213(91)90011-L.
- [89] R. Keith Ellis and Giulia Zanderighi. “Scalar One-Loop Integrals for QCD”. In: *Journal of High Energy Physics* 2008.02 (Feb. 1, 2008), pp. 002–002. ISSN: 1029-8479. DOI: 10.1088/1126-6708/2008/02/002. arXiv: 0712.1851.
- [90] Hung Jung Lu and Christopher A. Perez. “Massless One Loop Scalar Three Point Integral and Associated Clausen, Glaisher and L Functions”. In: *SLAC-PUB-5809* (May 1992).
- [91] Z. Bern, L. Dixon, and D. A. Kosower. “One-Loop Amplitudes for E^+E^- to Four Partons”. In: *Nuclear Physics B* 513.1-2 (Mar. 1998), pp. 3–86. ISSN: 05503213. DOI: 10.1016/S0550-3213(97)00703-7. arXiv: hep-ph/9708239.
- [92] Spencer Bloch and Dirk Kreimer. *Cutkosky Rules and Outer Space*. Dec. 5, 2015. arXiv: 1512.01705 [hep-th]. URL: <http://arxiv.org/abs/1512.01705> (visited on 07/13/2021).
- [93] C. Vergu. “On the Factorisation of the Connected Prescription for Yang-Mills Amplitudes”. In: *Physical Review D* 75.2 (Jan. 31, 2007), p. 025028. ISSN: 1550-7998, 1550-2368. DOI: 10.1103/PhysRevD.75.025028. arXiv: hep-th/0612250.
- [94] Samuel Abreu et al. “Cuts from Residues: The One-Loop Case”. In: *Journal of High Energy Physics* 2017.6 (June 2017), p. 114. ISSN: 1029-8479. DOI: 10.1007/JHEP06(2017)114. arXiv: 1702.03163.
- [95] Darren Forde. “Direct Extraction of One-Loop Integral Coefficients”. In: *Physical Review D* 75.12 (June 19, 2007), p. 125019. ISSN: 1550-7998, 1550-2368. DOI: 10.1103/PhysRevD.75.125019. arXiv: 0704.1835.
- [96] S. D. Badger. “Direct Extraction Of One Loop Rational Terms”. In: *Journal of High Energy Physics* 2009.01 (Jan. 20, 2009), pp. 049–049. ISSN: 1029-8479. DOI: 10.1088/1126-6708/2009/01/049. arXiv: 0806.4600.
- [97] William B. Kilgore. *One-Loop Integral Coefficients from Generalized Unitarity*. May 11, 2008. arXiv: 0711.5015 [hep-ph]. URL: <http://arxiv.org/abs/0711.5015> (visited on 01/27/2020).

- [98] Charalampos Anastasiou et al. “Unitarity Cuts and Reduction to Master Integrals in d Dimensions for One-Loop Amplitudes”. In: *JHEP 0703:111,2007* (Dec. 21, 2006). DOI: 10.1088/1126-6708/2007/03/111. arXiv: hep-ph/0612277v2.
- [99] Ruth Britto and Bo Feng. “Unitarity Cuts with Massive Propagators and Algebraic Expressions for Coefficients”. In: *Phys.Rev.D75:105006,2007* (Dec. 7, 2006). DOI: 10.1103/PhysRevD.75.105006. arXiv: hep-ph/0612089v3.
- [100] Ruth Britto and Bo Feng. “Integral Coefficients for One-Loop Amplitudes”. In: *Journal of High Energy Physics* 2008.02 (Feb. 26, 2008), pp. 095–095. ISSN: 1029-8479. DOI: 10.1088/1126-6708/2008/02/095. arXiv: 0711.4284.
- [101] Ruth Britto, Bo Feng, and Pierpaolo Mastrolia. “Closed-Form Decomposition of One-Loop Massive Amplitudes”. In: *Physical Review D* 78.2 (July 28, 2008), p. 025031. ISSN: 1550-7998, 1550-2368. DOI: 10.1103/PhysRevD.78.025031. arXiv: 0803.1989.
- [102] Andreas Brandhuber et al. “Loop Amplitudes in Pure Yang-Mills from Generalised Unitarity”. In: *Journal of High Energy Physics* 2005.10 (Oct. 4, 2005), pp. 011–011. ISSN: 1029-8479. DOI: 10.1088/1126-6708/2005/10/011. arXiv: hep-th/0506068.
- [103] Andreas Brandhuber and Massimiliano Vincon. “MHV One-Loop Amplitudes in Yang-Mills from Generalised Unitarity”. In: *Journal of High Energy Physics* 2008.11 (Nov. 25, 2008), pp. 078–078. ISSN: 1029-8479. DOI: 10.1088/1126-6708/2008/11/078. arXiv: 0805.3310.
- [104] Z. Bern et al. “One-Loop Self-Dual and $N=4$ Super Yang-Mills”. In: *Physics Letters B* 394.1-2 (Feb. 1997), pp. 105–115. ISSN: 03702693. DOI: 10.1016/S0370-2693(96)01676-0. arXiv: hep-th/9611127.
- [105] Z. Bern and A. G. Morgan. “Massive Loop Amplitudes from Unitarity”. In: *Nuclear Physics B* 467.3 (May 1996), pp. 479–509. ISSN: 05503213. DOI: 10.1016/0550-3213(96)00078-8. arXiv: hep-ph/9511336.
- [106] Walter Giele, Zoltan Kunszt, and Jan Winter. “Efficient Color-Dressed Calculation of Virtual Corrections”. In: *Nuclear Physics B* 840.1-2 (Nov. 2010), pp. 214–270. ISSN: 05503213. DOI: 10.1016/j.nuclphysb.2010.07.007. arXiv: 0911.1962.
- [107] Manuel Accettulli Huber et al. *Complete Form Factors in Yang-Mills from Unitarity and Spinor Helicity in Six Dimensions*. Oct. 10, 2019. arXiv: 1910.04772 [hep-ph, physics:hep-th]. URL: <http://arxiv.org/abs/1910.04772> (visited on 11/03/2019).
- [108] Wolfram Research. *PossibleZeroQ*. 2007. URL: <https://reference.wolfram.com/language/ref/PossibleZeroQ.html> (visited on 07/27/2021).
- [109] W. T. Giele and E. W. N. Glover. “Higher-Order Corrections to Jet Cross Sections in e^+e^- Annihilation”. In: *Physical Review D* 46.5 (Sept. 1, 1992), pp. 1980–2010. DOI: 10.1103/PhysRevD.46.1980.
- [110] Zoltan Kunszt, Adrian Signer, and Zoltan Trocsanyi. “Singular Terms of Helicity Amplitudes at One-Loop in QCD and the Soft Limit of the Cross Sections of Multi-Parton Processes”. In: *Nuclear Physics B* 420.3 (June 1994), pp. 550–564. ISSN: 05503213. DOI: 10.1016/0550-3213(94)90077-9. arXiv: hep-ph/9401294.
- [111] Stefano Catani and Michael H. Seymour. “A General Algorithm for Calculating Jet Cross Sections in NLO QCD”. In: *Nuclear Physics B* 485.1-2 (Feb. 1997), pp. 291–419. ISSN: 05503213. DOI: 10.1016/S0550-3213(96)00589-5. arXiv: hep-ph/9605323.

- [112] Zvi Bern, Lance J. Dixon, and David A. Kosower. “On-Shell Recurrence Relations for One-Loop QCD Amplitudes”. In: *Physical Review D* 71.10 (May 18, 2005), p. 105013. ISSN: 1550-7998, 1550-2368. DOI: 10.1103/PhysRevD.71.105013. arXiv: hep-th/0501240.
- [113] Kasper Risager. “A Direct Proof of the CSW Rules”. In: *Journal of High Energy Physics* 2005.12 (Dec. 1, 2005), pp. 003–003. ISSN: 1029-8479. DOI: 10.1088/1126-6708/2005/12/003. arXiv: hep-th/0508206.
- [114] Ruth Britto, Guy R. Jehu, and Andrea Orta. *The Dimension-Shift Conjecture for One-Loop Amplitudes*. Nov. 27, 2020. arXiv: 2011.13821 [hep-th]. URL: <http://arxiv.org/abs/2011.13821> (visited on 02/07/2021).
- [115] Simon Badger, Hjalte Frellesvig, and Yang Zhang. “A Two-Loop Five-Gluon Helicity Amplitude in QCD”. In: *Journal of High Energy Physics* 2013.12 (Dec. 2013), p. 45. ISSN: 1029-8479. DOI: 10.1007/JHEP12(2013)045. arXiv: 1310.1051.
- [116] Simon Badger et al. “A Complete Two-Loop, Five-Gluon Helicity Amplitude in Yang-Mills Theory”. In: *Journal of High Energy Physics* 2015.10 (Oct. 2015), p. 64. ISSN: 1029-8479. DOI: 10.1007/JHEP10(2015)064. arXiv: 1507.08797.
- [117] Nima Arkani-Hamed et al. “Local Integrals for Planar Scattering Amplitudes”. In: *Journal of High Energy Physics* 2012.6 (June 2012), p. 125. ISSN: 1029-8479. DOI: 10.1007/JHEP06(2012)125. arXiv: 1012.6032.
- [118] Nima Arkani-Hamed et al. “The All-Loop Integrand For Scattering Amplitudes in Planar $N=4$ SYM”. In: *Journal of High Energy Physics* 2011.1 (Jan. 2011), p. 41. ISSN: 1029-8479. DOI: 10.1007/JHEP01(2011)041. arXiv: 1008.2958.
- [119] Zvi Bern and David A. Kosower. “The Computation of Loop Amplitudes in Gauge Theories”. In: *Nuclear Physics B* 379.3 (July 27, 1992), pp. 451–561. ISSN: 0550-3213. DOI: 10.1016/0550-3213(92)90134-W.
- [120] Gerard 't Hooft and M. J. G. Veltman. “Regularization and Renormalization of Gauge Fields”. In: *Nucl. Phys.* B44 (1972), pp. 189–213. DOI: 10.1016/0550-3213(72)90279-9.
- [121] Z. Bern et al. “Supersymmetric Regularization, Two-Loop QCD Amplitudes and Coupling Shifts”. In: *Physical Review D* 66.8 (Oct. 10, 2002), p. 085002. ISSN: 0556-2821, 1089-4918. DOI: 10.1103/PhysRevD.66.085002. arXiv: hep-ph/0202271.
- [122] Walter T. Giele, Zoltan Kunszt, and Kirill Melnikov. “Full One-Loop Amplitudes from Tree Amplitudes”. In: *Journal of High Energy Physics* 2008.04 (Apr. 14, 2008), pp. 049–049. ISSN: 1029-8479. DOI: 10.1088/1126-6708/2008/04/049. arXiv: 0801.2237.
- [123] Th. Kaluza. “On the Unification Problem in Physics”. In: *International Journal of Modern Physics D* 27.14 (Oct. 1, 2018), p. 1870001. ISSN: 0218-2718. DOI: 10.1142/S0218271818700017.
- [124] Oskar Klein. “Quantentheorie und fünfdimensionale Relativitätstheorie”. In: *Zeitschrift für Physik* 37.12 (Dec. 1, 1926), pp. 895–906. ISSN: 0044-3328. DOI: 10.1007/BF01397481.
- [125] Clifford Cheung and Donal O’Connell. “Amplitudes and Spinor-Helicity in Six Dimensions”. In: *Journal of High Energy Physics* 2009.07 (July 21, 2009), pp. 075–075. ISSN: 1029-8479. DOI: 10.1088/1126-6708/2009/07/075. arXiv: 0902.0981.
- [126] Zvi Bern et al. “Generalized Unitarity and Six-Dimensional Helicity”. In: *Physical Review D* 83.8 (Apr. 21, 2011), p. 085022. ISSN: 1550-7998, 1550-2368. DOI: 10.1103/PhysRevD.83.085022. arXiv: 1010.0494.

- [127] John Joseph M. Carrasco and Ingrid A. Vazquez-Holm. “Loop-Level Double-Copy for Massive Quantum Particles”. In: *Physical Review D* 103.4 (Feb. 3, 2021), p. 045002. ISSN: 2470-0010, 2470-0029. DOI: 10.1103/PhysRevD.103.045002. arXiv: 2010.13435.
- [128] S. D. Badger et al. “Recursion Relations for Gauge Theory Amplitudes with Massive Particles”. In: *Journal of High Energy Physics* 2005.07 (July 14, 2005), pp. 025–025. ISSN: 1029-8479. DOI: 10.1088/1126-6708/2005/07/025. arXiv: hep-th/0504159.
- [129] Christian Schwinn and Stefan Weinzierl. “On-Shell Recursion Relations for All Born QCD Amplitudes”. In: *Journal of High Energy Physics* 2007.04 (Apr. 23, 2007), pp. 072–072. ISSN: 1029-8479. DOI: 10.1088/1126-6708/2007/04/072. arXiv: hep-ph/0703021.
- [130] David A. Kosower. “Next-to-Maximal Helicity Violating Amplitudes in Gauge Theory”. In: *Physical Review D* 71.4 (Feb. 11, 2005), p. 045007. ISSN: 1550-7998, 1550-2368. DOI: 10.1103/PhysRevD.71.045007. arXiv: hep-th/0406175.
- [131] Andrew Hodges. *Eliminating Spurious Poles from Gauge-Theoretic Amplitudes*. May 11, 2009. arXiv: 0905.1473. URL: <http://arxiv.org/abs/0905.1473> (visited on 05/21/2020).
- [132] Lucy Budge et al. *The One-Loop Amplitudes for Higgs + 4 Partons with Full Mass Effects*. Feb. 27, 2020. arXiv: 2002.04018 [hep-ph]. URL: <http://arxiv.org/abs/2002.04018> (visited on 03/03/2020).
- [133] Simon Badger. “Automating QCD Amplitudes with On-Shell Methods”. In: *Journal of Physics: Conference Series* 762 (Oct. 2016), p. 012057. ISSN: 1742-6588, 1742-6596. DOI: 10.1088/1742-6596/762/1/012057. arXiv: 1605.02172.
- [134] Francesco Buciuni. “Applications of Modern Methods for Scattering Amplitudes”. PhD thesis. Durham U., Dept. of Math., 2018.
- [135] Alexander C. Edison and Stephen G. Naculich. “SU(N) Group-Theory Constraints on Color-Ordered Five-Point Amplitudes at All Loop Orders”. In: *Nuclear Physics B* 858.3 (May 2012), pp. 488–501. ISSN: 05503213. DOI: 10.1016/j.nuclphysb.2012.01.019. arXiv: 1111.3821.
- [136] Zvi Bern, Lance J. Dixon, and David A. Kosower. “The Last of the Finite Loop Amplitudes in QCD”. In: *Physical Review D* 72.12 (Dec. 9, 2005), p. 125003. ISSN: 1550-7998, 1550-2368. DOI: 10.1103/PhysRevD.72.125003. arXiv: hep-ph/0505055.
- [137] Z. Bern and G. Chalmers. “Factorization in One-Loop Gauge Theory”. In: *Nuclear Physics B* 447.2-3 (Aug. 1995), pp. 465–518. ISSN: 05503213. DOI: 10.1016/0550-3213(95)00226-I. arXiv: hep-ph/9503236.
- [138] David A. Kosower and Peter Uwer. “One-Loop Splitting Amplitudes in Gauge Theory”. In: *Nuclear Physics B* 563.1-2 (Dec. 1999), pp. 477–505. ISSN: 05503213. DOI: 10.1016/S0550-3213(99)00583-0. arXiv: hep-ph/9903515.
- [139] Diana Vaman and York-Peng Yao. “The Space-Cone Gauge, Lorentz Invariance and On-Shell Recursion for One-Loop Yang-Mills Amplitudes”. In: *Continuous Advances in QCD 2008* (Dec. 2008), pp. 41–55. DOI: 10.1142/9789812838667_0004. arXiv: 0805.2645.
- [140] Andreas Brandhuber et al. “Recursion Relations for One-Loop Gravity Amplitudes”. In: *Journal of High Energy Physics* 2007.03 (Mar. 8, 2007), pp. 029–029. ISSN: 1029-8479. DOI: 10.1088/1126-6708/2007/03/029. arXiv: hep-th/0701187.

- [141] Z. Bern, J. J. M. Carrasco, and H. Johansson. “New Relations for Gauge-Theory Amplitudes”. In: *Physical Review D* 78.8 (Oct. 16, 2008), p. 085011. ISSN: 1550-7998, 1550-2368. DOI: 10.1103/PhysRevD.78.085011. arXiv: 0805.3993.
- [142] N. E. J. Bjerrum-Bohr, Poul H. Damgaard, and Pierre Vanhove. “Minimal Basis for Gauge Theory Amplitudes”. In: *Physical Review Letters* 103.16 (Oct. 16, 2009), p. 161602. ISSN: 0031-9007, 1079-7114. DOI: 10.1103/PhysRevLett.103.161602. arXiv: 0907.1425.
- [143] S. Stieberger. *Open & Closed vs. Pure Open String Disk Amplitudes*. June 23, 2010. arXiv: 0907.2211 [hep-th]. URL: <http://arxiv.org/abs/0907.2211> (visited on 07/29/2021).
- [144] Bo Feng, Rijun Huang, and Yin Jia. “Gauge Amplitude Identities by On-Shell Recursion Relation in S-Matrix Program”. In: *Physics Letters B* 695.1-4 (Jan. 2011), pp. 350–353. ISSN: 03702693. DOI: 10.1016/j.physletb.2010.11.011. arXiv: 1004.3417.
- [145] Yi-Xin Chen, Yi-Jian Du, and Bo Feng. “A Proof of the Explicit Minimal-Basis Expansion of Tree Amplitudes in Gauge Field Theory”. In: *Journal of High Energy Physics* 2011.2 (Feb. 2011), p. 112. ISSN: 1029-8479. DOI: 10.1007/JHEP02(2011)112. arXiv: 1101.0009.
- [146] Freddy Cachazo. *Fundamental BCJ Relation in $N=4$ SYM From The Connected Formulation*. June 26, 2012. arXiv: 1206.5970 [hep-th]. URL: <http://arxiv.org/abs/1206.5970> (visited on 07/29/2021).
- [147] Bo Feng, Yin Jia, and Rijun Huang. “Relations of Loop Partial Amplitudes in Gauge Theory by Unitarity Cut Method”. In: *Nuclear Physics B* 854.1 (Jan. 2012), pp. 243–275. ISSN: 05503213. DOI: 10.1016/j.nuclphysb.2011.08.024. arXiv: 1105.0334.
- [148] Johannes Henn, Bláithín Power, and Simone Zoia. “Conformal Invariance of the One-Loop All-Plus Helicity Scattering Amplitudes”. In: *Journal of High Energy Physics* 2020.2 (Feb. 2020), p. 19. ISSN: 1029-8479. DOI: 10.1007/JHEP02(2020)019. arXiv: 1911.12142.
- [149] David C. Dunbar, Guy R. Jehu, and Warren B. Perkins. “Two-Loop Gravity Amplitudes from Four Dimensional Unitarity”. In: *Physical Review D* 95.4 (Feb. 22, 2017), p. 046012. ISSN: 2470-0010, 2470-0029. DOI: 10.1103/PhysRevD.95.046012. arXiv: 1701.02934.
- [150] Z. Bern, L. Dixon, and D. A. Kosower. *New QCD Results from String Theory*. Nov. 3, 1993. arXiv: hep-th/9311026. URL: <http://arxiv.org/abs/hep-th/9311026> (visited on 06/29/2021).
- [151] Z. Bern, L. Dixon, and D. A. Kosower. “One-Loop Corrections to Five-Gluon Amplitudes”. In: *Physical Review Letters* 70.18 (May 3, 1993), pp. 2677–2680. ISSN: 0031-9007. DOI: 10.1103/PhysRevLett.70.2677. arXiv: hep-ph/9302280.
- [152] Z. Bern et al. “Multi-Leg One-Loop Gravity Amplitudes from Gauge Theory”. In: *Nuclear Physics B* 546.1-2 (Apr. 1999), pp. 423–479. ISSN: 05503213. DOI: 10.1016/S0550-3213(99)00029-2. arXiv: hep-th/9811140.
- [153] Zeno Capatti et al. *Local Unitarity: A Representation of Differential Cross-Sections That Is Locally Free of Infrared Singularities at Any Order*. Oct. 2, 2020. arXiv: 2010.01068 [hep-ph, physics:hep-th]. URL: <http://arxiv.org/abs/2010.01068> (visited on 10/06/2020).
- [154] Z. Bern and A. K. Grant. “Perturbative Gravity from QCD Amplitudes”. In: *Physics Letters B* 457.1-3 (June 1999), pp. 23–32. ISSN: 03702693. DOI: 10.1016/S0370-2693(99)00524-9. arXiv: hep-th/9904026.

- [155] Darren Forde and David A. Kosower. “All-Multiplicity Amplitudes with Massive Scalars”. In: *Physical Review D* 73.6 (Mar. 6, 2006), p. 065007. ISSN: 1550-7998, 1550-2368. DOI: 10.1103/PhysRevD.73.065007. arXiv: hep-th/0507292.
- [156] German Rodrigo. “Multigluonic Scattering Amplitudes of Heavy Quarks”. In: *Journal of High Energy Physics* 2005.09 (Sept. 30, 2005), pp. 079–079. ISSN: 1029-8479. DOI: 10.1088/1126-6708/2005/09/079. arXiv: hep-ph/0508138.
- [157] Christian Schwinn and Stefan Weinzierl. “SUSY Ward Identities for Multi-Gluon Helicity Amplitudes with Massive Quarks”. Version 2. In: *Journal of High Energy Physics* 2006.03 (Mar. 7, 2006), pp. 030–030. ISSN: 1029-8479. DOI: 10.1088/1126-6708/2006/03/030. arXiv: hep-th/0602012.
- [158] Paola Ferrario, German Rodrigo, and Pere Talavera. “Compact Multigluonic Scattering Amplitudes with Heavy Scalars and Fermions”. In: *Physical Review Letters* 96.18 (May 9, 2006), p. 182001. ISSN: 0031-9007, 1079-7114. DOI: 10.1103/PhysRevLett.96.182001. arXiv: hep-th/0602043.